Investigation of cytomegalovirus-based cancer vaccines

Silvia Gimeno Brias

A thesis submitted to Cardiff University in candidature for the Degree of Doctor of Philosophy

Systems Immunity Research Institute and Division of Infection and Immunity,

School of Medicine,

Cardiff University,

Heath Park,

Cardiff.

June 2018

Declaration

This work has not been submitted in substance for any other degree or award at this or any other university or place of learning, nor is being submitted concurrently in candidature for any degree or other award.

Signed ……(candidate) Date ……

STATEMENT 1

This thesis is being submitted in partial fulfilment of the requirements for the degree of PhD.

Signed …… (candidate) Date ……

STATEMENT 2

This thesis is the result of my own independent work/investigation, except where otherwise stated, and the thesis has not been edited by a third party beyond what is permitted by Cardiff University's Policy on the Use of Third Party Editors by Research Degree Students. Other sources are acknowledged by explicit references. The views expressed are my own.

Signed ……(candidate) Date ……

STATEMENT 3

I hereby give consent for my thesis, if accepted, to be available online in the University's Open Access repository and for inter-library loan, and for the title and summary to be made available to outside organisations.

Signed ……(candidate) Date ……

STATEMENT 4: PREVIOUSLY APPROVED BAR ON ACCESS

I hereby give consent for my thesis, if accepted, to be available online in the University's Open Access repository and for inter-library loans **after expiry of a bar on access previously approved by the Academic Standards & Quality Committee.**

Signed ……(candidate) Date ……

Acknowledgements

I would like to take this opportunity to thank the Medical Research Council (MRC) for funding my PhD. I would also like to thank my supervisor, Dr Ian Humphreys, for his constant support, guidance and excellent supervision throughout this journey. I would like to thank my co-supervisors, Dr Rich Stanton and Professor Awen Gallimore, for their support and advice during these years.

A big thank you goes to all the members of the Humphreys' lab who have helped provide a fun and yet professional environment. I would like to specially thank Morgan Marsden and Lucy Chapman for their technical support; Dr Mat Clement for his useful discussions and suggestions; Pragati Sabberrwal for staying with me counting cells until 11pm; and Dr Sandra Dimonte, Marta Williams and Catherine Rutley for their support and good company.

I would also like to thank Yasmin, Fede, Dani and Freya for making the first year of my PhD unforgettable. A special thanks to Patricia for those hour-long breaks, for allowing me to vent out about my project and for helping me stay calm in moments of stress – thank you! I would like to thank Silvia, Cristian and Victor for those visits to Southampton and surf trips, which allowed me to take a break and come back more motivated. Thank you Silvia for long conversations on the phone and supporting me despite my mood (thanks for putting up with me). I would also like to thank Tatiana, although miles apart we always find time to catch up and be there for each other.

Finally, I would like to thank my parents, specially my mum, who have helped me get to this point in life. A special thank you goes to my grandmother, Mercedes, for her unconditional love and support – thank you for believing I can achieve everything that I set out to do.

Summary

Cytomegalovirus (CMV) is a highly immunogenic beta-herpesvirus that establishes asymptomatic infection in immune competent individuals. The ability of CMV to induce high frequencies of functional effector memory $CD8^+$ T cells that increase over time (termed 'memory inflation') makes this virus an attractive vaccine vector. The primary focus of this thesis is centred on the hypothesis that engineering a CMV-based vector expressing a tumour-associated antigen will be able to induce a robust and long-lived anti-tumour $CD8^+$ T cell response. Using the murine CMV (MCMV) infection model, several MCMV-based vectors were constructed to express the tumour-associated antigens 5T4 and NY-ESO-1, from different locations within the *m123-m128* locus of the MCMV genome, which has been associated with the induction of memory inflation. Systemic immunisation with these vectors revealed that induction of tumour-specific $CD8^+$ T cells correlated with high tumour antigen expression during MCMV replication *in vitro* and in turn, depended on the site of insertion within the MCMV genome. MCMV-based vectors were also examined in prime-boost strategies that incorporated recombinant adenovirus expressing the corresponding tumour-associated antigen. Prime-boost immunisation resulted in the generation of polyfunctional tumour-specific $CD8^+$ T cells that delayed tumour onset. Interestingly, immunisation with the MCMV vector led to an increased influx of lymphocytes infiltrating the tumour. Finally, the immunogenicity of a spread-defective MCMV vector, ΔgL-MCMV, was investigated upon subcutaneous challenge. Encouragingly, although the magnitude of the response was reduced compared to wild-type MCMV, ΔgL-MCMV was able to drive memory inflation. Collectively, these data show the importance of vector construction in an effective CMV-based vaccine and highlight the potential of CMV in influencing lymphocyte infiltration into tumours. Ultimately, it provides further evidence of the potential use of CMV as a vaccine vector for cancer therapy.

Table of Contents

List of Figures

List of Tables

List of Abbreviations

ACT	Adoptive cell transfer
Ad	Adenovirus
ADCC	Antibody-dependent cellular cytotoxicity
AHR	Aryl hydrocarbon receptor
AIDS	Acquired immune deficiency syndrome
AML	Acute myeloid leukaemia
APCs	Antigen presenting cells
BAC	Bacterial artificial chromosome
bp	Base pair
Blimp-1	B lymphocyte induced maturation protein-1
CAR	Chimeric antigen receptor
CDC	Complement-dependent cytotoxicity
cDCs	Classical dendritic cells
CLL	Chronic lymphocytic leukaemia
CMC	Carboxymethyl cellulose
CMV	Cytomegalovirus
COX-2	Cyclooxygenase 2
CPE	Cytopathic effect
CRC	Colorectal cancer
CTA	Cancer-testis antigen
CTLA-4	Cytotoxic T lymphocyte antigen 4
cVAC	Cytoplasmic virus assembly compartment
DCs	Dendritic cells
DMOS	Dimethyl sulfoxide
DN	Double negative
DP	Double positive
DTT	Dithiothreitol
E	Early
EBV	Epstein-Barr virus
EEC	Early effector cells
EGFR	Epithelial growth factor receptor
FCS	Foetal calf serum
FcR	Fragment c receptor
FDA	Food and Drug Administration

FOXP3	Forkhead box P3
GATA-3	GATA-binding protein 3
GC	Gastric cancer
GM-CSF	Granulocyte-macrophage colony-stimulating factor
HBV	Hepatitis B virus
HCC	Hepatocellular carcinoma
HCMV	Human cytomegalovirus
HCV	Hepatitis C virus
HER2	Human epidermal growth factor receptor 2
HHV	Human herpesvirus
HIV	Human immunodeficiency virus
HL	Hodgkin's lymphoma
HLA	Human leukocyte antigen
HNC	Head and neck cancer
HPV	Human papilloma virus
HSV	Herpes simplex virus
HTLV	Human T lymphocytic virus
ICAM	Intracellular adhesion molecule
IDO	Indoleamine 2,3-dioxygenase
IE	Immediate early
IL	Interleukin
IFN	Interferon
i.m	Intramuscular
i.n	Intranasal
i.p	Intraperitoneal
ISG	IFN-stimulated genes
i.v	Intravenous
KLRG1	Killer lectin-like receptor G1
KSHV	Kaposi's sarcoma-associated herpes virus
L	Late
LAG-3	Lymphocyte activation gene 3
LCMV	Lymphocytic choriomeningitis virus
LFA-3	Lymphocyte function associated antigen 3
mAbs	Monoclonal antibodies
MCC	Merkel cell carcinoma
MCMV	Murine cytomegalovirus
MDSCs	Myeloid-derived suppressor cells

MFI	Mean fluorescence intensity
MHC	Major histocompatibility complex
MIE promoter	Major immediate-early promoter
MOI	Multiplicity of infection
MPEC	Memory precursor effector cell
Mtb	*Mycobacterium tuberculosis*
MVA	Modified vaccinia Ankara
NHL	Non-Hodgkin's lymphoma
NK cell	Natural killer cell
NSCLC	Non-squamous non-small cell lung carcinoma
ORF	Open reading frame
PCR	Polymerase chain reaction
pDCs	Plasmacytoid dentritic cell
PDGF	Platelet-derived growth factor
PDGFRα	Platelet-derived growth factor receptor α
PBS	Phosphate buffered saline
PD-1	Programmed cell death protein 1
PD-L1	Programmed cell death ligand 1
PEG_2	Prostaglandin-E_2
pfu	Plaque forming unit
p.i	Post-infection
PRR	Pattern recognition receptor
PSA	Prostate-specific antigen
RAd	Recombinant adenovirus
RAG	Recombination activating gene
RCC	Renal cell carcinoma
RE	Restriction enzyme
RhCMV	Rhesus cytomegalovirus
RORγt	Retinoic acid receptor related orphan receptor γt
s.c	Subcutaneous
SEM	Standard error of the mean
SEREX	Serological analysis of recombinant cDNA expression libraries
SIV	Simian immunodeficiency virus
SLEC	Short-live effector cells
SLPs	Synthetic long peptides
STAT3	Signal transducer and activator of transcription 3
TAMs	Tumour associated macrophages

T-bet	T-box expressed in T cells
TCE	Tetrachloroethylene
T_{CM} cell	Central memory T cell
TCR	T cell receptor
T_{EM} cell	Effector memory T cell
T_{FH} cell	Follicular helper T cell
T_H cell	Helper T cell
TILs	Tumour infiltrating lymphocytes
TIM-3	T cell immunoglobulin domain and mucin domain protein 3
TGF	Transforming growth factor
TLR	Toll-like receptor
TNF	Tumour necrosis factor
TRAIL	TNF-related apoptosis-inducing ligand
Tregs	Regulatory T cells
T_{RM} cell	Tissue-resident memory T cell
TRP2	Tyrosinase-related protein 2
TPBG	Trophoblast glycoprotein
UC	Urothelial carcinoma
U_L	Unique long
U_S	Unique short
VEGF	Vascular endothelial growth factor
VLA-4	Very-late antigen 4
VZV	Varicella zoster virus
VV	Vaccinia virus
WT	Wild type
ZP3	Zona pellucida 3

Chapter 1 - Introduction

1.1 T Lymphocytes

T lymphocytes (referred to hereafter as T cells) are part of the adaptive immune system, and along with B lymphocytes they form the second line of host defence after the innate immune response, eliminating pathogens in an antigen-specific manner and providing long-lasting protection.

1.1.1 T cell development

T cells originate from common lymphoid progenitor cells in the bone marrow (1) and migrate to the thymus where they undergo T cell receptor (TCR) gene rearrangement and thymic selection. The majority of cells in the thymus give rise to α/β T cells, however approximately 5% bear the γ/δ TCR (2). The function of the later cells is less well understood than those T cells expressing α/β TCRs, and will not be discussed further. Upon entry into the thymus, T cell precursors lack the expression of CD4 and CD8 ($CD4^-CD8^-$) and are called double negative (DN) cells. DN thymocytes move to the thymic cortex where rearrangement of the TCR genes occur. The process initially selects for cells that have successfully rearranged their TCR-β chain locus. The β chain then pairs with the surrogate chain, pre-Tα, and produces a pre-TCR that forms a complex with CD3 molecules, leading to their survival, proliferation and arrest in further β chain loci rearrangement. These cells further differentiate by upregulating CD4 and CD8, becoming double positive (DP; $CD4^+CD8^+$) cells. DP thymocytes rearrange their TCR-α chain loci, to produce an $\alpha\beta$-TCR. DP cells then undergo positive selection – cells interact with self-antigens on major histocompatibility complex (MHC) class I or class II molecules. Those that recognise the MHC bound self-peptides with an

appropriate affinity survive, while those cells that interact with a weaker affinity die by apoptosis. Thymocytes then migrate into the medulla where they undergo negative selection – they interact with epithelial cells and antigen presenting cells (APCs), such as dendritic cells (DCs) and macrophages, which present MHC bound self-antigens. Thymocytes that recognise the antigen below an acceptable threshold of reactivity develop into single positive $CD4^+$ or $CD8^+$ T cells via the downregulation of CD8 or CD4 expression, respectively. Those DP thymocytes that interact too strongly with the antigen undergo apoptosis. This process prevents the formation of unreactive or alloreactive T cells. Single positive $CD4^+$ and $CD8^+$ T cells exit the thymus as mature naïve T cells and circulate the periphery (reviewed in (3)).

1.1.2 $CD4^+$ helper T cells

Mature naïve $CD4^+$ helper T cells (T_H) enter secondary lymphoid organs, such as lymph nodes and epithelium-associated lymphoid tissues in the gastrointestinal and respiratory tracts and skin, where they search for specific antigen bound MHC class II molecules found on APCs. Interaction of the TCR with specific antigens results in differentiation and clonal expansion of the $CD4^+$ T cell. Depending on the cytokines in the microenvironment and costimulatory molecules involved in antigen presentation, in addition to the affinity of the antigen, $CD4^+$ T cells will differentiate into different effector T_H cells (4–8) classified into distinct populations, T_H1, T_H2, T_H9, T_H17 or T_H22 cells, based on the type of cytokine production.

Interleukin (IL)-12, produced by activated macrophages and DCs, stimulates the development of T_H1 cells (9, 10). T_H1 cells produce IL-2, interferon (IFN)-γ and tumour necrosis factor (TNF)-β; and protect the host from intracellular pathogens via the recruitment and activation of macrophages and enhancing their microbicidal action (5). In addition, cytokines produced by T_H1 cells, mainly IL-2 and IFN-γ, promote $CD8^+$ T

cell differentiation into active cytotoxic cells. T_H1 cells also induce B cells to produce IgG2a antibodies that can coat extracellular microbes and activate complement, thereby helping to eliminate some extracellular pathogens as well (5). T_H1 cytokine induction is associated with the expression of the transcription factor T-box expressed in T cells (T-bet) (11). The development of T_H2 cells from naïve $CD4^+$ T cells is induced by IL-4 (9) and mainly defend the host against extracellular pathogens. T_H2 cells produce IL-4, IL-5, IL-10 and IL-13 and is associated with the transcriptional regulator GATA-binding protein 3 (GATA-3) (12). These cytokines induce B cells to produce most classes of antibodies, including IgA, IgE and some subclasses of IgG (13) which initiate IgE-dependent mast cell-mediated reactions, in addition to eosinophil activation in the defence against parasite infections (5, 14). However, cytokines driving T_H2-associated inflammation, such as IL-13, have been associated with allergic disorders such as asthma, allergic rhinitis and eczema (15). Furthermore, T_H2 cells also have anti-inflammatory actions – IL-4 and IL-13 antagonise the action of IFN-γ while IL-10 suppresses various macrophages responses. T_H1 and T_H2 effector cells produce cytokines that serve as their own autocrine growth factor – IL-2 and IL-4 secreted by T_H1 and T_H2 cells, respectively, generate a positive feedback loop as they are potent inducers of T_H1 and T_H2 development, respectively. At the same time, the two subsets of T_H cells produce cytokines that cross-regulate each other's development and activity – IFN-γ produced by T_H1 cells inhibits the development of T_H2 cells, while IL-4 and IL-10 produced by T_H2 cells inhibit the development of T_H1 cells (5, 16). Naïve $CD4^+$ T cells can also develop into T_H17 cells when they are activated in the presence of transforming growth factor (TGF)-β, IL-6 and IL-23 (17). T_H17 produce IL-10, IL-17, IL-21 and IL-22, and are involved in the defence against extracellular bacteria and fungi, but also have a role in the development of autoimmune diseases (18). T_H17 cells are associated with the upregulation of the transcription factor retinoic acid receptor related orphan receptor (ROR) γt (19). Other less characterised subsets

include T_H9 and T_H22, which produce IL-9 and IL-22, respectively (reviewed in (20)). Another subset of $CD4^+$ T cells, regulatory T cells (Tregs), are characterised by the expression of the transcription factor forkhead box P3 (FOXP3), and are required to maintain self-tolerance (21, 22). Most Tregs are produced in the thymus as a functionally distinct and mature T cell subpopulation and are known as natural Tregs. However, a small portion are induced from mature $CD4^+$ T cells in the periphery upon TCR activation in the presence of TGF-β and are known as induced Tregs (iTregs) (23). A more recently described $CD4^+$ T cell subset are follicular helper T (T_{FH}) cells (reviewed in (24)). These are identified by the constitutive expression of the B cell homing receptor CXCR5 and develop upon antigen encounter in the presence of IL-6 and IL-21 (25). Moreover, T_{FH} cell development is associated with the transcriptional regulator BCL-6 which antagonises transcription factors important for T_H1, T_H2 and T_H17 differentiation (26). T_{FH} cells are located in the follicular area of secondary lymphoid organs where they are important for the formation of germinal centres and support B cell expansion and differentiation (27, 28). While some T_H cells are terminally differentiated, the majority of these cells retain some plasticity and can acquire different properties and functions upon antigenic re-stimulation and can switch subsets (reviewed in (29)). The development of the different $CD4^+$ T cell subsets is summarised in Figure 1.1.

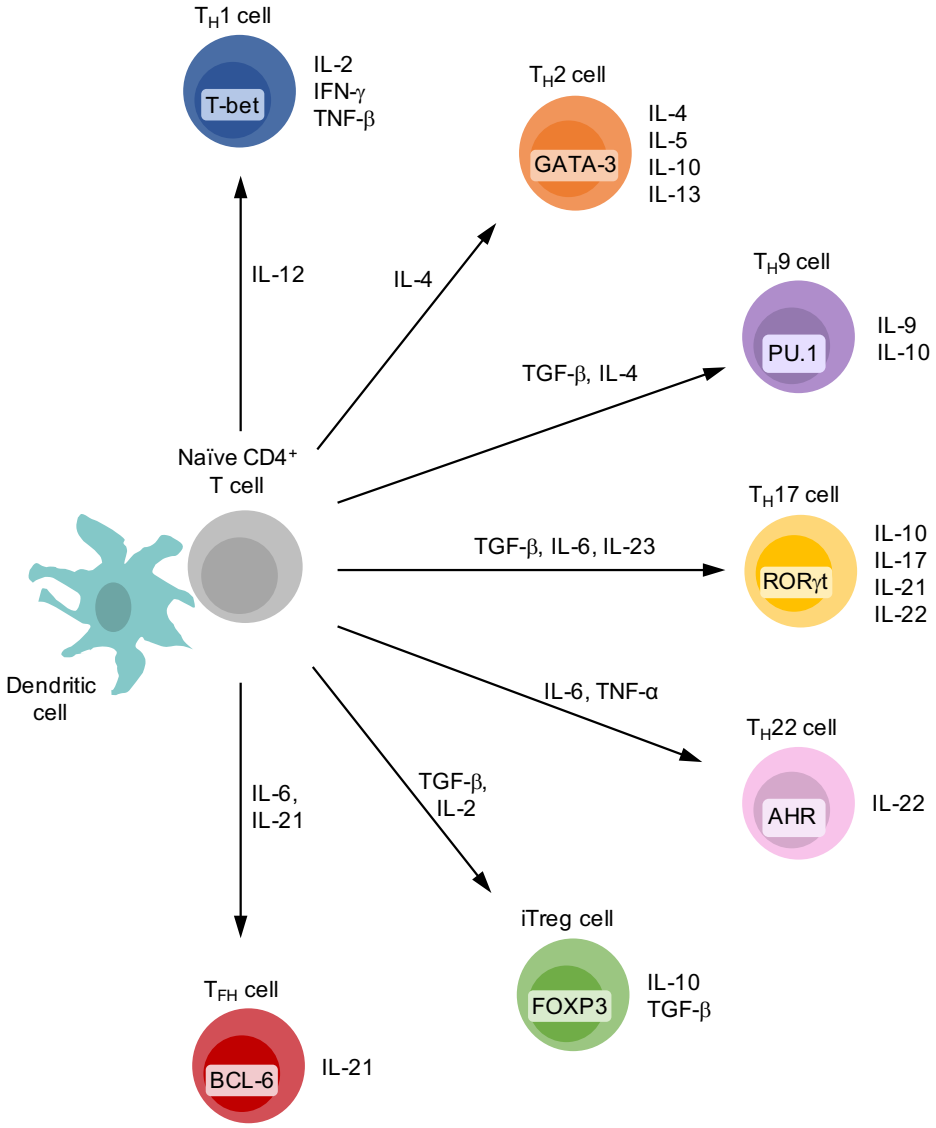

Figure 1.1 CD4⁺ helper T cell differentiation.

Following antigen recognition on APCs, naïve $CD4^+$ T cells differentiate into distinct T_H subsets via the exposure to different cytokines (shown next to the arrows). This leads to the induction of subset-specific transcription factors (shown inside each cell), which results in their own pattern of cytokines production (shown next to each cell type).

1.1.3 $CD8^+$ cytotoxic T cells

$CD8^+$ cytotoxic T cells play an important role in the defence against intracellular pathogens, including viruses and bacteria, and for tumour surveillance. Naïve $CD8^+$ T cells enter secondary lymphoid organs where they become activated by mature DCs bearing cognate antigen. Activation of naïve $CD8^+$ T cells require three distinct signals: engagement of the TCR with the peptide-bound MHC class I molecule and CD8 co-receptor stabilising the signal (signal 1); co-stimulatory signal such as, but not limited to, that from the interaction between CD28 on the T cell surface and either CD80 or CD86 on APCs (signal 2); and cytokines such as type 1 IFNs and IL-2 (signal 3) (30–33). Presentation of the antigen by immature DCs or in the absence of cytokines (signal 3), the antigen-stimulated $CD8^+$ T cells fail to develop into effector $CD8^+$ T cells and become tolerant (34).

Once activated, $CD8^+$ T cells undergo clonal expansion, differentiate into effector cells and travel throughout the host looking for cells expressing their cognate antigen. Upon encounter, activated $CD8^+$ T cells release cytotoxins, such as perforin and granzymes, which enter the target cell and induce apoptosis. Further to the cytotoxins, $CD8^+$ T cells can also induce apoptosis via the binding of FAS ligand on T cell surface to Fas receptor on the target cell membrane. Cells undergoing programmed cell death are rapidly engulfed by nearby phagocytic cells. Activated $CD8^+$ T cells also produce IFN-γ and TNF-α which contribute to host defence in several ways. IFN-γ is involved in the regulation of over 200 known IFN-stimulated genes (ISG), the products of which exert numerous functions contributing to host defence (reviewed in (35)). IFN-γ has anti-viral properties and induces the increased expression of MHC class I on cell surfaces, aiding recognition of infected cells by $CD8^+$ T cells. Moreover, IFN-γ activates macrophages, recruiting them to site of infection. TNF-α can synergise with IFN-γ to activate macrophages, and engage with TNF receptor-I on target cells to induce apoptosis (36).

1.1.3.1 Effector CD8$^+$ T cell Subsets

Once CD8$^+$ T cells become activated, changes in the cell phenotype occur – CD62L is downregulated early after CD8$^+$ T cells are primed allowing cells to leave secondary lymphoid organs and migrate to site of infection (37). Antigen experienced CD8$^+$ T cells upregulate the cellular adhesion molecule CD44 and high expression levels are maintained throughout the life of the T cell (38). Expression of CD44 and CD62L on CD8$^+$ T cells are commonly used as markers to identify different cell subsets. However, the expression pattern of many other molecules is also altered. Some examples are OX40, 4-1BB and very-late antigen (VLA)-4, which are upregulated, while CCR7 is downregulated upon CD8$^+$ T cell activation (39).

Furthermore, based on the expression pattern of the surface markers, killer cell lectin-like receptor G1 (KLRG1) and CD127 (IL-7 receptor α chain), three distinct effector CD8$^+$ T cell populations can be identified: early effector cells (EEC), short-lived effector cells (SLEC) and memory precursor effector cells (MPEC) (40–43). Naïve CD8$^+$ T cells are characterised by being CD127^{high} and KLRG1^{low} and upon activation, CD127 is downregulated and cells have been recently termed EEC (CD127^{low}KLRG1^{low}). Some EEC upregulate KLRG1 and become SLEC (CD127^{low}KLRG1^{high}), which are considered to be more terminally differentiated and most undergo apoptosis during the contraction phase, after the infection has been cleared. Other EEC can re-express CD127 and become MPEC (CD127^{high}KLRG1^{low}), which survive the contraction phase and retain the ability to differentiate into a long-lived memory population (44). The factors regulating the differentiation into SLEC and MPEC population are only recently being identified. It has been shown that IL-12 signalling during T cell priming regulates SLEC differentiation via the upregulation of T-bet activity (42). The transcription factor B lymphocyte induced maturation protein-1 (Blimp-1) has also been reported to be important in the generation of SLEC (45, 46).

In addition, $CD4^+$ T cell help and IL-2 signalling aid expansion and differentiation of effector $CD8^+$ T cells into SLEC via CD25 upregulation (41).

1.1.3.2 Memory $CD8^+$ T cells

Memory $CD8^+$ T cells are maintained by the actions of IL-7 and IL-15 which promote cell survival and self-renewal in an antigen-independent manner (47, 48). A unique feature of memory $CD8^+$ T cells is their ability to produce effector functions without the need of co-stimulation or cytokine signalling (49). This rapid activation allows $CD8^+$ T cells to quickly control and clear a secondary infection, resulting in reduced pathology. Memory $CD8^+$ T cells can be divided into three main groups, which can be distinguished by phenotypic markers, functions and location: central memory (T_{CM}), effector memory (T_{EM}) and tissue-resident memory (T_{RM}) T cells.

All memory $CD8^+$ T cell subsets are antigen-experienced, thus express high levels of CD44. $CD8^+$ T_{CM} cells express high levels of CD62L which enables them to home to secondary lymphoid organs. T_{CM} cells have greater proliferative potential than other memory subsets and produce IL-2, but have reduced effector functions. T_{CM} cells differentiate into effector cells in response to antigenic stimulation (49). In contrast, $CD8^+$ T_{EM} cells express low levels of CD62L and are predominantly found in non-lymphoid organs. T_{EM} cells have reduced proliferative capacity, but produce immediate effector functions upon antigen encounter (49). A more recently identified memory subset are T_{RM} cells, which reside long-term in mucosal tissues such as skin, lung and gut, and have limited migratory potential – they are not found in any lymphoid organ or in the circulation. $CD8^+$ T_{RM} cells are characterized by high expression of CD103 and CD69 and low expression of CD62L and CD27. They have very little proliferative capacity but have enhanced immediate effector function, expressing high levels of granzyme B (50). When and how these T_{RM} cells are established and how are they regulated is still an area of ongoing research. It has been suggested that cells

migrate to non-lymphoid tissues during the effector phase of a response and then become permanently established (reviewed in (50)). Recent observations in mice have shown that the precursors of T_{RM} cells in the skin and small intestines are derived from effector memory T cell precursors (MPECs) that express low levels of KLRG1 (51, 52). At these sites the cytokine milieu within the tissues, such as TGF-β, drive their differentiation into T_{RM} cells (51, 52). Table 1.1 shows a summary of memory $CD8^+$ T cell characteristics.

Table 1.1 Memory $CD8^+$ T cell characteristics.

Cell subset	Phenotype	Location	Functional properties
T_{CM} cell	$CD44^+CD62L^+$	Secondary lymphoid tissues and blood	↑ Proliferative capacity ↑ IL-2 production ↑ Migration ↓ Effector functions
T_{EM} cell	$CD44^+CD62L^-$	Spleen, blood and non-lymphoid tissues	↓ Proliferative capacity ↓ IL-2 production ↑ Migration ↑ Effector functions
T_{RM} cell	$CD103^+CD69^+$ $CD62L^-CD27^-$	Skin, lung, gut and brain	↓ Proliferative capacity ↓ IL-2 production ↓ Migration ↑ Effector functions

1.2 Cancer and Anti-Tumour Immunity

1.2.1 Initiation of cancer

Cancer is a collective name for the combination of different diseases characterised by uncontrollable cell division resulting in the invasion of the surrounding tissues and spread to other organs of the body. According to the World Health Organisation (WHO), cancer is the leading cause of death worldwide, accounting for approximately 29% of deaths in the UK in 2011. Tumourigenesis, the process underlying the transformation of normal cells into malignant derivatives, is a multistep mechanism involving epigenetic and genetic alterations that result in the upregulation of oncogenes and inactivation of tumour suppressor genes. This confers growth advantages, leading to unregulated cellular proliferation. In 2000, Douglas Hanahan and Robert Weinberg published the review 'The Hallmarks of Cancer', in which they described six alternations in cell physiology that govern this transformation (53):

- The ability to sustain proliferative signalling by promoting the production and release of growth factors and overexpressing growth factor receptors;
- Evading growth suppressors by downregulating or displaying mutant dysfunctional growth suppressor receptors, inactivating tumour suppressor genes or abolishing cell-cell contact inhibition;
- Evading apoptosis via the loss of pro-apoptotic regulators or upregulation of anti-apoptotic proteins;
- Unlimited replicative potential by maintaining the telomere length due to the upregulation of telomerase expression, preventing senescence or apoptosis;
- Sustained angiogenesis via production of vascular endothelial growth factors;

- Activating tissue invasion and metastasis by altering the expression of cell-cell adhesion molecules.

Over a decade later, in the course of remarkable progress in cancer research, two emerging hallmarks were added (54):

- Avoiding immune destruction by disabling immune components via production of immunosuppressive factors and recruiting immunosuppressive cells;
- Reprogramming of energy consumption – shifting from mitochondrial oxidative phosphorylation to aerobic glycolysis.

While these processes must occur for tumours to progress, cancer development depends on malignant cells actively interacting with neighbouring cells, comprised of multiple distinct cell types, all collaborating to create a complex tumour microenvironment that determines the outcome of tumour progression.

1.2.2 Cancer immune-surveillance and immune-editing

The concept of cancer immune-surveillance emerged in the 1950s, with Burnet and Thomas' proposing that thymus-dependent cells constantly circulated the host tissues for the presence of transformed cells resulting in their elimination (55–58). At the time, such work was considered controversial due to several experiments by Stutman describing no differences in tumour development between immunocompetent wild type mice and immunocompromised nude mice when these were given chemically induced tumours (59, 60). It was later reported that functional cytotoxic T cells, albeit in fewer numbers, were still present in these nude mice (61, 62). Furthermore, Stutman, following his experiments rejecting the existence of immune-surveillance, reported a new cell type with tumour-killing ability, the natural killer (NK) cell, that was also present

in nude mice (63), thus casting doubts over the interpretation of the previous findings in these mice.

Two decades later, technological advances in mouse genetics resulted in the generation of mice strains with defined immune-deficiencies, which helped support the hypothesis of cancer immune-surveillance. These included, but not limited to, recombination-activating gene (RAG) knock out mice, deficient in T, B and NKT cells; and mice lacking important immune components such as perforin or IFN-γ. These mice exhibited an increased frequency of spontaneous and/or chemically-induced tumours as compared to wild type mice (64–66). Furthermore, mice depleted of NK cells using monoclonal antibodies were more susceptible to chemically induced tumourigenesis than untreated controls (67). Thus, these data demonstrated a clear role for the innate and adaptive immune system in recognising and eliminating malignant cells. Nonetheless, studies have also shown that, despite the multiple effector functions of the immune system against tumourigenesis, immunocompetent mice still developed tumours, and that these were less immunogenic than those that developed in immunocompromised mice (66, 68, 69). Paradoxically, besides protecting from tumour development, the actions of the immune system leads to the selection and eventual out-growth of tumours that are more capable of escaping immune detection, indicating that cancer immune-surveillance represents one step of a broader immunological process.

This prompted the development of the cancer immune-editing hypothesis, which describes how the host immune responses can protect against and promote tumour development (70–72). This involves three phases: elimination, which represents the concept of cancer immune-surveillance; equilibrium, where many tumour cells are effectively eliminated but new ones arise carrying more mutations that provide them with increased resistance to immune attack; and escape, referring to tumour

out-growth from cells that have overcome the immunological restrain. The mechanisms underlying tumour immune escape will be discussed in section 1.2.3.

1.2.2.1 Cancer immune-editing in humans

Studies of tumour development in mice have served as the main driver for the establishment of the cancer immune-editing hypothesis. Nevertheless, evidence has since been obtained indicating that this also occurs in humans and can alter the course of tumour development in patients. Throughout the years it became apparent that immunocompromised patients, such as those with human immunodeficiency virus (HIV)/acquired immune deficiency syndrome (AIDS) and individuals receiving immune-suppressants for organ transplantation, had an increased risk of cancer (reviewed in (72)). Whilst the cancers arising in these patients are typically of viral origin such as lymphomas (Epstein-Barr virus, EBV), Kaposi's sarcoma (herpesvirus) and cervical cancer (human papilloma virus, HPV), there is evidence of greater risk for colon, pancreas, kidney, lung and non-melanoma skin cancers. In accordance with the cancer immune-surveillance hypothesis, the increased rates of cancer in immunocompromised individuals is a result of reduced recognition or elimination of aberrant cells. Furthermore, insights of the role of the immune system in human cancer have also come from anecdotal reports of cancers being transferred from an organ donor to the immunosuppressed recipient (73, 74), where *de novo* malignancies arise in the permissive environment created by the immune-suppressants.

1.2.3 Mechanisms of evasion from immune-surveillance

Tumour cells develop mechanisms driven by genomic instability and immune selection pressure, that enables their evasion from immune-surveillance (54, 71). At the tumour cell level, alternations leading to reduced immune recognition and resulting in loss of immunogenic tumour antigen expression, promotes tumour out-growth. This can occur

through the downregulation of MHC class I molecules that present these antigens to tumour-specific T cells (75–77); through loss of components involved in antigen processing and loading onto MHC class I molecules within the tumour cell (78–80); and through the emergence of tumour cells that express poor immunogenic antigens (54). Furthermore, tumour cells can overcome the cytotoxic effects of immune cells by upregulating anti-apoptotic molecules such as Bcl-2 (54, 81); via persistent activation of pro-oncogenic transcription factors such as signal transducer and activator of transcription 3 (STAT-3) (82); and by overexpressing PI-9, a serine protease inhibitor that inactivates granzyme B (83). Alternatively, immune escape may result from the establishment of an immunosuppressive state within the tumour microenvironment. Tumour cells may overproduce immunosuppressive cytokines, such as IL-10, vascular endothelial growth factor (VEGF) and TGF-β, which inhibit DC function and lymphocyte activation (84). The pro-inflammatory factor prostaglandin E_2 (PEG_2) is also expressed by tumours due to enhanced expression of the enzyme cyclooxygenase 2 (COX-2) (85). PGE_2 suppresses myeloid cell activation via induction of IL-10 production by lymphocytes and macrophages and inhibition of IL-12 production by macrophages (86). In addition, tumour cells produce inhibitors of T cell responses, such as galectin-1, which promotes apoptosis of activated T cells among other functions (87); and indoleamine 2,3-dioxygenase (IDO), which metabolises tryptophan, reducing its concentration in the surrounding environment, resulting in $CD8^+$ T cell proliferation arrest and $CD4^+$ T cell apoptosis (88). Other immune evasion mechanisms operate through the recruitment of Tregs and myeloid-derived suppressor cells (MDSCs), which can actively suppress the actions of cytotoxic lymphocytes. When stimulated, Tregs produce IL-10 and TGF-β and express the inhibitory co-stimulatory molecules CTLA-4 and PD-L1 (89). MDSCs are a heterogeneous cell population comprised of myeloid progenitor cells and immature myeloid cells. They induce expansion of Tregs; produce IL-10 and TGF-β; uptake or deplete the surroundings of the amino acids

arginine or cysteine, which are required for T cell activation and function; and/or produce highly reactive oxygen species and peroxynitrites, which nitrate TCRs or chemokine receptors on tumour-specific T cells blocking the interaction with their ligands (reviewed in (90)).

1.2.4 Tumour-associated antigens

Along with the development of new techniques such as the ability to grow T cells *in vitro* and establishing tumour cell lines, the first human tumour antigen recognised by T cells was identified in 1989 – an epithelial mucin, MUC1 (91). In the following years, a large number of tumour antigens were identified using tumour-reactive T cells, or using patient sera. The later approach, called serological analysis of recombinant cDNA expression libraries (SEREX), uses tumour-specific antibodies isolated from cancer patients to screen tumour gene expression libraries to identify target antigens (92). Since their discovery, tumour-associated antigens have been envisioned as targets for cancer therapy.

Tumour-associated antigens can be classified into five categories: (i) overexpression of oncogenes (e.g. HER2 and MUC1); (ii) mutated gene products (e.g. p53); (iii) differentiation antigens, (e.g. gp100 and MART-1); (iv) cancer-testis antigens (e.g. MAGE and NY-ESO-1); and (v) antigens of oncogenic viruses (e.g. HPV and EBV). The use of these antigens for cancer therapy is sometimes compromised by their expression profile. For example, overexpressed antigens and differentiation antigens are not solely restricted to tumour cells, but are still found in healthy tissue, thus targeting these antigens could result in autoimmunity against healthy normal cells. In contrast, cancer-testis antigens (CTAs) are ideally suited as targets for cancer therapy. CTAs expression is highly restricted to tumour cells showing little or no expression in healthy tissues except for normal testis, embryonic ovaries and placenta. These tissues are considered immune-privilege sites as in the healthy state, cells at these

sites do not express MHC class I molecules and therefore cannot present antigens to T cells (reviewed in (93)). Mutated tumour antigens frequently result from point mutations in ubiquitously expressed genes. The mutation usually changes one amino acid in the peptide or causes a frameshift leading to the production of a new peptide (neo-antigen) and consequently creates a novel epitope that can bind to the MHC class I molecule and/or be recognised by T cells (94). Mutations can also affect oncogenes, thus altering their function and enhancing tumourigenesis. Mutated tumour antigens can be attractive candidates for targeted immunotherapy if it can target the mutated or unique region of these peptides to reduce risks of toxicity. Furthermore, antigens from oncogenic viruses are ideal targets for cancer therapy due to their absence in healthy cells and their capacity to be recognised by T cells. The tumour-associated antigens that will be the focus of this thesis are 5T4 and NY-ESO-1, members of the CTA group, and are described below.

1.2.4.1 5T4

The transmembrane protein 5T4, also known as trophoblast glycoprotein (TPBG), is referred to as an oncofoetal antigen due to its expression in placental trophoblast and in multiple human carcinomas, including colorectal, ovarian and gastric tumours (95). 5T4 was identified in 1988 by a murine monoclonal antibody raised against purified human trophoblast glycoproteins (96). *In vitro* experiments in which 5T4 was overexpressed, cells showed reduced adherence, E-cadherin downregulation, increased motility and cytoskeletal disruption (97–99). Thus, indicating a possible involvement of 5T4 in cell invasion processes in tumours. Indeed, there have been studies showing an association between the expression of 5T4 in tumours with metastasis and an unfavourable clinical outcome (100–102). Upregulation of 5T4 expression is associated with very early embryonic stem cell differentiation (103, 104) and forms an integrated component of epithelial-to-mesenchymal transition, a process

important during embryonic development, but also considered to contribute to metastatic spread of epithelial tumours (105, 106). Wnt signalling is a key component of many aspects of cellular regulation, such as cell fate, proliferation and migration, which are critical for normal development, homeostasis and regeneration, but its dysregulation can lead to disease, including cancer (review in (107)). Indeed, 5T4 has been shown to interfere with Wnt/β-catenin canonical signalling and activate non-canonical Wnt pathways (108). Furthermore, 5T4 has been reported to be involved in the functional expression of CXCR4 leading to CXCL12-medaited chemotaxis in tumour cells, which has been associated with tumourigenesis in many cancers (109, 110). Human $CD4^+$ and $CD8^+$ T cells recognising HLA-restricted 5T4 peptides have been identified in healthy individuals using peptide-pulsed DCs and monocyte-derived DCs infected with replication defective adenovirus encoding 5T4 to stimulate peripheral blood lymphocytes (111–113). More importantly, 5T4-specific T cells in colorectal cancer (CRC) patients have been associated with better prognosis (114, 115). Thus, the selective pattern of 5T4 expression and involvement with cancer spread, in addition to the presence of 5T4-specific T cells in humans and its correlation with better prognosis, have lend 5T4 as a valuable target for anti-cancer therapies aiming at inducing and/or enhancing tumour-specific T cell responses.

1.2.4.2 NY-ESO-1

NY-ESO-1 belongs to the group of cancer-testis antigens and was first identified in 1997 using SEREX technology (116). It is expressed in a variable proportion of a wide range of human cancers including melanoma, ovarian cancer, breast cancer, prostate cancer and hepatocellular carcinoma (117–120); while its expression in normal tissue is restricted to the germ line cells (spermatogonia) in the testis (119). The expression of NY-ESO-1 has been shown to correlate with aggressive ovarian cancer (120). NY-ESO-1 has a strong spontaneous immunogenicity in humans, inducing both

cellular and humoral responses (121–123). Notably, adoptive transfer of genetically engineered lymphocytes reactive to NY-ESO-1 improved the clinical response rates and overall survival of patients with metastatic melanoma and synovial cell sarcoma (124, 125), suggesting that NY-ESO-1-specific T cells mediate anti-tumour effects. Although its function remains unknown, the exceptional immunogenicity of NY-ESO-1 and association with anti-tumour activity, together with its extensive distribution among many cancer types, make it a very good vaccine candidate with the potential to be used in vaccines against many types of cancers.

1.2.5 Tumour infiltrating immune cells

The correlation between tumour infiltrating immune cells and improved prognosis for numerous cancers has been established for many years now. In 1931, an American oncologist made the observation that excised tumours with greater immune cell infiltrates led to an improved post-operative survival (126). But it was not until 1989 when the first study formally identifying the positive correlation between tumour infiltrating lymphocytes (TILs) and favourable patient prognosis was published (127). This study was carried out in melanoma patients and reported that patients with high levels of $CD8^+$ T cell infiltration had an 8-year survival rate of 88.5% compared to 59.3% in patients with a sparse or absent immune cell infiltration. Since then, multiple studies have reported similar observations in other types of cancer such as colorectal (128), oesophageal (129), ovarian (130), breast (131), lung (132), head and neck (133) and prostate (134) carcinomas.

Though the presence of immune cells within the tumour is of clinical relevance, further studies have revealed that their phenotype and activation status is as important. Enhanced survival is associated with certain subsets of T cells, such as $CD8^+$ and T_H1 cells, at the tumour site (129–132, 135–137); while tumour infiltration by other immune cells, such as macrophages and Tregs, have been shown to have a negative impact

on patient survival (138–140). However, there has been some discrepancies concerning the significance of Tregs in tumours – some groups have found a correlation between the presence of this cell type and poor prognosis in colorectal, ovarian, pancreatic and hepatocellular carcinoma (138, 141–143), while the contrary has been reported for follicular lymphoma, Hodgkin's lymphoma and, in some studies, with colorectal cancer patients (144–147). The reasons for the different outcomes in colorectal cancer are not clear, but might be due to the methodology used to quantify Tregs (e.g. immunohistochemistry or flow cytometry) or tumour stage (e.g. early or late) (148).

1.2.5.1 Tumour-specific T cells

Although tumour cells express antigens that can be recognised by T cells and these have the potential to counteract cancer progression, challenges exist that often result in the inability to control the disease. Since the majority of tumour-associated antigens are self-proteins, the T cells expressing high-affinity TCRs specific for those antigens are usually deleted in the thymus during negative selection (central tolerance) (refer to section 1.1.1), or rendered inactive in the periphery (peripheral tolerance) (149). Nevertheless, self-tolerance mechanisms are 'leaky', allowing survival of low affinity self/tumour-specific T cells (150). This results in low numbers of self/tumour-specific T cells bearing low affinity TCRs, limiting the efficacy of anti-tumour T cell responses (151, 152). In addition, the process of antigen presentation is impaired in the tumour microenvironment, leading to insufficient priming and boosting of T cells (153). Furthermore, TILs have been reported to show a phenotype that resembles that of T cell exhaustion defined in chronic viral infections. TILs expressing elevated levels of multiple co-inhibitory receptors, such as programmed cell death protein 1 (PD-1), cytotoxic T lymphocyte antigen-4 (CTLA-4), lymphocyte activation gene-3 protein (LAG-3) and T-cell immunoglobulin domain and mucin domain protein 3 (TIM-3), have

been observed in several human cancers, including in melanoma, ovarian cancer and chronic lymphocytic leukaemia (154–157). These cells often have impaired effector cytokine production (e.g. IFN-γ, TNF-α and IL-2) (154–156, 158) and cytotoxic activity (157). In addition, transcriptional profiling of MART-1-sepcific $CD8^+$ T cells in metastases from melanoma patients showed a very similar exhaustion profile to LCMV-specific T cells (159). This suggests that T cell dysfunction in cancer limits the effectivity of TILs to counteract tumour cells, resulting in disease progression. Deciphering the mechanisms mediating T cell dysfunction in tumours will be important for the design of effective immunotherapies.

1.3 Cancer Immunotherapy

The first insights of the potential of manipulating the host's immune system to target tumours dates to 1893 when an American oncologist, William Coley, reported that cancer regressed when patients received a mixture of attenuated cultures of *Streptococci* (known as Coley's toxins) (160). Since then our knowledge regarding the molecular and cellular role of the host's immune system in tumourigenesis, in addition to our understanding of tumours evading immune-surveillance, has significantly increased. This has led to more informed attempts to target tumours via immunotherapy focusing on increasing the quality and quantity of effector immune cells, discovering additional protective tumour-specific antigens and overcoming the immunosuppressive environment at the tumour site.

Various approaches have been explored to achieve these objectives and will be described below in more detail: (i) adoptive transfer of *in vitro* expanded natural arising or genetically engineered tumour-specific lymphocytes; (ii) therapeutic administration of monoclonal antibodies to target and eliminate tumour cells (e.g. directed to CD20 on leukaemia and lymphoma cells and against HER2 on breast cancer cells); (iii)

approaches that inhibit molecular or cellular mediators of cancer-induced immunosuppression (e.g. anti-CTLA-4 and anti-PD-1); (iv) vaccines to elicit strong tumour-specific immune responses.

1.3.1 Adoptive T cell therapy

Adoptive T cell therapy (ACT) was initially described in 1988 (161) and since then it has become the most powerful immunotherapeutic strategy to treat patients with metastatic melanoma, revealing great efficacy in clinical trials with an objective response rate between 40% and 70% (162–164). ACT involves the identification and isolation of TILs with anti-tumour activity from the patient, their expansion *in vitro* via co-culture with patient's tumour in the presence of IL-2 and the transfer of these cells back into the patient (Figure 1.2A). Before infusing the expanded tumour-specific T cells, the patient is usually treated with chemotherapy or irradiation for a short period of time to eliminate Tregs and MDSCs, which have immunosuppressive activities that can significantly interfere with the anti-tumour activity of the infused lymphocytes; and eliminate other lymphocytes that can compete with the transferred cells for growth promoting cytokines such as IL-7 and IL-15 (162, 163, 165, 166). Likewise, IL-2 can also be administered along with the expanded cells to improve their survival since the persistence of the transferred lymphocytes correlates with cancer regression in patients receiving ACT (163, 166, 167). However, the success of ACT using autologous TILs only seems feasible in patients with melanoma due to its higher immunogenicity that naturally gives rise to high levels of tumour-specific TILs compared to other types of cancer.

Over the years, ACT has improved to be able to target other types of cancer where cells with anti-tumour activity are rarely identified. This involves the generation of genetically modified T cells using a retroviral or lentiviral vector to insert genes for high affinity TCRs (168) or genes encoding molecules that increase their anti-tumour activity

(Figure 1.2B). The latter may include genes encoding cytokines such as IL-2 and IL-15 (169, 170), enabling tumour-specific T-cells to generate their own growth-promoting cytokines; genes encoding for co-stimulatory, anti-apoptotic or trafficking molecules such as CD80, Bcl-2 and CD62L (166, 171–173), respectively; and introduction of telomerase, which prevents telomere shortening, enhancing proliferative potential of the cells transferred (174). Clinical trials have shown that measurable responses can be achieved using genetically engineered T cells in cancers other than melanoma, including colorectal cancer (175) and synovial cell sarcoma (124). Furthermore, genetically engineered T cells reactive to NY-ESO-1 displayed a good safety profile with improved overall survival in patients with metastatic melanoma and synovial cell sarcoma (124, 125). However, this novel method is still in its early stages and need further exploration as enhanced potency of genetically modified lymphocytes comes with increased risk of toxicity due to healthy cells and organs being recognised and destroyed by the transferred cells (175, 176). An example is a study in which melanoma patients were treated with genetically modified lymphocytes that had genes encoding TCRs recognising MART-1 and gp100 introduced. Although it resulted in up to 30% of the patient exhibiting objective cancer regression, patients also exhibited visual or auditory dysfunction due to the transferred T cells targeting normal melanocytes in the eye and in the ear (176).

Another approach is the development of anti-tumour T cells harbouring chimeric antigen receptors (CAR), where the heavy and light chains of antibodies are genetically fused to intracellular T cell signalling molecules (177). Thus, the lymphocyte gains the ability to recognise cell surface tumour-associated antigens rather than being limited to recognising these on MHC molecules. In addition to proteins, CAR T cells can recognise non-protein surface molecules such as carbohydrates and glycolipids, which can also be uniquely associated with tumours (178). Cells expressing CAR have significantly widened the potential of ACT for cancers other than melanoma. The first

evidence of clinical response using CAR was described for treating patients with neuroblastoma, where administration of T cells expressing CAR targeting the tumour-specific antigen disialoganglioside GD2 resulted in tumour regression (179). Further success of this approach has been reported in a study using CARs directed to CD19 in lymphoma which resulted in tumour regression, although some toxicities were noted, such as hypotension, fever and eradication of B-lineage cells since they also express CD19 (180, 181). A disadvantage of CAR T cells is the requirement of the tumour antigen to be expressed on the cell surface, while TCRs can recognise both intracellular and extracellular processed peptides. Furthermore, many of the antibodies used for CAR design are murine monoclonal antibodies, which could limit their long-term clinical use due to the induction of human anti-mouse antibody immune responses (182). In addition, clinical responses in patients treated with genetically engineered TCRs and CARs have demonstrated the importance of the choice of antigen to avoid toxicity.

Despite its high clinical efficacy, ACT comes with some disadvantages. The process of generating large numbers of tumour-specific T cells is complex, requiring specialised cell production facilities and highly trained laboratory and medical staff. Furthermore, and probably the biggest issue is the fact that ACT is a highly-personalised treatment where a new and different reagent (i.e. tumour-specific T cells) has to be produced for each patient.

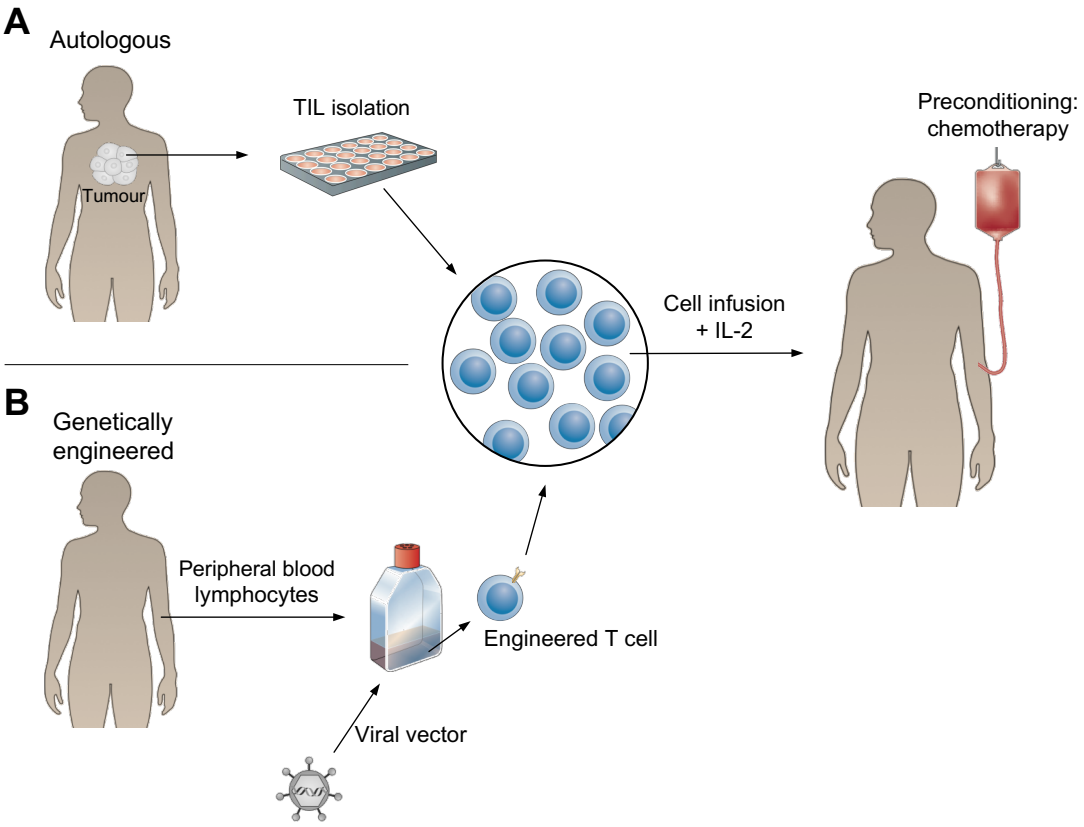

Figure 1.2 Clinical application of adoptive T cell therapy.

Adoptive cell therapy using either **(A)** autologous TILs obtained from resected tumours or using **(B)** peripheral lymphocytes which have been genetically transduced with a retroviral or lentiviral vector to express anti-tumour T cell receptors or CARs. Cells are expanded *in vitro* and infused, along with IL-2, back to the patient after having received a preparative lymphoablation regimen.

1.3.2 Monoclonal antibodies against tumour cells

The administration of tumour-targeting monoclonal antibodies (mAbs) has proven to be a successful form of cancer immunotherapy. The manufactured mAbs can be generated to target a specific antigen with an optimal affinity and to exhibit strong immunogenicity to activate immune mechanisms. The mechanisms of mAb actions include inhibition and neutralisation, where mAbs prevent signalling downstream of their targets; complement-dependent cytotoxicity (CDC), where mAbs activate complement, resulting in direct cytotoxicity via complement pore formation; and antibody-dependent cellular cytotoxicity (ADCC), where mAbs activate immune cells, such as neutrophils and NK cells, via fragment c receptor (FcR) binding (183)

Nine mAbs targeting six tumour-associated antigens have been approved for cancer therapy. Their target and use are described in Table 1.2. Monoclonal antibodies generally have been viewed as being less toxic than chemotherapy agents, however, toxicities have been described. The animal origin of mAbs (e.g. mice) can lead to hypersensitivity reactions, which can be quite severe requiring the discontinuation of the therapy (184). In addition, human anti-mouse antibodies can target therapeutic mAbs, interfering with the therapeutic actions of these agents. This can be overcome by the generation of humanised antibodies generated in transgenic mice. Other toxicities result from the binding of the mAb to its target antigen on healthy tissues. Cetuximab and panitumumab therapy has been reported to cause skin eruption due to the expression of EGFR in skin (185, 186). Targeting HER2 with trastuzumab has resulted in cardiac toxicity because heart tissue express small amounts of this protein (184). Finally, the mAb targeting VEGF, bevacizumab, can induce hypertension, bleeding and thrombosis which is thought to be related to interference with normal VEGF-driven biology (187, 188).

Table 1.2. Therapeutic monoclonal antibodies approved for cancer immunotherapy.

Generic name	Target	Cancer Indication	Ref
Alemtuzumab	CD52	CLL	(189)
Gemtuzumab	CD33	NHL	(190)
Rituximab	CD20	NHL	(191)
Ibritumomab tiuxetan	CD20	NHL	(192)
Tositumomab	CD20	NHL	(193)
Trastuzumab	HER2	Breast cancer	(184)
Cetuximab	EGFR	Colorectal cancer	(185)
Panitumumab	EGFR	Colorectal cancer	(186)
Bevacizumab	VEGF	NSCLC, colorectal cancer, breast cancer, renal cancer and pancreatic cancer	(187, 188, 194–196)

AML – acute myeloid leukaemia; CLL – chronic lymphocytic leukaemia; EGFR – epidermal growth factor receptor; HER2 – human epidermal growth factor receptor 2; NHL – non-Hodgkin's lymphoma; NSCLC – non-squamous non-small cell lung cancer; VEGF – vascular endothelial growth factor.

1.3.3 Immune-checkpoint blockade therapy

In the immune system, there are several key regulators, termed immune-checkpoints (inhibitory signals), that manage the magnitude of the immune response to restore homeostasis. Under normal physiological conditions, these immune-checkpoints are crucial for the maintenance of self-tolerance, preventing autoimmunity; and to protect from damage during infection. However, in the cancer setting, tumours can upregulate the expression of immune-checkpoint proteins to escape from immune attack. Thus, blocking those immune-checkpoint inhibitory signals in order to enhance anti-tumour immune responses is an area of great interest. Indeed, immune checkpoint blockade therapy has been the focus of interest since cancer immunotherapy was selected as Breakthrough of the Year by Science magazine in 2013. Of all the immune-checkpoint inhibitors, CTLA-4 and PD-1 have been the most actively studied for cancer immunotherapy.

The immune checkpoint inhibitor CTLA-4 was the first to be targeted in the clinic. CTLA-4 is expressed on T cells and binds to CD80 and CD86 with higher affinity and avidity than the co-stimulatory receptor CD28, resulting in proliferation and activation arrest (197). Ipilimumab and tremelimumab are two anti-CTLA-4 antibodies that entered clinical testing for patients with advanced melanoma in 2000. But it was not until 2011 when the U.S. Food and Drug Administration (FDA) granted the approval of ipilimumab following two large phase III trials reporting that ipilimumab significantly extended survival in metastatic melanoma (198, 199). Ipilimumab therapy causes toxicities resulting from tissue-specific inflammation and includes enterocolitis, inflammatory hepatitis and dermatitis (200). Tremelimumab is still under investigation in clinical trials along with new CTLA-4-blocking agents.

PD-1 is a receptor expressed on T cell that binds to PD-L1, which is widely expressed by many somatic cells upon exposure to pro-inflammatory cytokines as well as tumour

cells; and PD-L2, which its expression is restricted to APCs (200). Upon binding to its ligand, PD-1 signalling leads to the inhibition of T cell responses. The first evidence that PD-1 blockade could result in anti-tumour activity was described in 2010 in a phase I clinical trial where nivolumab (anti-PD-1 agent) was given to patients with different types of carcinomas resulting in 37.5% objective tumour responses (200, 201). This triggered accelerated clinical trials with PD-1 and PD-L1 blocking agents that resulted in the approval of the first two anti-PD-1 antibodies, pembrolizumab and nivolumab for the treatment of melanoma in 2014, and advanced NSCLC in 2015. Since then the clinical development of anti-PD-1 and anti-PD-L1 as anti-cancer agents has picked up considerable momentum (200). There are currently five anti-PD-1 or anti-PD-L1 antibodies approved by the FDA for a wide range of cancers including melanoma, NSCLC, renal cancer (RCC), hepatocellular carcinoma (HCC), head and neck cancer (HNC), urothelial cancer (UC) and Hodgkin's lymphoma (HL) (200) (Table 1.3). Studies using these agents reported successful outcomes with high objective tumour response rates and a more limited toxicity compared to CTLA-4 blockade (200, 202).

Table 1.3 Immune checkpoint inhibitors approved for cancer immunotherapy.

Generic name	Target	Cancer Indication	Ref
Ipilimumab	CTLA-4	Melanoma	(200)
Nivolumab	PD-1	Melanoma, NSCLC, RCC, HL, HNC, UC and HCC	(200)
Pembrolizumab	PD-1	Melanoma, NSCLC, HNC, HL, UC and GC	(200)
Atezolizumab	PD-L1	UC and NSCLC	(200)
Avelumab	PD-L1	MCC and UC	(200)
Durvalumab	PD-L1	UC	(200)

GC – gastric cancer; HCC – hepatocellular carcinoma; HL – Hodgkin's lymphoma; HNC – head and neck cancer; MCC – Merkel cell carcinoma; NSCLC - non-squamous non-small cell lung cancer; RCC – renal cell carcinoma; UC – urothelial carcinoma.

1.3.4 Immunisation strategies

Most cancer vaccines aim to activate tumour-specific $CD8^+$ T cells as studies have supported their key role in cancer therapy. Cancer vaccines can be optimised by the careful selection of antigens, adjuvants, delivery systems and schedules to generate, amplify and/or skew anti-tumour immunity without the side effects of other less precisely targeted therapies. The development of cancer vaccines can be divided into two groups: prophylactic and therapeutic; which can be further divided into type of vaccine: DNA-, peptide-, DC- and viral- based vaccines.

1.3.4.1 Prophylactic cancer vaccines

Prophylactic cancer vaccines have been used to prevent the chance of tumourigenesis caused by various viral infections. Due to the foreign nature of viruses, the immune system is able to recognise antigens derived from these, thus classic vaccination strategies to induce protective immunity can be used without having to overcome the barriers encountered when targeting sporadic tumours. Currently, there are seven human viruses which have been associated to cancer: hepatitis B virus (HBV), HPV, EBV, human T-lymphocytic virus (HTLV), hepatitis C virus (HCV), Kaposi's sarcoma-associated herpes virus (KSHV) and Merkel cell carcinoma virus (203). To date, there are only vaccines for HBV and HPV, but there are ongoing efforts developing vaccines for HCV, EBV and HTLV.

The first preventive cancer vaccine was against HBV, approved by the FDA in 1981, and it is now part of the scheduled routine vaccination for infants and has resulted in reduced incidence of hepatocellular carcinoma (204, 205). More recently, vaccines against HPV16 and HPV18, consisting of non-infectious viral-like particles containing HPV capsid proteins, have been developed and are commercially available (Gardasil by Merck and Cervarix by GlaxoSmithKline) to prevent cervical cancer, where HPV16

and HPV18 have been associated with 70% of these tumours (206, 207). In a study, vaccination of uninfected women against HPV induced potent anti-viral immunity that prevented viral acquisition, leading to 98% efficacy against the HPV-associated cervical carcinoma (207).

1.3.4.2 Peptide-based vaccines

This type of cancer vaccine uses a short peptide derived from a tumour-specific antigen for immunisation, and aims to activate specific $CD8^+$ T cells that react against self/tumour antigens. Advantages of peptide-based vaccines include that short peptides are simple and cheap to manufacture, and multiple peptides can be given at the same time, targeting several antigens at once (208, 209). Although data from animal models have been promising, reporting the potential therapeutic effect of such vaccines (210–212), clinical benefits of peptide-based cancer vaccines have been disappointing in most trials so far, despite inducing anti-tumour immunity. Tecemotide, a MUC1 vaccine for NSCLC, did not result in a significant difference in overall survival rate in a phase II trial (213). Furthermore, phase II clinical trials of multi-peptides (IMA901) for metastatic renal cell carcinoma (214) and multi-peptides for advanced pancreatic cancer did not show survival benefit either (215).

Improvements have led to the generation of peptide-based vaccines that consist of synthetic long peptides (SLPs) that incorporate both class I and class II epitopes (216). These may cover multiple, overlapping epitopes, therefore not restricting the therapy to patients with specific HLA types. Moreover, in contrast to short peptides, SLPs are not able to bind directly to MHC class I molecules and require uptake and processing by APCs before being presented to T cells. Thus, properly activated APCs will provide the necessary signals, ensuing a strong T cell response. Also, several strategies have been developed to improve the immunogenicity of the administered peptides (reviewed in (217)). For example, by epitope enhancement, where the modification of the amino

acid sequence of the epitope can improve the efficacy of the vaccine by increasing the affinity of the peptide for the MHC molecule (218); increasing the affinity of the peptide-MHC complex for the TCR (219); or inhibiting peptide degradation by serum peptidases (220). In addition, peptide-based vaccines can be delivered along with adjuvants, cytokines, or in combination with other cancer therapies, to amplify and direct the immune response (reviewed in (221)). These have proven to improve immune responses in preclinical and clinical studies (reviewed in (221)).

1.3.4.3 DNA-based vaccines

DNA-based vaccines are being developed to encode tumour-associated antigens in order to mount an immune response against an existing tumour, as well as to encode other immunomodulatory molecules to direct the resulting immune response. Plasmid DNA constructs are easier and less time consuming to generate compared to peptides, and bacterial DNA plasmids possess endogenous adjuvant activity due to the presence of unmethylated CpG dinucleotide motifs that stimulate toll-like receptor (TLR) 9 in mammalian immune cells (222, 223). Such vaccines have shown potent immunogenicity and potential therapeutic effects in several mouse models (224–226). However in human trials, immunisation with naked DNA plasmids were mostly ineffective and minimally immunogenic (227–229). Subsequent studies have investigated various strategies to enhance the potency of DNA-based vaccines: addition of more potent adjuvants, improved delivery techniques (e.g. liposome, electroporation and Gene Gun delivery), and prime/boost regimes (i.e. priming with DNA followed by boosting with a viral-based or protein-based vaccine). The latter has been shown to be quite efficient at inducing more potent responses but further studies are needed to evaluate the effectiveness of this therapy (230).

1.3.4.4 Dendritic cell-based vaccines

A very promising approach in therapeutic cancer vaccines is the use of DCs. Patient's DC precursor cells (i.e. peripheral blood monocytes or haematopoietic progenitor cells) are isolated and differentiated into DCs with the use of cytokines such as granulocyte-macrophage colony-stimulating factor (GM-CSF) and IL-4. These are then loaded with tumour-associated peptides and activated before being infused back into the patient. DC-based vaccines have been evaluated in multiple types of cancer, including melanoma (231), B cell lymphoma (232), AML (233) and renal cell carcinoma (234). These studies have shown that such vaccines are safe, immunogenic and can promote tumour regression in some patients. The limited successful clinical outcome could be, in part, because most of these studies have been performed in cancer patients with advanced disease stage, often with compromised immune system. Thus, DC-based vaccines need to be tested in early-stage cancer patients.

Sipuleucel-T, also known as Provenge, is currently the only DC-based vaccine that has been approved. Sipuleucel-T is a personalised vaccine used for metastatic prostate cancer. It is prepared by culturing the patient's APCs with a fusion protein composed of prostatic acid phosphatase (an antigen found in 95% of prostate cancer) and GM-CSF before being infused back into the patient. Although clinical trials showed no reduction in tumour size or decreased disease progression, it demonstrated an increase in median survival compared to placebo (235, 236), which led to its FDA approval. However, the extent to which this vaccine is based on DCs and not on other constituents has been debated.

Although the results are promising, several limitations have delayed the applicability of DC-based vaccines. Firstly, the generation of DCs is labour intensive, patient-specific and expensive. DCs are very sensitive to experimental manipulation resulting in changes in the activation status and their phenotype. Furthermore, poor survival and migration to the lymph nodes is observed when DC-based vaccines are injected

subcutaneously (237). Hence, a novel strategy involving the *in vivo* targeting of antigens to DCs via the coupling of antigens to antibodies specific for DC surface receptors (e.g. DEC205 and CLEC9A) is being studied. The administration of these vaccines along with DC activators (e.g. TLR3 and CD40 agonists) enables the maturation of DCs and the induction of immune responses (reviewed in (238)). Several studies in mouse models of cancer have provided evidence that this approach induces protective anti-tumour $CD4^+$ and $CD8^+$ T cells (239–242) and is under development for use in cancer patients. Further research is necessary to determine the actual influence of the DC receptor targeted, and thus, the DC subset activated, on shaping the immune response.

1.3.4.5 Viral-based vaccines

The aforementioned cancer immunisation strategies have been marginally effective in clinical trials. However, other approaches, such as viral-based vaccines, are being explored. After the first promising report of a viral-based vaccination strategy using recombinant vaccinia virus (VV) expressing a hepatitis B antigen (243), further viral vectors have been examined (reviewed in (244)). The aim of using viral-based vector vaccines is to induce a protective immune response in the host without establishing viral disease. Such vectors can be engineered to express heterologous antigens and activate $CD8^+$ and $CD4^+$ T cell responses, along with induction of antibodies, without the need of co-administrating exogenous adjuvants (245). A variety of virus-based vaccines exist differing in several characteristics such as cell tropism, genetic carrying capacity, and type, quality and magnitude of immune responses (245). Viruses that are currently in preclinical and clinical stages of development include, but not limited to, adenovirus, poxvirus, lentivirus and alphavirus. Due to safety concerns, current viral-based vaccines use viruses which are either completely replication defective or spread defective and are unable to establish a persistent infection. These vaccines

have been successfully used in controlling diseases such as smallpox (VV), measles (live attenuated measles virus), rubella (live attenuated rubella virus) and a number of other viral diseases (246). Thus, recombinant viral vectors have become an attractive platform to exploit for cancer immunotherapy and some have been tested in advanced phase clinical trials.

1.3.4.5.1 Adenovirus-based vectors

Adenoviruses (Ad) are non-enveloped DNA viruses. The Ad genome is well characterised and permissive of genetic modifications which allows retargeting the virus's tropism to a specific cell in addition to the insertion of exogenous DNA (247). Consequently, it has been used in the fields of vaccination, gene therapy and oncolytic therapy. The gene of interest is often inserted into the E1 locus, rendering the virus replication-deficient. The initial cancer vaccination studies have used replication-deficient variants of serotype Ad2 and Ad5 due to their ability to induce exceptionally strong antibody and $CD8^+$ T cell responses, in addition to the ability to generate high viral titres during the manufacturing process (248). However, their use has been limited by the high levels of pre-existing immunity in humans (specifically, neutralising antibodies), which has led to variable vaccine responses and little therapeutic effects in clinical trials (249, 250). In addition, results from the unsuccessful STEP study, where an Ad5-based vector was tested as a vaccine against HIV, suggested there was a correlation between increased susceptibility to HIV and individuals displaying a higher level of neutralising antibodies against Ad5 (251). Thus, many groups are now exploring the use of Ad that exist at a lower prevalence in the human population (e.g. alternative human Ad serotypes or simian Ad) and/or Ad5 with alterations in the viral capsid in order to overcome the anti-Ad immunity (reviewed in (247)). In addition, simian Ad-based vectors have been tested in pre-clinical models of infectious disease, some of which have progressed to clinical studies where results

have been encouraging (reviewed in (244)). In addition to using Ad-based vectors to drive anti-tumour immune responses, Ads have also been explored as oncolytic viruses and have proven to be a powerful tool in the elimination of tumours via their direct lytic effects (reviewed in (247)).

1.3.4.5.2 Poxvirus-based vectors

Poxviruses are the most broadly studied viral vectors and have a long and successful history in vaccination programs – most notably, VV was used to vaccinate over one billion people against smallpox, leading to its eradication in 1978 (252). In the cancer therapy setting, VV (253–257), fowlpox virus (257, 258) and canarypox virus (259, 260) have been investigated clinically. Although the attenuated Wyeth strain of VV has a good safety profile, modified vaccinia Ankara (MVA) is often preferred due to its reduced replication in primary human cells (261). Similarly, canarypox and fowlpox are unable to productively infect humans because they cannot complete their life cycle to generate virions, but these vectors are less immunogenic than VV and MVA (262). MVA has been used to express the tumour-associate antigen 5T4 in a vector known as TROVAX. TROVAX has been evaluated in patients with metastatic colorectal cancer (263, 264), prostate cancer (265) and renal cell carcinoma (266–268). These studies showed that MVA-5T4 was able to elicit a humoral and cellular response against 5T4, but efficacy of the vaccine was variable and was limited to a slight improvement in patient overall survival.

1.3.4.5.3 Limitations of current viral-based vectors

Recombinant viral vectors frequently show significant anti-tumour activity in pre-clinical animal models that it is not translated to human trials. This could be due to factors such as tolerance to the antigen in humans and the immunosuppressive tumour microenvironment. Furthermore, as it is the case for VV, MVA and Ad5 vectors,

vector-specific limitations include the induction of neutralising antibodies against the vector itself that can restrict successful immunisation and impede their repeated use. In addition, the strong immunogenic nature of the viral vector might 'compete' with the inserted tumour-associated antigen. Both matters can be overcome by the use of heterologous viral vectors expressing the same tumour-associated antigen in a prime-boost regimen. This approach is exemplified by the cancer vaccine PROSTVAC-VF used in patients with prostate cancer. PROSTVAC-VF consists of two recombinant viral vectors, vaccinia and fowlpox virus, carrying prostate-specific antigen (PSA) along with genes encoding the costimulatory molecules CD80, intracellular adhesion molecule 1 (ICAM-1) and lymphocyte function-associated antigen 3 (LFA-3) (269). A phase II clinical trial reported a significant improvement in overall survival in patients receiving the vaccine (30%) than the control group (17%), and longer median survival by 8.5 months (269). Yet, the immune response induced by the fowlpox-based vector is not as robust as with VV, thus needing continuous booster immunisation to maintain T cell responses.

Thus, new viral-based vectors that induce a strong tumour-specific immune response with a single immunisation or that can still elicit an immune response in subsequent boosting vaccinations without being dampened by the host immune system would be advantageous. Furthermore, current viral-based vaccines aiming at inducing a T cell response have used non-persistent vectors that result in an acute effector immune response, which, once the vector is eliminated, develop into T_{CM} cells located in secondary lymphoid tissues. This type of immunisation may not be suitable for inducing a population of cells capable of long-term immune-surveillance, which is necessary in preventing tumour recurrence or metastasis. Instead, a viral-based vector that can induce an T_{EM} response would be beneficial for cancer therapy due to their capability for a rapid response and their localisation in different tissues.

1.3.4.6 Challenges facing cancer vaccines

Despite the success of these vaccines in eliciting tumour-specific T cells, the overall efficacy of therapeutic vaccination against established tumours remain suboptimal, with clinical benefit for patients being described mainly as prolonged survival. One aspect that limits the further development of cancer vaccines is the selection of an appropriate antigen to target and the need to break self-tolerance. Other aspects may be the low numbers of tumour-specific T cell induced and their low avidity for tumour recognition as well as lack of capacity to infiltrate the tumour. In addition, the host tolerance mechanisms including anergy and regulatory T cells, and the immunosuppressive environment within the tumour also prevent tumour elimination by immune cells. As noted above, some recent and relatively successful vaccination approaches have included combination of vaccine elements (e.g. VV vector plus fowlpox vector; or DNA-vaccines followed by viral-based vaccine) and vaccines combined with other cancer immunotherapies such as immune checkpoint blockade. Thus, strategies to reduce tumour-induced immunosuppressive cells after vaccination are also being tested. The development of combinational therapies is challenging as the correct sequence, the appropriate timing of administration and the dosage of the two combined agents need to be studied when designing future clinical studies.

1.4 Cytomegalovirus

1.4.1 Herpesviridae

Human cytomegalovirus (HCMV) is one of the nine recognized herpesviruses that infects humans. Herpesviruses are a large family of DNA viruses with diverse animal hosts including mammals, birds, and reptiles. They have been collectively assigned to the family *Herpesviridae* (270–272). Herpesviruses are divided into 3 subfamilies based on their genome sequence and biological characteristics: *alpha*-, *beta*- and *gamma*- herpesvirinae. The alpha-herpesviruses usually establish latency in sensory nerve ganglia (272) and to date 3 human alpha-herpesviruses have been identified: herpes simplex virus (HSV)-1, responsible for cold sores, HSV-2, responsible for genital herpes, and varicella zoster virus (VZV) causative agent of chickenpox and shingles (272). Beta-herpesviruses display a broader cell tropism and members of this subgroup include HCMV, human herpesvirus- (HHV) 6A and 6B and HHV-7. Gamma-herpesviruses typically establish latency in lymphoid cells and includes the human pathogens KSHV and EBV, responsible for infectious mononucleosis (272).

All human herpesviruses have a relatively large linear double-stranded DNA genome ranging from 125 kbp to 235 kbp enclosed within an icosahedral capsid. This is surrounded by an amorphous layer composed of viral proteins termed the tegument, which in turn is bounded by a lipid bilayer envelope containing membrane-associated proteins and various viral glycoproteins which are responsible for viral entry into host cells (270). Further to the virion structure, human herpesviruses share other biological characteristics – replication and transcription of viral DNA and capsid assembly-occurs in the infected cell's nucleus, production of infectious virions is accompanied by cell lysis and they establish a persistent life-long latent infection within a specific target cell. Latent viral genomes persist as a closed circular episomal DNA in the nucleus with

minimal virus gene transcription, but can reactivate by an environmental cue producing infectious virions that can spread from cell to cell (273).

This thesis focuses on the beta-herpesvirus cytomegalovirus (CMV). CMVs are found across a broad range of mammalian hosts including human, primate and rodents, and have adapted to their respective host over millions of years of co-evolution. For this reason, CMVs are highly species-specific, with no cross-species infection having been reported in the literature. Some CMV species can replicate to a certain extent in cells of closely related species *in vitro*, such as Rhesus CMV (RhCMV) in human epithelial and endothelial cells (274). However, replication in cells of more distant species is generally not possible. CMVs have acquired inhibitors of apoptosis for their host cells, allowing successful replication and subsequent spread within the host and this might be the determinant of species specificity as the virus is unable to inhibit apoptosis in cells of distant species. Indeed, it has been reported that murine CMV (MCMV) infection of human fibroblast activates apoptosis, preventing efficient viral DNA replication and expression of late genes. But infection with a recombinant MCMV expressing the Bcl-2-like protein of HCMV allowed successful MCMV replication in human cells (275, 276). CMVs have the largest genomes of all the members of the *herpesviridae* family, and HCMV is the best studied in terms of pathogenesis and is a major human pathogen that infects a large proportion of the human population.

1.4.2 Human cytomegalovirus

HCMV has the largest genome, of all human viruses with 235kbp (277), encoding at least 167 protein-coding genes, with extensive alternate mRNA splicing, in addition to non-coding RNAs, including microRNAs (273, 278). The HCMV genome has a unique long (U_L) and a unique short (U_S) segment that are flanked by inverted repeat sequences denoted TR_L/TR_S at the termini and IR_L and IR_S at the U_L/U_S junction (Figure 1.3) (279). The terminal repeats contain signals for genome packaging and cleavage

(280, 281). Due to the inverse orientation of the repeated sequences at the junction between the U_L and U_S segments, homologous recombination can occur during replication giving rise to four isomeric genome arrangements that contain the U_L and U_S segments in alternative orientations with respect to one another that appear to package with equal efficiency (282).

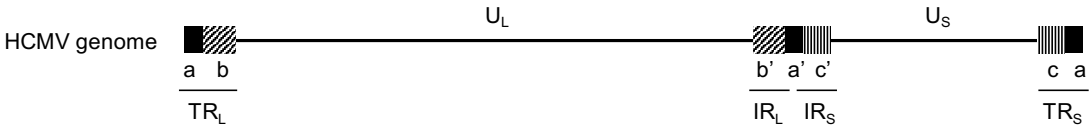

Figure 1.3 HCMV genome structure.

In HCMV, the unique long (U_L) and unique short (U_S) regions are flanked by inverted repeat sequences, denoted TR_L/TR_S at the termini and IR_L and IR_S at the U_L/U_S junction (shown by the solid and striped boxes, inverted sequence are represented by '). Both TR_L/TR_S share a sequences only – b and c sequences differ in the nucleotide sequence.

HCMV has a tropism for a wide variety of cell types such as fibroblasts, hepatocytes, epithelial, endothelial, smooth muscle, neuronal and myeloid cells (monocytes/macrophages and DCs) (283–285). While fibroblasts, endothelial, epithelial, smooth muscle cells and terminally differentiated cells of the myeloid lineage are fully permissive for HCMV infection (286, 287), bone-marrow derived $CD34^+$ progenitor cells and $CD14^+$ monocytes take up virus but do not support productive infection and it is believed that these cells act as sites of latent infection *in vivo* (288–292). The reactivation of latent HCMV in these cells occurs following differentiation into macrophages and DCs (290, 293, 294).

HCMV-infected cells exhibit a characteristic cytopathology with nuclear and cytoplasmic inclusions. In the laboratory HCMV is most frequently propagated in fibroblasts, but extensive passaging in this cell type has led to the accumulation of mutations in a process of adaptation (295). As a result, replication and release of

progeny has improved in fibroblasts, while the ability to infect endothelial and epithelial cells in addition to macrophages and DCs has been compromised (295–297). Consequently, laboratory strains such as AD169 and Towne, are genetically distinct from wild-type strains (277, 298–300). Of the current strains used in research, Merlin is considered to be the most similar to wild-type HCMV due to its limited passage number in fibroblasts before being sequenced (277).

1.4.2.1 HCMV life cycle

HCMV entry into host cells is a complex, multistep process (Figure 1.4). Infection with cell-free virus is initiated with the binding of viral envelope glycoproteins to specific cell surface receptors. This involves glycoprotein B (gB) interacting with cell surface heparan sulfate proteoglycans, in addition to various integrins and to EGFR which promote virus entry (301, 302). Of note, the need of EGFR binding by HCMV for cell entry is controversial – studies have reported that EGFR-negative cells were not susceptible to infection, but this could be reversed by transfecting the cells with a EGFR-expressing plasmid (302); whilst others described no reduction in virus infection efficiency when EGFR was blocked using antibodies (303). Furthermore, the heterodimer formed by glycoprotein H (gH) and glycoprotein L (gL), gH/gL, also has an essential role in virus entry via binding of integrins (304). gH/gL further associates with glycoprotein O (gO) forming a trimer that facilitates HCMV entry into fibroblasts via interaction with platelet-derived growth factor receptor α (PDGFRα) (305–307); or as recently reported, with proteins UL128, UL130 and UL131 forming a pentameric complex that is necessary for infection of endothelial cells (308–311). How these complexes work with gB in virus entry is still unknown. Following receptor binding, the viral envelope fuses with the cellular membrane, either by direct fusion at the plasma membrane (fibroblasts) or with the endosomal membrane after internalisation by receptor-mediated endocytosis (endothelial and epithelial cells), depending on the cell

type (312). This releases the nucleocapsid into the cytoplasm which translocates to the nucleus where the viral genome is delivered into the nucleus through the nuclear pore complex (313). Simultaneously, tegument proteins are released into the cytoplasm and traffic to specific sites where they perform a wide range of functions such as priming the cellular environment for viral replication and modulating the initial host response to infection (314). Once in the nucleus, the linear viral genome circularises (315) and viral DNA replication and gene transcription occurs. Viral gene expression occurs in a tightly regulated cascade and is divided into three phases based on their time of synthesis after infection: immediate early (IE), early (E) and late (L). IE gene products are regulatory proteins that activate other viral genes. Early gene products are involved in DNA synthesis, capsid maturation, and host immune evasion. Late genes encode viral structural components for virion maturation and egress from the cell (316).

In the nucleus, HCMV DNA replication occurs by the rolling circle mode of replication where viral DNA replication occurs unidirectional producing a continuous DNA molecule that contains multiple copies of the viral genome linked in series, known as concatamers. These are subsequently cleaved into single genome-length copies and packed into individual, preformed capsids (315). Tegument proteins are added to the nucleocapsid as it traffics from the nucleus to the cytoplasm, providing stability during translocation and directing the nucleocapsid to the site of envelopment in the cytoplasm, termed cytoplasmic virus assembly compartment (cVAC) (317). The cVAC is a virus-induced structure composed of modified and rearranged host organelles that support virion maturation and egress from cells. During nuclear egress, nucleocapsids obtain a temporary envelope at the inner nuclear membrane, which is followed by a de-envelopment event at the outer nuclear membrane releasing the nucleocapsid into the cytoplasm (318). At the cVAC, the nucleocapsids acquire remaining tegument proteins and obtain a final viral envelope resulting in the formation of a mature virion

(317). Once formed, mature virions are translocated to the cell surface within small vesicles which are released from the cell by exocytosis. Alternatively, HCMV can spread via direct cell-to-cell transmission (319). Although the mechanism is still poorly understood, a recent study reported the involvement of the pentameric complex gH/gL/UL128/UL130/UL131 in this pathway (320).

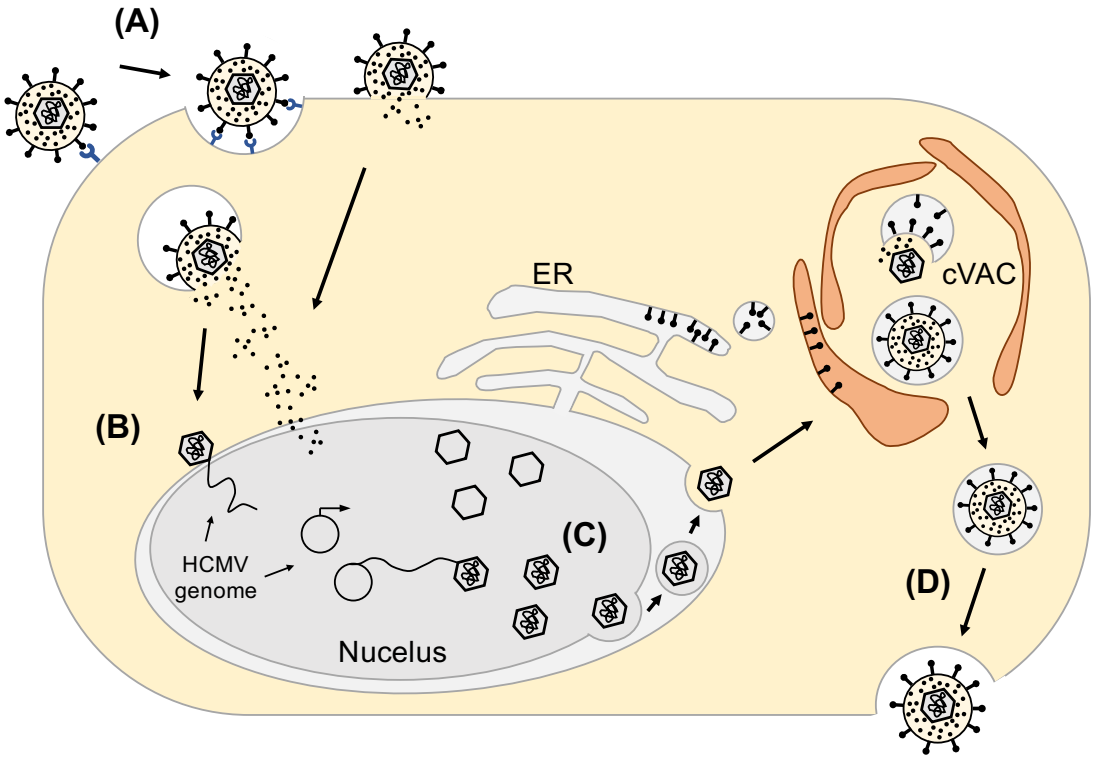

Figure 1.4 HCMV life cycle.

(A) HCMV virions interact with specific receptors at plasma membrane and enters the host cell either through direct fusion with the plasma membrane or through the endocytic pathway. This releases the nucleocapsid and tegument proteins into the cytosol. **(B)** The nucleocapsid is translocated to the nucleus, where the viral genome is delivered and circularised. Tegument proteins modulate host immune response and initiate a cascade of viral gene expression – IE genes are expressed first, followed by E genes that initiate viral DNA replication and L genes. **(C)** L gene expression initiate DNA packaging and capsid assembly in the nucleus, followed by nuclear egress. The nucleocapsid traffics to the cytosolic virus assembly compartment (cVAC) where it acquires tegument proteins and a viral envelope. **(D)** The mature enveloped virion is released by exocytosis at the plasma membrane.

1.4.2.2 Pathogenesis of HCMV

HCMV has a prevalence of 40-100% of the population depending on the geographical location and socioeconomic status (273). After primary infection, HCMV is shed for months to years, depending on age, in bodily secretions such as saliva, urine, semen and breast milk (273). HCMV is transmitted through direct contact with the infected fluids and frequently occurs in organ transplantations, blood transfusions, during sexual contact, and in the context of childcare. An additional route of transmission is through the placenta during pregnancy, or via contact with infected maternal genital secretions during delivery (i.e. congenital infection) (273). HCMV is generally asymptomatic in immunocompetent individuals but can cause severe disease and sometimes death in immunocompromised patients such as HIV-infected persons, organ transplant recipients and those with hereditary severe combined immunodeficiency, in addition to the immunologically immature (new-born infants) (321, 322).

HCMV is the most common intrauterine infection, affecting approximately 0.6% of life births in developed countries (323). Congenital HCMV can manifest in a wide range of symptoms including hearing loss, visual impairment and intellectual disability (321). Symptomatic congenital infection at birth is estimated to account for approximately 10% of the cases, and approximately 14% of those with asymptomatic infection develop symptoms during the first 5 years of life (323–325). Maternal immunity against HCMV from women exposed to the virus prior to pregnancy provides some protection against damaging HCMV infection in the new-born compared to women experiencing primary infection, however, it does not prevent the acquisition of HCMV by the developing foetus (321, 326, 327). Overall, it is predicted that approximately 0.5% of all congenital HCMV infections result in death and that 17-20% of surviving children develop permanent neurological sequelae (325).

HCMV is considered an opportunistic pathogen in immune-compromised/ immune-suppressed individuals where their adaptive immune response is compromised and have a reduced ability to respond to primary infection. Furthermore, these individuals are at high risk of reactivation of latent HCMV. Clinical manifestation of HCMV infection in this group includes hepatitis, retinitis, colitis and pneumonitis (328). Over 75% of solid organ transplant patients become newly infected with HCMV or reactivate latent virus after transplantation. This has been associated with allograft rejection and increased morbidity and mortality (329, 330). Most HIV-infected individuals are positive for HCMV and several studies have shown a positive correlation between quantity of HCMV and enhanced progression of HIV disease (331). Clinical manifestations of HCMV disease in this cohort of patients include retinitis, gastroenteritis, encephalopathy and polyradiculopathy (328).

HCMV disease can be treated with the antiviral drugs ganciclovir, cidofovir and foscarnet, but are associated with adverse reactions and toxic effects (332). Furthermore, therapeutic effectiveness of these drugs is frequently compromised by the emergence of drug-resistance strains (332). Hence, their use is limited to patients who are at risk for serious disease.

1.4.2.3 Immune response to HCMV

Primary HCMV infection is controlled by both the innate and adaptive immune system. HCMV infection triggers the activation of TLR2, TLR3 and TLR9 and other pattern recognition receptors (PRRs) (333–335). This leads to the production of type I IFNs and inflammatory cytokines (e.g. TNF-α and IL-6) which recruit and activate phagocytes and APCs. Furthermore, type I IFNs induce an 'antiviral state' in cells via the induction of ISG which exert numerous functions to limit viral replication and contribute to host defence (336). NK cells are also recruited to the site of infection where they eliminate infected cells via perforin-mediated cytolysis or via expression of

TNF-related apoptosis-inducing ligand (TRAIL) (337). In addition, NK cells can stimulate the infected cell to produce IFN-β which acts in an autocrine fashion; and in combination with NK cell-produced IFN-γ, inhibit virus replication (338, 339). Moreover, the importance of NK cells in the immediate control of viral infection is highlighted by the severe HCMV disease outcome seen in an NK-deficiency setting (340), in addition to the extensive immune evasion mechanisms that HCMV encodes to prevent NK cell activation (reviewed in (341)). Further HCMV-encoded proteins are designed to disrupt antigen presentation and subsequent activation of the adaptive immune system via the downregulation of MHC class I and II molecules (342–347). Additionally, infected DCs undergo apoptosis (287). Despite this, infected macrophages are still able to efficiently induce T cell activation by presenting viral antigens (348) and uninfected DCs can phagocytise infected apoptotic cells and cross-present viral antigens to T cells (349–351). This serves as a link between innate and adaptive immunity, where a sustained adaptive immunity is crucial in maintaining long-term control of HCMV. Although the contribution of the humoral arm of the immune system in controlling HCMV has been debated, there is evidence supporting a role for humoral immunity in the defence against HCMV by restricting viral dissemination and limiting the severity of the disease. The major targets for neutralizing antibodies include envelope glycoproteins (e.g. gB, gH/gL and gM/gN), structural tegument proteins (e.g. pp65 and pp150), and non-structural proteins such as IE1 (352–354). Pre-existing anti-HCMV maternal antibodies prior to conception can confer protection to the foetus *in utero* (321).

T cell immunity is necessary to limit HCMV viral replication and prevent disease, however it does not eliminate the virus or prevent transmission (355). Virus-specific $CD8^+$ T cells are crucial in controlling HCMV during primary infection and reactivation (355–358). In addition, there is increasing evidence that $CD4^+$ T cells are also important in the control of HCMV infection. Immunocompetent children who have recently acquired HCMV have heightened viral shedding in urine and saliva compared to adults,

and is associated with reduced numbers of CMV-specific IFN-γ^+ $CD4^+$ T cells (359). Furthermore, low levels of CMV-specific $CD4^+$ T cells significantly correlates with increased frequency of HCMV-related disease in lung transplant recipients (360). A defining immunological hallmark of HCMV infection includes the extremely large proportion of CMV-specific T cells present in HCMV seropositive individuals, with approximately 10% of the $CD4^+$ and $CD8^+$ T cell memory compartment in the peripheral blood being specific for CMV (361). These HCMV-specific responses accumulate in the host with age, a phenomenon termed memory inflation (362–364). Unlike in some chronic viral infections such as hepatitis C where sustained stimulation leads to virus-specific T cell 'exhaustion', HCMV-specific $CD8^+$ T cells retain a phenotype associated with T_{EM} cells and remain functional (365, 366).

1.4.3 Murine cytomegalovirus – a model for HCMV-inducing immune responses

Due to the strict host specificity of CMV, HCMV can only be studied in humans, which has limited the understanding of many aspects of HCMV biology to extrapolation of *in vitro* findings. Investigations of CMV *in vivo* have been performed using animal models such as in primates (e.g. chimpanzee and rhesus macaque) and rodents (e.g. mouse, rat and guinea pig). Although primate CMVs are the most closely related to HCMV, the use of primates are costly and have strict ethical and logistical limitations (367). Therefore, rodent CMVs have been used as an alternative. Among these, MCMV is the most widely used model and has served a major role in the study of CMV biology.

Like HCMV, MCMV is a beta-herpesvirus member of the *Herpesviridae* family. It is a double stranded DNA virus that has a 230 kbp genome in a single long unique sequence with short direct repeats at either end (368, 369). MCMV genome is predicted to contain 170 genes with approximately 45% homology with the HCMV

genome and 78 shared open reading frames (369). There are two MCMV strains commonly used in research – Smith and K181. MCMV Smith strain was originally isolated in 1954 from the salivary gland tissue of laboratory mice infected with a wild-type isolate (370). MCMV K181 is a variant of the Smith strain isolated from salivary glands of mice after serial passage *in vivo* (371). The K181 strain has been described as a more virulent variant and has been reported to replicate to higher titres *in vivo* (371).

Further to genome similarities, MCMV and HCMV share many other features. MCMV can cause severe disease or lethality in immunologically immature and immune-deficient mice, resulting in symptoms mimicking that of humans (e.g. pneumonitis, hepatitis and retinitis) (372–375). Moreover, as with HCMV, MCMV can infect a variety of haematopoietic and non-haematopoietic cells with epithelial, endothelial and mature myeloid cells being significant sites of virus production (376). MCMV transmission is similar to HCMV, via shedding into bodily fluids such as saliva and breast milk (377). A notable difference between MCMV and HCMV is the fact that MCMV is not able to cross the placenta to infect the embryos. However, methods for intra-placental infection of embryos and models of congenital infection have been developed involving direct inoculation of MCMV into the central nervous system or uterus (378–380).

1.4.3.1 Immune responses to MCMV

Activation of the immune system during primary MCMV infection resembles that of HCMV. MCMV activates similar TLRs in DCs and macrophages as HCMV (e.g. TLR3, TLR7 and TLR9) (381–383) that result in a strong production of type I IFNs and other pro-inflammatory cytokines such as IFN-γ, TNF-α, IL-6, IL-1, IL-12, IL-18 and IL-15 (384–386), which recruit leukocytes to the site of infection. Similar to HCMV infection, NK cells play an important role in the defence against MCMV during the early stages

of infection (day 4-5 post-infection (p.i)) as demonstrated in various studies where NK cell depletion and adoptive transfer have resulted in increased susceptibility and resistance, respectively, to MCMV (387–389). In addition, similarly to HCMV, antibodies directed against MCMV are not essential for the control of primary MCMV infection (390), but it is thought be involved in limiting virus dissemination after reactivation (391).

1.4.3.1.1 T cell responses to MCMV

$CD8^+$ T cells play an important role, although dispensable, in controlling MCMV infection in most organs with the exception of the salivary glands (392). Depletion of $CD8^+$ T cells during acute MCMV infection results in a compensatory increased antiviral activity of NK cells and $CD4^+$ T cells (392, 393). $CD4^+$ T cells have an important role in controlling primary MCMV infection in the salivary glands via the secretion of IFN-γ (394–396). The absence of MHC class I molecules on infected acinar glandular epithelial cells due to viral immune evasion, along with the lack of cross-presenting APCs in the salivary gland, prevent the activation of local MCMV-specific $CD8^+$ T cells in this tissue (396, 397). Thus, viral control is confined to the $CD4^+$ subset. Interestingly, $CD4^+$ T cells are not necessary for the generation of MCMV-specific $CD8^+$ T cells during acute infection (394, 398), but are involved in supporting inflationary MCMV-specific $CD8^+$ T cell responses (398, 399).

Memory inflation

Like HCMV, MCMV induces memory inflation, and it was in the mouse model of CMV where this phenomenon was first described by Karrer *et al.* in 2003. (400). The mouse model of CMV has served as an important tool in the investigation of the mechanisms underlying memory inflation. In mice, not all MCMV-specific $CD8^+$ T cells induced during the acute response expand overtime. Some MCMV epitope-specific $CD8^+$ T cell responses contract rapidly after acute infection and develop into stable low frequency

long-term memory or become undetectable and are termed ‘non-inflationary’ epitopes (in C57BL/6 mice: M45, m141 and M57; in BALB/c mice: m04, m18 and M45) (401–405). These cells exhibit a typical central memory phenotype (405). On the contrary, ‘inflationary’ epitopes (in C57BL/6 mice: IE3, M38 and m139; in BALB/c mice: pp89 and m164) (401–405) increase overtime with some remaining at high frequencies, displaying an effector memory phenotype (405). As in humans, inflationary MCMV-specific $CD8^+$ T cells represent 10-20% of the total $CD8^+$ T cell compartment in the blood (400, 401) and can be found in diverse lymphoid and non-lymphoid tissues. Inflation of CMV-specific $CD4^+$ T cells has been observed in humans, but in the mouse model MCMV-specific $CD4^+$ T cells seem to undergo less pronounced inflation and so far only m09-specific $CD4^+$ T cells in C57BL/6 mice have been described (406, 407). Similarly to HCMV, despite the persistent nature of MCMV, inflationary MCMV-specific T cells retain their functionality, including proliferative capacity, cytotoxicity and cytokine secretion; and do not show features of exhaustion (e.g. PD-1 expression, loss of cytokine production) as observed with certain chronic viral infections, such as during LCMV infection (408, 409).

The mechanism driving memory inflation is still unclear, however, evidence suggests it is a consequence of low-level persistence of antigen due to sporadic viral reactivation events, leading to repeated antigen stimulation (410, 411). These inflationary $CD8^+$ T cells have been identified as short-lived effector cells, with a half-life of approximately 1-2 months, which are constantly being replaced by new effector cells that differentiate from a pool of memory cells with higher proliferative capacity established early in infection (408). In addition, it has been recently reported that intraperitoneal infection with a spread-defective single-round MCMV does not impair the development of memory $CD8^+$ T cell inflation, suggesting that once infection is established full viral reactivation, such as the production of new infectious virions, is not a prerequisite, and only the presence of latent virus is sufficient to drive inflation (410). Furthermore, data

from recent studies suggest that memory inflation is dependent on antigen presentation by latently infected non-hematopoietic cells in which these cells directly re-stimulate inflationary memory $CD8^+$ T cells inducing their expansion and differentiation into effector cells (411–413). This is consistent with the increasing evidence that non-hematopoietic cells are a major site of MCMV latency (412–414). In relation with the above idea, in addition to cross-presentation via APCs during latency is not necessary for maintaining memory inflation (412, 413, 415), a recent study reported that non-inflationary MCMV-specific $CD8^+$ T cells displayed a higher immunoproteasome dependence compared to inflationary MCMV-specific $CD8^+$ T cells (416). The immunoproteasome is constitutively expressed in APCs such as macrophages and DCs, while in non-immune cells it is only transiently induced by IFN-γ (417). Consequently, during MCMV latency, infected non-hematopoietic cells would only process proteins through the conventional constitutive proteasomes. In addition, the co-stimulatory receptors 4-1BB and OX40 expressed on T cells after activation have also been shown to contribute to MCMV-specific $CD8^+$ T cell inflation (418, 419). Interestingly, only $CD8^+$ T cells specific for certain MCMV epitopes undergo memory inflation, but this is not well understood yet. Current evidence suggests that the kinetics of gene expression during viral reactivation could determine which T cell specificities undergo inflation – memory inflation of a HSV-1 epitope was observed only when the peptide was fused to the end of MCMV *ie2* and not to *M45* (420). However, other criteria, such as epitope processing, protein half-lives and peptide affinity for MHC molecules, must also be involved since a single MCMV protein can contain epitopes that drive memory inflation as well as those that do not (401, 421).

1.4.4 Cytomegalovirus as a vaccine vector

The interest to explore CMV as a viral vector stems from the observation that CMV induces robust effector memory T cell responses that are widely distributed throughout the body (refer to sections 1.4.2.3 and 1.4.3.1.1). Furthermore, the ability to super-infect individuals with pre-existing CMV immunity (422), along with the ease of engineering recombinants expressing multiple antigens, make CMV a very attractive vector for vaccination strategies.

The potential of CMV-based vaccines was initially established by the ability of RhCMV expressing simian immunodeficiency virus (SIV) antigens (RhCMV-SIV) to induce an immune response against SIV in rhesus macaques. Regardless of pre-existing RhCMV immunity, macaques could be immunised with RhCMV-SIV and develop SIV-specific $CD4^+$ and $CD8^+$ T cell responses that predominantly exhibited an effector memory phenotype, which could be detected for more than 3 years post-immunisation (423). A subsequent study compared the phenotype of SIV-specific T cells responses using the RhCMV-SIV vector and traditional DNA prime-Ad5 boost immunisation. Both immunisation strategies induced SIV-specific $CD4^+$ and $CD8^+$ T cells to similar magnitudes by day 400 post-vaccination (424). In contrast to the T_{EM} phenotype induced by the RhCMV vector, DNA-Ad5 immunisation induced T cells that exhibited predominantly a T_{CM} phenotype (424). At day 400 after initial immunisation, macaques were challenged with SIV_{MAC239}. Macaques receiving the RhCMV-SIV vector controlled SIV infection and approximately 50% of animals were protected for over a year, which correlated with the magnitude of $CD8^+$ T_{EM} cells induced. In contrast, all DNA-Ad5-vaccinated macaques manifested progressive infection, although with reduced mean plasma viral load compared to un-vaccinated macaques (424). Recently, a similar study using RhCMV expressing *Mycobacterium tuberculosis* (Mtb) antigens (RHCMV-TB) reported that subcutaneous administration of the vector induced circulating Mtb-specific $CD4^+$ and $CD8^+$ T_{EM} cells (425). Upon intrabronchial

Mtb challenge a year after immunisation, 68% of vaccinated animals displayed reduced pulmonary Mtb-induced disease compared to unvaccinated controls (425). Furthermore, the use of CMV as a vaccine vector has also been demonstrated in the mouse model of CMV – several studies using recombinant MCMV constructs have shown protective immunity against a variety of pathogens and toxins, inducing the accumulation of T cells reactive to peptides derived from heterologous antigens. The protective immunity has been demonstrated in tetanus (426), HSV (420), vaccinia (427), Ebola virus (428) and *Mycobacterium tuberculosis* (429) challenge models in mice.

Unlike the pathogens aforementioned, tumour-associated antigens are usually self-antigens and non-immunogenic, and tolerance mechanisms make it harder to generate efficient anti-tumour immune responses. However, a study using recombinant MCMV expressing the self ovarian antigen zona pellucida 3 (ZP3) reported that a single dose of the vector was able to break tolerance and induce an immune response against ZP3 , rendering the immunised mice infertile (430). Subsequently, studies describing the protective efficacy of MCMV-based vectors expressing tumour-associated antigens have emerged. The first encouraging study describing tumour protection by an MCMV vector was in 2012 by Klyushnenkova *et al*. (431). They reported that MCMV expressing the human prostate antigen, PSA, induced $CD8^+$ T cell responses in 'humanised' mice that inflated with time (431). Upon tumour challenge, immunised mice had delay of tumour growth (431). Another MCMV vector expressing the melanoma antigen mouse tyrosinase-related protein 2 (TRP2) prevented tumour outgrowth in a mouse model of melanoma (B16) with a single immunisation, regardless of pre-existing CMV infection (432). Notably, it conferred long-term protection – five months after a single dose, mice were still protected from tumour challenge (432). A more recent study reported an MCMV vector expressing the tumour-associated antigen gp100 containing a mutated epitope, which could induce a potent anti-tumour

$CD8^+$ T cell response that was detected 10 months after a single immunisation (433). In addition, gp100-specific $CD8^+$ T cells could be elicited despite prior MCMV infection. Furthermore, both prophylactic and therapeutic immunisations with the vector protected mice from intravenous B16 tumour challenge (433).

The above vaccination studies carried out in the mouse model were done via intraperitoneal (i.p) administration of the vector. This route of vector administration is not clinically relevant for vaccination strategies, thus other routes, such as subcutaneous (s.c) (as conducted in the rhesus macaques' studies), intranasal (i.n) and/or intramuscular (i.m) immunisations need to be examined in MCMV to examine whether a similar T cell immune profile can be achieved. Furthermore, the use of persistent viral vectors for vaccination rises safety and bioethical concerns due to the potential of transmission between individuals, which could generate pathological immune responses or lead to disease in immune-compromised individuals. The use of attenuated CMV vectors need to be fully explored for their ability to induce a sustained anti-tumour immune response. These will be discussed in more detail in Chapter 5 of this thesis.

1.5 Thesis Hypothesis and Objectives

It is well established that tumour infiltrating $CD8^+$ T cells, in addition to 5T4- and NY-ESO-1-specific $CD8^+$ T cells, have been associated with better prognosis in cancer patients. Efforts have been made to generate new cancer therapies that aim to augment these tumour-specific T cells in the clinic. Viral-based vectors are a promising platform to achieve this as they are naturally immunogenic and can induce a wide range of immune responses. However, current viral-based vaccines expressing tumour-associated antigens have induced modest T cell responses that have resulted in minimal clinical benefit. In addition, these T cell responses have been described as transient, rendering them ineffective against metastasis. Hence, new viral vectors, such as CMV which induces a robust, long-lasting $CD8^+$ T_{EM} cell response have the potential to overcome the limitations observed with current viral-based cancer vaccines.

I hypothesise that CMV-based vectors engineered to express tumour-associated antigens may be immunogenic and afford protection from tumour development.

To test this, in this thesis I will be using the mouse model of CMV to address the following objectives:

1. Generate MCMV-based vectors expressing the tumour-associated antigens 5T4 and NY-ESO-1;

2. Examine the immunogenicity and efficacy of MCMV-based vectors expressing 5T4 and NY-ESO-1;

3. Investigate the immunogenicity of MCMV immunisation using a clinically relevant route of delivery in the skin.

Chapter 2 - Materials and Methods

2.1 Buffers, Solutions and Media

Unless otherwise stated, all chemicals used were purchased from Sigma or Fisher, and all tissue culture reagents used were purchased from Gibco, Life Technologies.

D10:	DMEM containing 4.5g/L L-glucose, 10% (v/v) heat inactivated foetal calf serum (FCS) (Invitrogen), 250units penicillin/streptomycin, 0.26mg/mL L-Glutamine, and 97mg/mL sodium pyruvate.
R10:	RPMI, 10% (v/v) FCS, 250units penicillin/streptomycin, 0.26mg/mL L-Glutamine, and 97mg/mL sodium pyruvate.
LB broth:	20g/L of LB low salt broth (Melford) in ddH_2O.
LB Agar:	LB broth, 15% (w/v) agar (Oxoid).
LB Agar + Sucrose:	1% (w/v) tryptone, 0.5% (w/v) yeast extract (Oxoid), 15% (w/v) agar (Oxoid), 5% (w/v) sucrose in ddH_2O.
Ampicillin solution:	100mg/mL ampicillin sodium salt (Melford) in ddH_2O, sterilised through 0.22µm filter.
Chloramphenicol solution:	12.5mg/mL chloramphenicol (Melford) in 100% ethanol.
Kanamycin solution:	15mg/mL kanamycin (Melford) in ddH_2O, sterilised through 0.22µm filter.

Streptomycin solution:	200mg/mL streptomycin sulphate (Melford) in ddH_2O, sterilised through 0.22µm filter.
IPTG solution:	100mM isopropyl1 β-D-1-thiogalactopyranoside (Melford) in ddH_2O, sterilised through 0.22µm filter.
X-gal solution:	40mg/mL 5-bomo-4chloro-3-indolyl β-D-galactopyranoside (Melford) in dimethyle sulfoxide (DMSO).
Sorbitol cushion:	20% (w/v) sorbitol (Acros Organics) in PBS, sterile filtered through a 0.22µm filter.
CMC media:	Autoclaved 4g carboxymethyl cellulose (CMC) in 500mL D10.
Crystal violet solution:	0.1% (w/v) crystal violet in ddH_2O.
PBST:	0.05% (v/v) Tween 20 in PBS.
Blocking buffer:	5% (w/v) fat-free milk proteins in PBST.
Lysis buffer:	150mM NH_4Cl, 10mM $KHCO_3$, 1mM EDTA in ddH_2O.
Digestion mix:	RPMI, 5% FCS, 1mg/mL collagenase D (Roche), 5mM sterile $CaCl_2$, 50µg/mL DNase I (Sigma-Adlrich).
FACS buffer:	2% (v/v) FCS, 0.05% (w/v) sodium azide in PBS.
Saponin buffer:	2% (v/v) FCS, 0.05% (w/v) sodium azide, 0.5% (w/v) saponin (Acros Organics) in PBS.
Dialysis buffer:	1mM $MgCl_2$, 135mM NaCl. 10mM Tris-HCl pH7.8, 10% glycerol in ddH_2O.

2.2 Mice

Female BALB/c and C57BL/6 mice were purchased from Charles River (UK) or Envigo (UK). All studies were performed under the UK Home Office-approved Project Licenses PPL 30/2969, 30/2891, 30/3428, 30/2927 and P7867DADD. All animals were treated according to Home Office regulations and were kept in pathogen-free Scantainer housing at the Home Office designated facility at Heath Park Cardiff University.

2.3 Cells

NIH-3T3 (ATCC CRL-1658), SGC1 (ATCC), LL/2 (LLC1) (ATCC 1642) and T-Rex-293 cells (Life technologies/Invitrogen) were grown in D10. gL-3T3 cells (kindly supplied by Dr. Christopher Snyder, Thomas Jefferson University, USA) were grown in D10 containing 0.5mg/mL G418 (Enzo Life Sciences). CT26 (ATCC 2638) were grown in R10 and CT26-NY-ESO-1 cells (kindly supplied by Prof. Hiroshi Shiku, Mie University, Japan) were grown in R10 supplemented with 0.35mg/mL G418. The cultures were maintained in a humidified incubator at 37°C with an atmosphere of 5% CO_2. For sub-culturing, 70-80% confluent cell monolayers were washed with PBS and incubated with trypsin (Gibco, Life Technologies) for 3-5 minutes at 37°C to detach cells from the flask surface. Subsequently, media was added to inactivate the trypsin. The cells were centrifuged for 5 minutes at 1500rpm, the supernatant discarded and the cell pellet resuspended in the corresponding media. Flasks (150cm^2, Thermo Fisher Scientific) containing the cells were prepared and incubated. T-Rex-293 cells were grown in 'Cell Bind' flasks (Corning) due to them being less adherent. Confluent cells were passaged every 2-3 days and split in a ratio of 1:5 or 1:6.

2.4 Vector Design and Strategy

Recombineering experiment strategies, primers and oligonucleotides design along with sequencing data analysis was performed using CLC MAIN 6 software (CLC Bio). Primers were designed to have a melting temperature of 55-65°C, as well as, where possible, reduced self/pair-annealing or secondary structure formation. All primers and oligonucleotides were obtained from Eurofins Genomics as salt free purified lyophilised DNA. Primers and oligonucleotides were reconstituted in 10mM Tris (Fisher), pH8 to a final concentration of 100μM.

2.5 Recombinant MCMV Vector Construction

A bacterial artificial chromosome (BAC) containing the entire genome of the MCMV K181 strain was provided by Dr. Richard Stanton (Cardiff University, UK) and used to generate the recombinant MCMVs containing the chosen cancer antigen (designated MCMV-antigen) replacing the open reading frame (ORF) of the non-essential *ie2* gene; or fused to the end of the ORF of the *ie1* or *ie3* gene with a P2A linker. Refer to Table 2.1 for the complete list of viral constructs.

Table 2.1 Virus constructs generated.

Virus Construct	Gene	Viral insertion site	Method
MCMV-ΔIE2	*ie2* KO	Delete *ie2* ORF	2.5.1
MCMV-NY-ESO-1	*NY-ESO-1*	Replace *ie2* ORF	2.5.1
MCMV-5T4	*5T4*	Replace *ie2* ORF	2.5.1
MCMV-MIE-5T4	*HCMV-MIEp-5T4*	Replace *ie2* ORF	2.5.2
MCMV-IE1-P2A-5T4	*P2A-5T4*	Fused to *ie1* ORF	2.5.1
MCMV-IE3-P2A-5T4	*P2A-5T4*	Fused to *ie3* ORF	2.5.1
RAd-NY-ESO-1	*NY-ESO-1*	Replace *E1*	2.6

KO – knock out; HCMV – human cytomegalovirus; MIEp – major immediate-early promoter; ORF – open reading frame.

2.5.1 Two-step BAC-based mutagenesis

MCMV-based vectors were generated using a two-step BAC-based mutagenesis (as described in (434)) using a selectable cassette, *neo/lacZα/rpsL*, encoding kanamycin resistance, lacZ, and streptomycin sensitivity genes, respectively.

2.5.1.1 Generation of selectable cassette

The selectable cassette was amplified by polymerase chain reaction (PCR) using primers with overlapping homology of ~20 base pairs (bp) to the cassette and ~80 bp to the target insertion region in the K181 BAC (primer sequences are listed in Appendix I). Fragments were amplified using Roche Expand HiFi kit, which contains a combination of 5'-3' *Taq* DNA polymerase and a 3'-5' proofreading exonuclease for improved amplification yield and fidelity. For each 50μL reaction, the following components were added: 40.5μL double distilled water (ddH_2O), 5μL buffer 2 (containing $MgCl_2$), 1.5μL DMSO, 1μL dNTPs (New England Biolabs), 0.5μL forward primer, 0.5μL reverse primer, 0.5μL template DNA and 0.5μL enzyme. PCR products were synthesised using a T3000 Thermocycler (Biometra) under the following parameters:

1. Incubate at 94°C for 2 minutes
2. Incubate at 94°C for 15 seconds
3. Incubate at 55°C for 30 seconds
4. Incubate at 72°C for 3 minutes
5. Go to step 2 for 34 cycles
6. Incubate at 4°C and pause

The PCR product was then run on a 0.7% agarose gel alongside a sample of HighRanger 1kb DNA ladder (Norgen Biotek Corp.) and visualised using a G:Box gel doc (Syngene), or a bench-top transilluminator (Spectroline). DNA was purified using the Q-Spin gel Extraction/PCR purification Kit (Geneflow). Briefly, the DNA fragment

from the agarose gel was excised using a sharp scalpel and weight. Buffer QC was added in a 3:1 ratio (300μL:100mg), incubated at 50°C until the gel slice was completely dissolved and transferred into a QIAquick spin column. This was centrifuged at 13000rpm for 1 minute, the flow-through discarded, PE wash buffer added to the column and centrifuged again. The QIAquick column was placed into a clean 1.5mL eppendorf and EB elution buffer was added to the centre of the column. The column was left to stand for 1 minute before being centrifuged for 1 minute to elute the DNA.

2.5.1.2 First round of recombineering (Positive selection)

SW102 bacteria transduced to express phage λ Red recombinant proteins and containing the K181 BAC were incubated overnight in 5mL LB containing 12.5μg/mL chloramphenicol in a shaking incubator at 32°C. 0.5mL of the overnight culture was then incubated in 25mL LB containing chloramphenicol until an optical density$_{600}$ (OD_{600}) of approximately 0.6 was reached (Biomate 3 Spectronic, Thermo Fisher Scientific). To make the bacteria competent and activate the λ Red genes, the culture was then incubated in a water bath at 42°C for 15 minutes and then placed on ice for 20 minutes to halt further bacteria growth and ensure they remained competent. The bacteria culture was then centrifuged (4000rpm, 5 minutes, 0°C), the pellet washed twice with ice-cold ddH_2O and then resuspended in ~400μL ddH_2O. 25μL of competent bacteria were added to an eppendorf along with ~3μL PCR product and transferred to a pre-cooled 0.2cm cuvette (Geneflow), left on ice for 5 minutes and then electroporated at 2.5KV (Biorad Micropulser). Bacteria were then recovered in 1mL LB for 1 hour at 32°C in a shaking incubator. 150μL of the recovered bacteria was spread onto an LB agar plate containing 12.5μg/mL chloramphenicol, 12.5μg/mL kanamycin, 80μg/mL X-gal and 0.2mM IPTG and incubated at 32°C for 48-72 hours to select for

bacteria containing the cassette. To check for *rpsL* functionality different blue colonies were picked and streaked onto kanamycin- or 400μg/mL streptomycin-containing LB plates. Also, 5mL of LB media was inoculated with these colonies and incubated overnight at 32°C in a shaking incubator.

2.5.1.3 Miniprep and restriction enzyme digests

For the colonies where the *rpsL* gene was working, DNA was isolated using the QIAprep Spin Miniprep kit (Qiagen). Briefly, the overnight bacteria culture was spun (4000rpm, 5 minutes, 4°C) and the pellet resuspended in P1 buffer. P2 lysis buffer was then added and incubated at room temperature for 5 minutes followed by the addition of P3 neutralisation buffer. This was then centrifuged at 13000rpm for 10 minutes. To precipitate DNA, isopropanol was added, centrifuged at 13000rpm for 10 minutes at 4°C, the supernatant discarded, 70% (v/v) ethanol added and spun at 13000rpm for 10 minutes. The supernatant was then discarded and pellet was left to air dry before resuspending the pellet in 10mM Tris, pH8. Restriction enzyme (RE) digest was performed using *Hind*III (New England Biolabs) by combining 8μL DNA, 1μL buffer and 1μL enzyme, and incubated for 1 hour at 37°C. This mix was loaded and run on a 0.7% agarose gel. Colonies with the correct RE digestion pattern were stored at -80°C as glycerol stocks.

2.5.1.4 Second round of recombineering (Negative selection)

SW102 bacteria containing the *rpsL* cassette were prepared and made competent as described in section 2.5.1.2. PCR products for the human antigens 5T4 and NY-ESO-1 were prepared as described in section 2.5.1.1. To delete the *ie2* ORF, 1μL of an oligonucleotide (Appendix I) with ~50 bp of homology to the left and to the right of the *ie2* coding DNA sequence was used to electroporate competent SW102 bacteria

instead of a PCR product. For inserting *5T4* gene fused to the *ie1* or *ie3* ORF with a P2A linker, a DNA molecule containing the *P2A-5T4* gene with *ie1* overhangs was ordered to be synthesised by Invitrogen. The required DNA fragment was flanked by *Bam*HI RE sites to facilitate its isolation from the plasmid backbone. Consequently, the plasmid containing the *P2A-5T4* gene was incubated with *Bam*HI, run on a 0.7% gel and purified the wanted fragment as described in section 2.5.1.1. 3μL of the purified DNA was used for electroporation. In addition, it was also used as the DNA templated to amplify *P2A-5T4* with *ie3* hangouts (refer to Appendix I for primers), which was then used in electroporation as described in section 2.5.1.2. Following electroporation, the bacteria were recovered in 4mL LB for 3 hours to ensure the rpsL protein was cleared, before being spread onto LB plates containing chloramphenicol, streptomycin, X-gal and IPTG. After 48-72 hours, white colonies were picked and minipreps and RE digest were performed as described in section 2.5.1.3.

2.5.1.5 DNA sequencing analysis

For sequencing, two primers (Table 2.2) were used which read out the gene inserted. Firstly, the region of interest was amplified using primers that bind just beyond where recombination occurred within the BAC. The PCR product was run on a 0.7% agarose gel and the DNA purified as described in section 2.5.1.1. The amplified fragments and primers were prepared as described by SmarSeq Kit (Eurofins Genomics, Germany) and send to sequence. SW102 bacteria containing the correct sequence were stored at -80°C as glycerol stocks.

Table 2.2 Primers used for DNA sequencing.

Primer		Sequence
IE2seq	Forward	ATACTACTGCATGCCCCT
	Reverse	CGCTCGATCCATTCTTCT
IE1seq	Forward	GTACAGAGAATAAAAGAGGGG
	Reverse	TGATGATGAGGTGACCCG
IE3seq	Forward	ACAAGACACAAGTGCTCAA
	Reverse	GACCTGTCTGCATTTGAG
RAd_seq	Forward	AATGTCGTAACAACTCCG
	Reverse	ACCTGATGGTGATAAGAA

2.5.2 En passant mutagenesis

En passant mutagenesis was used to insert a fragment containing the HCMV major immediate-early (MIE) promoter with the human *5T4* gene to replace the *ie2* ORF (as described in (435)). The GS1783 *E. coli* strain was obtained from Dr. Gregory Smith (Northwestern University, USA).

2.5.2.1 Gene fragment for En passant mutagenesis

The DNA fragment containing the HCMV MIE promoter with the *5T4* gene as well as a kanamycin resistance gene was ordered to be synthesised by Invitrogen. The DNA fragment was flanked by *Hind*III restriction sites to facilitated the isolation of the required fragment from the plasmid backbone. Briefly, the DNA was incubated with *Hind*III and *Age*I (New England biolabs) for 1 hour at 37°C before running it on a 0.7% agarose gel. The correct size DNA band was purified from the gel as mentioned in section 2.5.1.1 and stored at -20°C until further use.

2.5.2.2 Transforming K181 BAC into GS1783

SW102 bacteria containing the K181 BAC was grown in LB containing chloramphenicol at 32°C in a shaking incubator overnight. The BAC DNA was isolated as described in section 2.5.1.3. GS1783 bacteria were grown until an OD_{600} of approximately 0.6 was reached as mentioned in section 2.5.1.2. The bacteria culture was washed twice in cold ddH_20 before being transferred to a pre-cooled 0.2cm cuvette along with 3μL of the isolated K181 BAC DNA. Bacteria were electroporated at 2.5KV and then recovered in 1mL LB for 2 hours at 32°C in a shaking incubator. 150μL of the recovered bacteria was spread onto an LB agar plate containing 12.5μg/mL chloramphenicol. Three single colonies were picked and grown overnight in 5mL LB containing chloramphenicol. DNA from these cultures was isolated and RE digest was performed with *Xho*I, *Eco*RI and *Hind*III (all from New England Biolabs) as described in section 2.5.1.3. Bacteria showing matching digestion pattern to K181 BAC were stored at -80°C as glycerol stocks.

2.5.2.3 Recombineering

GS1783 bacteria containing the K181 BAC was grown overnight in LB containing chloramphenicol in a shaking incubator at 32°C. Bacteria were made competent as described in section 2.5.1.2. Competent bacteria were centrifuged at 4000rpm for 5 minutes at 4°C and washed twice in 10% ice-cold glycerol before being resuspended in a total volume of 50μL. 3μL of the purified DNA was added to the competent bacteria and transferred to a pre-cooled 0.2cm cuvette which was then electroporated at 2.5KV. Bacteria were recovered in 1mL LB for 2 hours in a shaking incubator at 32°C. 100μL of the recovered bacteria was plated on an LB plate containing chloramphenicol and kanamycin and incubated for 24 hours at 32°C. Four colonies were picked and grown overnight in LB containing chloramphenicol. DNA was isolated from these bacteria

cultures and incubated with *Hind*III as mentioned in section 2.5.1.3 to identify clones with the correct digestion pattern.

2.5.2.4 Resolution of co-integrates

Bacteria harbouring positive clones were grown in 1mL LB containing chloramphenicol in a shaking incubator at 32°C for 2 hours. 1mL of pre-warmed LB containing chloramphenicol and 2% (w/v) arabinose was added to the culture and incubated for an additional hour. The bacteria culture was transferred to a 42°C water bath for 30 minutes and then returned to the 32°C shaking incubator for 2-3 hours. The OD_{600} was measured at this point; 10μL of a 1:100 ($OD_{600} \leq 0.50$) or a 1:1000 ($OD_{600} > 0.50$) dilution was plated onto LB agar plates containing chloramphenicol and 1% (w/v) arabinose and incubated at 32°C for 24-48 hours. Four colonies were picked, the DNA isolated and RE digest performed as in section 2.5.1.3 to check for correct BAC pattern. Positive clones were sent to sequence as described in section 2.5.1.5 and bacteria with the correct DNA sequence were stored at -80°C as glycerol stocks.

2.6 Recombinant Adenovirus Vector Construction

A BAC containing the entire genome of the adenovirus serotype 5 was provided by Dr. Richard Stanton (Cardiff Univeristy, UK). This is a replication-deficient vector with the *E1* and *E3* regions deleted. In place of the deleted regions, the vector provided had an HCMV MIE promoter, followed by a selectable cassette occupying the transgene insertion site, and an HCMV MIE polyadenylation sequence. This BAC was used to generated the recombinant adenovirus (RAd) containing *NY-ESO-1* replacing the selectable cassette. In this case, the selectable cassette contained an ampicillin resistance, lacZ and sucrose sensitivity gene, *amp^r/lacZα/sacB*. The same method of recombineering as in section 2.5.1 was used though instead of using kanamycin and

streptomycin LB plates, ampicillin and sucrose LB plates, respectively, were used to select for and against the cassette.

2.7 Reconstitution and Growth of BAC-derived Viruses

Bacteria containing the correct insert were grown in 500mL LB containing chloramphenicol overnight in a shaking incubator at 32°C and BAC DNA was isolated by maxiprep using the Nucleobond BAC 100 kit (Machery-Nagel, Germany). Briefly, bacteria cultures were centrifuged at 6000rpm for 15 minutes at 4°C, the pellet resuspended in S1 buffer, followed by the addition of buffer S2. After 5 minutes at room temperature, S3 buffer was added for 5 minutes at 4°C. Subsequently, it was centrifuged at 6000rpm for 15 minutes, poured onto a filter paper and into a column provided. The column was then washed twice with N3 buffer and the DNA eluted with N5 buffer. The DNA was then precipitated by adding isopropanol and centrifuged at 15000rpm for 30 minutes at 4°C. The supernatant was discarded and 70% ethanol was added. This was centrifuged at 15000rpm for 10 minutes, the ethanol was then removed, the pellet allowed to dry for 20 minutes and then resuspended in 10mM Tris, pH8. The concentration of DNA was measured using an NDG1000 Nanodrop spectrophotometer (Thermo Fisher Scientific).

MCMV BAC DNA was transfected into NIH-3T3 cells while RAd BAC DNA was transfected into T-Rex-293 cells. Both transfections were carried using the Effectene Transfection kit (Qiagen). $1x10^6$ cells were seeded into a T25 flask (Corning) and incubated overnight at 37°C. The following day, 4μg of BAC DNA was mixed with Buffer EC to make up a total volume of 150μL. 8μL of enhancer was added, mixed and incubated at room temperature for 5 minutes. Next, 25μL of effectene was added, mixed and incubated at room temperature for 5-10 minutes. 1mL of D10 was added to

the DNA mix, which was then added dropwise onto the cells. Cells were incubated at 37°C to allow virus growth.

2.7.1 Generation of MCMV stocks

For generating MCMV stocks, media was changed every 2-3 days and once regions of cytopathic effect (CPE) were apparent, supernatant was collected and stored at -80°C or used to infect more NIH-3T3 cells. When all the cells were infected, these were scraped and stored at -80°C.

2.7.2 Generation of RAd stocks

For RAd stock generation, the virus propagated through the T25 flask. Once CPE was completed, cells with the media were collected and spun at 1500rpm for 5 minutes. The supernatant was discarded and the pellet resuspended in 1mL PBS. An equal volume of tetrachloroethylene (TCE) (Fisher) was added and shaken vigorously until a single phase formed to lyse the cells and release cell-associated adenovirus virions. This was centrifuged at 2000rpm for 20 minutes and the top layer containing the virus was transferred and aliquoted in 100μL to be stored at -80°C or used to infect more T-Rex-293 cells.

2.8 Virus Purification

2.8.1 Recombinant MCMV

The collected infected cells and supernatants were centrifuged at 2000rpm for 5 minutes at 4°C. The pellet was resuspended in cold D10 and sonicated in an icy water bath for 7 minutes. This was followed by centrifugation (3000rpm, 5 minutes, 4°C) to

pellet the cell debris, which was subsequently discarded. The supernatant containing the virus was centrifuged at high speed (10000rpm, 100 minutes, 4°C) to pellet the virus. This was resuspended in cold D10 and then overlaid onto a 20% sorbitol cushion and centrifuged at high speed (18100rpm, 100 minutes, 4°C). The virus pellet was resuspended in D10 and sonicated for 5 minutes on ice. The sample was centrifuged at 3000rpm for 5 minutes at 4°C and the supernatant was aliquoted and stored at -80°C. Virus stocks were tittered by plaque assay (Section 2.9.1) on 2-3 separate occasions and an average titter taken.

2.8.2 Recombinant adenovirus

Recombinant adenovirus was purified using a caesium chloride gradient to remove cellular debris. 2mL of 3.6M CsCl solution was added into an ultra-clear Beckman centrifuge tube (Beckman Coulter, 331372) followed by 3mL of 1.6M CsCl solution. The TCE-extracted adenovirus was gently added on top of the gradient drop-by-drop and spun at 23000rpm for 2 hours at room temperature (Ultra Beckman L8-M ultracentrifuge). The adenovirus appeared as an opalescent band resting between the two CsCl layers and was collected by piercing the side of the tube just beneath the adenovirus band using a 21-gauge needle and a 5mL syringe. A new CsCl gradient was prepared as above and the collected virus was added to the top and centrifuged overnight (approximately 18 hours) at 23000rpm, room temperature. The adenovirus was collected as mentioned above and dialysed against a buffer solution to eliminate the CsCl solution. Dialysis tubing (Medicell International Ltd) was pre-warmed by submerging it in a beaker containing distilled water and allowed to cool to room temperature. The tubing was then transferred to dialysis buffer and closed at one end by a clip. The purified adenovirus was pipetted into the tube and the end clipped. The tube was then placed in 1L dialysis buffer in a beaker on a magnetic stirrer. The dialysis

buffer was replaced with fresh buffer after 2 hours and left overnight at 4°C. The adenovirus was removed from the dialysis tube, aliquoted and stored at -80°C.

2.9 Plaque Assay

NIH-3T3 cells were seeded into Corning flat bottom 24-well cell-bind plates (Appleton Woods, Birmingham, UK) at a concentration of 1 x 10^5 cells per well and incubated overnight.

2.9.1 MCMV stock titration

Purified virus stocks were serially diluted in DMEM and 200μL of each dilution was added to the cells in duplicates. Plates were incubated at 37°C, 5% CO_2 for one hour. DMEM containing the virus was removed and pre-warmed semi-viscous CMC media was added to each well. Cells were incubated for 6 days at 37°C, 5% CO_2. The CMC media was then removed and cells were fixed and stained for 4 hours with 10% formaldehyde in PBS and 0.5% crystal violet solution, respectively. Plates were then washed under running water and left to air-dry. Plaques were counted and replicating virus titre calculated using the formula:

$$\textit{plaque forming unit}\ (\textit{pfu})/\textit{mL} = \textit{average number of plaques} \times \textit{dilution factor} \times 5^{\dagger}$$

---

† 200μL of the viral dilution was added to the cells (i.e. 1/5th of 1mL), thus this is accounted for by multiplying by 5 to obtain pfu/mL.

2.9.2 MCMV IE1 immuno-fluorescence titration

As above, purified virus was serially diluted and added to the cells followed by one-hour incubation before adding CMC media and incubating for 10 days at 37°C, 5% CO_2. CMC media was removed and the cells washed in PBS. 1mL 50/50 acetone/methanol was added for 10 minutes at room temperature to fix infected cells. This was then removed and cells washed with PBS. IE1 antibody (Clone IE1.01, CapRi) diluted 1:1000 in PBS was added and incubated for 30 minutes at 37°C on a rocking platform. The antibody was removed and cells washed twice with PBS. Anti-mouse AlexaFluor 594 (Life Technologies, Thermo Fisher Scientific) diluted 1:500 in PBS was added and incubated at 37°C on a rocking platform for another 30 minutes. Stained cells were washed in excess PBS and visualised under a microscope (Leica). Plaques were counted and virus titre was calculated using the above formula (Section 2.9.1).

2.9.3 Virus quantification in organs

Mouse organs were homogenised in RPMI, dilutions of the suspension were prepared and 200μL was added onto confluent NIH-3T3 cells. MCMV was tittered by centrifugal enhancement at 1000 *x g* for 30 minutes. The suspension was then removed and CMC media was added. Cells were incubated for 6 days and fixed and stained as mentioned in section 2.9.1. Plaques were counted and virus quantification was calculated as pfu/g using the formula:

$$pfu/g = \frac{average\ number\ of\ plaques \times dilution \times 5^{\ddagger}}{organ\ weight}$$

---

‡ 200μL of the viral dilution was added to the cells (i.e. 1/5th of 1mL), thus this is accounted for by multiplying by 5 to obtain pfu/mL.

2.10 Recombinant Adenovirus Stock Titration

T-Rex-293 cells were seeded into a 12-well plate at a concentration of 2.5 x 10^5 cells per well and incubated overnight. Purified RAd stock was serially diluted in DMEM and 100μL of each dilution was added to the cells. To prevent disturbance of the loosely adhered cells, the culture supernatant was not removed prior to infection. The cells were then incubated at 37°C, 5% CO_2 for 48 hours before being fixed and permeabilised in acetone:methanol (1:1) for 10 minutes. Cells were washed with PBS and stained with polyclonal goat anti-adenovirus primary antibody (Abcam, AB1056) diluted 1:5000 in PBS for 1 hour at 37°C on a rocking platform. Excess primary antibody was removed by washing cells with excess PBS, before adding HRP-conjugated donkey anti-goat antibody (SantaCruz, 2056) diluted 1:1000 in PBS for a further one-hour incubation at 37°C. Cells were subsequently washed in PBS and HRP substrate was added. DAB substrate (Vector Labs, SK100) was used according to manufacturer's instructions and prepared by the addition of DAB substrate and supplied buffers to ddH_2O. Recombinant adenovirus titres were calculated using the following formula:

$$pfu/mL = \frac{average\ number\ of\ infected\ cells\ per\ field\ of\ view \times number\ of\ fields\ per\ well}{virus\ volume\ (mL) \times dilution\ factor}$$

2.11 Extraction of Viral DNA from Cell-Free Virions

Viral DNA was purified using the QIAamp MinElute Virus Spin Kit (Qiagen). In brief, cell-free virions were incubated at 56°C for 15 minutes with proteases and lysis buffer. 100% ethanol was added to the lysate and pulse-vortexed for 15 seconds before allowing it to stand at room temperature for 5 minutes. This was then transferred onto a QIAamp MinElute column and centrifuged at 8000rpm for 1 minute. Bound DNA was washed twice by the addition of wash buffer to the column followed by one wash with

100% ethanol. The column was incubated at 56°C for 3 minutes to allow the membrane to dry completely before viral DNA was eluted.

2.12 Western blot

Western blotting was used to examine the expression of NY-ESO-1 and 5T4 by the MCMV and RAd vectors generated. SGC1 cells were infected with recombinant MCMV at a multiplicity of infection (MOI) of 1 for 6, 24, 48 and 72 hours, while infections with RAd were done at an MOI of 500 for 48 hours. Cells were washed with PBS, scraped, lysed and added to NuPAGE LDS Sample Buffer (Life Technologies) along with 10mM dithiothreitol (DTT) (Sigma Aldrich) and heated to 90°C for 10 minutes. Samples were then loaded onto a pre-cast NuPAGE Novex 4-12% Bis-Tris protein gel (Life Technology) along with a sample of Novex Sharp Pre-stained Protein Standard and run at 200V for 40 minutes. Proteins were transferred onto a PVDF membrane (GE Healthcare Life Sciences), which had been previously soaked in methanol for 5 minutes, at 30V for 70 minutes. The membrane was then blocked with 5% non-fat milk in PBST for 1 hour at room temperature and probed overnight at 4°C on a rocking platform with the primary antibody (See Table 2.3 for antibody list) in PBST containing 1% milk. The following day, the membrane was washed three times with PBST before being incubated with the secondary antibody (Table 2.3) for 1 hour at room temperature. The membrane was washed three times with PBST before incubating it for 5 minutes with SuperSignal West Pico chemiluminescent substrate (Thermo Fisher Scientific) and imaged using G:Box gel doc. To re-probe the membrane, it was washed in PBST and incubated with stripping buffer (Thermo Fisher Scientific) for 30 minutes at 37°C. It was then washed in PBST, blocked and re-probed as above.

Table 2.3 Antibodies used for western blotting.

Primary Antibody	Host	Clone	Concentration	Company
α-mouse 5T4	Sheep	Polyclonal	1:2000	R&D Systems
α-human NY-ESO-1	Mouse	E978	1:5000	EMD Millipore
α-MCMV m123	Mouse	IE1.01	1:1000	CapRi
α-actin	Rabbit	Polyclonal	1:2000	Sigma-Aldrich
Secondary Antibody	**Host**	**Clone**	**Concentration**	**Company**
α-sheep-HRP	Donkey	n/a	1:2000	Sigma Aldrich
α-mouse-HRP	Goat	n/a	1:5000	Bio-Rad Laboratories
α-rabbit-HRP	Goat	n/a	1:2000	Bio-Rad Laboratories

2.13 Animal Experiments

Virus immunisations were performed intraperitoneally or subcutaneously with the stated dose of recombinant or control MCMV strains or RAds.

2.13.1 Blood collection

For tail bleeds, mice were placed in a heating cabinet at 37°C for 20 minutes. Mice were then placed in a restraining tube and Ethyl Chloride anaesthesia (Vidant Pharma) sprayed on the tail before blood collection. Approximately 50μL of blood was withdrawn from the lateral tail vein with lithium-heparin containing tubes for capillary blood collection (Microvette CB300 LH, Sarstedt).

2.13.2 Tumour induction and monitoring

For tumour induction, BALB/c or C57BL/6 mice were injected subcutaneously with 1 x 10^5 cells suspended in 100μL sterile PBS into the left flank. Following cell challenge, mice were monitored for tumour development every other day. Tumour-bearing mice were sacrificed before their tumours reached 17mm in diameter or if tumours caused apparent discomfort. Tumour size was measured using a caliper every 2 to 3 days. Tumour width and length was measured, and the tumour volume calculated using the following formula:

$$Tumour\ volume\ \left(mm^3\right) = length \times width \times smallest\ value \times \frac{\pi}{6}$$

2.14 Lymphocyte Isolation

Spleens, lungs, salivary glands and lymph nodes were harvested from mice. Spleens were passed through a 70μm nylon cell strainer to obtain a single cell suspension. This was spun for 5 minutes at 1500rpm and the cell pellet resuspended and incubated in lysis buffer (section 2.1) for 5 minutes. Cells were then washed in PBS and resuspended in R10. Salivary glands and lungs were cut into small pieces and incubated in digestion mix (section 2.1) at 37°C with agitation for 45 minutes. Cells were then passed through a 70μm nylon cell strainer, washed with PBS, and resuspended in R10. Lymph nodes were incubated in HBBS (with Ca^{2+} and Mg^{2+}) containing 100ug/mL DNase I and 1.6mg/mL collagenase D for 30 minutes at 37°C with agitation. Subsequently, cells were passed through a 70μm nylon cell strainer, washed in PBS and resuspended in R10. Blood withdrawn from the lateral tail vein was incubated for 5 minutes with lysis buffer, washed with PBS and cells resuspended in R10. Lymphocytes were quantified using trypan blue (Thermo Fisher Scientific).

2.15 Peptides

A peptide library covering the complete sequence of human 5T4 protein was obtained from Prof. Awen Gallimore (Cardiff University, UK). The library consisted of 41 20-mer peptides overlapping by 10 amino acids (Table 2.4). Peptides were pooled in a total of 13 pools, each consisting of 5-7 peptides (as shown in Table 2.5). These 13 peptide pools were used for the screening of 5T4-reactive $CD8^+$ T cell responses in an IFN-γ Enzyme-Linked ImmunoSpot (ELISpot) assay.

The class I restricted MCMV-derived peptides $pp89_{168-176}$ (YPHFMPTNL), $m164_{257-265}$ (AGPPRYSRI), $M38_{316-323}$ (SSPPMFRV), $m139_{419-426}$ (TVYGFCLL) and $IE3_{416-423}$ (RALEYKNL); the class-II restricted MCMV-derived peptides $M53_{285-299}$ (IAHQRITLTARCLRL) and $M78_{417-431}$ (SQQKMTSLPMSVFYS); class I restricted NY-ESO-1_{81-88} peptide (RGPESRLL); and class I-restricted peptides $5T4_{170-178}$ (SAPSPLVEL), $5T4_{244-252}$ (NSLVSLTYV) and $5T4_{253-260}$ (VSFRNLTHL) were synthesised at a purity of >95% by Peptide Synthetics (Fareham, UK). NY-ESO-1 peptide pool consisting of 15-mer sequences with 11 amino acids overlap, covering the complete protein sequence was obtained from Miltenyi Biotec (Germany).

Table 2.4 Human 5T4 20-mer peptide sequences.

No.	Sequence	No.	Sequence
1	MPGGCSRGPAAGDGRLRLAR	22	GLRRLELASNHFLYLPRDVL
2	AGDGRLRLARLALVLLGWVS	23	HFLYLPRDVLAQLPSLRHLD
3	LALVLLGWVSSSSPTSSASS	24	AQLPSLRHLDLSNNSLVSLT
4	SSSPTSSASSFSSSAPFLAS	25	LSNNSLVSLTYVSFRNLTHL
5	FSSSAPFLASAVSAQPPLPD	26	YVSFRNLTHLESLHLEDNAL
6	AVSAQPPLPDQCPALCECSE	27	ESLHLEDNALKVLHNGTLAE
7	QCPALCECSEAARTVKCVNR	28	KVLHNGTLAELQGLPHIRVF
8	AARTVKCVNRNLTEVPTDLP	29	LQGLPHIRVFLDNNPWVCDC
9	NLTEVPTDLPAYVRNLFLTG	30	LDNNPWVCDCHMADMVTWLK
10	AYVRNLFLTGNQLAVLPAGA	31	HMADMVTWLKETEVVQGKDR
11	NQLAVLPAGAFARRPPLAEL	32	ETEVVQGKDRLTCAYPEKMR
12	FARRPPLAELAALNLSGSRL	33	LTCAYPEKMRNRVLLELNSA
13	AALNLSGSRLDEVRAGAFEH	34	NRVLLELNSADLDCDPILPP
14	DEVRAGAFEHLPSLRQLDLS	35	DLDCDPILPPSLQTSYVFLG
15	LPSLRQLDLSHNPLADLSPF	36	SLQTSYVFLGIVLALIGAIF
16	HNPLADLSPFAFSGSNASVS	37	IVLALIGAIFLLVLYLNRKG
17	AFSGSNASVSAPSPLVELIL	38	LLVLYLNRKGIKKWMHNIRD
18	APSPLVELILNHIVPPEDER	39	IKKWMHNIRDACRDHMEGYH
19	NHIVPPEDERQNRSFEGMVV	40	ACRDHMEGYHYRYEINADPR
20	QNRSFEGMVVAALLAGRALQ	41	YRYEINADPRLTNLSSNSDV
21	AALLAGRALQGLRRLELASN		

Table 2.5 Human 5T4 peptide pools.

pp	1	2	3	4	5	6
7	1	2	3	4	5	6
8	7	8	9	10	11	12
9	13	14	15	16	17	18
10	19	20	21	22	23	24
11	25	26	27	28	29	30
12	31	32	33	34	35	36
13	37	38	39	40	41	

2.16 IFN-γ ELISpot

Ninety-six-well plates (MAIP-S-4510) (Millipore, Moslheim, France) were used for ELISpot assays and all antibodies were purchased from Mabtech (Natka, Sweden). Initially, plates were treated with 70% ethanol for 2 minutes followed by 5 washes with sterile water. Wells were then coated with 100μL of anti-IFN-γ capture antibody (AN18) at a concentration of 15μg/mL and incubated at 4°C overnight. Excess antibody was removed and the plate washed 5 times with sterile PBS before blocking the wells with D10 for 30 minutes at room temperature. This was then removed and the stimuli followed by the isolated splenocytes were added to the wells. The plate was covered in aluminium foil and incubated for approximately 18 hours at 37°C, 5% CO_2. Next, cells were removed, the plate was washed 5 times with PBS and the detection antibody (biotinylated anti-IFN-γ, R4-6A2) was added at a concentration of 1μg/mL. This was incubated for 2 hours at room temperature before washing as above and adding the Streptavidin-ALP, diluted 1:1000, for 1 hour. The plate was washed and substrate solution BCIP/NBT (Thermo Fisher Scientific) was added and left until distinct spots emerged. To stop colour development, the plate was washed thoroughly with water. It was left to dry before counting the spots using an automated ELISpot plate reader (ImmunoSpot, CTL) and analysed with the ELISpot 5.0 software package to ensure consistent analysis of spots between wells. Spot counts were verified manually.

2.17 Assessment of Antigen-specific T cells

$CD8^+$ and/or $CD4^+$ T cells specific for MCMV, NY-ESO-1 and 5T4 were detected by peptide stimulation with the MHC class I and class II restricted peptides mentioned in section 2.15. Lymphocytes were incubated for 6 hours at 37°C in the presence of 3μg/mL peptides and 2μg/mL Brefeldin A (Sigma-Aldrich). A medium control without peptides was run alongside the stimulations. Following stimulation, cells were stained for surface markers and intracellular proteins (section 2.18).

2.18 Flow Cytometry

2.18.1 Cell surface staining

Single cell suspensions were plated out onto a V-bottom 96 well plate (Fisher). Cells were washed twice in PBS before staining for dead cells using Zombie Aqua Fixable Viability Kit (BioLegend) diluted 1:500 in PBS and incubated in the dark at room temperature for 10 minutes. Cells were then washed in PBS and incubated at room temperature for 10 minutes with anti-CD16/32 (BioLegend) diluted 1:50 in FACS buffer to block Fc receptors. This was followed by cell surface staining with various antibody panels diluted in FACS buffer and incubating at 4°C for 20 minutes. Surface antibodies are listed in Table 2.6.

Table 2.6 Antibodies used in flow cytometry for detecting cell-surface proteins.

Antibody	Conjugate	Clone	Company	Dilution for $1x10^6$ cells
α-CD3ε	PerCP	145-2C11	BioLegend	1:50
α-CD3ε	APC/Cy7	145-2C11	BioLegend	1:100
α-CD4	APC	GK1.5	BioLegend	1:100
α-CD4	AF700	GK1.5	BioLegend	1:50
α-CD8a	AF700	53-6.7	BioLegend	1:50
α-CD8a	PE/Cy7	53-6.7	BioLegend	1:100
α-CD8a	PerCP	53-6.7	BioLegend	1:100
α-CD8a	BV605	53-6.7	BioLegend	1:100
α-CD11b	BV785	M1/70	BioLegend	1:100
α-CD11c	BV605	N418	BioLegend	1:100
α-CD44	APC/Cy7	IM7	BioLegend	1:100
α-CD62L	PE/Cy7	MEL-14	Abcam	1:100
α-CD69	BV711	H1.2F3	BioLegend	1:100
α-CD80	PE/Cy7	16-10A1	BioLegend	1:100
α-CD86	APC/Cy7	GL-1	BioLegend	1:100
α-CD103	PerCP/Cy5.5	2E7	BioLegend	1:100
α-CD127	BV711	A7R34	BioLegend	1:50
α-IA/IE	FITC	M5/114.15.2	BioLegend	1:500
α-KLRG1	FITC	2F1/KLRG1	BioLegend	1:100
α-PD-1	PE/Dazzle 594	29F.1A12	BioLegend	1:100
α-SigelcH	PB	551	BioLegend	1:100

2.18.2 Intracellular cytokine staining

Following cell surface staining, cells were fixed with 4% paraformaldehyde (Fisher) and permeabilised with saponin buffer. Subsequently, staining with intracellular antibodies (listed in Table 2.7) was performed.

Table 2.7 Antibodies used in flow cytometry for detecting intracellular proteins.

Antibody	Conjugate	Clone	Company	Dilution for $1x10^6$ cells
α-IFN-γ	FITC	XGM1.2	BioLegend	1:100
α-TNF-α	PE	MP6-XT22	BioLegend	1:100

2.18.3 MHC Class I tetramers

NY-ESO-1_{81-88} (H2-D^d), pp89 (H2-L^d), M38 (H2-K^b), m139 (H2-K^b), IE3 (H2-K^b), $5T4_{170-178}$ (H2-D^b), $5T4_{244-252}$ (H2-D^b) and $5T4_{253-260}$ (H2-D^b) monomers conjugated to biotin were obtained from the NIH Tetramer Core Facility (Atlanta, USA). Tetramers where formed by using ExtrAvidin-PE (Sigma-Aldrich), Streptavidin-APC (Thermo Fisher Scientifics), Streptavidin-BV421 (BioLegend). Briefly, to 10μg of monomer, 14.4μL of ExtrAvidin-PE, or 8μL of Streptavidin-APC, or 3μL Streptavidin-BV421 was added in 5 times every 20 minutes at 4°C. Tetramers were used at a concentration of 1μg per stain for 15 minutes at 37°C. This was followed by cell surface staining as described above.

2.18.4 Flow cytometry analysis

Cells were washed in FACS buffer and data acquired on FACSCanto II (BD Biosciences), FACSARIA III (BD Biosciences) or Attune NxT Flow Cytometer (Thermo Fisher Scientifics). Compensation was carried out with antibody-capture beads (BD Pharmingen) stained with individual antibodies used in each study. A minimum of 50,000 lymphocyte events were acquired and data was analysed using FlowJo software (TreeStar Inc, Ashland, OR). Total numbers of different cell populations were calculated by multiplying the total number of viable cells by percentage of positive cells detected by flow cytometry. Unless otherwise stated, $CD8^+$ and $CD4^+$ T cell responses

shown as frequency of IFN-γ^+, includes both single positive (IFN-γ^+ TNFα^-) and double positive (IFN-γ^+ TNFα^+) cells minus background levels.

2.19 Statistical Analysis

GraphPad prism Version 7 was used for all statistical analyses. All results are expressed as mean values together with the standard error of the mean (SEM) where appropriate and unless otherwise stated. Specific statistical test is indicated in each experiment. P values ≤ 0.05 were considered statistically significant and displayed by * in the figures (**p<0.01, ***p<0.005).

Chapter 3 - Generation of viral vectors expressing tumour-associated antigens

3.1 Introduction

3.1.1 Generation of recombinant viral vectors using bacterial artificial chromosome-based technology

Construction of viral-based cancer vaccine vectors has been aided by the development of bacterial artificial chromosomes (BACs). BACs are large plasmids widely used for cloning and modifying large DNA sequences of different origins in *Escherichia coli* (*E. coli*), such as viral genomes (436–439). They have become the tool of choice due to their high stability and large insert size (100-300kbp) (440). Recombination-mediated genetic engineering (recombineering) is used to manipulate the BAC DNA, allowing the deletion and insertion of target genes into the vector. This is achieved by the Red recombination system, originating from λ bacteriophages, that mediates homologous recombination between DNA molecules with as few as 30 bp of homology. This system consists of three genes: *exo*, *bet* and *gam*. Exo is a 5'-3' exonuclease that degrades double stranded (ds) DNA from the 5' end, generating 3' overhangs from the introduced dsDNA targeting fragment. *bet* encodes the protein beta that binds to the 3' overhang and mediates its annealing to complementary DNA present in the BAC, thereby integrating the DNA fragment into replicating DNA. Gam inhibits the *E. coli* RecBCD exonuclease from degrading the linear DNA targeting fragment. The expression of these genes is driven by the strong phage promoter *p*L, under the control of the temperature sensitive λ cI-repressor that prevents their transcription when bacteria are kept at 32°C. The λ cI-repressor can be inactivated when the temperature is shifted to

42°C, allowing the expression of *exo*, *bet* and *gam* genes and homologous recombination to occur (441–443). To facilitate the use of the Red system for BAC engineering, Copeland and colleagues stably integrated the Red genes into the chromosome of the BAC DH10B *E. coli* strain, creating DY380 *E. coli* (443). This allows tighter control of the Red genes, as plasmid expression systems are often 'leaky' resulting in low level constitutive Gam and Red activity. In addition, since Red genes are expressed from the bacterial chromosome rather than a plasmid, the recombination functions are not lost during cell replication. DY380 *E. coli* was further modified to integrate a functional galactose (*gal*) operon with the *galK* gene missing, in the bacterial chromosome, creating SW102 *E. coli* strain (434). This enables positive/negative selection of clones during BAC manipulation using the GalK system described by Warming *et al*. (434), which uses galactose as the carbon source for bacterial growth. This will not be discussed further as this selection method was not used in this thesis.

3.1.1.1 Methods for modifying BACs

The use of selectable markers in conjunction with recombineering enables relatively fast and easy cloning of genetic fragments into a vector. There are several methods for modifying BACs, all based on homologous recombination. A simple and widely used approach is based on positive/negative selection using selectable markers such as *neo* and *rpsL* genes. *Neo* confers kanamycin resistance and is used for positive selection while streptomycin sensitivity resulting from *rpsL* expression is used for negative selection. First the selectable cassette containing both genes is inserted by homologous recombination and positive clones are identified by resistance to kanamycin. Next the desired DNA fragment is introduced to replace the selectable cassette and clones that have acquired the DNA fragment are identified by their ability to grow in streptomycin. A disadvantage of this selection system is that spontaneous point mutations in the *rpsL* gene can occur without influencing the bacteria's ability to

grow in the presence of streptomycin, thus increasing the background after negative selection. Another method of homologous recombineering is *en passant* mutagenesis, which uses I-SceI, an endonuclease that recognises an 18 bp site rarely present in genome sequences. Briefly, the DNA fragment to be inserted harbours a sequence duplication, a selection marker, targeting flanks and a single I-*Sce*I site. The DNA fragment is inserted into the target site by homologous recombination and positive clones are identified by antibiotic resistance. Next, the expression of I-SceI is induced resulting in the cleavage of the I-*Sce*I site producing a dsDNA end which can undergo Red recombination, removing the marker cassette (Figure 3.1). For *en passant*, the I-*Sce*I gene was inserted in the DY380 *E. coli* chromosome under the control of an arabinose-inducible promoter, creating the *E. coli* strain GS1783 (444).

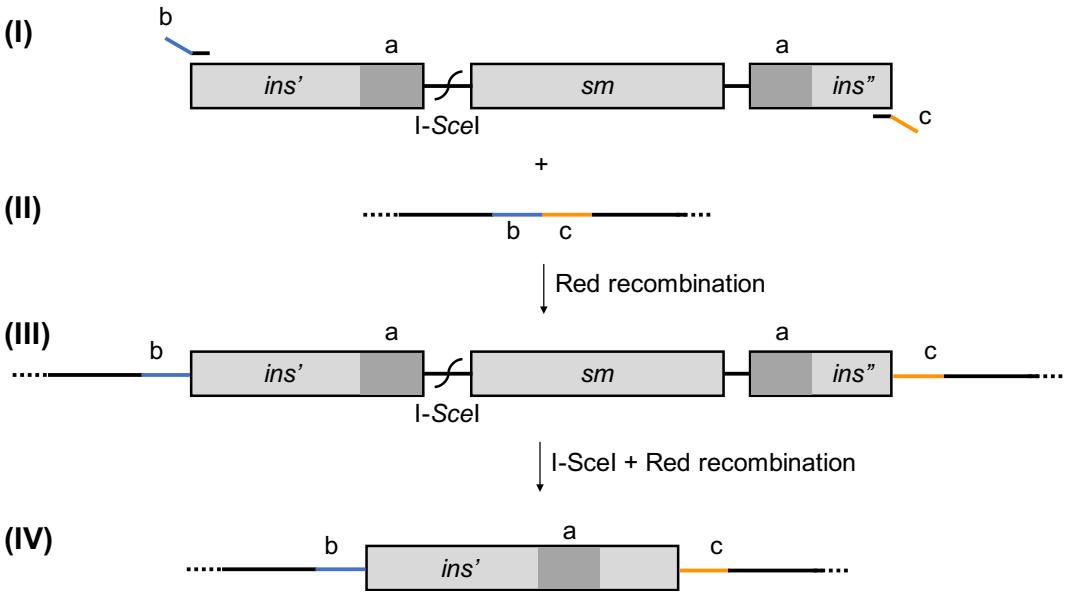

Figure 3.1 *En passant* mutagenesis – overview.

(I) A DNA construct consisting of the sequence to be inserted (ins), a selection marker (sm), and a I-*Sce*I restriction site is amplified by PCR using primers that have approximately 50 bp 5' overhang homology to the insertion site (blue and orange lines) to allow Red-based recombination into the **(II)** target sequence. **(III)** Intermediate co-integrate. The selection marker is released from the co-integrate by cleavage of the I-*Sce*I site allowing a second Red recombination to occur **(IV)**. a-c: identical sequences of approximately 50 bp. ins' and ins'': sequence to be inserted.

3.1.2 K181 MCMV BAC

The capture of CMV genomes as BAC clones allows modification of viral genomes and paves the way for a plethora of applications, such as using cloned viruses for vaccine development. The K181 BAC (pARK25), containing the whole K181 MCMV viral genome was produced by Redwood *et al.* (445). It was generated to contain a 249 bp duplication flanking the BAC cassette at the viral *m07* locus that allows self-excision of the BAC cassette by homologous recombination once transfected into eukaryote cells. This recombination is efficient and it is suggested to be selected for by size exclusion as viruses that have lost the BAC backbone are packaged more efficiently into the capsids compared to those containing the BAC backbone. This has been observed in other viruses such as adenoviruses and EBV where the length of the insert affects the efficiency with which the DNA is packaged (446, 447). For example in adenoviruses, those vectors containing an insert that exceeded the wild type adenovirus genome by over 5% undergo genome rearrangements that eventually results in the loss of the insert (447). Furthermore, the K181 BAC backbone contains a *gfp* gene, thus correct recombination in eukaryote cells can be observed by the loss of GFP expression.

3.1.3 AdZ BAC

Stanton *et al.* (448) developed an adenovirus BAC, designated AdZ (Ad with zero cloning steps), that allows rapid and efficient generation of recombinant adenoviruses (RAds) using recombineering technology. The AdZ vector contains the entire Ad5 genome with the *E1* and *E3* genes deleted and an expression cassette, comprised of a HCMV major immediate early (MIE) promoter along with its polyadenylation signal, in place of the *E1* region. In addition, to allow genes to be inserted directly into the vector a selectable cassette consisting of amp^r, *lacZ*α and *sacB* encoding genes for ampicillin resistance, β-galactosidase and sensitivity to sucrose, respectively, was included in the vector. The AdZ vector is ‘self-excising’ due to the incorporation of

I-*Sce*I recognition sites at either end of the Ad genome, in addition to an I-*Sce*I gene under the Rous sarcoma virus (RSV) promoter within the BAC backbone. Thus, transfection of the circular AdZ BAC into eukaryote cells results in expression of I-*Sce*I, which in turn excises the BAC backbone from the viral genome (for the schematic of the AdZ BAC vector see Figure 3.2).

3.1.4 Aims

The aims of this chapter were the following:

1. Generate MCMV vectors expressing 5T4 and NY-ESO-1;
2. Generate a RAd vector expressing NY-ESO-1;
3. Examine the expression of 5T4 and NY-ESO-1 by the vectors generated.

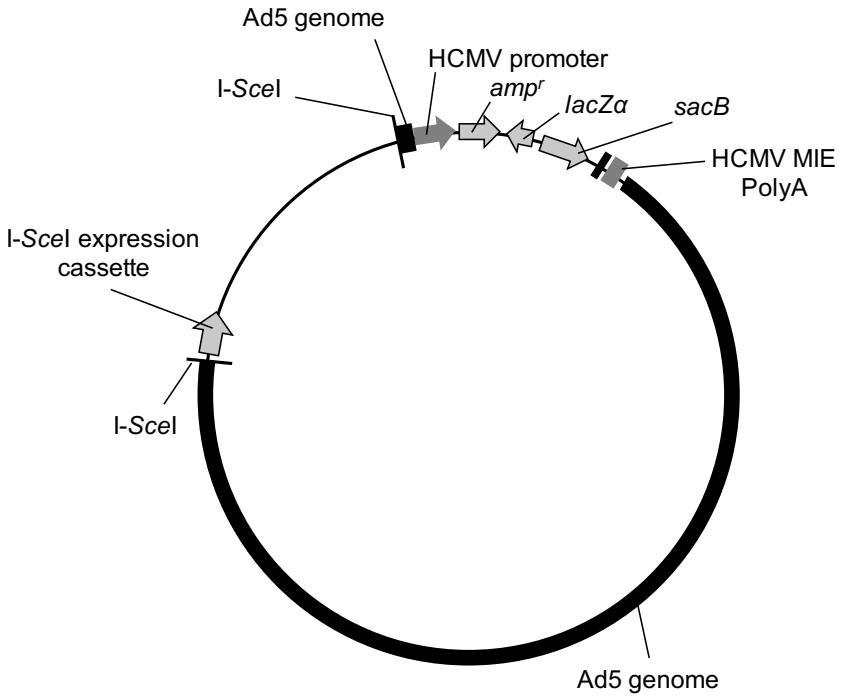

Figure 3.2 Schematic of AdZ BAC.

Diagram of the complete AdZ BAC showing the HCMV MIE promoter, the selectable marker cassette and the polyadenylation sequence. The vector includes I-SceI restriction sites at the start and end of the Ad5 genome as well as I-SceI expression cassette within the BAC backbone.

3.2 Results

3.2.1 Criteria for generating MCMV vectors

Choice of tumour-associated antigens

NY-ESO-1 and 5T4 were chosen to be inserted into the MCMV genome because, as described in sections 1.2.4.1 and 1.2.4.2 (Chapter 1), NY-ESO-1- and 5T4- specific $CD8^+$ T cells have been associated with better prognosis in cancer patients. Mice do not have a homologue of the NY-ESO-1 tumour-associated antigen, thus the human gene was used. 5T4 is expressed in human and mice and exhibit 81% amino acid homology (449). The human *5T4* gene was chosen to be inserted into the MCMV vector since it harboured some differences in the amino acid sequence, which might have the potential to break tolerance and increase vector immunogenicity. Indeed, the use of modified tumour-associated antigens was reported by Qiu *et al*. where an MCMV vector expressing mouse gp100 that contained a modified epitope was able to induce a gp100-specific T cell response while that expressing the native mouse protein was not (433).

Choice of insertion site within the MCMV genome

The site of insertion for the tumour-associated antigens was decided based on the properties of the MCMV vector. Ideally, the tumour-specific T cell responses induced by the MCMV vector should inflate overtime as observed with some MCMV-specific responses. In addition, the tumour-associated antigens should be expressed during latency because, as mentioned in section 1.4.3.1 (Chapter 1), inflationary T cell responses might be determined by the expression kinetics during MCMV latency.

MCMV-specific epitopes that inflate over time in both C57BL/6 and BALB/c mice can be found in the *m123* locus (IE3 and pp89 (also known as IE1), respectively). This harbours the immediate early genes *ie1*, *ie2* and *ie3*. The MCMV *ie2* gene is expressed in the immediate early phase of virus replication and encodes a non-essential protein

that can be deleted or modified without affecting i*n vitro* or *in vivo* virus replication (450). Thus, the initial cloning strategy was to insert the tumour-associated antigen genes, *5T4* and *NY-ESO-1*, replacing the *ie2* ORF, meaning that their expression would be driven by the endogenous promoter without affecting replication. Figure 3.3 shows a schematic of the constructs where *NY-ESO-1* (construct 1) and *5T4* (construct 2) genes replaced the *ie2* ORF and are designated MCMV-NY-ESO-1 and MCMV-5T4, respectively.

As it will be discussed in Chapter 4, further MCMV vectors expressing 5T4 were constructed as it was thought that the expression of the tumour-associated antigens driven by the endogenous *ie2* promoter was very low. Hence, a new construct where *5T4* expression was driven by a strong constitutive promoter, the HCMV major immediate early (MIE) promoter, was generated (designated MCMV-MIE-5T4, Figure 3.3, construct 3). Other sites for gene insertion were also examined. The genes *ie1* and *ie3* contain inflationary epitopes and are also expressed in the immediate early phase of viral replication. In addition, there is evidence for episodes of *ie1* and *ie3* transcription during MCMV latency and recurrence, respectively (451, 452). Hence, *5T4* was fused to the end of the ORF of either *ie1* or *ie3* via a P2A linker, and were designated MCMV-IE1-P2A-5T4 (Figure 3.3, construct 5) and MCMV-IE3-P2A-5T4 (Figure 3.3, construct 6), respectively. The P2A linker allows cleavage of the 5T4 from the endogenous protein during translation to avoid any disruption of the IE1 and IE3 protein functions as these are essential for MCMV (453). Finally, a construct with the *ie2* ORF deleted was generated to use as a control for those vectors where the antigen was replacing the *ie2* ORF (Figure 3.3, construct 4); and was designated MCMV-ΔIE2. Unless otherwise stated the method of homologous recombineering used was based on positive/negative selection of clones; Figure 3.4 shows an overview of the method. The K181 BAC in SW102 *E. coli* was made available by Dr. Richard Stanton.

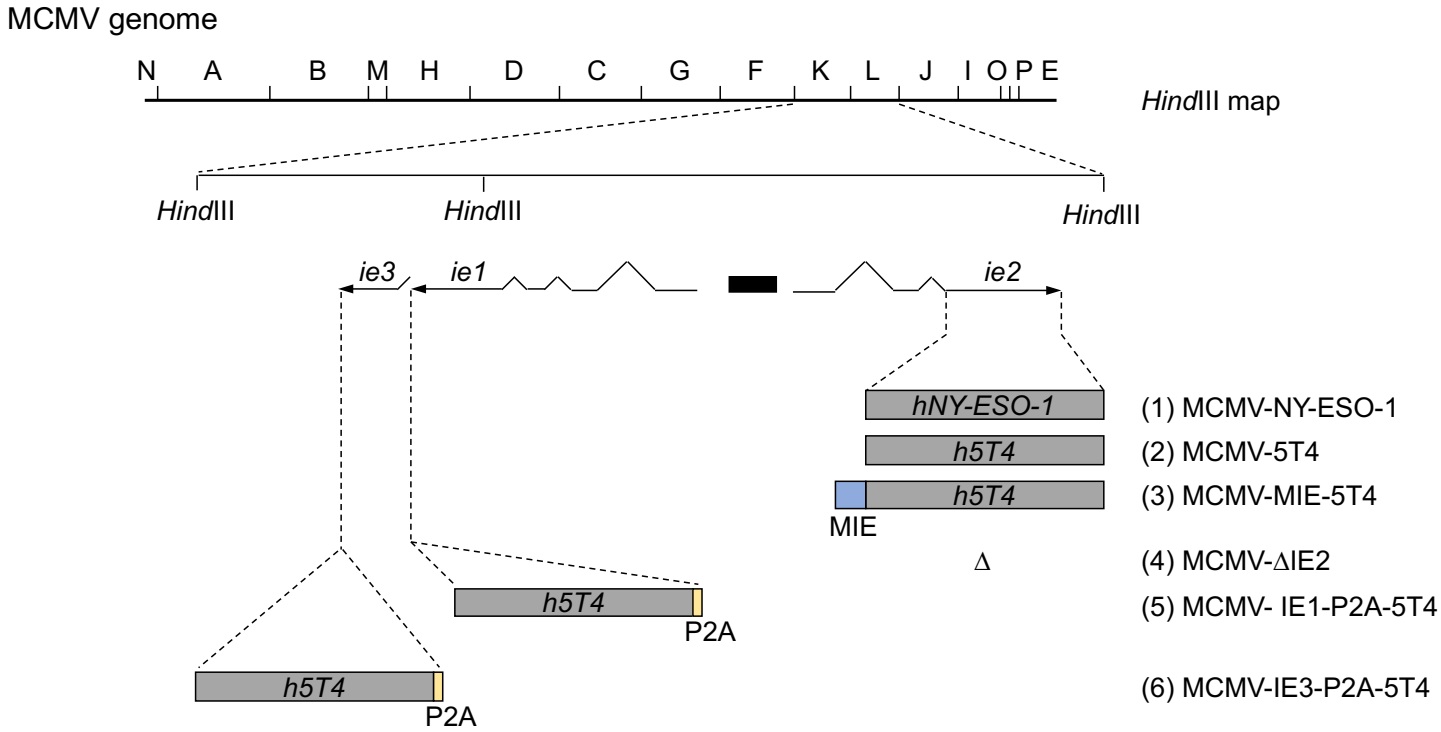

Figure 3.3 Schematic of the MCMV vectors generated.

The top line shows the *Hind*III digestion map of the K181 MCMV genome. The *ie1*, *ie2* and *ie3* gene transcripts are shown under the expanded region and the enhancer is indicted by the black box. Recombinant vectors were constructed by λ-based linear recombination: (1) MCMV-NY-ESO-1: human *NY-ESO-1* was inserted under the control of the endogenous *ie2* promoter, replacing the *ie2* ORF. (2) MCMV-5T4: codon optimized human *5T4* ORF was inserted under the control of the endogenous *ie2* promoter, replacing the *ie2* ORF. (3) MCMV-MIE-5T4: codon optimized human *5T4* ORF driven by the HCMV MIE promoter, replacing the *ie2* ORF. (4) MCMV-ΔIE2: *ie2* ORF deleted. (5) MCMV-IE1-P2A-5T4: codon optimized human *5T4* ORF fused in frame to the end of the *ie1* gene via a P2A linker. (6) MCMV-IE3-P2A-5T4: codon optimized human *5T4* ORF fused in frame to the end of the *ie3* gene via a P2A linker.

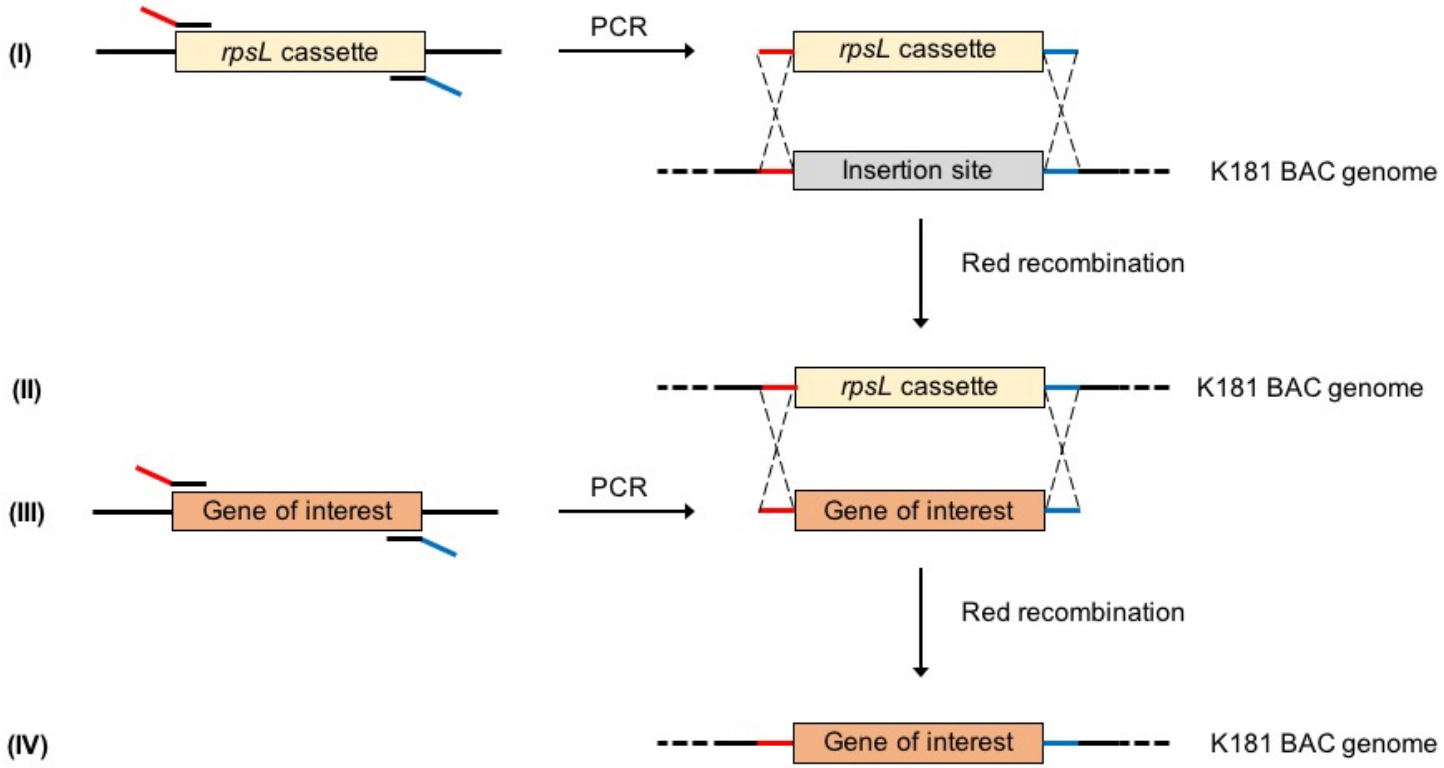

Figure 3.4 Overview of K181 BAC recombineering.

(I) The *rpsL* selection cassette was amplified using primers with 5' overhanging arms homologous to the insertion site in the K181 BAC genome and used in the first round of recombineering. **(II)** Recombinants harbouring the *rpsL* cassette were identified by positive selection on kanamycin plates. **(III)** Cancer antigen genes were amplified using primers with 5' overhanging arms homologous to the insertion site and used in the second round of recombineering replacing the selection cassette. **(IV)** Recombinants containing the gene of interest were identified by negative selection on streptomycin plates.

3.2.1.1 5T4 and NY-ESO-1 insertion into the MCMV BAC genome

The selectable marker cassette *neo/lacZ*α*/rpsL,* (*rpsL* cassette) encoding the genes for kanamycin resistance, β-galactosidase and streptomycin susceptibility, respectively, was inserted within the *ie2* DNA coding region or at the end of the *ie1* or *ie3* ORF of the K181 MCMV BAC. The cassette was amplified by PCR using primers with 5' overhangs homologous to the regions contiguous to the insertion site (Appendix I) and introduced into competent SW102 bacteria by electroporation. The λ Red genes were transiently induced by incubating bacteria at 42°C for 15 min, and following homologous recombination the cassette was inserted into the BAC. Recovered SW102 bacteria were grown on kanamycin plates that also contained IPTG, which induces the expression of β-galactosidase, and X-gal, a modified galactose sugar. Correct insertion of the selectable cassette resulted in the bacteria being resistant to kanamycin and appearing blue after ~24 hours (Figure 3.5A). The functionality of the genes in the *rpsL* cassette was checked by picking four colonies and streaking them on plates containing either kanamycin or streptomycin in addition to IPTG and X-gal. Colonies with a fully functional *rpsL* gene could grow on kanamycin plates but not on those containing streptomycin (Figure 3.5B). BAC DNA from colonies with functional *rpsL* cassette was extracted and treated with *Hind*III endonuclease to check for the presence of K181 BAC since cleavage with this enzyme gives a recognisable band pattern on agarose gel (Figure 3.5C&D). The resultant band pattern was consistent with the retention of the K181 MCMV genome, thus one of the clones for each insertion site was selected and used for the next round of recombineering.

The tumour associated antigens, *5T4* and *NY-ESO-1*, were amplified using different sets of primers with 5' overhangs homologous to the regions contiguous to the different insertion sites (i.e. *ie1*, *ie2* and *ie3*). For those vectors where *5T4* would be replacing the *rpsL* cassette, a codon optimised version of the gene was used since the original

5T4 sequence resulted in a 50 bp deletion during recombineering due to the presence of a duplicative sequence (data not shown). A plasmid containing the P2A linker and the codon optimised *5T4* gene flanked by 80 bp with homology to the *ie1* insertion site and *Bam*HI restriction sites was incubated with *Bam*HI to release the *P2A-5T4* DNA fragment with *ie1* arms of homology for use in recombineering. This was also used as the DNA template for amplifying *5T4* alone or *P2A-5T4* using primers with *ie2* and *ie3* 5' arms of homology, respectively. To generate the *ie2*-deficient MCMV vector, an oligonucleotide consisting of ~50 bp of homology to the left and right of the *ie2* DNA coding sequence was used as the recombination DNA fragment. The DNA fragments were introduced into competent bacteria by electroporation and the antigen was inserted into the BAC by homologous recombineering, replacing the *rpsL* cassette.

Recovered bacteria were grown on plates containing streptomycin, ITPG and X-gal. *rpsL* expression makes bacteria susceptible to streptomycin, allowing selection against the parental vector. The lacZ marker differentiated recombinant colonies from a background of false positives arising from spontaneous mutations in the *rpsL* gene. Therefore, when *rpsL* cassette was replaced by the DNA fragment, the colonies appeared white in colour (Figure 3.6A). DNA from white colonies from each construct was extracted and restriction enzyme digestion performed with *Hind*III (Figure 3.6B-F). Samples exhibiting cleavage pattern indicative of successful recombination were used to amplify the region where recombination had occurred, sent to sequence and analysed to ensure no mutations had been introduced. Glycerol stocks where then generated from those clones that had the gene inserted with no mutations.

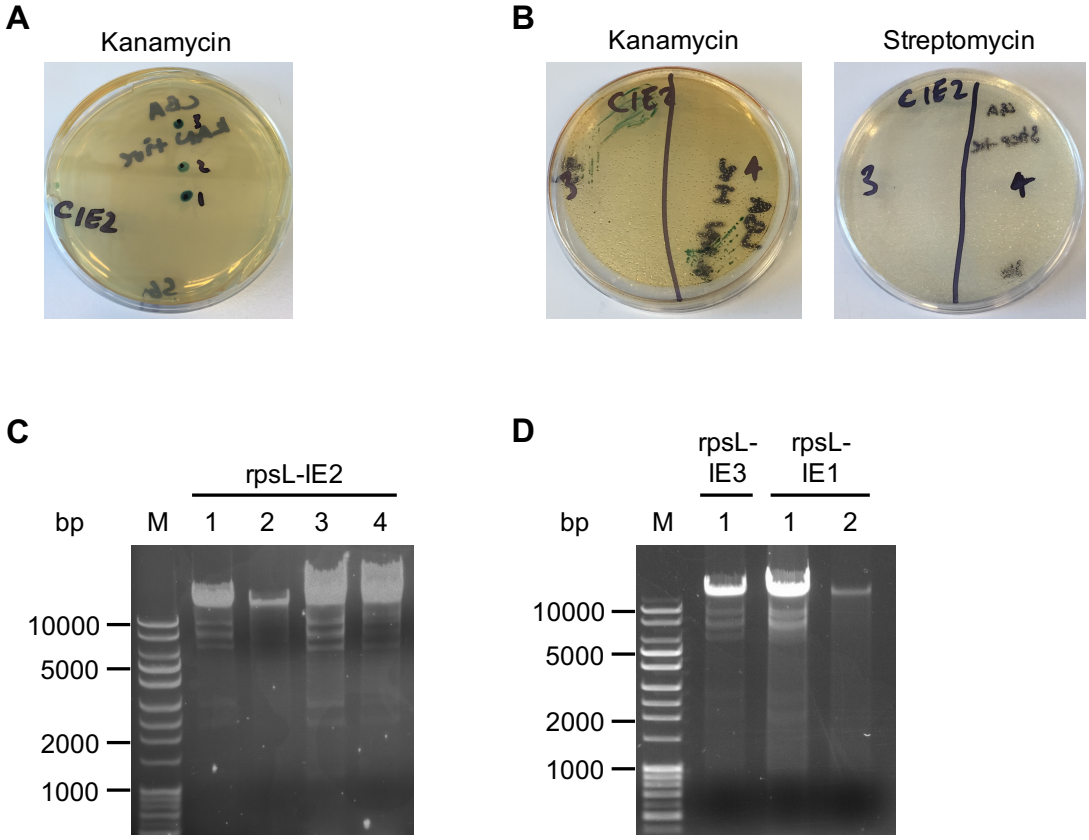

Figure 3.5 Selection of colonies containing functional *rpsL* cassette.

A) Representative image of SW102 bacteria recombineered to insert the *rpsL* cassette into the K181 MCMV BAC genome grown for 48 hours on kanamycin plates. **(B)** Representative images where single positive clones where streaked on both kanamycin and streptomycin plates to test the functionality of the cassette. **(C-D)** *Hind*III digestion of positive colonies where the *rpsL* cassette was inserted **(C)** within the *ie2* ORF, **(D)** at the end of *ie1* or at the end of *ie3*. Lanes M: 1 kbp DNA ladder, Lanes 1-4: different colonies picked.

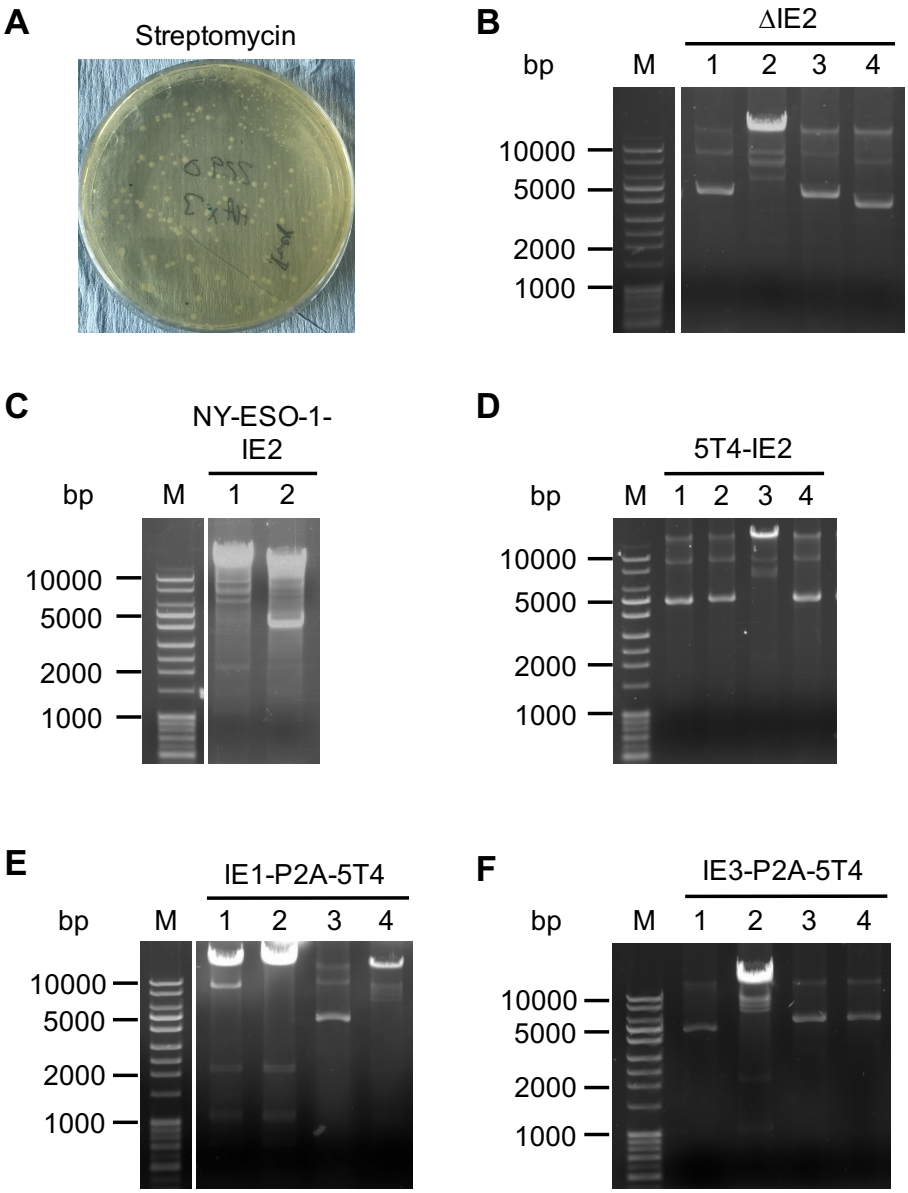

Figure 3.6 Selection of clones where the target gene has replaced the *rpsL* cassette in the K181 BAC.

(A) Representative image of SW102 bacteria recombineered to replace the *rpsL* cassette by the cancer antigen, grown for 48 hours on streptomycin plates. **(B-F)** *Hind*III digestion of DNA from white colonies where **(B)** the *ie2* ORF has been deleted, **(C)** *NY-ESO-1* and **(D)** *5T4* have replaced the selection cassette in *ie2* locus, and **(E&F)** *P2A-5T4* has replaced the *rpsL* cassette at the *ie1* and *ie3* locus, respectively. Lanes M: 1 kbp DNA ladder, lanes 1-4: different colonies picked.

3.2.1.2 MIE-5T4 inserted into the MCMV BAC genome

For inserting the *MIE-5T4* within the MCMV genome, replacing the *ie2* ORF, the *en passant* method of recombineering was used due to the high percentage of random recombineering encountered when inserting such a large fragment into the K181 BAC. Due to time constraints, the DNA fragment used in recombineering was assembled using CLC Main Workbench and send to be synthesised by Invitrogen (referred to as MIE-5T4-neo). Figure 3.7 shows how the genes were arranged in the DNA fragment, which was flanked by 80 bp homologous to the site of insertion in the BAC. Along with the HCMV-MIE promoter and *5T4* gene, a I-*Sce*I restriction site and a kanamycin resistance gene (*neo*) that allowed positive selection of clones containing the DNA fragment were included. *Hind*III restriction sites were added at the ends of the DNA fragment to allow easy excision from the plasmid backbone.

For *en passant* mutagenesis, GS1783 *E. coli* was used instead of SW102 as it contains the I-*Sce*I gene in addition to the Red genes in the chromosome of the bacteria. Hence, GS1783 *E. coli* was transformed with the K181 BAC as described in section 2.5.2.2 of the Materials and Methods (Chapter 2) and clones containing the BAC were identified by correct restriction enzyme digestion pattern using *Xho*I, *Eco*RI and *Hind*III (Figure 3.8A) and glycerol stocks generated. The *MIE-5T4-neo* DNA fragment was isolated from the plasmid vector by restriction enzyme digest, introduced into competent GS1783 bacteria by electroporation and inserted into the K181 BAC by homologous recombination. Recovered bacteria were plated on kanamycin plates which would allow the growth of those with the DNA fragment inserted. BAC DNA from few clones was extracted and treated with *Hind*III to check for the K181 BAC pattern (Figure 3.8B). Positive clones were then used in PCR along with the IE2seq primers to check for correct insert size (2838 bp). All clones picked had an insert size around 3000 bp, matching the predicted size (Figure 3.8C). Next, the expression of I-*Sce*I was induced by growing the bacteria in l-arabinose, inducing cleavage of the I-*Sce*I site within the

DNA fragment. This resulted in double-stranded DNA end with adjoining homologous sequence which underwent recombination, removing the marker cassette. Bacteria were then grown on chloramphenicol plates containing l-arabinose. The BAC DNA from a few clones was extracted and digested with *Hind*III. Two clones with the correct digestion pattern were chosen and the site of recombination amplified with IE2seq primers and send to sequence. Glycerol stocks where made from clones with the correct sequence.

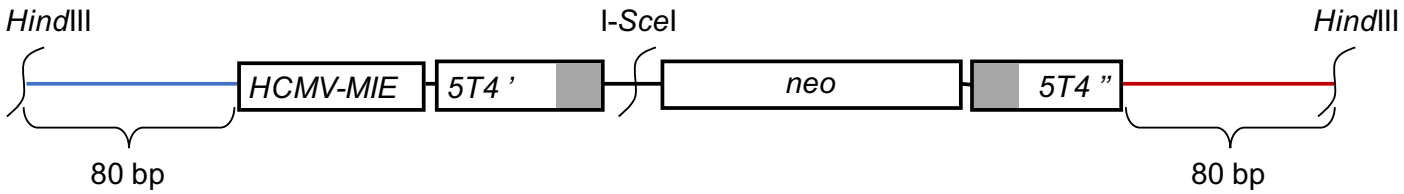

Figure 3.7 DNA fragment used for *en passant* mutagenesis (*MIE-5T4-neo*).

The DNA fragment was constructed to have the HCMV-MIE promoter followed by part of the codon optimized *5T4* gene (*5T4'*), a I-*Sce*I restriction site, a kanamycin resistance gene (*neo*) and the remaining part of the *5T4* gene (*5T4"*). The 50 bp at the end of the *5T4'* fragment and the 50 bp at the beginning of the *5T4"* fragment (grey boxes) were identical to allow recombination. This is flanked by 80 bp homologous to the site of insertion in the BAC and by *Hind*III restriction sites to allow easy excision of the DNA fragment from the plasmid backbone.

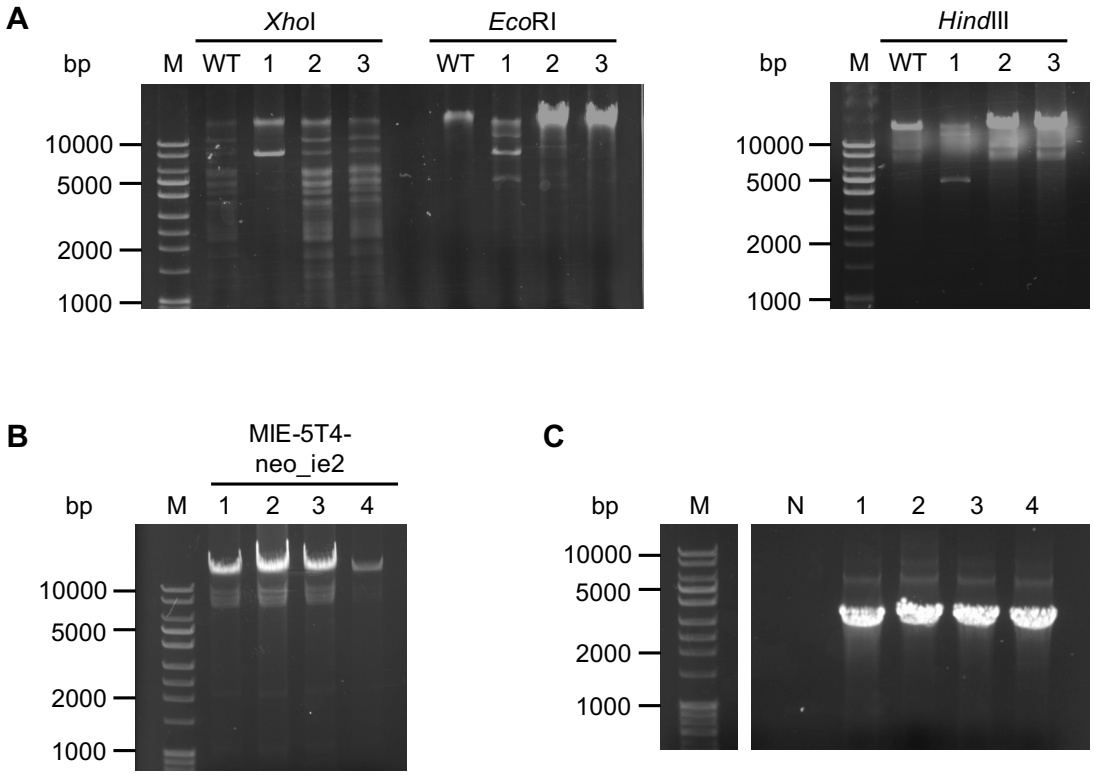

Figure 3.8 Selection of colonies with correct K181 BAC and insert.

(A) Three different clones (lanes 1-3) of GS1783 transformed with the K181 BAC genome along with the parent K181 BAC (WT) were digested with *Xho*I, *Eco*RI and *Hind*III and run on an agarose gel. **(B)** *Hind*III digest of K181 BAC in GS178 bacteria containing the *MIE-5T4-neo* DNA fragment. Lane M: 1 kbp DNA ladder, lanes 1-4: different clones picked. **(C)** DNA of recombinant clones amplified with primers flanking the insertion site (IE2seq). Lane M: 1 kbp DNA ladder, lane N: negative control, lanes 1-4: different clones.

3.2.2 Cloning 5T4 and NY-ESO-1 into AdZ

AdZ BAC in SW102 *E. coli* was obtained from Dr. Richard Stanton. *NY-ESO-1* was inserted between the HCMV MIE promoter and the polyadenylation signal (PolyA) replacing the *amp^r/lacZα/SacB* selection cassette (*sacB* cassette). The *NY-ESO-1* gene was amplified by PCR using primers with 5' overhangs homologous to the region flanking the insertion site (Appendix I). The amplification product was transformed into SW102 bacteria containing the AdZ BAC, and the λ *Red* genes were transiently induced to allow homologous recombination to occur. Recombinant bacteria were recovered on plates containing chloramphenicol, X-Gal, IPTG and 5% sucrose. In the presence of sucrose, *sacB* expression in gram-negative bacteria leads to their death, allowing selection of those clones without the selection cassette. As with the *rpsL* cassette, positive clones where the *sacB* cassette had been replaced by the *NY-ESO-1* gene would be identifiable by white colonies. Four white colonies were picked and DNA extracted to perform restriction enzyme digest with *Bam*HI (Figure 3.9). DNA from positive clones with the recognisable digest pattern were sequenced and glycerol stocks generated. An Ad vector with the codon optimised human *5T4* gene inserted into the same site as *NY-ESO-1*, and a control RAd lacking an insert were generated previously by Evelina Statutke.

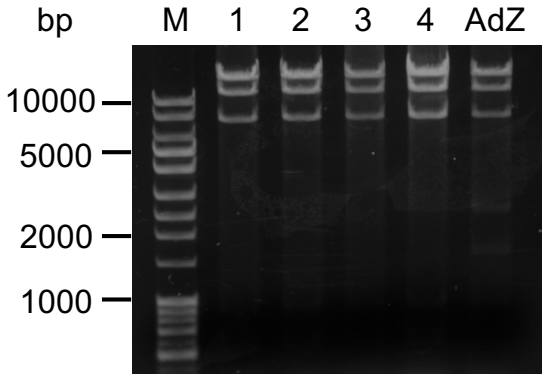

Figure 3.9 Analysis of AdZ clones harbouring the NY-ESO-1 gene.

*Bam*HI digest of DNA from different white colonies where the *SacB* cassette in the AdZ BAC has been replaced by the tumour associated antigen *NY-ESO-1*. Lane M: 1 kbp DNA ladder, lanes 1-4: different colonies, lane AdZ: parental AdZ BAC.

3.2.3 Growth of viral vectors and detection of antigen expression

BAC DNA from the MCMV and AdZ BAC clones generated was extracted from bacteria and transfected into NIH 3T3 cells and 293TREx cells, respectively. The MCMV and RAd vectors were propagated, grown and purified as described in Materials and Methods (Chapter 2, section 2.7 and 2.8). DNA from MCMV vectors generated was extracted and the regions where the tumour-associated antigen was inserted was examined by PCR using the sequencing primers IE1seq, IE2seq or IE3seq. MCMV-ΔIE2, MCMV-NY-ESO-1, MCMV-5T4, MCMV-MIE-5T4, MCMV-IE1-P2A-5T4 and MCMV-IE3-P2A-5T4 would give amplification products with sizes 343 bp, 831 bp, 1551 bp, 1929 bp, 1701 bp and 1698 bp, respectively. As a control, the *m157* locus, which is distant from the site of recombineering, was also amplified using m157seq primers (Appendix I) and would give a product size of 844 bp. DNA from RAd-NY-ESO-1 was also extracted and amplified using primers that bind within the HCMV MIE promoter and polyA sequence (RAd_seq), giving an amplification product of 880 bp. PCR confirmed that all the vectors had the correct insert (Figure 3.10).

Subsequently, expression of cancer antigens was confirmed by western blot. MCMV-ΔIE2 and RAd-CTL were used as negative control. For expression analysis, mouse salivary gland epithelial cells, SGC1, were infected with individual vectors. Ad5 cell entry requires the coxsackievirus and adenovirus receptor (CAR) (454, 455) and its expression on SGC1 cells is unknown. Thus, SGC1s were infected with a RAd expressing green fluorescence protein (GFP; RAd-GFP). Due to the replication-deficient nature of the RAds, the infection was carried out at a high MOI of 500 (500 pfu per cell) to maximise the expression of the protein. GFP expression was examined at 24, 48 and 72 hours post infection (Figure 3.11). Although expression was weak, GFP was detected as early as 24 hours p.i, with increased intensity after 48 hours, demonstrating that RAds could infect SGC1. Hence, SGC1s were infected at an MOI of 500 with either RAd-CTL, RAd-5T4 or RAd-NY-ESO-1 and lysates prepared

at 48 hours post infection. For the MCMV vectors, SGC1 cells were infected at an MOI of 0.1 (1 pfu per 10 cells) and samples collected at day 2, 3, 4 and 6 p.i. NY-ESO-1 expression was detected in those lysates infected with either MCMV-NY-ESO-1 or RAd-NY-ESO-1 (Figure 3.12A). Interestingly, expression of this tumour associated antigen was much higher in the RAd vector than in the MCMV vector (Figure 3.12A). 5T4 expression was detectable in samples infected with all the MCMV vectors generated: MCMV-5T4 (Figure 3.12B), MCMV-MIE-5T4 (Figure 3.12C), MCMV-IE1-P2A-5T4 (Figure 3.12D) and MCMV-IE3-P2A-5T4 (Figure 3.12E). However, expression level of 5T4 varied depending on where the tumour-associated antigen gene was inserted within the K181 MCMV genome. MCMV-MIE-5T4 and MCMV-IE1-P2A showed highest expression with levels comparable to that of the RAd-5T4 (Figure 3.12C&D).

To examine whether the inserts were affecting viral replication, growth curve assays were performed to assess the growth phenotype. The growth kinetics of the MCMV vectors generated were compared to wild-type (WT)-MCMV (parental K181 MCMV). MCMV-ΔIE2 (Figure 3.13A), MCMV-NY-ESO-1 (Figure 3.13B), MCMV-5T4 (Figure 3.13C), MCMV-MIE-5T4 (Figure 3.13D), and MCMV-IE3-P2A-5T4 (Figure 3.13F) replicated to the same extent as WT-MCMV. In contrast, the MCMV-IE1-P2A-5T4 vector did not replicate to comparable titres as WT-MCMV, resulting in a log difference by day 4 p.i (Figure 3.13E). This indicated that 5T4 fused to the end of *ie1* ORF might be affecting the vector's replication capacity.

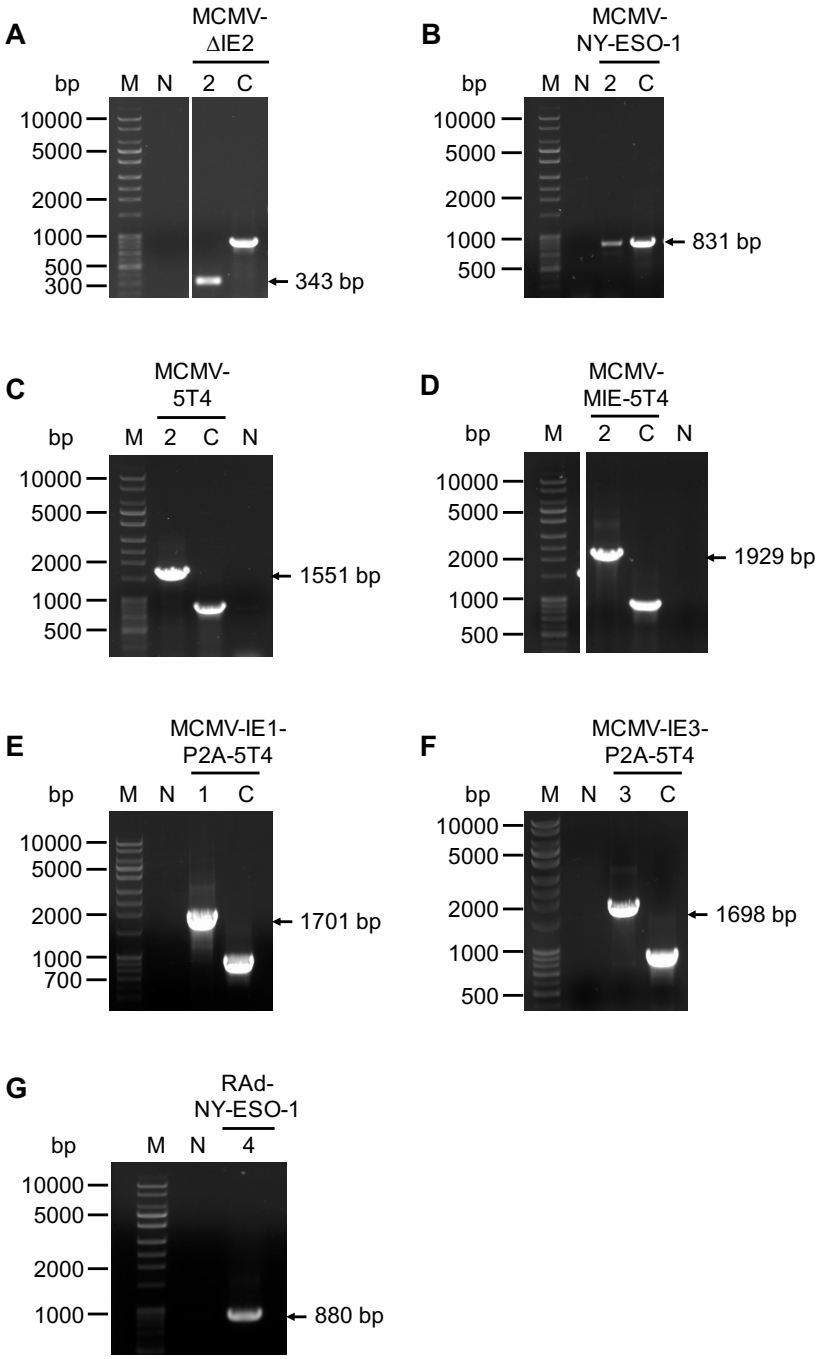

Figure 3.10 PCR analysis of viral DNA.

DNA from the MCMV and RAd vectors generated was isolated from cell free virions and the region where the antigen was inserted was amplified by PCR using primers contiguous to the inserted site. **(A)** MCMV-ΔIE2, **(B)** MCMV-NY-ESO-1, **(C)** MCMV-5T4 and **(D)** MCMV-MIE-5T4 DNA were amplified using IE2seq and m157 primers. **(E)** MCMV-IE1-P2A-5T4 and **(F)** MCMV-IE3-P2A-5T4 DNA were amplified using m157 primers and IE1seq and IE3seq respectively. **(G)** RAd-NY-ESO-1 DNA was amplified using RAd_seq primers. Lane M: 1 kbp, Lane N: no template, Lane C: positive control using primers to amplify m157 locus, Lane 1: amplification using IE1seq primers, Lane 2: amplification using IE2seq primers, Lane 3: amplification using primers IE3seq primers, Lane 4: amplification using RAd_seq.

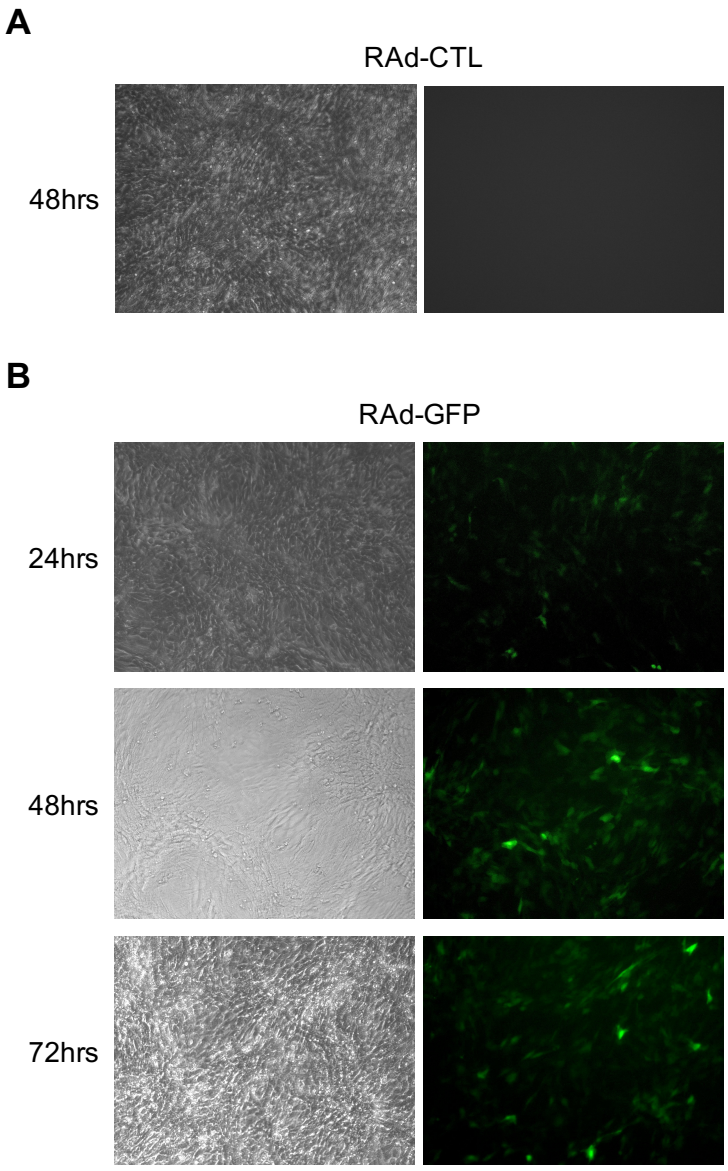

Figure 3.11 SGC1 infected RAds.

SGC1 cells were infected with **(A)** RAd-CTL and **(B)** RAd-GFP vectors at an MOI of 500 and examined for GFP expression at 24, 48 and 72 hours post-infection. Left-hand images: light microscopy images of cells infected with either virus. Right-hand images: fluorescence images of cells infected with either virus. All images were taken under x20 magnification.

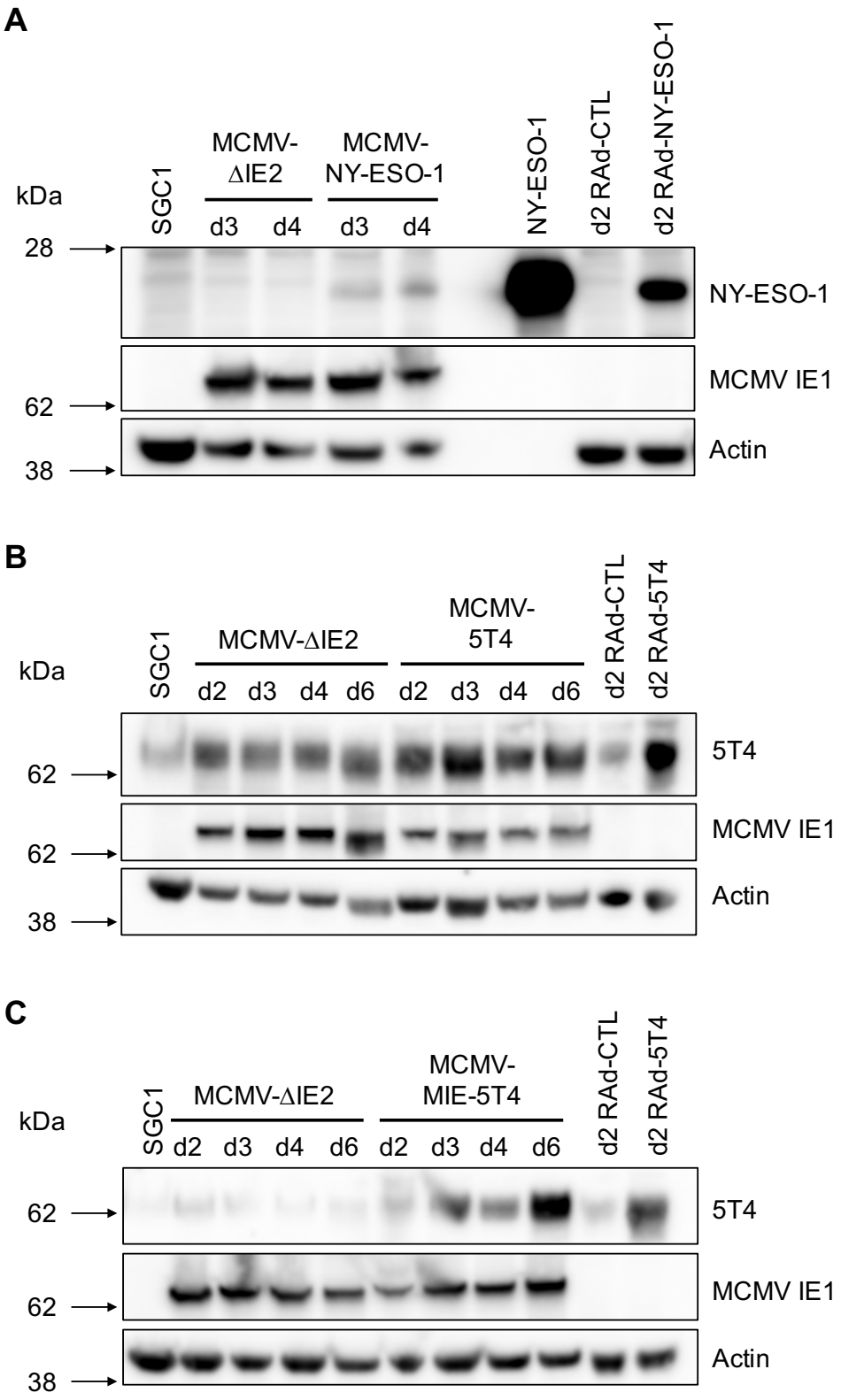
A
kDa
SGC1
MCMV-ΔIE2
MCMV-NY-ESO-1
d3 d4 d3 d4
NY-ESO-1
d2 RAd-CTL
d2 RAd-NY-ESO-1
28
62
38
NY-ESO-1
MCMV IE1
Actin
B
kDa
SGC1
MCMV-ΔIE2
MCMV-5T4
d2 d3 d4 d6 d2 d3 d4 d6
d2 RAd-CTL
d2 RAd-5T4
62
62
38
5T4
MCMV IE1
Actin
C
kDa
SGC1
MCMV-ΔIE2
MCMV-MIE-5T4
d2 d3 d4 d6 d2 d3 d4 d6
d2 RAd-CTL
d2 RAd-5T4
62
62
38
5T4
MCMV IE1
Actin

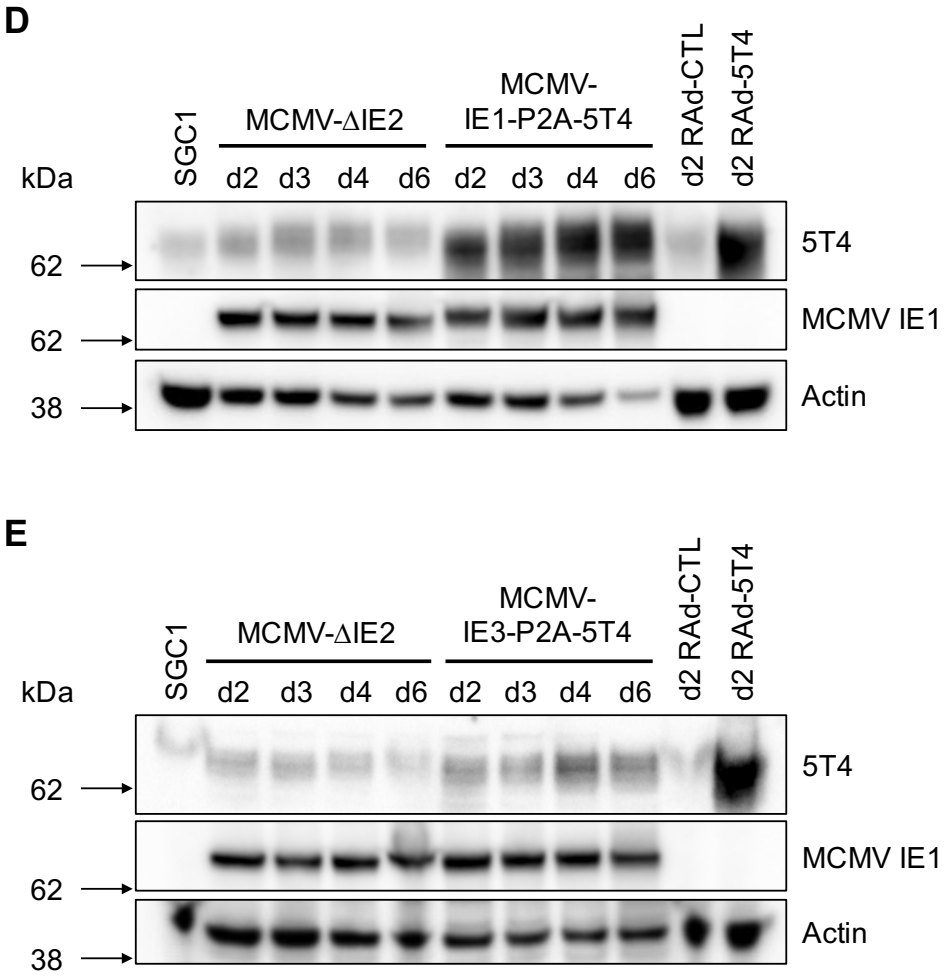

Figure 3.12 Expression of NY-ESO-1 and 5T4 by the viral vectors.

SGC1 cells were infected with the MCMV vectors at an MOI of 0.1 and the RAd vectors at an MOI of 500. Cell lysates were prepared at day 2, 3, 4 and 6 p.i and samples separated by SDSPAGE and transferred to a nitrocellulose membrane. NY-ESO-1 and 5T4 were detected using the respective antibodies. Membranes were stripped and re-probed for MCMV IE1 and actin. MCMV-ΔIE2 and RAd-CTL lysates were used as negative controls. **(A)** MCMV-NY-ESO-1 and RAd-NY-ESO-1 lysates along with 50ng of NY-ESO-1 protein, **(B)** MCMV-5T4 lysates, **(C)** MCMV-MIE-5T4 lysates, **(D)** MCMV-IE1-P2A-5T4 lysates and **(E)** MCMV-IE3-P2A-5T4 lysates.

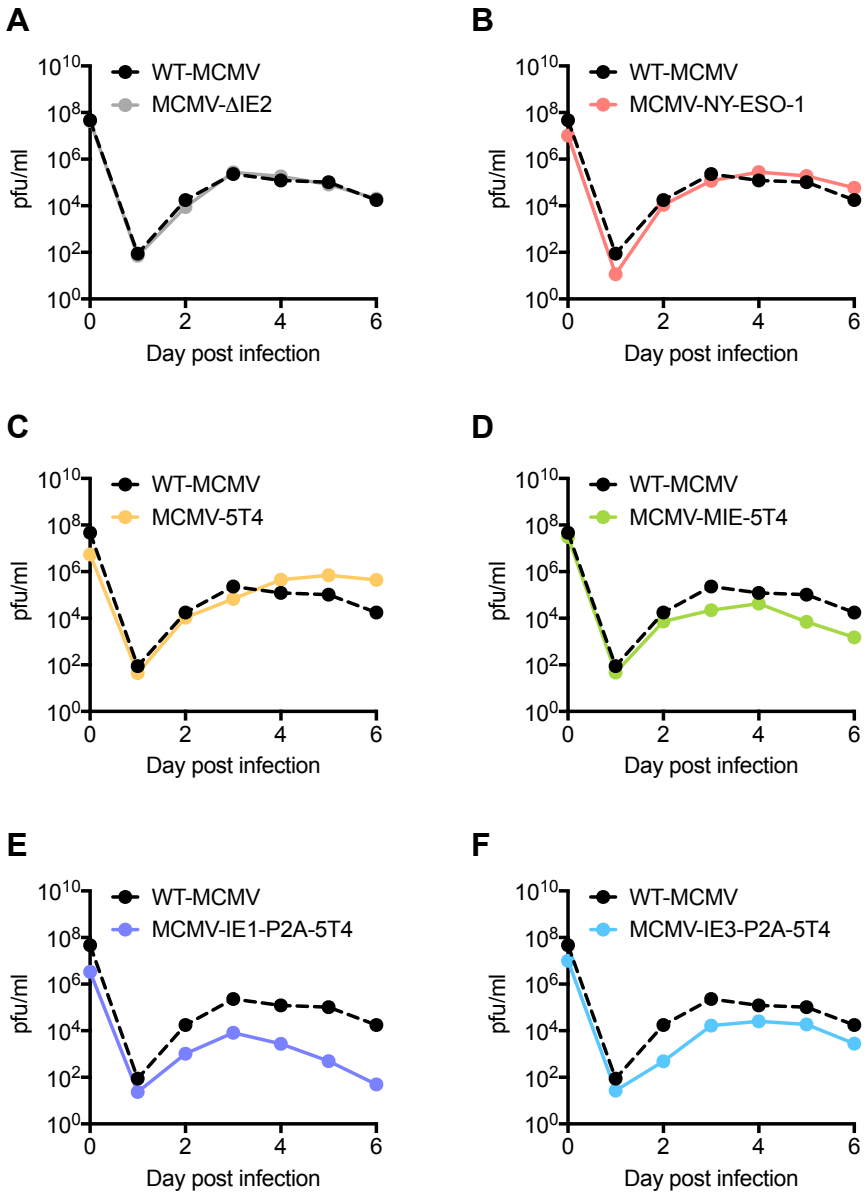

Figure 3.13 Growth curve analysis of the MCMV vectors generated.

NIH-3T3 cells were infected with **(A)** MCMV-ΔIE2, **(B)** MCMV-NY-ESO-1, **(C)** MCMV-5T4, **(D)** MCMV-MIE-5T4, **(E)** MCMV-IE1-P2A-5T4 and **(F)** MCMV-IE3-P2A-5T4 at an MOI of 0.1. **(A-F)** The same WT-MCMV infection was used as a control for all vectors generated. Supernatants from infected cultures were collected at the time points shown and virus was quantified by plaque assay. Data shown as mean ± SEM from two different assays.

3.3 Discussion

Initially, MCMV vectors expressing NY-ESO-1 and 5T4 were constructed with the tumour-associated antigens expressed directly downstream of the MCMV *ie2* promoter, replacing the *ie2* ORF – MCMV-NY-ESO-1 and MCMV-5T4, respectively. Growth curve analysis revealed that the replicative nature of the MCMV vector was not affected by the insertion of genes at this site (Figure 3.13B&C). Although the expression of 5T4 and NY-ESO-1 by their respective vectors could be detected by western blot (Figure 3.12A&B), the level of expression observed appeared to be quite low. Regarding NY-ESO-1, its expression by the MCMV vector was much lower compared to that expressed by the RAd vector. This could be due to RAd expression of the tumour-associated antigen being driven by the HCMV MIE promoter, which is a known strong constitutive promoter; thus, the endogenous *ie2* promoter might not be as strong in driving NY-ESO-1 expression in the MCMV vector. In relation to the expression of 5T4 by the MCMV-5T4 vector, the western blot showed that although 5T4 was detected, 5T4 background level was high, most probably due to the high exposure time used (Figure 3.12B), suggesting that MCMV-5T4 expressed 5T4 at low levels as observed with MCMV-NY-ESO-1. Furthermore, in addition to a weaker promoter driving 5T4 and NY-ESO-1 expression in the MCMV vectors, the tumour associated antigens might be degraded quickly, consequently resulting in low levels detected by western blot.

Several groups have developed recombinant MCMVs expressing the gene of interest placed under the control of the HCMV MIE promoter and cloned in between the two *Hpa*I sites of the *Hind*III-L fragment, within *ie2* exon 1 (430, 432, 433). Hence, a new construct was generated to maximise the expression level of 5T4, with the HCMV MIE promoter driving 5T4 expression, replacing the whole *ie2* ORF, and thus still being downstream of the enhancer and not influencing the inflationary properties of the region – MCMV-MIE-5T4. The introduction of the HCMV MIE promoter did not affect viral

replication as assessed by growth curve assay (Figure 3.13D) and expressed 5T4 to higher levels than that observed by the MCMV-5T4 vector (Figure 3.12B&C). In addition, two more MCMV vectors expressing 5T4 were generated. For these two vectors, 5T4 was fused to the end of *ie1* or *ie3* and consequently, under the control of the endogenous promoter – MCMV-IE1-P2A-5T4 and MCMV-IE3-P2A-5T4, respectively. Although 5T4 was detectable by western blot in samples infected with both vectors, a higher expression of the tumour-associated antigen was observed in cells infected with MCMV-IE1-P2A-5T4 than with MCMV-IE3-P2A-5T4 (Figure 3.12D&E). This correlates with published data where IE1 was observed to be the most abundant protein of the IE gene products (456). Furthermore, while MCMV-IE3-P2A-5T4 replicated to similar titres as WT-MCMV, MCMV-IE1-P2A-5T4 replication was hampered (Figure 3.13E&F), indicating that fusing 5T4 to the end of *ie1* might be interfering with its function, resulting in reduced replicative capacity. IE1 has been reported to act as an activator of gene expression for genes expressed later in the infection cycle, thereby promoting lytic replication of CMV (457). However, different groups have reported opposite results when examining the role of IE1 in MCMV replication – one states that an MCMV with the *ie1* gene knocked out grew at similar rates as the parental WT-MCMV (458); while another observed slightly impaired growth kinetics in an MCMV with a truncated *ie1* gene (438).

Overall, RAd and several MCMV vectors were successfully generated to express either 5T4 or NY-ESO-1. Western blots indicated the importance of the insertion site, as well as the promoter, to achieve an adequate level of gene expression. Different degrees of protein expression might influence the magnitude of immune responses induced by the MCMV vectors; thus, all the MCMV vectors generated were tested for anti-tumour responses *in vivo* and experiments are described in Chapter 4.

Chapter 4 - Examining the immunogenicity and efficacy of MCMV vectors expressing tumour-associated antigens

4.1 Introduction

4.1.1 Viral vector-based cancer vaccines

In cancer, there is a strong association between $CD8^+$ T cells and overall patient survival. For an effective T cell-based cancer vaccine, the viral vector must be able to overcome immune tolerance and induce a strong tumour-specific $CD8^+$ T cell response that recognises the tumour-associated antigen with high avidity and can infiltrate the tumour tissue. Once there, T cells must be able to overcome the immunosuppressive tumour environment and remain active. Results from clinical trials examining viral-based cancer vaccines encoding tumour-associated antigens that aimed to generate a strong tumour-specific $CD8^+$ T cell immune response have been modest (459, 460).

4.1.1.1 Current viral-based vaccines targeting 5T4 and NY-ESO-1

The rationale for the development of vaccines that induce immune responses reactive to 5T4 and NY-ESO-1 is underpinned by the high expression of these antigens in a wide range of human carcinomas, while their expression in healthy tissues is restricted to germ-line cells (refer to Chapter 1, section 1.2.4). Several clinical studies have described a correlation between 5T4- and NY-ESO-1- expressing tumours with disease progression and worse clinical outcome in human carcinomas (100–102, 461–

463). Furthermore, T cells specific for 5T4 and NY-ESO-1 have been detected in cancer patients and they have been associated with better prognosis (114, 121–123). In addition, reports have demonstrated the ability of 5T4 specific and NY-ESO-1 $CD8^+$ T cells to lyse 5T4- and NY-ESO-1- expressing tumour cells, respectively (257, 464). Together, these data show the potential therapeutic importance of enhancing anti-5T4 and anti-NY-ESO-1 specific responses in cancer patients.

The first viral vector targeting 5T4 was reported more than a decade ago – human 5T4 expressed by MVA (trade name: TroVax). In preclinical studies using a mouse model of colorectal cancer, MVA-5T4 was able to protect against intravenous (i.v) tumour challenge, albeit tumour-specific T cells were not detected. However this was not as effective as active therapy when administered after tumour establishment (465). In clinical studies, TroVax has been tested as a homologous prime-boost vaccine, with or without other anti-tumour therapies, in patients with renal, prostate and colorectal cancer (reviewed in (466)). Although TroVax had a good safety profile, tumour-specific $CD8^+$ T cell responses and clinical efficacy were modest (466). Results showed a trend towards improved progression-free survival in those patients with highest 5T4-specific antibody titers (466). Importantly, early phase trials with TroVax reported that 5T4-specific immune responses, in particular T cells, induced by MVA-5T4 were often transient (263, 264), resulting in the need for ongoing booster immunisations. Lastly, a phase III clinical trial where patients with renal cancer where given MVA-5T4 + IL-2 or IFN-α did not show any overall survival benefit compared to placebo + IL-2 or IFN-α (467).

Prime-boost immunisation with recombinant vaccinia and fowlpox viruses expressing NY-ESO-1 have been evaluated in patients with various advanced solid tumours. The vectors were well tolerated and induced humoral and cellular immune responses in most of the candidates following four vaccinations (257). This anti-tumour therapy is still in its early stages with only one phase II clinical trial having been conducted –

immunisation of patients with melanoma and epithelial ovarian cancer at high risk of recurrence demonstrated some clinical improvement (468).

Homologous prime-boost immunisation with VV or MVA is not ideal as the host will develop neutralising antibodies against the vector, rendering it less effective in subsequent immunisations. Although, boosting with fowlpox virus can overcome this problem, the immune response elicited is not as robust as with VV. Hence, new viral vectors that induce a strong tumour-specific immune response with a single immunisation or that can still elicit an immune response in subsequent boosting vaccinations without being targeted by the host immune system would be beneficial.

4.1.2 Cytomegalovirus as a cancer vaccine vector

In recent years, new viral vectors have emerged aiming to exploit the viruses' properties in order to improve the vaccine's immunogenicity and efficacy. As discussed in detail in section 1.4.4 (Chapter 1), CMV-based vaccines represents a promising vaccine vector platform. Briefly, CMV vectors are unique in that they are potent inducers of immune responses, with some MCMV-specific T cells remaining at high frequencies for the life of the host. Furthermore, CMV induces effector memory T cells that are widely distributed in lymphoid and non-lymphoid organs. Consequently, a CMV vaccine could target metastasis in different organs. In addition, CMV seropositive individual can become re-infected with CMV and still elicit a strong immune response. Importantly, it has been demonstrated that MCMV can break tolerance in mice. Thus, it is possible that a CMV vector expressing 5T4 or NY-ESO-1 will be able to induce a robust tumour-specific $CD8^+$ T cell response.

4.1.3 Aims

The aims of this chapter were the following:

1. To examine the immunogenicity of 5T4- and NY-ESO-1-expressing MCMV vectors;
2. Examine whether priming and boosting with RAd expressing tumour-associated antigen enhances the immune response against the tumour-associated antigen;
3. Investigate the protective capacity of 5T4- and NY-ESO-1- expressing vectors against tumour challenge.

4.3 Results

4.3.1 Immunogenicity and protective efficacy of MCMV-NY-ESO-1

4.3.1.1 Single inoculation with MCMV-NY-ESO-1 does not induce detectable NY-ESO-1-specific CD8$^+$ T cell responses

The recombinant MCMV-NY-ESO-1 vector was first tested *in vivo* for its ability to induce CD8$^+$ T cell immune responses reactive to the tumour-associated antigen. Immunogenicity studies were performed in H-2^d-restricted mice (BALB/c) as BALB/c mice are able to develop a more robust CD8$^+$ T cell response to NY-ESO-1 compared to C57BL/6 mice (469). Mice were inoculated intraperitoneally with a single dose of 2x10^5 pfu of MCMV-NY-ESO-1. Naïve mice were used as control. Blood was withdrawn from the lateral tail vein at different time points for a period of 6 months, when mice were sacrificed and the spleens harvested to analyse T cell responses via 6-hour *ex vivo* stimulation with NY-ESO-1 immunodominant peptide (NY_{81-88}) and MCMV control peptide (pp89).

The MCMV-NY-ESO-1 vector induced a robust CD8$^+$ T cell response in the peripheral blood and in the spleen (Figure 4.1). A strong immune response against pp89 was detected, which followed the pattern of memory inflation in the periphery blood with an initial peak of 5.4% pp89-specific CD8$^+$ T cells that contracted slightly to ~4% at week 5 post-infection (p.i) but increased by week 12 and remained at high frequency thereafter (Figure 4.2A). Levels of pp89-specific CD8$^+$ T cells reached comparable levels to published data (400), indicating that MCMV-NY-ESO-1 vector was functional, which correlated with the *in vitro* growth assay (Chapter 3). In contrast, MCMV-NY-ESO-1 did not generate a detectable CD8$^+$ T cell response against NY_{81-88} in the peripheral blood nor in the spleen (Figure 4.2B&C). In addition, splenocytes were

stimulated with NY-ESO-1 peptide pool and analysed for $CD4^+$ T cell responses. Although no significant difference was observed in the total numbers of splenic $CD4^+$ T cells (Figure 4.3A), a $CD4^+$ response towards the peptide pool was detected in the spleen of the vaccinated mice (Figure 4.3B). Moreover, these NY-ESO-1-specific $CD4^+$ T cells were polyfunctional, producing both IFN-γ and TNF-α (Figure 4.3C). Thus, although the MCMV-NY-ESO-1 vector was not able to induce NY-ESO-1-specific $CD8^+$ T cells, it did induce NY-ESO-1-specific $CD4^+$ T cells that might aid NY-ESO-1-specific $CD8^+$ T cell activation during tumour challenge and/or may have a direct anti-tumoural function.

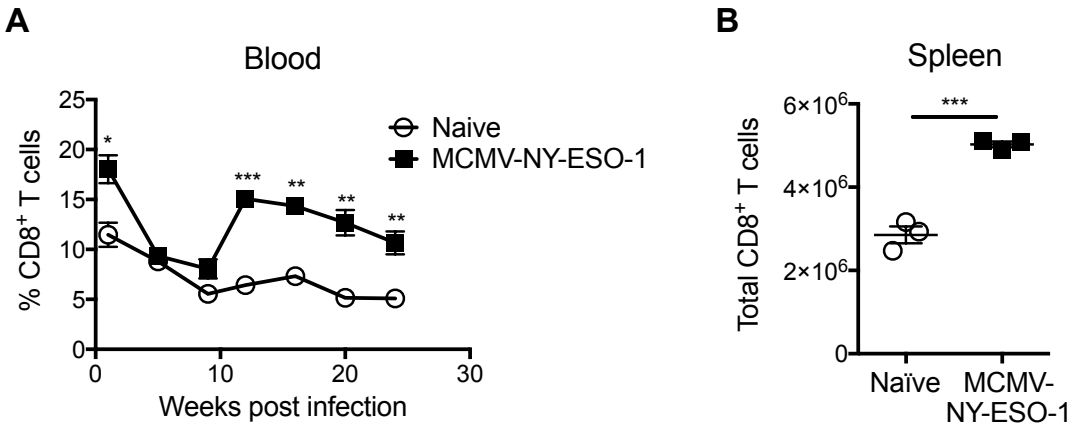

Figure 4.1 Systemic challenge with MCMV-NY-ESO-1 induces $CD8^+$ T cell responses.

BALB/c mice were challenged i.p with $2x10^5$ pfu MCMV-NY-ESO-1. Naïve mice were used as control. **(A)** Blood was taken from the lateral tail vein at week 1, 5, 9, 12, 16, 20 and 24 p.i. Cells were stained for CD8α to obtain frequency of $CD8^+$ T cells in the peripheral blood. Data shown as mean ± SEM (n=3 mice/group). Significance was assessed by unpaired *t* test on individual time points. **(B)** At week 26 p.i mice were culled, spleens were harvested and processed into single cell suspension. Cells were stained for CD8α to obtain total number of $CD8^+$ cells in the spleen. Data shown as individual mice with mean ± SEM (n=3 mice/group). Significance was assessed by unpaired *t* test. *p<0.05, **p<0.01 and ***p<0.005.

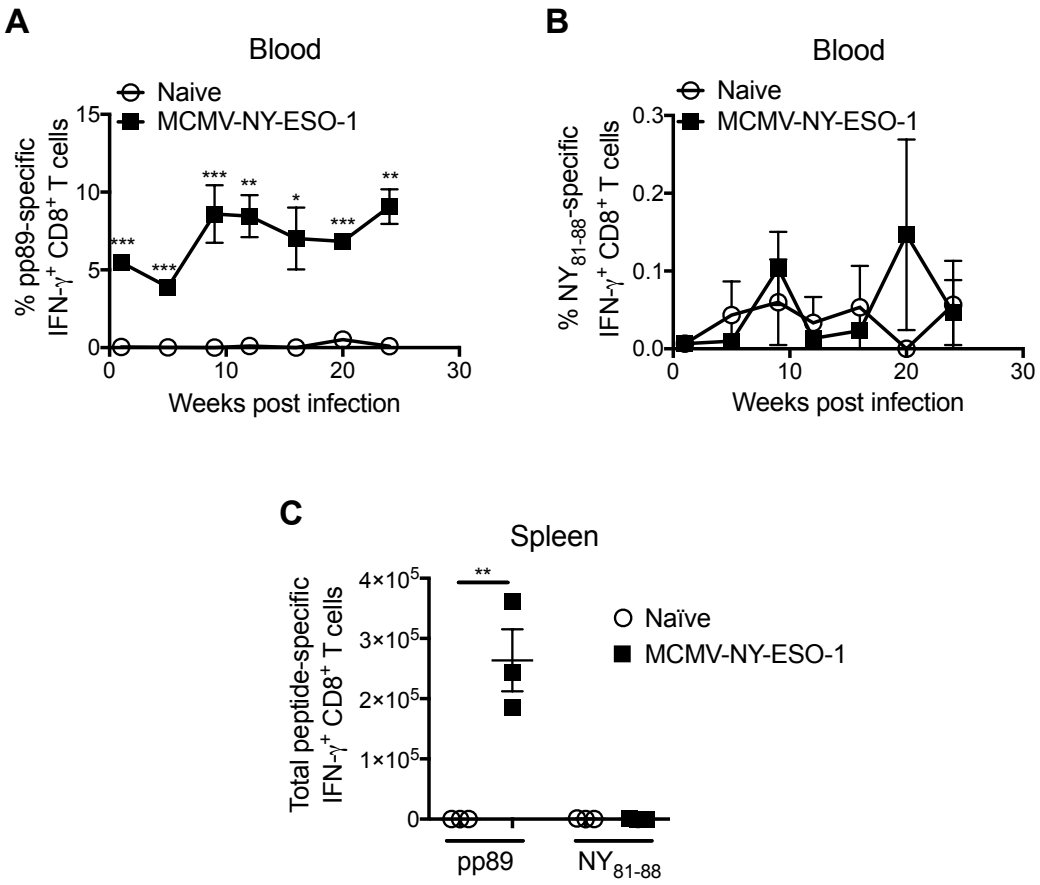

Figure 4.2 Systemic infection with MCMV-NY-ESO-1 does not induce detectable levels of NY_{81-88}-specific $CD8^+$ T cells.

BALB/c mice were infected i.p or not with $2x10^5$ pfu MCMV-NY-ESO-1. **(A&B)** Blood was withdrawn at week 1, 5, 9, 12, 16, 20 and 24 p.i and **(C)** at week 26 splenocytes were isolated. All cells were stimulated *ex vivo* with pp89 or NY_{81-88} for 6 hours and then stained for CD8α and IFN-γ to measure virus- and tumour- specific T cell responses. Data is expressed as **(A)** % pp89- or **(B)** % NY-ESO-1- specific cells in the blood and **(C)** total numbers of pp89- and NY-ESO-1- specific $CD8^+$ T cells in the spleen. Data is shown as **(A&B**) mean ± SEM or **(C)** as individual mice with mean ± SEM (n=3 mice/group). Significance was assessed by unpaired *t* test on individual time points. *p<0.05, **p<0.01 and ***p<0.005.

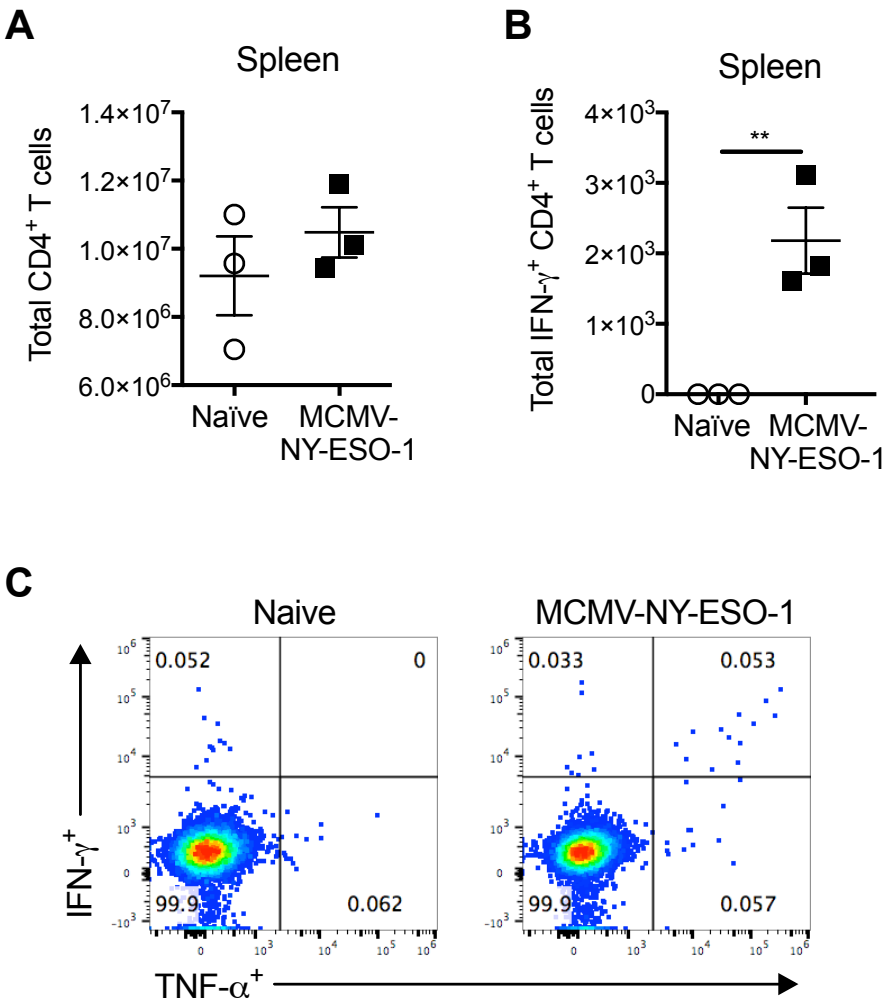

Figure 4.3 Systemic infection with MCMV-NY-ESO-1 induces detectable levels of NY-ESO-1-specific CD4$^+$ T cells in the spleen.

(A-C) BALB/c mice were infected i.p or not with 2x10^5 pfu MCMV-NY-ESO-1 and culled at week 26. Spleens were harvested and processed into single cell suspension. Cells were stimulated *ex vivo* with NY-ESO-1 peptide pool for 6 hours and then stained for CD4, IFN-γ and TNF-α to measure NY-ESO-1-specific CD4$^+$ T cell responses. **(A)** Total numbers of CD4$^+$ and **(B)** IFN-γ$^+$ CD4$^+$ T cells in the spleen. Data shown as individual mice with mean ± SEM (n=3 mice/group). Significance was assessed by unpaired *t* test. **p<0.01. **(C)** Representative flow cytometry plots showing IFN-γ and TNF-α expression by CD4$^+$ T cells stimulated with NY-ESO-1 peptide pool. Data is representative of 3 mice per group.

4.3.1.2 Prime-boost immunisation using recombinant adenovirus and/or MCMV induces a robust, long-lived NY-ESO-1-specific CD8$^+$ T cell response

Clinical studies have demonstrated an association between tumour-specific immune responses and increased progression-free survival in addition to overall survival in patients with cancer (114, 121–123). Current cancer vaccines, such as DNA- and peptide- based vaccines, induce modest anti-tumour T cell responses on their own, but these responses can be augmented when such vaccines are used in combination with other cancer therapies, including other immunisation strategies in a prime-boost regimen (221, 230, 269). Adenoviruses have been proven to be effective in prime-boosting strategies due to their ability to induce potent CD8$^+$ T cell responses in preclinical and clinical studies (230, 470). Hence, to improve the CD8$^+$ T cell response against NY-ESO-1 a prime-boost immunisation approach using recombinant adenovirus expressing the same tumour-associated antigen (RAd-NY-ESO-1) was investigated.

BALB/c mice were primed with either RAd-NY-ESO-1 or MCMV-NY-ESO-1 and 31 days later boosted with either viral vector. PBS was used as a control. Immune responses were measured at various time points post-boost to study the response kinetics. Figure 4.4A shows the experimental design. At day 7 post-boost, circulating lymphocytes were examined for NY_{81-88} reactivity. Surprisingly, those mice receiving RAd-NY-ESO-1 + RAd-NY-ESO-1 exhibited a large response against the NY_{81-88} peptide, reaching approximately 30% of CD8$^+$ T cells (Figure 4.4B&C). Furthermore, RAd-NY-ESO-1 alone also induced a strong NY_{81-88}-specific CD8$^+$ T cell response with a mean response of 21% NY-ESO-1 specific CD8$^+$ T cells (Figure 4.4B&C). Mice immunised with the combination of vectors, RAd-NY-ESO-1 + MCMV-NY-ESO-1 and vice versa, displayed a lower frequency of NY_{81-88}-specific CD8$^+$ T cells compared to the aforementioned groups – 10% and 8%, respectively (Figure 4.4B&C). In all the groups exhibiting an NY_{81-88}-specific CD8$^+$ T cell response, the majority of cells

secreting IFN-γ also produced TNF-α (Figure 4.4C), indicating that prime-boost immunisation has the ability to induce highly functional $CD8^+$ T cells against tumour-associated antigens.

NY_{81-88}-specific $CD8^+$ T cell responses were further analysed at day 29 post-boost to examine the persistence of the response. All immunised mice exhibiting an immune response against NY_{81-88} at day 7 post-boost still had NY_{81-88}-specific effector $CD8^+$ T cells present in the circulation at day 29 post-boost (Figure 4.5A). However, over this time the frequency of NY_{81-88}-specific $CD8^+$ T cell responses significantly decreased in all the immunised groups except for that primed with MCMV-NY-ESO-1 and boosted with RAd-NY-ESO-1, which maintained frequencies comparable with those measured 7 days after vaccination (Figure 4.5B). Consequently, RAd-NY-ESO-1 + RAd-NY-ESO-1, which initially induced the highest response at day 7 post-boost, resulted in comparable levels of NY_{81-88}-specific $CD8^+$ T cells as MCMV-NY-ESO-1 + RAd-NY-ESO-1 by day 29 post-boost. This suggests that priming with an MCMV vector may stabilise the magnitude of tumour-specific response. Furthermore, $CD4^+$ T cell responses were also examined at day 29 post-boost by stimulating circulating lymphocytes with NY-ESO-1 peptide pool. No significant differences were observed in the frequency of $CD4^+$ T cells in the peripheral blood of vaccinated mice (Figure 4.6A), but mice immunised with RAd-NY-ESO-1 + RAd-NY-ESO-1 exhibited significantly higher frequencies of NY-ESO-1-specific $CD4^+$ T cell responses in the circulation. Mice receiving MCMV-NY-ESO-1 + RAd-NY-ESO-1 and RAd-NY-ESO-1 + PBS also displayed some $CD4^+$ T cell responses, suggesting these were induced by the RAd-NY-ESO-1 vector (Figure 4.6B). In contrast and in accordance with data shown in section 4.3.1.1, single immunisation with MCMV-NY-ESO-1 did not induce detectable levels of NY_{81-88}-specific $CD8^+$ T cells or $CD4^+$ T cell responses in this experiment (Figure 4.5A and Figure 4.6B).

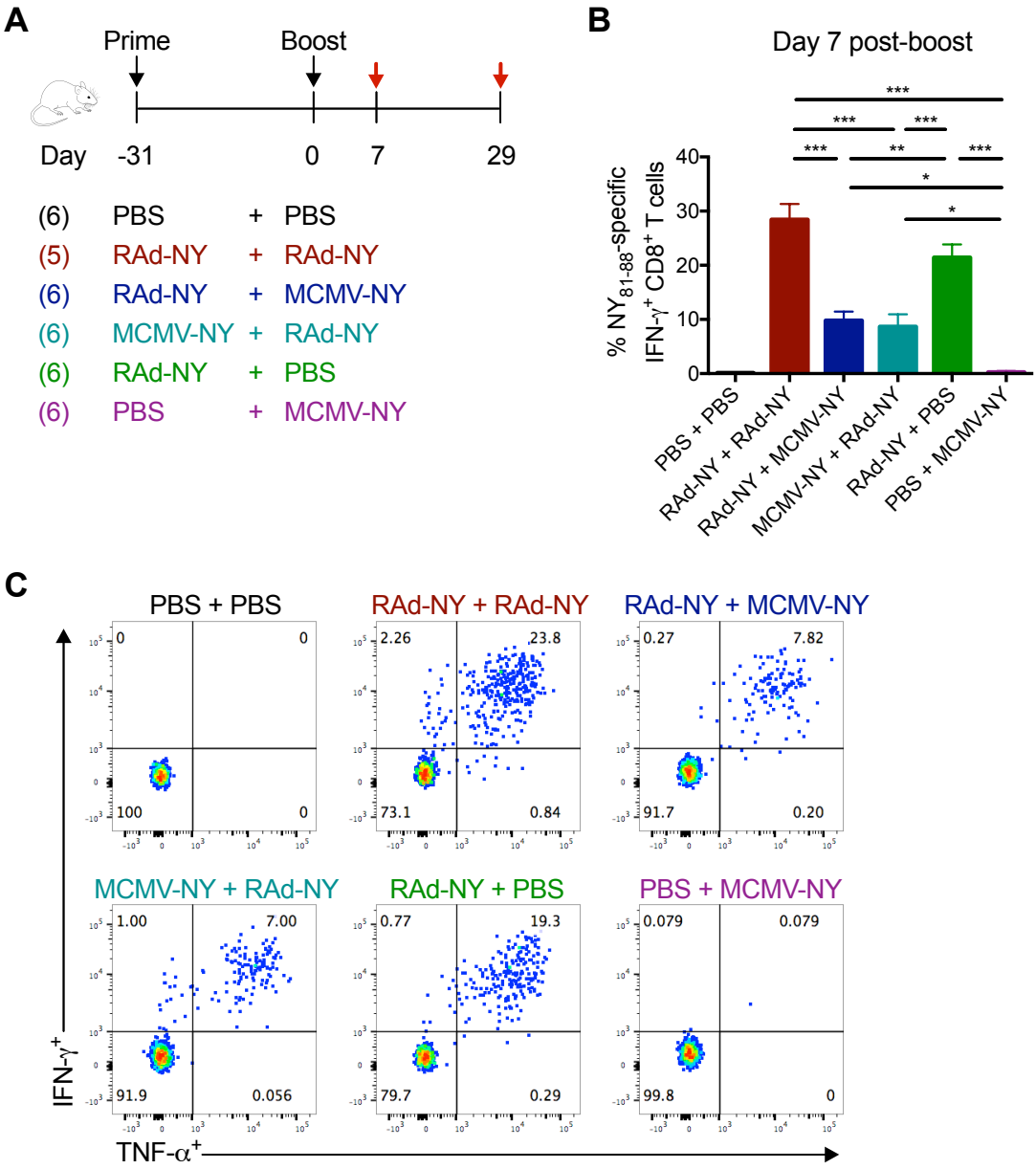

Figure 4.4 Sequential infection with RAd-NY-ESO-1 and MCMV-NY-ESO-1 induced detectable levels of NY_{81-88}-specific $CD8^+$ T cells.

BALB/c mice were immunised with either $5x10^8$ pfu RAd-NY-ESO-1 (RAd-NY) s.c or $2x10^5$ pfu MCMV-NY-ESO-1 (MCMV-NY) i.p, then 31 days later were boosted with either RAd-NY-ESO-1 or MCMV-NY-ESO-1. PBS was used as control. **(A)** Schematic of the experimental design. Numbers in brackets represent the number of mice in the corresponding group. Red arrows indicate when blood was withdrawn. **(B&C)** At day 7 blood was withdrawn from the lateral tail vein and stimulated *ex vivo* with NY_{81-88} peptide, followed by staining for CD8α, IFN-γ and TNF-α to measure tumour-specific responses. **(B)** Frequency of IFN-γ^+ $CD8^+$ T cells responding to NY_{81-88}. Data shown as mean + SEM (n=5-6 mice/group). Significance was assessed by one-way ANOVA with Bonferroni's correction for multiple comparisons. *p<0.05, **p<0.01 and ***p<0.005. **(C)** Representative flow cytometry plots showing IFN-γ and TNF-α expression of live, $CD8^+$ cells. Data is representative of 5-6 mice.

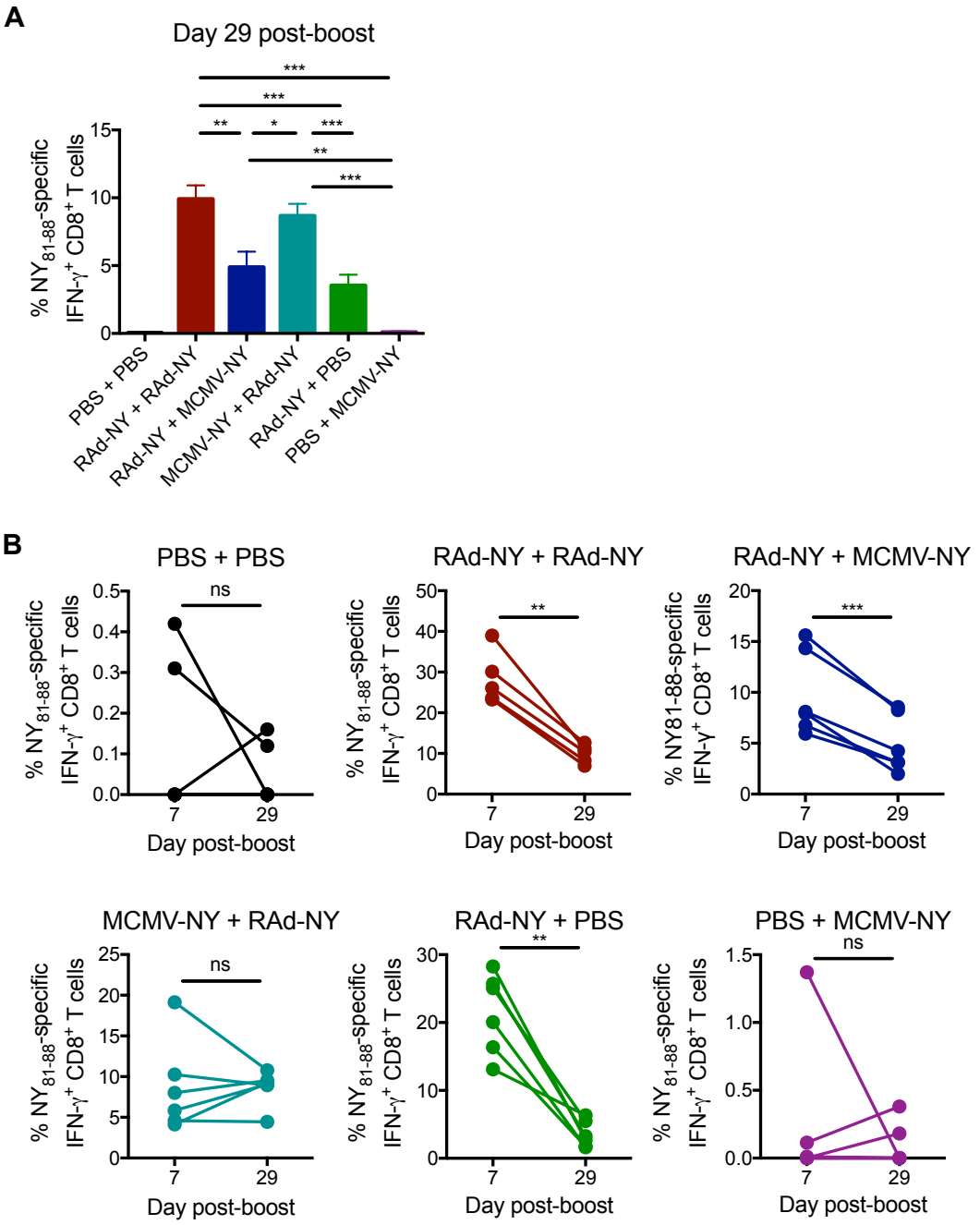

Figure 4.5 NY-ESO-1-specific CD8$^+$ T cells persist in the circulation 29 days after the boost.

Mice from the experiment described in Figure 4.4 were bled again at day 29 post-boost. Circulating lymphocytes were stimulated *ex vivo* with NY_{81-88} peptide, followed by staining for CD8α and IFN-γ to measure tumour-specific responses. **(A)** Frequency of IFN-γ^+ CD8$^+$ T cells responding to NY_{81-88}. Data shown as mean + SEM (n=5-6 mice/group). Significance was assessed by one-way ANOVA with Bonferroni's correction for multiple comparisons. **(B)** Frequency of NY_{81-88}-specific IFN-γ^+ CD8$^+$ T cells at day 7 and 29 post-boost in the different vaccinated groups. Data shown as individual mice. Paired *t* test was performed on the different vaccinated groups. *p<0.05, **p<0.01 and ***p<0.005.

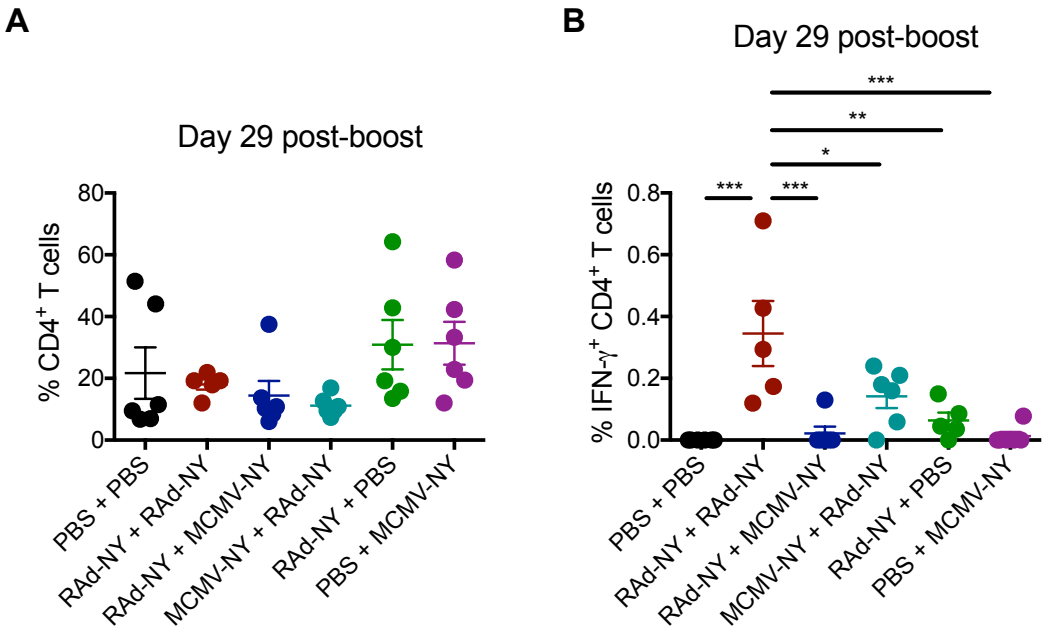

Figure 4.6 Prime-boost immunisation induces NY-ESO-1-specific CD4$^+$ T cells.

Circulating lymphocytes from the vaccinated mice in Figure 4.4 were obtained at day 29 post-boost and stimulated *ex vivo* with NY-ESO-1 peptide pool, followed by staining for CD4 and IFN-γ to obtain frequency of **(A)** CD4$^+$ T cells and **(B)** NY-ESO-1-specific CD4$^+$ T cell responses. Data shown as individual mice with mean ± SEM (n=5-6 mice/group). Significance was assessed by one-way ANOVA with Bonferroni's correction for multiple comparisons. *p<0.05, **p<0.01 and ***p<0.005.

4.3.1.3 Prime-boost immunisation delays tumour onset

In order to examine the protective efficacy of the RAd-NY-ESO-1 and MCMV-NY-ESO-1 vectors, vaccinated mice were injected subcutaneously with $1x10^5$ CT26-NY-ESO-1 cells in the left flank at day 31 post-boost – the full experimental timeline is shown in Figure 4.7. CT26-NY-ESO-1 cells were first palpable on day 5 after injection and were large enough to begin measuring on day 7 in the control group and the group receiving PBS + MCMV-NY. Tumours were measured three times a week using digital calipers, taking two perpendicular measurements across the tumours. CT26-NY-ESO-1 tumours grew in 91% (32 out of the 35 mice in the study) of injected mice. One of the mice that did not develop a tumour belonged to the control group (PBS + PBS), indicating that the injection was not successful and was removed from the study. Consequently, the other two mice that did not develop tumours (one from the group receiving RAd-NY-ESO-1 + MCMV-NY-ESO-1 and another from MCMV-NY-ESO-1 + RAd-NY-ESO-1) were also discarded from the study as it was not possible to know whether the tumours did not grow due to the vaccination or because of unsuccessful implantation of tumour cells. In addition, one mouse from the group receiving RAd-NY-ESO-1 + PBS had the tumour injected i.p. and so was also removed from the study. Due to rapid tumour growth, small necrotic areas prone to scabbing and ulceration were often observed in the centre of the tumour. Mice were checked every other day for the development of necrosis and were sacrificed if a crater-like appearance or discharge was observed. In addition, mice were sacrificed when the tumour measurement (either width or length) reached 15-16 mm.

Tumour volume was calculated to obtain tumour growth curves. The average tumour growth of each group until day 21 is shown in Figure 4.8A. After this point, mice bearing tumours with the above features were sacrificed, thus tumour growth curves from individual mice from each vaccinated group are shown in Figure 4.8B. In all the groups the tumours grew uniformly, however mice receiving prime-boost immunisations

regardless of the vectors, had a delay in tumour onset compared to control group. Mice in the control group started to develop measurable tumours at day 7 post-challenge, with all animals bearing measurable tumours by day 12 post-challenge (Figure 4.8B). Tumours in the mice receiving RAd-NY-ESO-1 either during priming or boosting were not measureable for 5 to 7 days later than the control group (at days 12 and 14 post-challenge), with some of the mice not developing measurable tumours past 21 days post-challenge (Figure 4.8B). Mice receiving PBS + MCMV-NY-ESO-1 developed measurable tumours 2 days later than control group, with some mice not developing measureable tumours until day 14 and 16 post-challenge (Figure 4.8B). As shown in Figure 4.8C, delay in measurable tumour development was statistically significant in those mice receiving RAd-NY-ESO-1, suggesting that the observed initial protection is dependent on the ability of the RAd-NY-ESO-1 vector inducing tumour-specific immune responses. Interestingly, once the tumour was established in the vaccinated mice, the growth rate was comparable to that of the control group (Figure 4.9). CT26-NY-ESO-1 cell line is derived from the colon carcinoma cell line CT26 and has been stably transfected with human NY-ESO-1. CT26-NY-ESO-1 is grown *in vitro* in the presence of the antibiotic G418 that selects for those cells expressing the resistance marker and thus, NY-ESO-1. Therefore, in the *in vivo* setting in the absence of selection pressure of the antibiotic, immune pressure on NY-ESO-1 expression by tumour cells may have led to tumour escape and loss of NY-ESO-1 expression. Consequently, the NY-ESO-1-specific effector $CD8^+$ T cells induced by the vaccines would no longer be able to target the tumour resulting in the out-growth of tumour cells that have lost NY-ESO-1 expression. To examine this further, a small fraction of the tumours from some mice were assessed for NY-ESO-1 expression. Although it is important to note that the blot does not have the appropriate controls, such as CT26 and CT26-NY-ESO-1 grown *in vivo* in unvaccinated mice, it suggests that the tumours that developed in the vaccinated mice are not expressing NY-ESO-1 at the time of sacrifice (Figure 4.10). This suggests that the transient protection afforded by

NY-ESO-1 expressing vaccines may be due to loss of NY-ESO-1 by CT26 tumour cells *in vivo*.

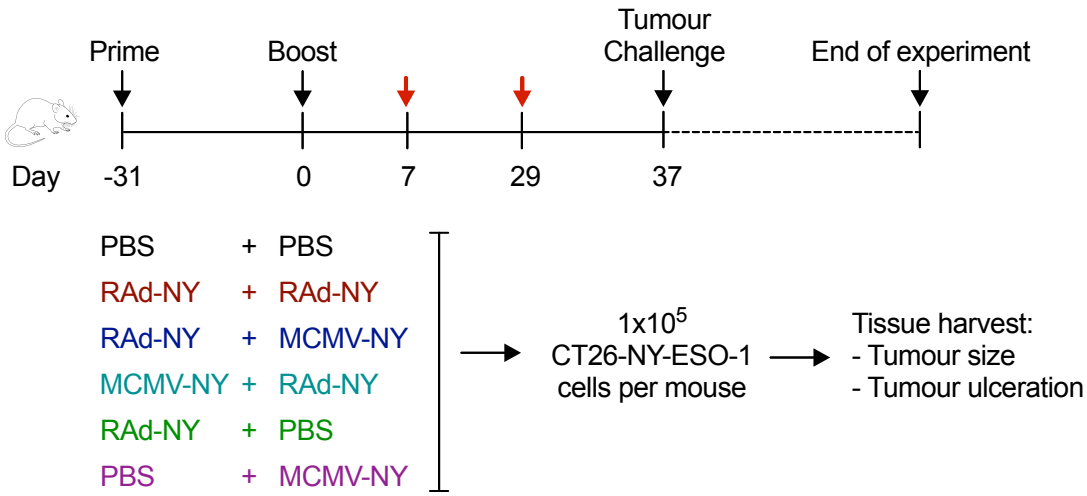

Figure 4.7 Experimental timeline investigating the protective efficacy of prime-boost NY-ESO-1 vaccination strategy.

The protective efficacy of the vaccines from the experiment shown in Figure 4.4 was examined by challenging the mice with $1x10^5$ CT26-NY-ESO-1 cells 37 days after the boost. Tumours were measured three times a week until the tumour grew to 15-16mm or became ulcerated, point at which mice were sacrificed. The tumour and the spleen of each mouse was harvested for further analysis.

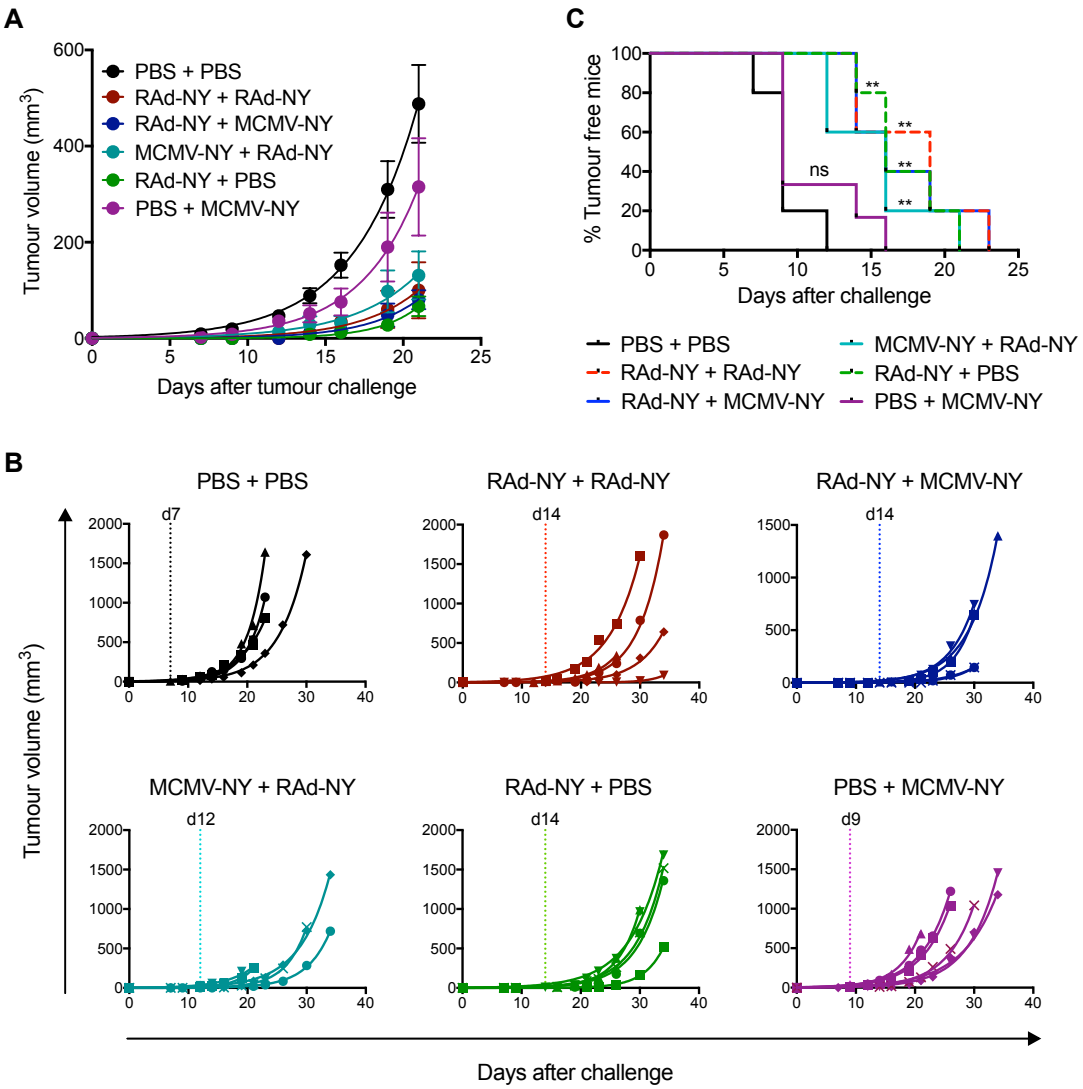

Figure 4.8 Prime-boost vaccination delays tumour onset.

BALB/c mice were immunised with either $5x10^8$ pfu RAd-NY-ESO-1 (RAd-NY) or $2x10^5$ pfu MCMV-NY-ESO-1 (MCMV-NY), then 31 days later were boosted with either RAd-NY-ESO-1 or MCMV-NY-ESO-1. PBS was used as control. Mice were challenged with $1x10^5$ CT26-NY-ESO-1 cells at day 37 post boost. Tumours were measured three times a week until mice were sacrificed. **(A)** Average tumour volumes over time up to day 21 post-challenge. Data shown as mean ± SEM (n=5-6 mice/group). **(B)** Tumour volume over time of individual mice in each vaccination group. Dotted vertical line represent the start of tumour measurements in the corresponding group. **(A&B)** The line through the set of measurements represents the best fit exponential growth of the tumour **(C)** Percentage of tumour-free mice. Significance relative to PBS + PBS was assessed by log-rank test; **p<0.01, ns = not significant.

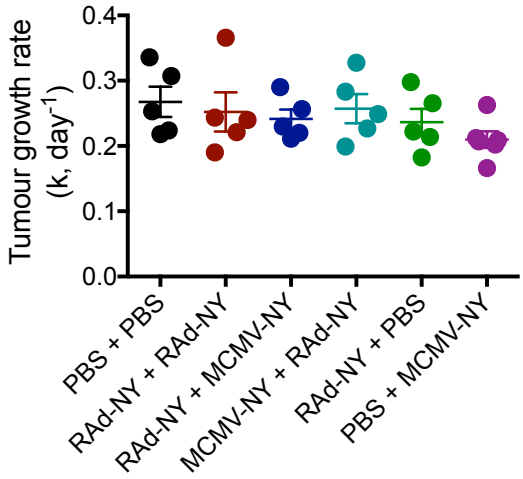

Figure 4.9 Vaccination does not affect tumour growth rate after tumour establishment.

Tumours were measured every other day during the length of the study shown in Figure 4.8 and tumour growth rates (k, days^{-1}) were calculated. Individual mice are depicted with mean ± SEM (n=5-6 mice/group).

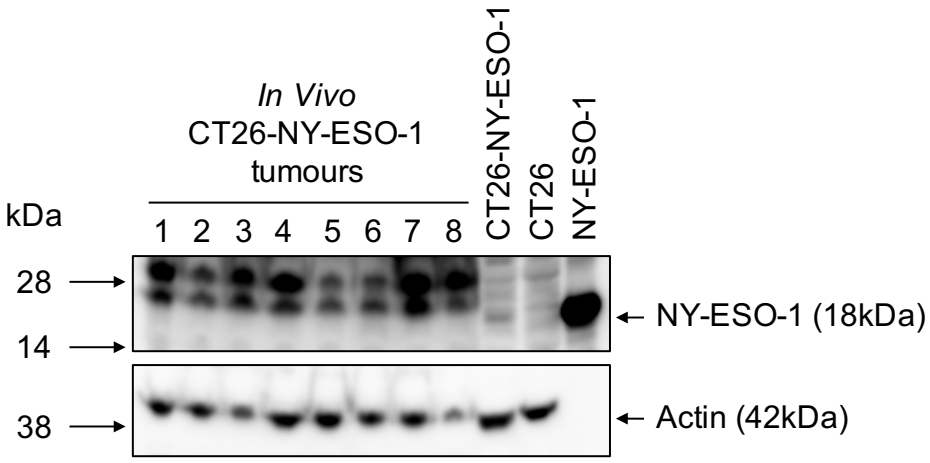

Figure 4.10 NY-ESO-1 expression by tumours *ex-vivo*.

Tumours from the experiment described in Figure 4.7 were homogenised and run on an SDSPAGE, followed by transfer to a nitrocellulose membrane. NY-ESO-1 was detected prior to membrane stripping and re-probing for actin. CT26-NY-ESO-1 cell lysate from *in vitro* culture and NY-ESO-1 protein was used as positive control and CT26 cell lysate from *in vitro* culture was used as a negative control. Lane 1 and 2: tumour lysates from mice receiving RAd-NY + RAd-NY; lane 3: RAd-NY + MCMV-NY; lane 4: MCMV-NY + RAd-NY; lane 5 and 6: RAd-NY + PBS; lane 7 and 8: PBS + MCMV-NY.

4.3.1.4 Prime-boost immunisation promoted the accumulation of tumour-infiltrating lymphocytes

Next, the extent to which $CD8^+$ T cell infiltration was associated with control of tumour onset was examined. At the point of sacrifice, tumours were harvested, processed into single cell suspensions and stained for CD8α, CD3 and with NY_{81-88}-tetramer. One mouse from the group receiving RAd-NY-ESO-1 + MCMV-NY-ESO-1 had to be eliminated from the study as the harvested tumour tissue had a blood clot attached to the tissue. A significant increase in the frequency of infiltrating $CD8^+$ T cells was observed in the tumours of all the vaccinated mice compared to control group (Figure 4.11A). Immunisation with either viral vector and in combination increased the frequency of NY_{81-88}-specific $CD8^+$ T cells within the tumours compared to control group receiving PBS + PBS, as measured by tetramer staining (Figure 4.11B&C). The combination of RAd-NY-ESO-1 + MCMV-NY-ESO-1 and RAd-NY-ESO-1 + PBS displayed a higher frequency of NY_{81-88}-specific TILs than the other vector combinations (RAd-NY-ESO-1 + RAd-NY-ESO-1 and MCMV-NY-ESO-1 + RAd-NY-ESO-1) (Figure 4.11B). This contrasts with the frequency of NY_{81-88}-specific $CD8^+$ T cells observed in the peripheral circulation before tumour challenge, where mice receiving RAd-NY-ESO-1 + MCMV-NY-ESO-1 and RAd-NY-ESO-1 + PBS displayed lower frequencies of NY_{81-88}-specific $CD8^+$ T cells as compared to RAd-NY-ESO-1 + MCMV-NY-ESO-1 and RAd-NY-ESO-1 + RAd-NY-ESO-1 (Figure 4.5A). Furthermore, the NY-ESO-1-specific $CD8^+$ T cells in all the vaccinated groups exhibited a higher frequency of effector memory cells ($CD44^+CD62L^-$) compared to control-vaccinated mice (Figure 4.12). Functional assays examining production of IFN-γ and TNF-α by tumour infiltrating NY-ESO-1-specific $CD8^+$ T cells could not be performed as most of the cells died after 6-hour *ex vivo* peptide stimulation. Furthermore, analysis of splenocytes is not presented because the PBS used during

the isolation process might have been compromised, resulting in a very low proportion of live cells. Consequently, the data obtained was not reliable.

To conclude, prime-boost vaccination with RAd-NY-ESO-1 and MCMV-NY-ESO-1 is a promising immunisation strategy as suggested by the delay in tumour onset and the high magnitude of tumour infiltrating $CD8^+$ lymphocytes in addition to the magnitude of effector memory tumour-specific $CD8^+$ T cells at the tumour site. Indeed, the protective efficacy of NY-ESO-1 specific T cell responses induced by these vaccines may be under-estimated by these experiments due to the possible loss of NY-ESO-1 by the tumour cell line used in these experiments. Thus, a better tumour model is needed to assess the full potential of RAd + MCMV prime-boost strategies.

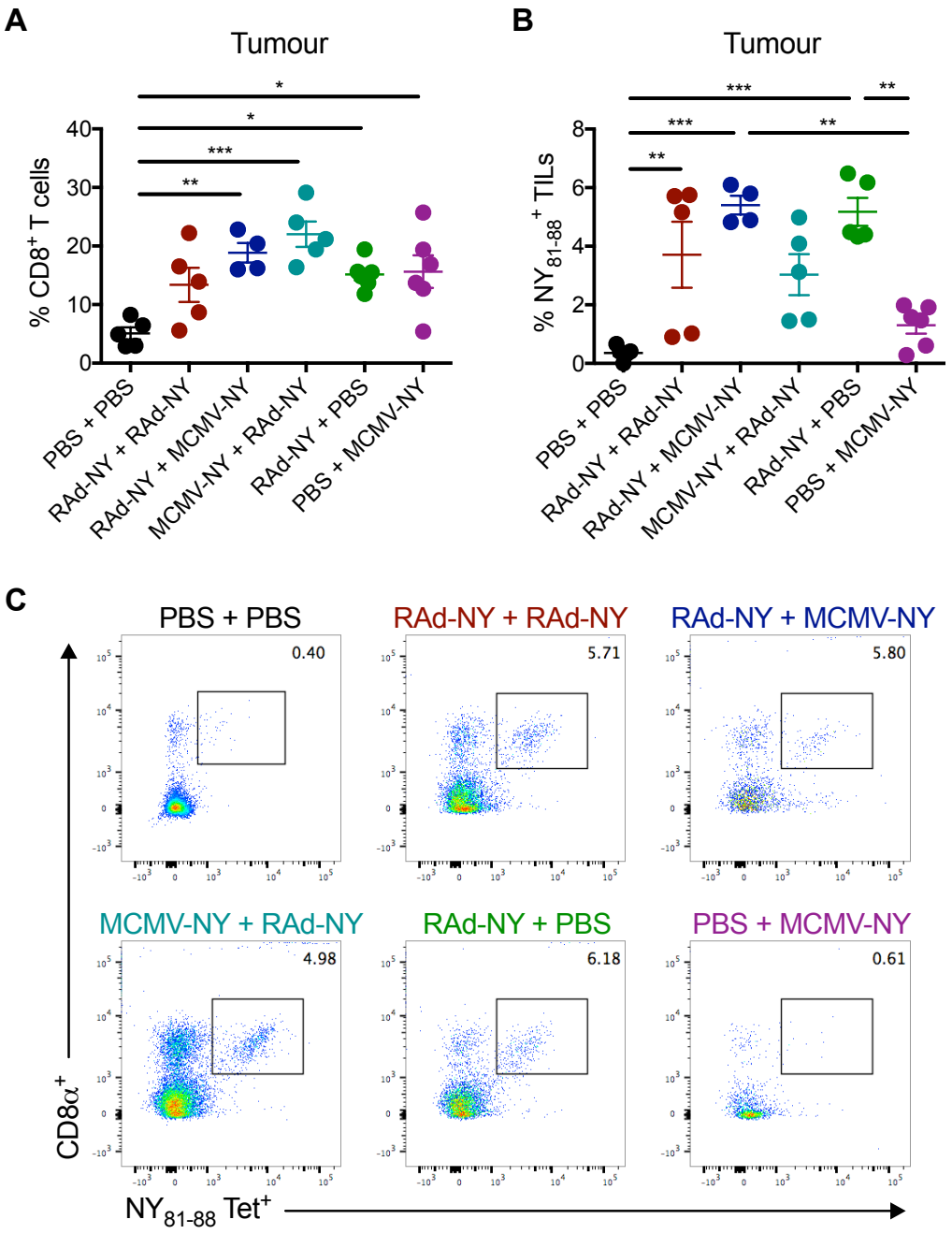

Figure 4.11 Vaccinated mice display a higher frequency of $CD8^+$ T cells and NY_{81-88}-specific tumour infiltrating lymphocytes in the tumour at time of sacrifice.

Vaccinated BALB/c mice bearing tumours from the study described in Figure 4.7 were sacrificed when the tumour reached 15-16mm in diameter or became ulcerated. Tumours were harvested and processed in single cell suspensions. Cells were stained for CD8α, CD3 and with NY_{81-88}-tetramer. **(A)** Frequency of $CD8^+$ $CD3^+$ T cells. **(B)** Frequency of NY_{81-88}-$tetramer^+$ $CD8^+$ T cells, gated on live cells. **(A&B)** Data shown as individual mice with mean ± SEM (n=4-6 mice/group). Significance was assessed by one-way ANOVA with Bonferroni's correction for multiple comparisons. *p<0.05, **p<0.01 and ***p<0.005. **(C)** Representative flow cytometry plots of CD8α versus NY_{81-88}-tetramer. Data is representative of 4-6 mice/group.

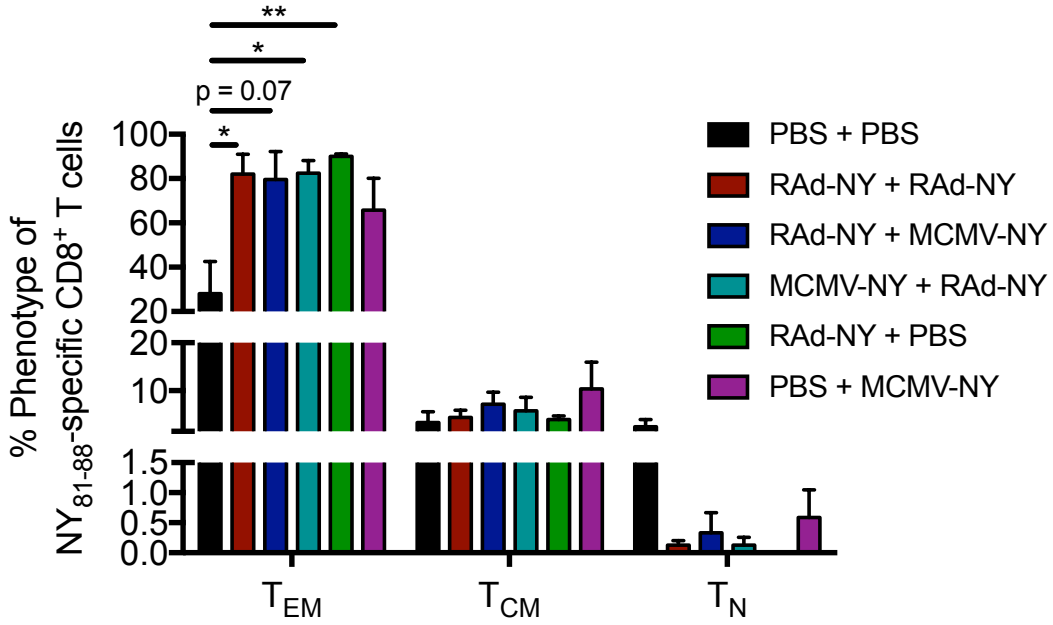

Figure 4.12 Vaccination with viral vectors induces tumour infiltrating NY-ESO-1-specific CD8$^+$ T_{EM} cells.

The phenotype of NY_{81-88}-specific CD8$^+$ T cells in the tumours from the experiment shown in Figure 4.11B was determined by co-staining cells with antibodies for CD44 and CD62L. Frequencies of effector memory (T_{EM}; CD44$^+$CD62L$^-$). central memory (T_{CM}; CD44$^+$CD62L$^+$) and naïve (T_N; CD44$^-$CD62L$^+$) cells of NY_{81-88}-tetramer$^+$ CD8$^+$ T cells are expressed as mean + SEM (n=4-6 mice/group). Significance was assessed by one-way ANOVA with Bonferroni's correction for multiple comparisons within the individual phenotypes (i.e. T_{EM}, T_{CM} and T_N). *p<0.05 and **p<0.01.

4.3.2 Immunogenicity and anti-tumour efficacy of 5T4-expressing MCMV vectors

4.3.2.1 MCMV-5T4 immunisation in BALB/c mice does not induce detectable 5T4-specific T cell responses

Unlike NY-ESO-1, the immunodominant $CD8^+$ T cell H-2^d restricted antigenic peptides from human 5T4 have not been mapped in BALB/c mice. This mouse strain was initially chosen to enable the study of the 4T1 cancer model in BALB/c, which has already been established by Prof. Gallimore's lab and shown to express 5T4 *ex vivo*. Furthermore, this model could be used to study both primary tumour development and metastasis. To map the T cell responses against 5T4, BALB/c mice were challenged with $2x10^5$ pfu MCMV-5T4. At day 7 post-infection, isolated splenocytes were used in an *ex vivo* IFN-γ ELISpot assay. Forty-one 20mer peptides, overlapping by 10 amino acids and covering the entire human 5T4 protein were combined into 13 pools as described in Materials and Methods (Chapter 2, section 2.15) and used to stimulate splenocytes. As shown in Figure 4.13A&B, a strong response towards the MCMV peptide pp89 was observed in those mice receiving MCMV-5T4. However, 5T4-specific responses could not be detected 7 days post-infection. An explanation might be that 5T4-specific T cells may be present at too low frequencies to be detected using this assay. In addition, a study using MCMV expressing an immunodominant epitope from the nucleoprotein of Ebola virus reported responses specific to the peptide inserted only after 8 weeks post-infection (428). Hence, a similar experiment was set up, assessing 5T4-specific responses at day 62 post-infection. Even at this later time point, T cells reactive to 5T4 were not detectable (Figure 4.13C) and it was concluded that the MCMV-5T4 vector could not induce a strong, detectable 5T4-specific T cell responses in BALB/c mice.

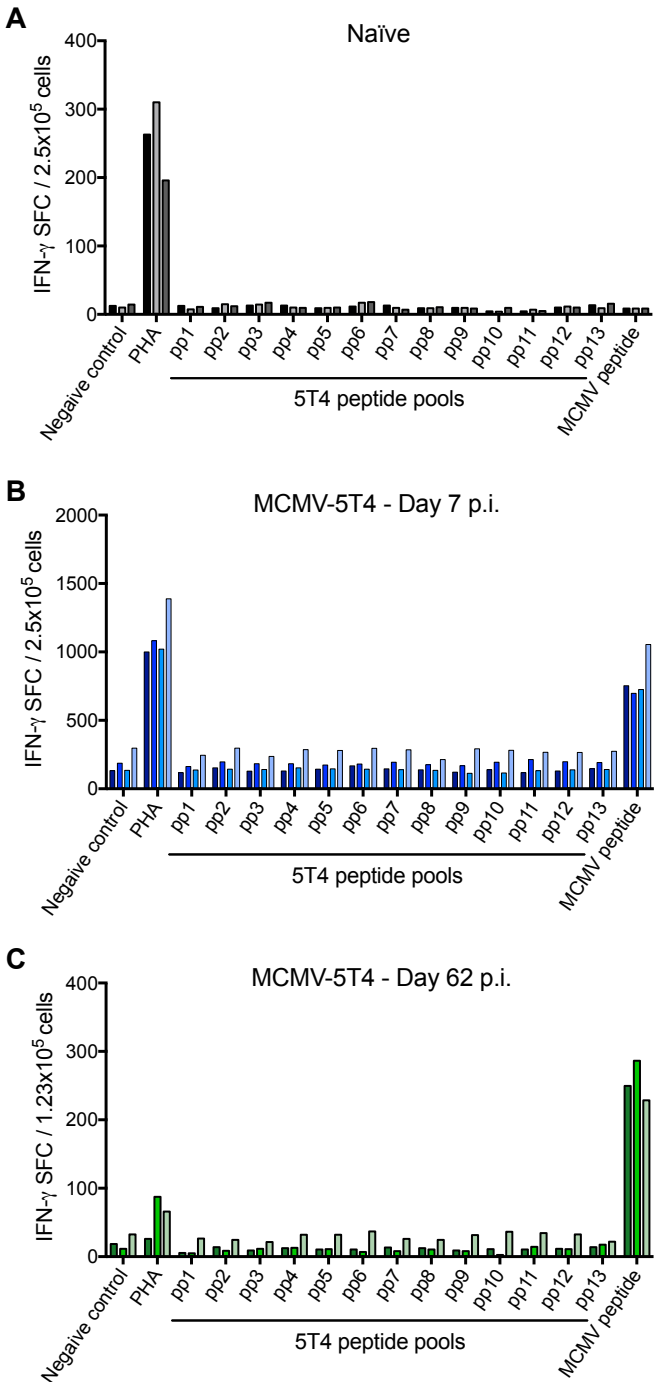

Figure 4.13 5T4-specific T cell responses after MCMV-5T4 challenge in BALB/c mice are not detectable.

BALB/c mice were challenged i.p with $2x10^5$ pfu MCMV-5T4 or left uninfected and spleens harvested **(A&B)** 7 days p.i or **(C)** 62 days p.i Splenocytes were isolated and stimulated overnight with a panel of 13 peptide pools covering the entire 5T4 sequence. IFN-γ production in response to the 5T4 peptide pools was enumerated by ELISpot assay. Media alone was used as a negative control, PHA was used as a positive control and the MCMV peptide pp89 was used as a vector control. **(A)** Naïve mice. **(B)** Day 7 MCMV-5T4 infected mice. **(C)** Day 62 MCMV-infected mice. Each bar represents an individual mouse and data is shown as mean spot forming cell (SFC) per $2.5x10^5$ or $1.23x10^5$ cells + SEM of duplicates.

4.3.2.2 Epitope mapping of human 5T4 in C57BL/6 and BALB/c mice using a RAd vector expressing 5T4

Given that the MCMV-NY-ESO-1 vector did not induce detectable NY-ESO-1-specific T cell responses upon single vector challenge (section 4.3.1.1) despite RAd-NY-ESO-1 inducing robust NY-ESO-1-specific $CD8^+$ T cell responses (section 4.3.1.2), the induction of 5T4-specific T cell responses in BALB/c mice was examined using RAd expressing 5T4. Thus, a colleague (Evelina Statkute) generated a RAd expressing human 5T4 (RAd-5T4) and mapped the immunodominant T cell responses to 5T4 in BALB/c mice. In parallel, she examined induction of 5T4-specifc T cell responses in C57BL/6 mice. Mice were primed and boosted with $5x10^8$ pfu of either RAd-CTL or RAd-5T4 prior to tissue harvest. Splenocytes were stimulated overnight with pools of 20mer 5T4 peptides spanning the entire protein and IFN-γ production was assessed by ELISpot. These experiments revealed that C57BL/6 mice elicited a stronger 5T4-specific immune response compared to BALB/c (Figure 4.14). For C57BL/6 mice, peptide pools 1,2,5,6,8,9, and 11 were positive (Figure 4.14A) suggesting candidate peptides containing immunogenic epitopes are peptides 7, 8, 11, 12, 13, 14, 17, 18, 25, 26, 29 and 30 (see matrix, Table 2.5). From these peptides, three potential immunodominant MHC class I restricted epitopes were identified using an epitope prediction programme and blocking antibodies to MHC class-I. These were: SAPSPLVEL ($5T4_{170-178}$), NSLVSLTYV ($5T4_{244-252}$) and VSFRNLTHL ($5T4_{253-260}$). The immunogenicity of these peptides was verified by stimulating splenocytes from the RAd-CTL and RAd-5T4 vaccinated C57BL/6 mice with the single peptides (Figure 4.15). Accordingly, subsequent experiments examining the immunogenicity of the 5T4 MCMV vectors were conducted on C57BL/6 mice.

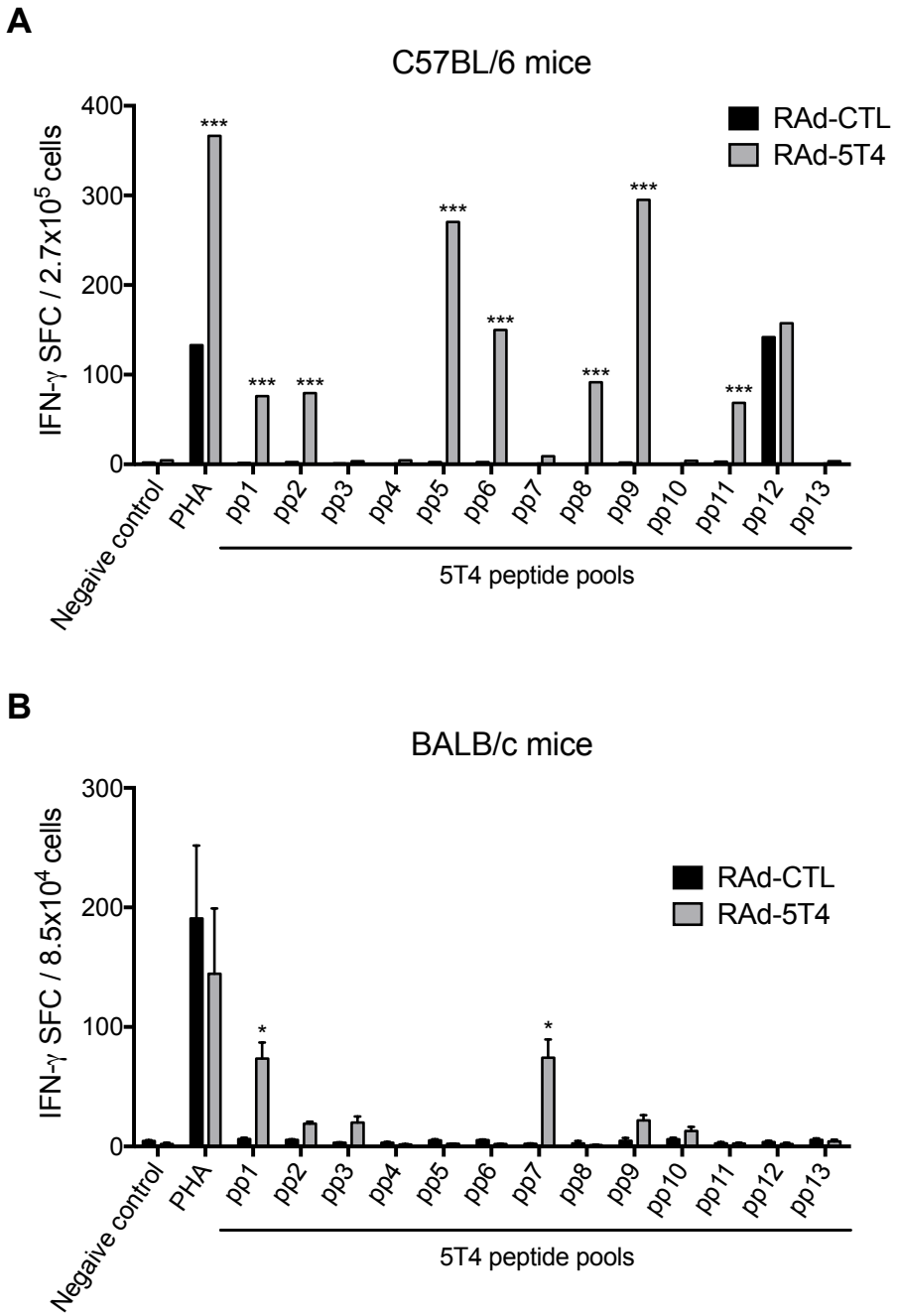

Figure 4.14 C57BL/6 mice elicit a more robust response towards 5T4 than BALB/c mice.

Splenocytes from **(A)** C57BL/6 or **(B)** BALB/c mice vaccinated with either RAd-CTL or RAd-5T4 were stimulated overnight with the 13 5T4 peptide pools and assessed for IFN-γ production by an ELISpot assay. Media alone was used as a negative control and PHA was used as a positive control. Data shown as mean spot forming cell + SEM (n=2-3 mice/group). Significance was assessed by two-way ANOVA with Bonferroni's correction for multiple comparisons. *$p<0.05$ and ***$p<0.005$. The injections and tissue harvest on C57BL/6 mice were performed by Prof Awen Gallimore while those in BALB/c were performed by myself. The ELISpot assay for both mouse strains was performed by Evelina Statkute.

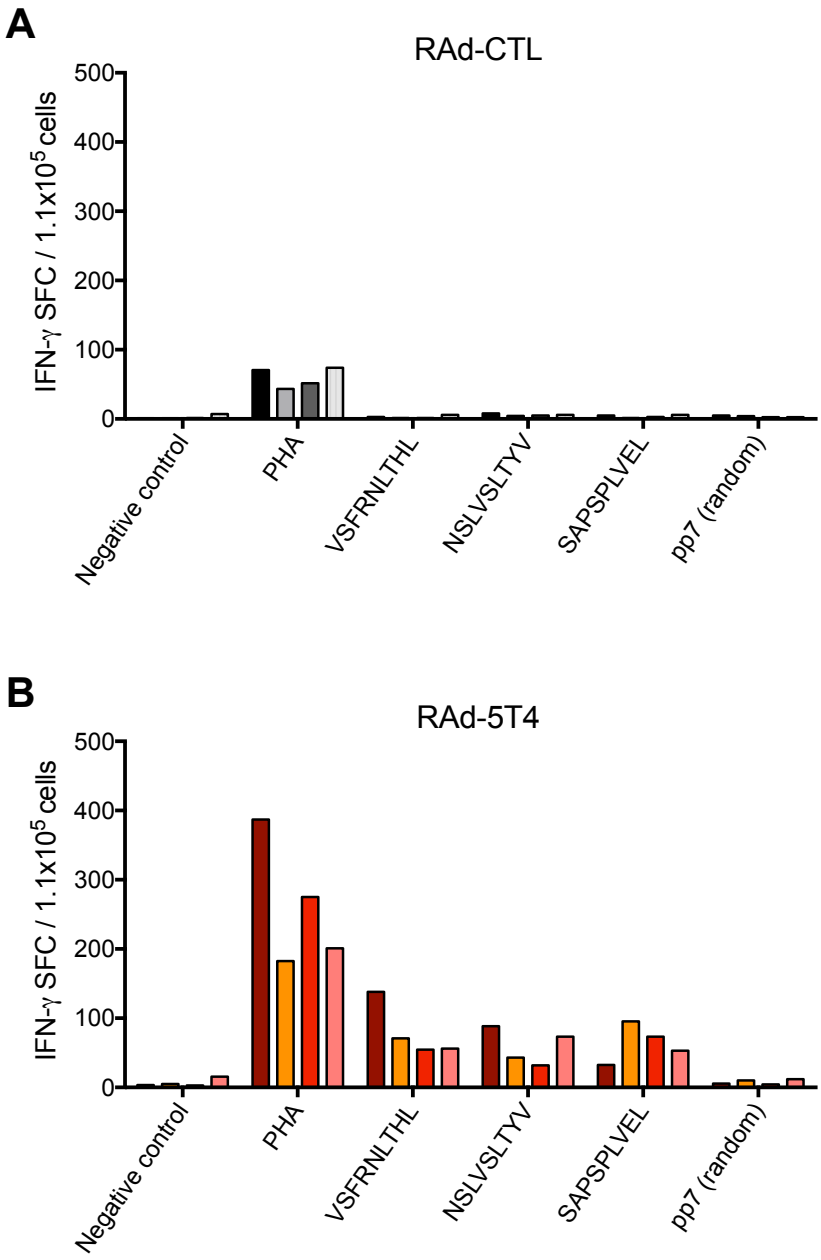

Figure 4.15 5T4 peptide-specific T cell responses in C57BL/6 mice immunised with RAd-5T4.

Splenocytes from C57BL/6 mice vaccinated with either **(A)** RAd-CTL or **(B)** RAd-5T4 from the experiment in Figure 4.14 were stimulated overnight with individual 5T4 peptides and assessed for IFN-γ production by ELISpot assay. Media alone and peptide pool 7 were used as negative controls and PHA was used as a positive control. Each bar represents an individual mouse and data is shown as mean spot forming cell (SFC) per $1.1x10^5$ cells + SEM of duplicates.

4.3.2.3 MCMV-IE1-P2A-5T4 induces detectable 5T4-specific CD8$^+$ T cell responses but display a reduced response to endogenous viral peptides

The difference in the ability of RAd-NY-ESO-1 to induce high frequency tumour-specific CD8$^+$ T cells as compared to the MCMV-NY-ESO-1 vector might lie in the level of tumour-associated antigen that is expressed by each vector. As described in Chapter 3, the RAd vector expressed higher levels of NY-ESO-1 protein than the MCMV vector due to the HCMV MIE promoter, which drives the expression of the tumour-associated antigen in the former. Thus, three new MCMV vectors were generated to improve the expression levels of 5T4: (1) *5T4* fused to *ie1* ORF (MCMV-IE1-P2A-5T4); (2) *5T4* fused to *ie3* ORF (MCMV-IE3-P2A-5T4); and (3) *5T4* under the HCMV MIE promoter, replacing ie2 ORF (MCMV-MIE-5T4) (refer to Chapter 3).

To examine the ability of these vectors to induce 5T4-specific CD8$^+$ T cell responses, C57BL/6 mice were immunised with 2x10^5 pfu of either WT-MCMV (negative control), MCMV-IE3-P2A-5T4 or MCMV-IE1-P2A-5T4. At day 7 post-infection blood was withdrawn from the lateral tail vein and cells were stimulated *ex vivo* with either a mix of three 5T4 peptides (section 4.3.2.2) or a combination of three MCMV inflationary peptides (i.e. M38, m139 and IE3) to identify tumour- or viral- specific CD8$^+$ T cells, respectively. Both 5T4 MCMV vectors induced very high frequencies of MCMV-specific CD8$^+$ T cells comparable to that induced by WT-MCMV (Figure 4.16A). Additionally, 5T4-specific CD8$^+$ T cells were detected in the peripheral circulation of mice immunised with MCMV-IE1-P2A-5T4, but not in those receiving MCMV-IE3-P2A-5T4 (Figure 4.16B). Further analysis revealed that the majority of 5T4-specific CD8$^+$ T cells induced were polyfunctional, secreting both IFN-γ and TNF-α (Figure 4.16C).

MCMV- and 5T4- specific responses were assessed in the peripheral blood over 7 months, analysing CD8$^+$ T cell responses on weeks 4, 8, 12, 16 and 28 post-infection. Encouragingly, 5T4-specific CD8$^+$ T cell responses in MCMV-IE1-P2A-5T4 vaccinated

mice followed the pattern seen for inflationary MCMV peptides - after peaking at day 7 post-infections (~0.25% 5T4-specific $CD8^+$ T cells), responses contracted to 0.12% of $CD8^+$ T cells, but subsequently inflated and were maintained at a higher frequency thereafter, with a mean response of approximately 0.5% of $CD8^+$ T cells being specific for 5T4 (Figure 4.17A). However, when individual responses from mice receiving MCMV-IE1-P2A-5T4 were examined in greater detail, it was observed that only one mouse in the group had a high 5T4-specific $CD8^+$ T cell response, reaching 1.7% of $CD8^+$ T cells by day 28 post-infection (Figure 4.17B). Two mice exhibited some reactivity to 5T4 that followed a similar pattern, but these 5T4-specific $CD8^+$ T cell responses did not inflate to the same extend and only reached ~0.5% of $CD8^+$ T cells (Figure 4.17B). In contrast, one of the mice did not exhibit a detectable 5T4 response (Figure 4.17B). Intriguingly, these 5T4-specific responses were associated with a much lower frequency of MCMV-specific $CD8^+$ T cells in the peripheral blood of these MCMV-IE1-P2A-5T4 vaccinated mice as compared to those receiving WT-MCMV (Figure 4.17C). Although MCMV-specific $CD8^+$ T cells in MCMV-IE1-P2A-5T4 mice exhibited comparable levels to those observed in WT-MCMV on weeks 1 and 4 post-infection, these did not increase in frequencies thereafter, with MCMV-IE1-P2A-5T4-challenged mice displaying an MCMV-specific response three times lower than WT-MCMV at week 28 post-infection – 5.7% vs 17.1%, respectively (Figure 4.17C). Of note, the mouse receiving MCMV-IE1-P2A-5T4 that exhibited a high 5T4-specific $CD8^+$ T cell response displayed an MCMV-specific $CD8^+$ T cell response comparable to that of other mice in the group.

Thus, these data implied that although the MCMV-IE1-P2A-5T4 vector was capable of inducing 5T4-specific T cell responses, it is perhaps impaired in terms of replication and/or persistence *in vivo*. Reduced MCMV-specific $CD8^+$ T cell response observed during MCMV-IE1-P2A-5T4 immunisation could be due to several reasons. First, the presence of various immunogenic antigens in a vector (i.e. MCMV and 5T4) can result

in competition between individual MHC class I epitopes, thereby diminishing responses to some of these. Indeed, this has been previously reported where mice challenged with MCMV vectors expressing either the immunodominant peptide from Ovalbumin, SIINFEKL, or from HSV-1 glycoprotein B, SSIEFARL, displayed a reduced inflationary response against the endogenous T cell epitopes M38, m139 and IE3 (420, 471). A second explanation of the differences in MCMV inflationary response between MCMV-IE1-P2A-5T4 and WT-MCMV may be due to a mutation in the MCMV-IE1-P2A-5T4 genome. Lastly, it was possible that the location where the tumour-associated antigen was inserted (i.e. fused to the end of the *ie1* gene) interfered with the expression and/or function of the IE1 protein, which has an essential role in driving the expression of various viral proteins (457) and may thus affect viral replication and virulence. This last possibility seems the most reasonable since virus growth assessed by a multistep growth kinetic assay in NIH 3T3 cells, showed that MCMV-IE1-P2A-5T4 did not replicate to titres comparable to that of WT-MCMV (Chapter 3, Figure 3.13). Consequently, the whole viral genome of the MCMV vector generated was sent for sequencing. The sequencing data from MCMV-IE1-P2A-5T4 was aligned against the WT-MCMV genome (accession number in GenBank AM886412) and revealed that a high percentage of the MCMV-IE1-P2A-5T4 viral genomes had a fragment deleted – from 6523 bp to 19431 bp. This region comprises genes from *m07* to *m18*. The proteins encoded by the genes *m07* to *m16* are members of the *m02* gene family (369). Although the function of most of them remain unknown, as a group they have been implicated in evasion of NK cell mediated immunity. Thus, these data suggest that the lack of long-lived 5T4-specific T cell responses may be due to impaired virus persistence due to a defective vector.

In contrast, the MCMV-IE3-P2A-5T4 vector induced no significant 5T4 responses during the 7 months studied (Figure 4.17A). However, this vector induced frequencies of MCMV-specific $CD8^+$ T cells being comparable to those observed in WT-MCMV

challenged mice (Figure 4.17C), suggesting that although the MCMV-IE3-P2A-5T4 vector was replication competent, it did not induce 5T4-specific T cell responses.

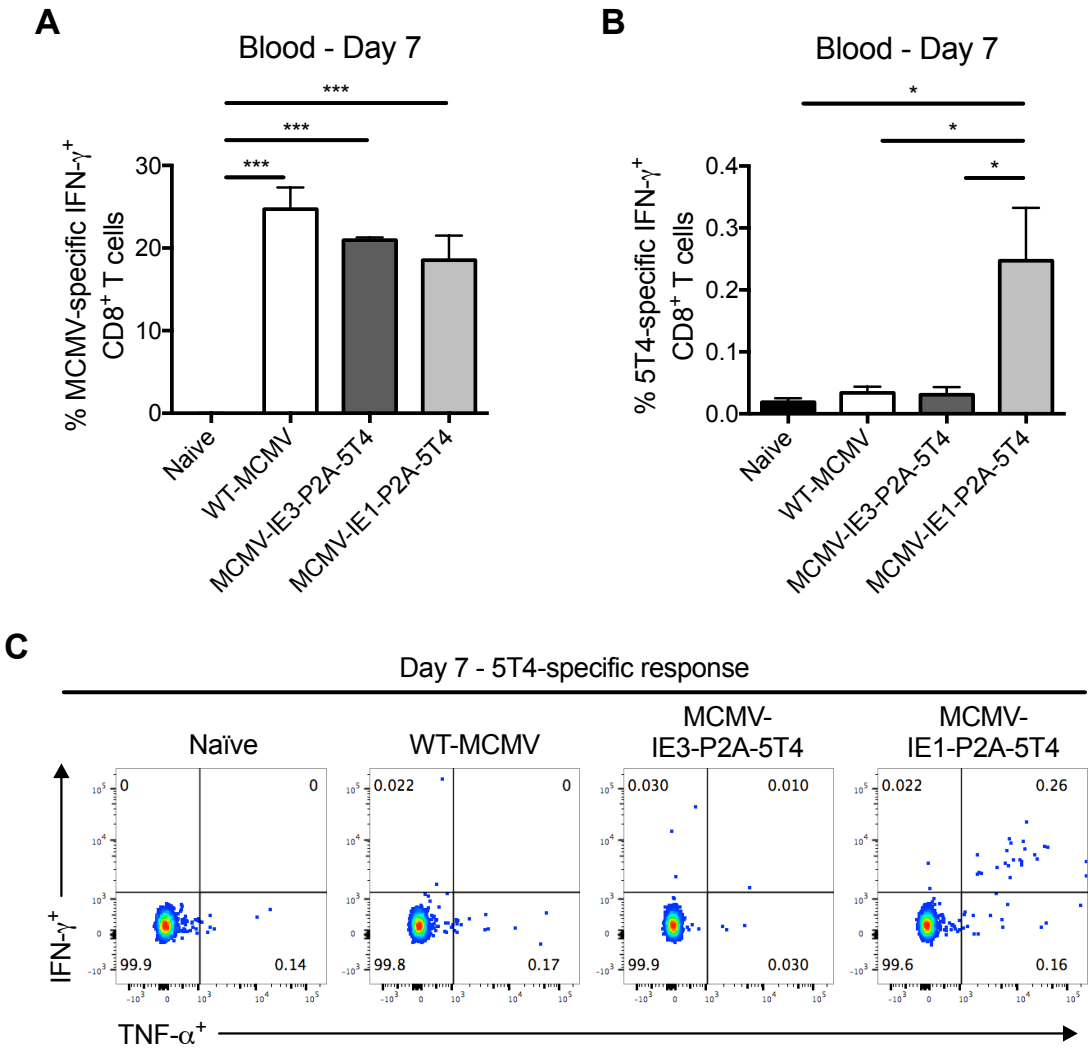

Figure 4.16 MCMV-IE1-P2A-5T4 induces 5T4-specific CD8$^+$ T cell responses.

C57BL/6 mice were challenged i.p with 2x10^5 pfu WT-MCMV, MCMV-IE3-P2A-5T4 or MCMV-IE1-P2A-5T4. Naïve mice were used as control. At day 7 p.i, blood was withdrawn from the lateral tail vein and cells were stimulated for 6 hours with a mix of either MCMV peptides (M38, m139 and IE3) or 5T4 peptides (5T4$_{170\text{-}178}$, 5T4$_{244\text{-}252}$ and 5T4$_{253\text{-}260}$). Frequency of **(A)** MCMV-specific and **(B)** 5T4-specific IFN-γ$^+$ CD8$^+$ T cells were measured. Data shown as mean + SEM (n=4 mice/group). Significance was assessed by one-way ANOVA with Bonferroni's correction for multiple comparisons. *p<0.05 and ***p<0.005. **(C)** Representative flow cytometry plots showing IFN-γ and TNF-α expression of live, CD8$^+$ cells. Data is representative of 4 mice/group.

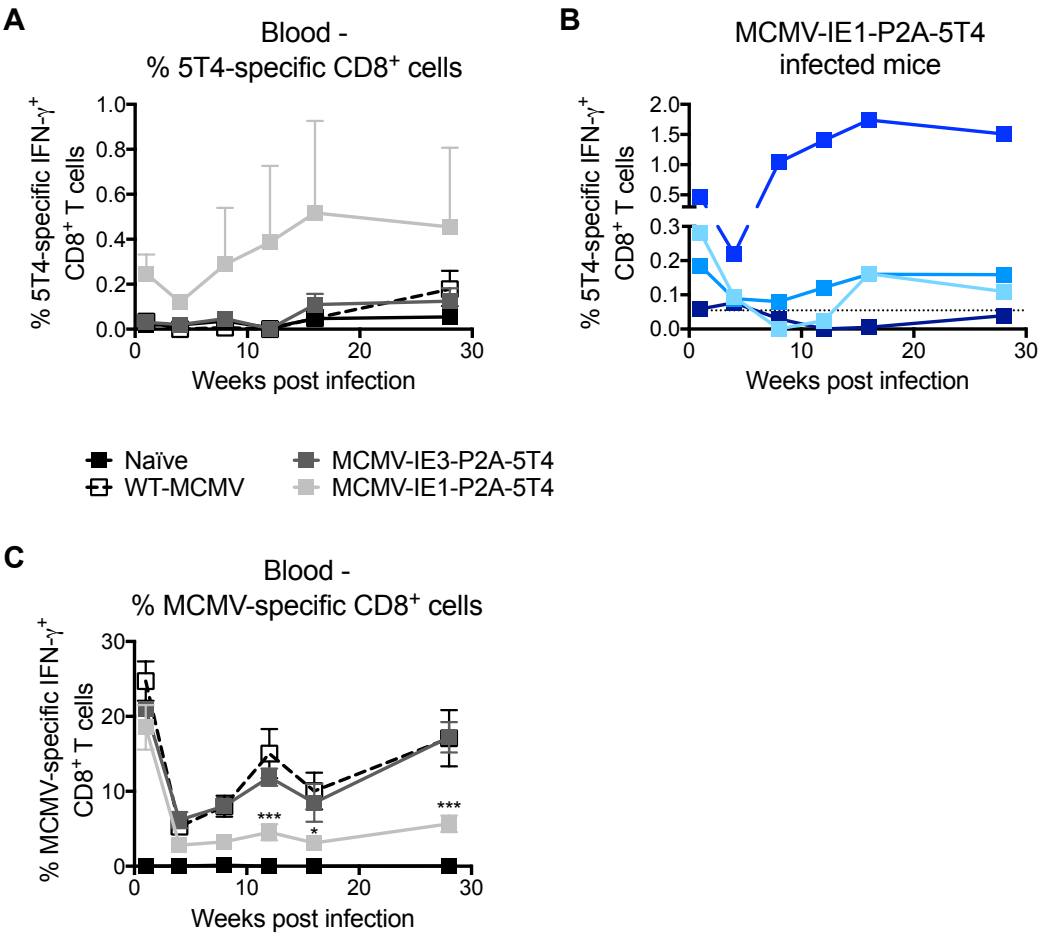

Figure 4.17 MCMV-IE1-P2A-5T4 vector can induce functional 5T4-specific CD8$^+$ T cells but responses to endogenous MCMV peptides is diminished.

C57BL/6 mice were challenged i.p with 2x10^5 pfu WT-MCMV, MCMV-IE3-P2A-5T4 or MCMV-IE1-P2A-5T4. Naïve mice were used as control. At week 1, 4, 8, 12, 16 and 28 p.i. blood was withdrawn from the lateral tail vein and cells were stimulated for 6 hours with a mix of either MCMV peptides (M38, m139 and IE3) or 5T4 peptides ($5T4_{170-178}$, $5T4_{244-252}$ and $5T4_{253-260}$). Subsequently, cells were stained for CD8α and IFN-γ. **(A)** Frequency of 5T4-specific IFN-γ^+ CD8$^+$ T cells. Data shown as mean + SEM (n=4 mice/group). **(B)** Frequency of 5T4-specific IFN-γ^+ CD8$^+$ T cells of individual mice vaccinated with MCMV-IE1-P2A-5T4. Dotted line represents the limit of detection. **(C)** Frequency of MCMV-specific IFN-γ^+ CD8$^+$ T cells. Data shown as mean $\pm$ SEM (n=4 mice/group). Significance was assessed by two-way ANOVA with Dunnett's correction comparing MCMV-IE3-P2A-5T4 and MCMV-IE1-P2A-5T4 with control WT-MCMV group. *p<0.05 and ***p<0.005.

4.3.2.4 MCMV-MIE-5T4 induces a modest 5T4-specific response

The final MCMV vector engineered expressing 5T4 under the HCMV MIE promoter, MCMV-MIE-5T4, was also tested *in vivo*. C57BL/6 mice were challenged i.p with $2x10^5$ pfu MCMV-MIE-5T4 or MCMV-ΔIE2 (negative control) and responses assessed over time. Longitudinal analysis of MCMV-specific responses did not reveal any significant differences in virus-specific responses in MCMV-MIE-5T4 challenged mice as compared to those receiving MCMV-ΔIE2 (Figure 4.18A).

Tumour-specific responses were detected at week 1 post-infection in MCMV-MIE-5T4 challenged mice, reaching 1.9% of circulating $CD8^+$ T cells (Figure 4.18B). However, mice receiving MCMV-ΔIE2 also exhibited a response towards the three 5T4 peptides at day 7 post-infection, reaching a magnitude of 0.9% of circulating $CD8^+$ T cells (Figure 4.18B). Following a contraction in the frequency of 5T4-specific $CD8^+$ T cells at week 4 post-infection in both challenged groups, 5T4 responses increased by week 8 in mice receiving MCMV-MIE-5T4 and were maintained at ~0.35% for the subsequent analyses until week 28, when these decreased to 0.15% of circulating $CD8^+$ T cells (Figure 4.18B). On the contrary, the 5T4 responses observed in MCMV-ΔIE2 challenged mice did not increase to similar magnitudes after the contraction period as in those receiving MCMV-MIE-5T4 (Figure 4.18B).

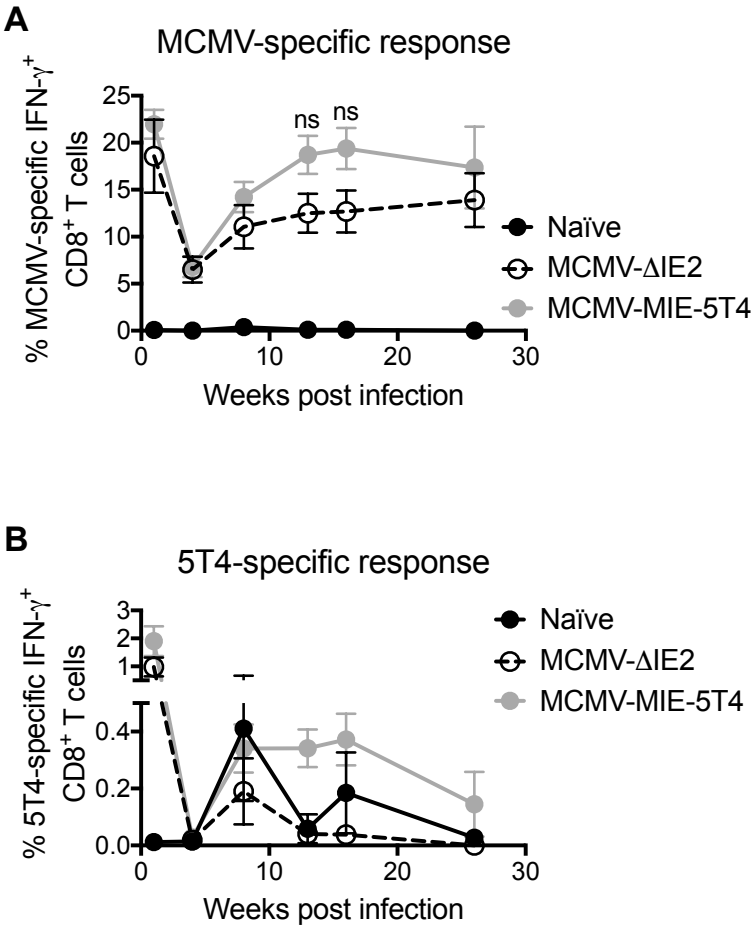

Figure 4.18 MCMV-MIE-5T4 induces a very modest 5T4-specific response.

C57BL/6 mice were challenged i.p with $2x10^5$ pfu MCMV-ΔIE2 or MCMV-MIE-5T4. Naïve mice were used as control. At week 1, 4, 8, 12, 16 and 26 p.i. blood was withdrawn from the lateral tail vein and cells were stimulated for 6 hours with a mix of either MCMV peptides (M38, m139 and IE3) or 5T4 peptides ($5T4_{170-178}$, $5T4_{244-252}$ and $5T4_{253-260}$). Subsequently, cells were stained for CD8α and IFN-γ. **(A)** Frequency of MCMV-specific IFN-γ^+ $CD8^+$ T cells overtime. Two-way ANOVA with Bonferroni's correction was used to compare MCMV-MIE-5T4 and MCMV-ΔIE2 groups. Adjusted p values (MCMV-MIE-5T4 versus MCMV-ΔIE2) are as follows: >0.99, >0.99, >0.99, 0.51, 0.38 and >0.99. **(B)** Frequency of 5T4-specific IFN-γ^+ $CD8^+$ T cells overtime. Data shown as mean ± SEM (n=4 mice/group).

4.3.2.5 Prime-boost immunisation with RAd-5T4 and MCMV-MIE-5T4 induces robust T cell responses reactive to 5T4

5T4-specific T cell responses induced by the three MCMV vectors generated were modest at best. This is not surprising given that human 5T4 exhibits 81% amino acid homology to mouse 5T4 (449) and mouse 5T4-specific T cells will therefore likely undergo negative selection during T cell development. To improve the magnitude of 5T4 responses, a prime-boost regime with RAd-5T4 was investigated. Although MCMV-IE1-P2A-5T4 vector has the potential to induce the highest magnitude of 5T4-specific $CD8^+$ T cells, this vector had a portion of its genome deleted, thus the MCMV-MIE-5T4 construct was chosen for these studies.

C57BL/6 mice were primed with $5x10^8$ pfu of either RAd-5T4 or RAd-CTL (control) and 35 days later boosted with $2x10^5$ pfu of either MCMV-MIE-5T4, MCMV-ΔIE2 (control), or $5x10^8$ pfu RAd-5T4. Figure 4.19A shows the experimental design and the groups with the different vaccine combinations. Blood was withdrawn from the lateral tail vein on day 7 post-prime and day 7 post-boost to examine 5T4-specific responses via peptide stimulation and flow cytometry. As shown in Figure 4.19B, 5T4-specific $CD8^+$ T cell responses could be detected after a single prime immunisation with RAd-5T4, reaching a magnitude between 0.4 and 0.8% of circulating $CD8^+$ T cells. Frequencies of 5T4-specific T cells were significantly amplified following the RAd-5T4 boost, reaching a mean response of 1.8% of $CD8^+$ T cells (Figure 4.19B). Furthermore, boosting with MCMV-ΔIE2 led to a reduction in 5T4-specific $CD8^+$ T cells (0.14% of $CD8^+$ T cells) whereas MCMV-MIE-5T4 boost maintained the level of 5T4 immune responses (~0.9% of $CD8^+$ T cells) (Figure 4.19B). Further assessment of 5T4-specific $CD8^+$ T cell responses at day 7 post-boost, revealed that most of these cells secreted both IFN-γ and TNF-α (Figure 4.19C).

Peripheral immune responses reactive to 5T4 were further examined on day 41 and 68 post-boost. Longitudinal analysis showed that in both groups displaying a robust 5T4 response on day 7 post-boost (RAd-5T4 + MCMV-MIE-5T4 and RAd-5T4 + RAd-5T4), the frequency of 5T4-specific T cells contracted by day 41 post-boost to 0.23% and 0.71% of $CD8^+$ T cells, respectively (Figure 4.20A). While the level of 5T4 response was maintained four weeks later (day 68 post-boost) in mice receiving RAd-5T4 + MCMV-MIE-5T4, 5T4-specific responses continued to decrease in the RAd-5T4 + RAd-5T4 vaccinated group, exhibiting a frequency of 0.5% 5T4-specific $CD8^+$ T cells (Figure 4.20A). Furthermore, mice receiving RAd-5T4 + MCMV-ΔIE2 that displayed very low 5T4 responses on day 7 post-boost, continued to decline, with responses falling below 0.1% by day 41 post-boost and remaining low, similar to that of the control group receiving PBS + PBS (Figure 4.20A). In addition, MCMV-specific responses were monitored alongside. All the mice receiving an MCMV vector (either MCMV-MIE-5T4 or MCMV-ΔIE2) exhibited a robust MCMV-specific immune response at day 7 post-boost (Figure 4.20B). These slightly contracted on day 41 post-boost in the group receiving MCMV-ΔIE2, but then inflated by day 68, consistent with previous data (Figure 4.20B). The same pattern was observed in mice receiving RAd-5T4 + MCMV-MIE-5T4, however, MCMV-specific $CD8^+$ T cells contracted significantly more and did not inflate to levels comparable to that seen in MCMV-ΔIE2 (Figure 4.20B). This might be due to the presence of 5T4 in the vector and the prime-boost regime which might be skewing the immune response towards 5T4 rather than MCMV endogenous antigens. In support of this hypothesis, mice receiving RAd-CTL + MCMV-MIE-5T4 exhibited comparable levels of MCMV-specific $CD8^+$ T cells to those observed in MCMV-ΔIE2 infected mice (Figure 4.20B).

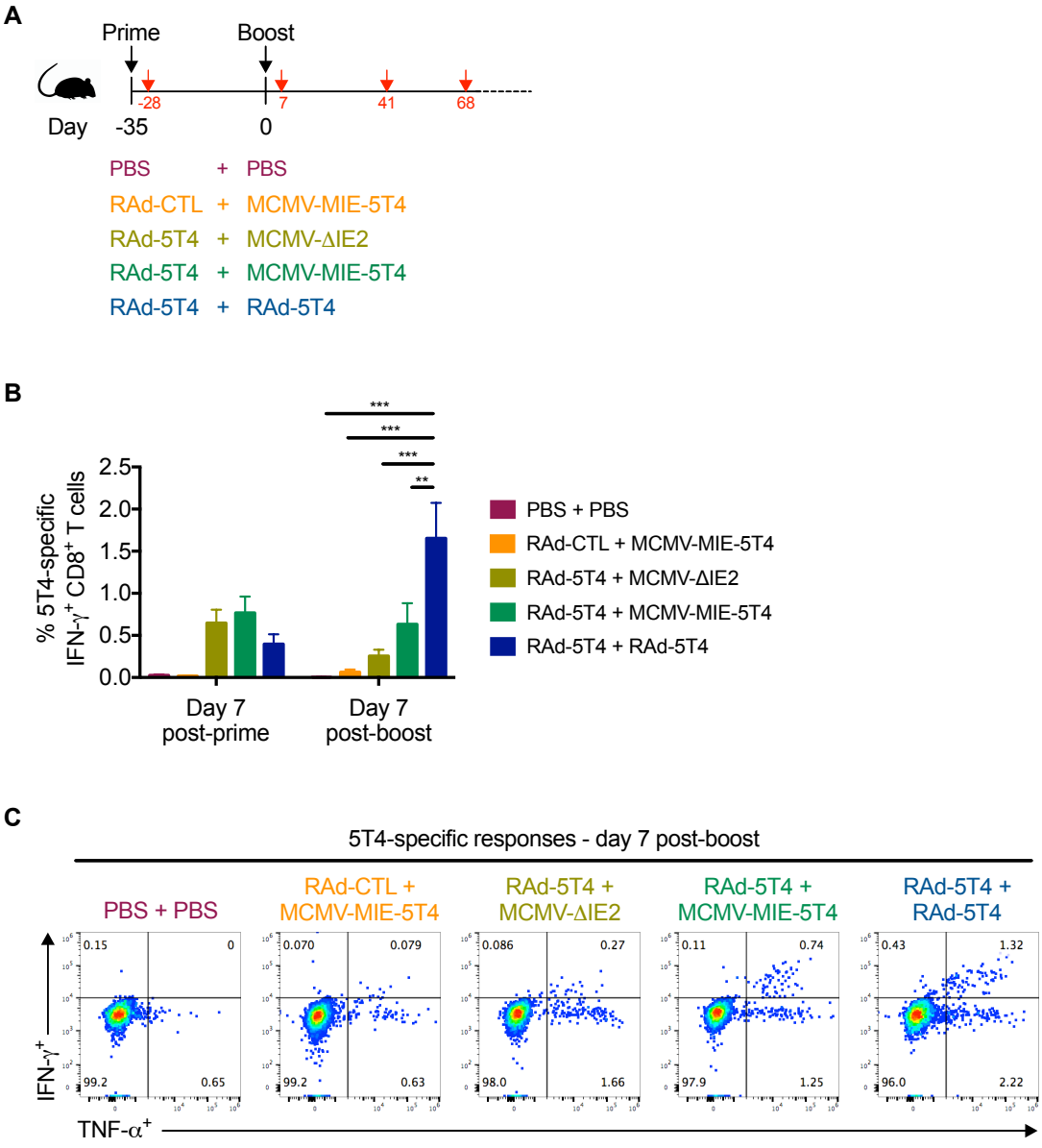

Figure 4.19 RAd-5T4/MCMV-MIE-5T4 prime-boost induces a strong polyfunctional 5T4-specific CD8$^+$ T cell response.

C57BL/6 mice were primed with 5x10^8 pfu RAd-5T4 or RAd-CTL (control) s.c followed by a boost with either 2x10^5 pfu MCMV-MIE-5T4, MCMV-ΔIE2 (control) i.p or 5x10^8 pfu RAd-5T4 s.c.. PBS was used as a control. **(A)** Schematic of the experimental design. Red arrows and numbers indicate the time point when T cell responses were analysed. **(B)** Blood was withdrawn at day 7 post-prime (d-28) and at day 7 post-boost (d7). Cells were stimulated *ex vivo* with a mix of three 5T4 immunodominant peptides ($5T4_{170-178}$, $5T4_{244-252}$ and $5T4_{253-260}$), followed by staining for CD8α and IFN-γ to obtain frequency of 5T4-specific IFN-γ$^+$ CD8$^+$ T cells. Data shown as mean + SEM (n=4 mice/group). Significance was assessed by two-way ANOVA with Bonferroni's correction for multiple comparisons. **p<0.01 and ***p<0.005. **(C)** Representative flow cytometry plots showing IFN-γ and TNF-α expression of live, CD8$^+$ cells responding to 5T4 stimulation on day 7 post-boost. Data representative of 4 mice per group.

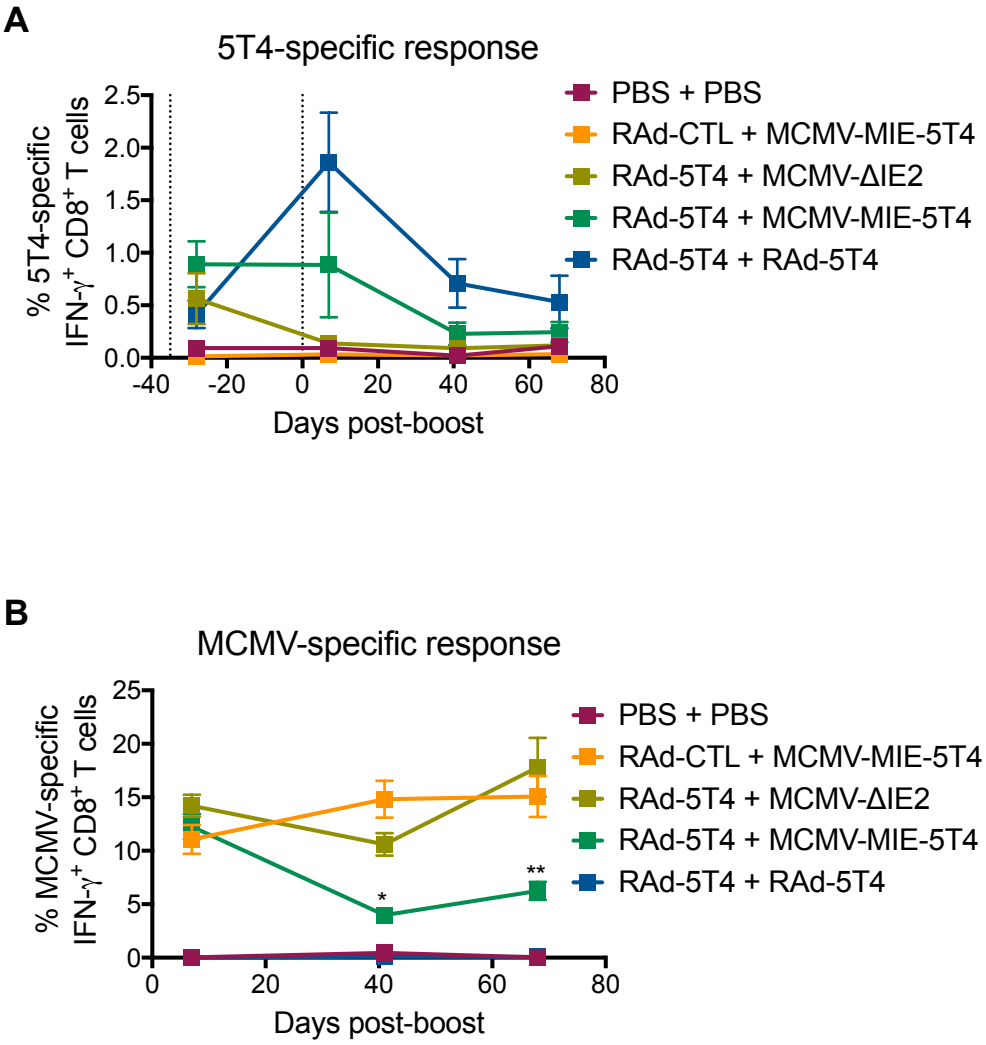

Figure 4.20 5T4-specific T cell response decrease over time after vaccination with 5T4-expressing viral vectors.

Blood from C57BL/6 mice (Figure 4.19A) was withdrawn from the lateral tail vein at days -28 (d7 post-prime), 7, 41 and 68 post-boost. Cells were stimulated *ex vivo* with a mix of three 5T4 peptides ($5T4_{170\text{-}178}$, $5T4_{244\text{-}252}$ and $5T4_{253\text{-}260}$) or three MCMV inflationary peptides (M38, m139 and IE3), followed by staining for CD8α and IFN-γ.**(A)** Frequency of 5T4-specific IFN-γ^+ $CD8^+$ cells. Dotted line represents prime and boost time points. **(B)** Frequency of MCMV-specific IFN-γ^+ $CD8^+$ cells. Data shown as mean ± SEM (n=3-4 mice/group). Significance of **(B)** was assessed by one-way ANOVA with Dunnett's correction, comparing those groups receiving MCMV-MIE-5T4 with control group receiving MCMV-ΔIE2 at each time point. *p<0.05 and **p<0.01.

4.3.2.6 Priming with RAd-5T4 followed by boosting with MCMV-MIE-5T4 has the potential to elicit protective immunity against tumour challenge

To determine whether the observed 5T4-specific $CD8^+$ T cell responses could protect against tumour growth, immunised mice were challenged s.c with 1 $x10^5$ LLC1 cells, that express mouse 5T4 (Appendix II), in the left flank 4.75 months post-boost. The experimental time line is shown in Figure 4.21A. LLC1 tumours were palpable on day 10 after tumour injection and were large enough to measure by day 12 in the control group receiving PBS + PBS. Tumours were measured three times a week as described before. LLC1 tumours were very aggressive and due to their rapid growth, tumours were prone to ulceration, thus mice were checked every other day and were sacrificed if a crater-like appearance or discharge was observed.

LLC1 tumours developed in 61% (11 out of the 18 mice in the study) of injected mice during the period studied (61 days) (Figure 4.21B). The seven mice that did not develop palpable tumours during the 61 days studied were from the following groups: three mice from RAd-CTL + MCMV-MIE-5T4; two from RAd-5T4 + MCMV-ΔIE2; and two from RAd-5T4 + MCMV-MIE-5T4. Only one mouse from those receiving RAd-CTL + MCMV-MIE-5T4 developed a tumour and it did so at a similar time as those in control group (2 days later) (Figure 4.22A). In contrast, tumour onset in mice receiving RAd-5T4 + MCMV-ΔIE2 and RAd-5T4 + MCMV-MIE-5T4 was delayed by 11 days and up to 19 days in one mouse receiving RAd-5T4 + MCMV-MIE-5T4 (Figure 4.22A). Furthermore, tumours in the group immunised with RAd-5T4 + RAd-5T4 developed tumours between day 12 and day 19 after tumour challenge (Figure 4.22A). Although delays were observed in the date of tumour onset, the growth rate of immunised mice was not statistically different to the control group (Figure 4.22B). However, this might be due to the low numbers of animals in each group.

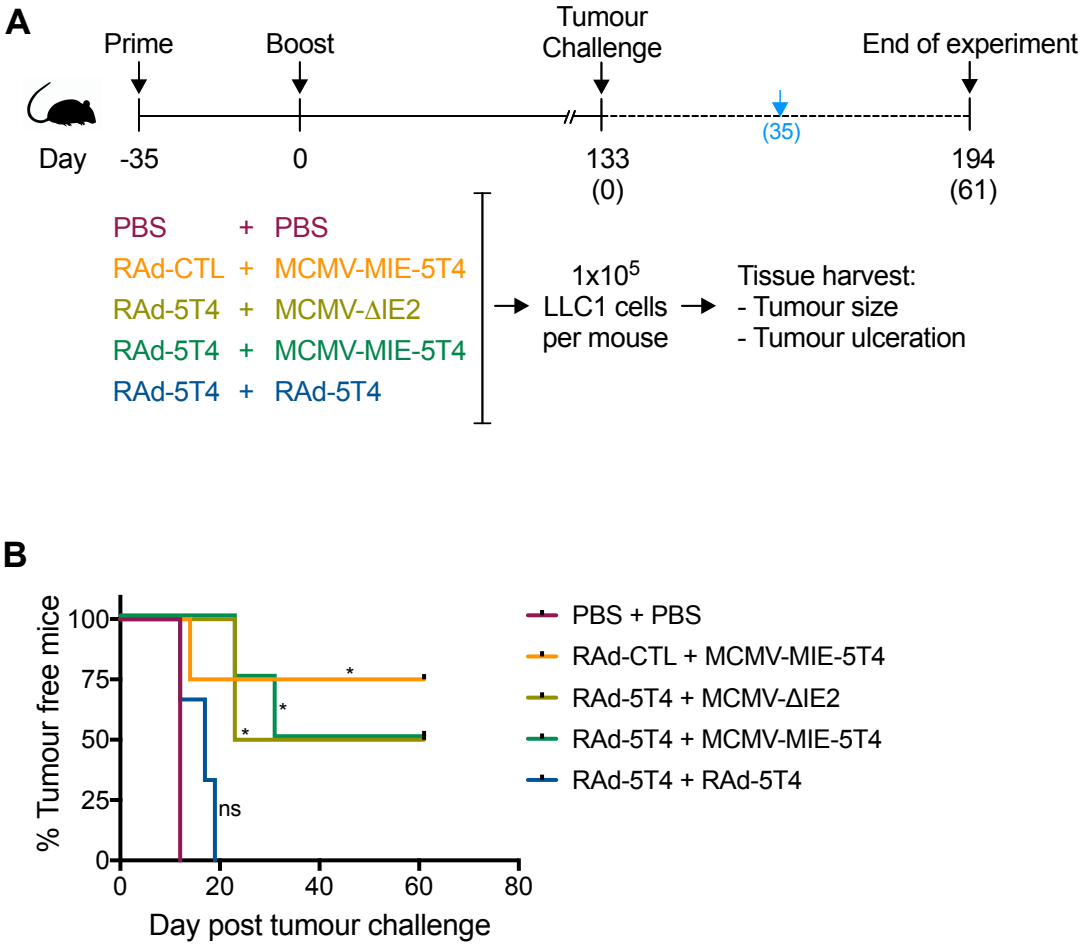

Figure 4.21 Vaccination with RAd-5T4 and MCMV-MIE-5T4 offers protection against tumour challenge.

The protective efficacy of the vaccines shown in Figure 4.19A was investigated by challenging the mice with 1x10^5 LLC1 cells 133 days after the boost. Tumours were measured three times a week until tumours grew to 15-16mm or became ulcerated, at which point mice were sacrificed. **(A)** Experimental timeline. Blue arrow indicates when the last mice bearing tumours were sacrificed. Mice that did not develop tumours were monitored until day 61 after tumour challenge. **(B)** Percentage of mice that did not develop palpable tumours. ns = not significant, *p<0.05, relative to PBS + PBS control group; log-rank test with Bonferroni's correction for multiple comparisons.

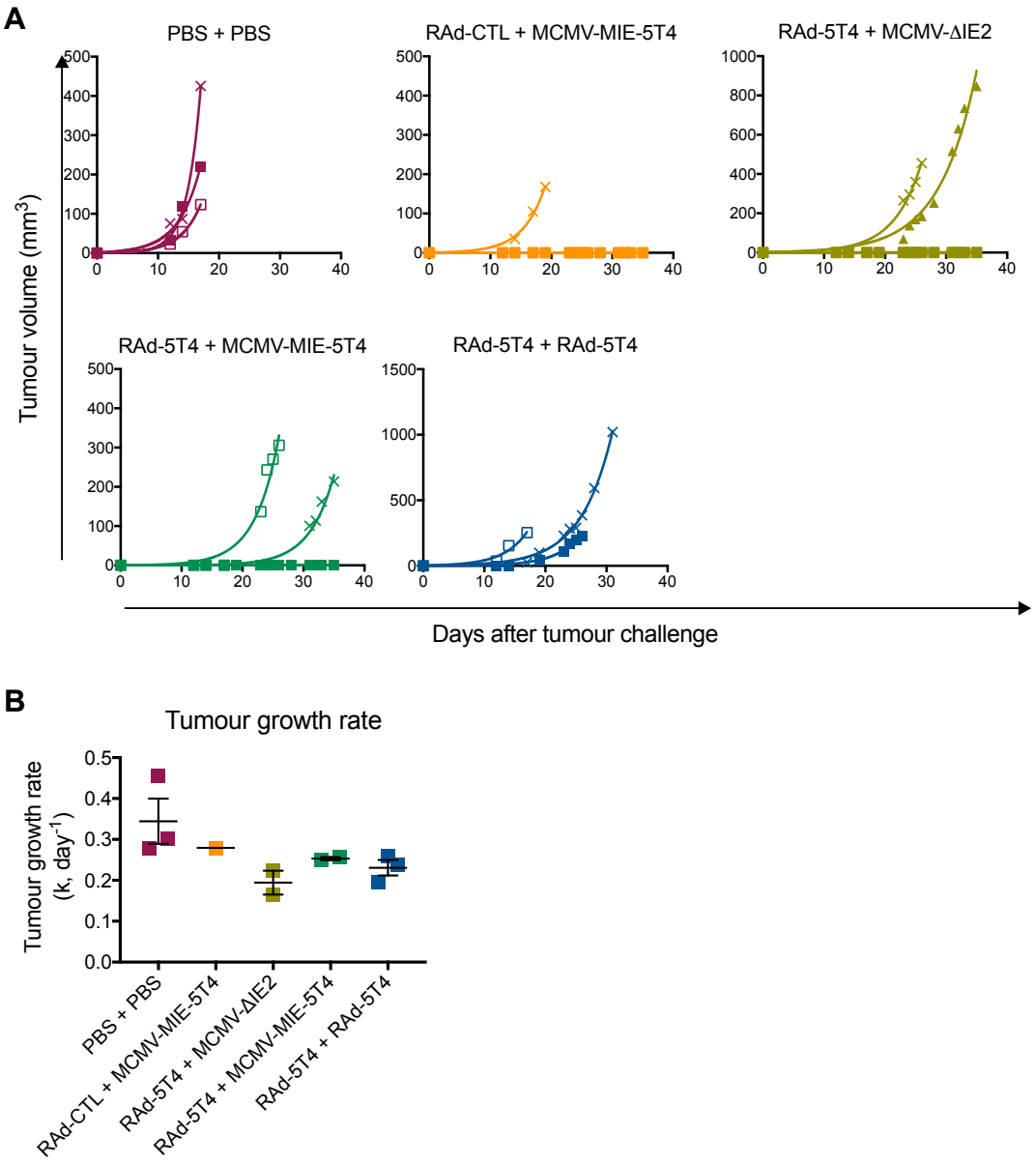

Figure 4.22 LLC1 tumour growth in mice immunised with 5T4-expressing vectors.

Vaccinated mice were challenged with $1x10^5$ LLC1 cells at day 133 after the boosting immunisation. Tumours were measured three times per week until mice were sacrificed. **(A)** Tumour volume over time of the individual mice in each group: PBS+PBS n=3; RAd-CTL+MCMV-MIE-5T4 n=4; RAd-5T4+MCMV-ΔIE2 n=4; RAd-5T4+MCMV-MIE-5T4 n=4; and RAd-5T4+ RAd-5T4 n=4. The line through the sets of measurements represents the best fit exponential growth of the tumour. **(B)** Tumour growth rates (k, $days^{-1}$). Data shown as individual mice with mean ± SEM.

4.3.2.7 MCMV immunisation is associated with a higher frequency of tumour infiltrating CD8$^+$ lymphocytes

Next, tumour infiltrating lymphocytes were analysed to determine their association with anti-tumour protection afforded by vector immunisation. Tumours were harvested on the day of sacrifice, processed into single cell suspensions and stained for CD8, CD3 and with tetramers specific for three different 5T4 epitopes ($5T4_{170\text{-}178}$, $5T4_{244\text{-}252}$ and $5T4_{253\text{-}260}$), followed by assessment via flow cytometry. CD8$^+$ T cells specific for 5T4 were detected in the tumour of all the vaccinated groups as well as in the control group receiving PBS + PBS (Figure 4.23A). Conclusions cannot be drawn from this data due to the small number of mice in each group and the spread of the data. Further analysis, such as expression of CD44, CD62L and PD-1 could not be performed due to the low frequency of 5T4-tetramer$^+$ cells in the tumours (Figure 4.23B). Nonetheless, the magnitude and phenotype of tumour infiltrating CD8$^+$ lymphocytes (CD8$^+$ TILs) was assessed. Mice primed with RAd-5T4 followed by MCMV-MIE-5T4 or MCMV-ΔIE2 boost displayed a trend towards a higher frequency of CD8$^+$ TILs, suggesting that MCMV vaccination might induce increased infiltration of CD8$^+$ T cells into the tumour site (Figure 4.24A).

No differences in the expression of PD-1 by CD8$^+$ TILs were observed between the immunised groups nor with the control group (Figure 4.24B). Furthermore, tumours from mice receiving RAd-5T4 + MCMV-MIE-5T4 had the highest frequency of infiltrating T_{EM} CD8$^+$ cells (CD44$^+$CD62L$^-$) out of the five groups (Figure 4.24C), as assessed by CD44 and CD62L expression. In addition, those mice receiving RAd-5T4 had an increased frequency of KLRG1$^-$CD127$^+$ T_{EM} CD8$^+$ TILs, markers of MPECs (Chapter 1, section 1.1.3.1), which are associated with high proliferative potential. In contrast, T_{EM} CD8$^+$ TILs from mice challenged with PBS + PBS and RAd-CTL + MCMV-MIE-5T4 exhibited a more differentiated phenotype, KLRG1$^+$CD127$^-$ (Figure 4.24C) associated with SLECs (Chapter 1, section 1.1.3.1).

As stated above, robust conclusions cannot be drawn from this data. However, it suggests that RAd-5T4 + MCMV-MIE-5T4 prime-boost vaccination has an advantage over the other immunisations. Taken together, these data suggest that the MCMV vector promotes $CD8^+$ cell infiltration into the tumour, resulting in a higher frequency of $CD8^+$ TILs exhibiting an effector memory phenotype (Figure 4.24). Furthermore, RAd-5T4 + MCMV-MIE-5T4 induced effector memory $CD8^+$ TILs with the phenotype $KLRG1^-CD127^+$, indicating their potential to proliferate in the presence of IL-7 and generate more effector cells which can target tumour cells. In addition, the lack of PD-1 expression on $CD8^+$ TILs (Figure 4.24) indicates their potential to exhibit effector functions despite the immunosuppressive tumour environment.

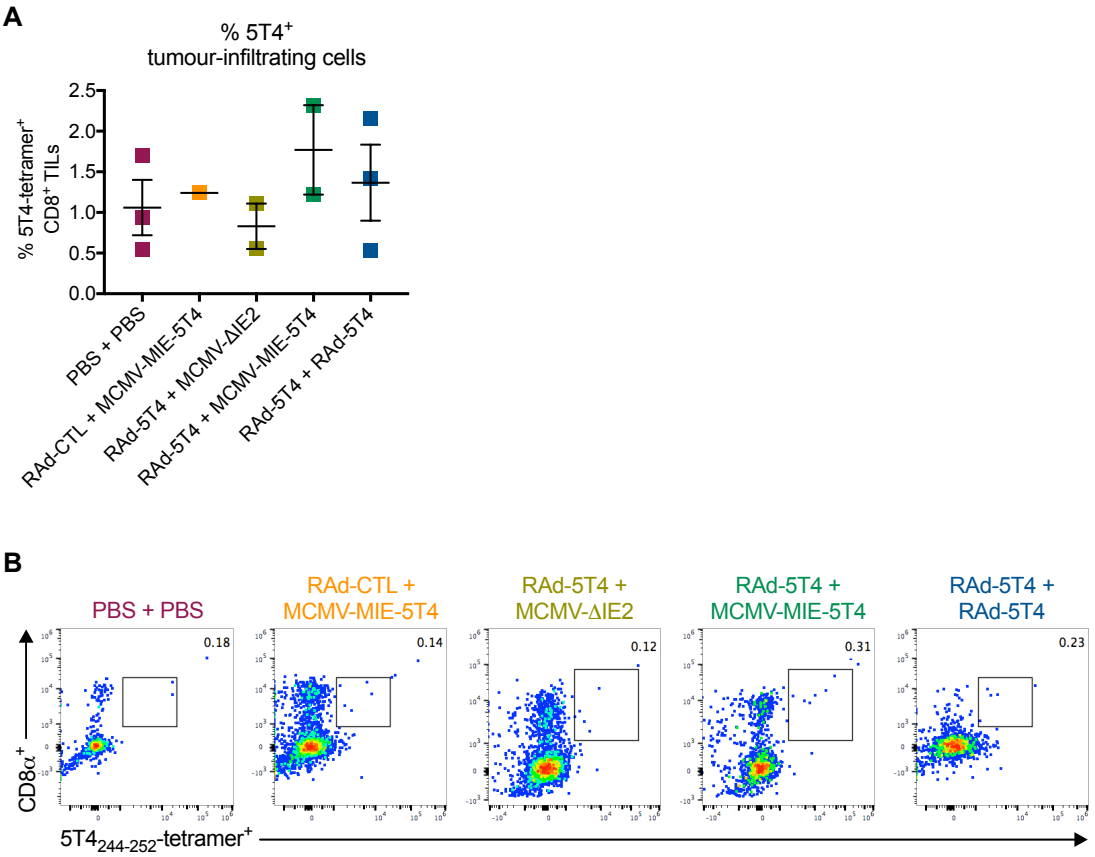

Figure 4.23 5T4-specific tumour infiltrating lymphocytes are present in all the tumours.

Immunised C57BL/6 mice bearing tumours were sacrificed when the tumours become ulcerated or reached 15-16mm in diameter. Tumours were harvested and processed in single cell suspensions. Cells were stained for CD8α and with tetramers specific for the three immunodominant 5T4 peptides ($5T4_{170-178}$, $5T4_{244-252}$ and $5T4_{253-260}$) to obtain the frequency of 5T4-specific tumour infiltrated lymphocytes. **(A)** Graph displays the frequency of the three 5T4-tetramers^{+} combined. Data shown as individual mice with mean ± SEM. **(B)** Representative flow cytometry plots of CD8α versus $5T4_{244-252}$-tetramer.

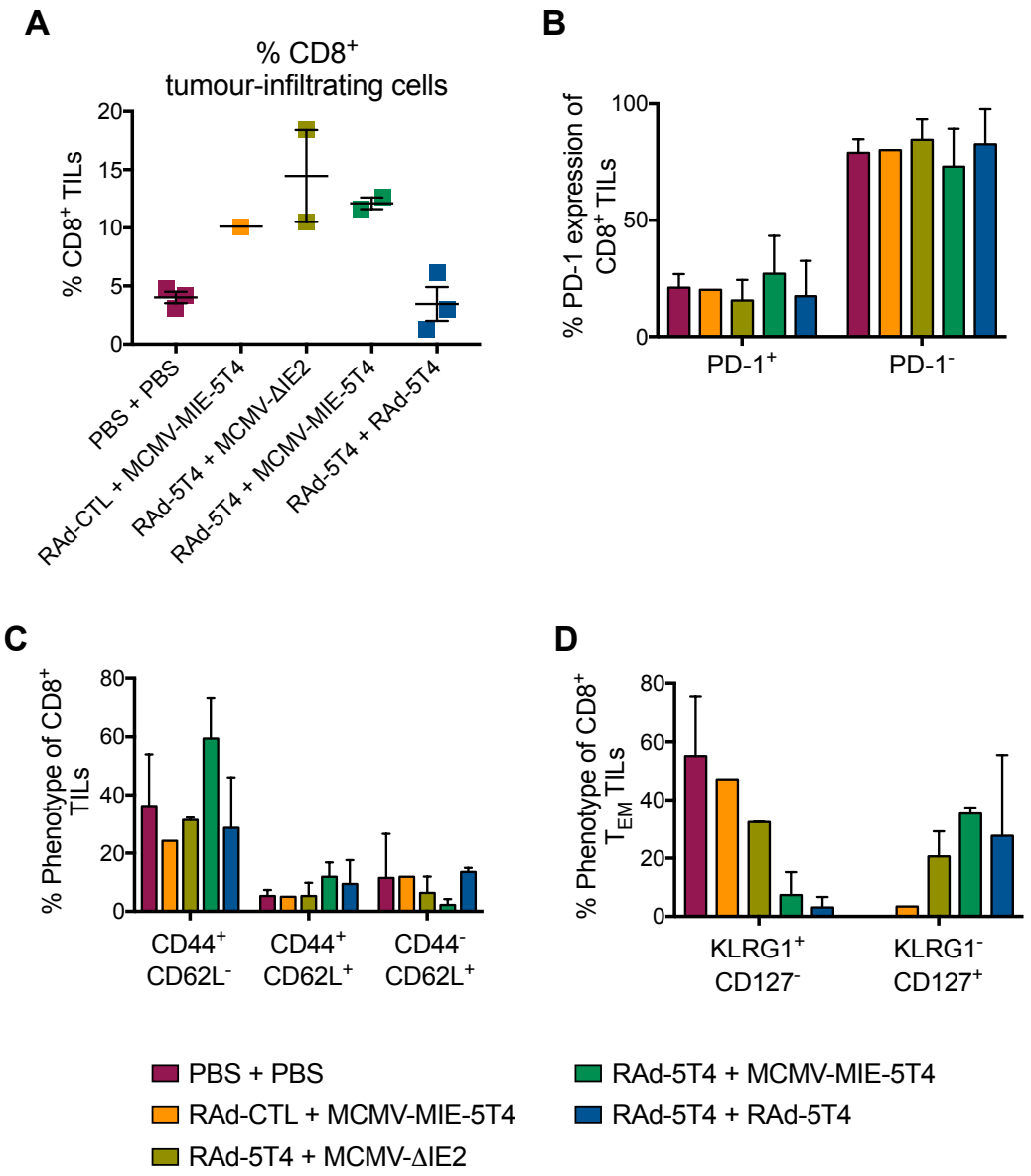

Figure 4.24 Tumours from mice primed with RAd-5T4 and boosted with MCMV-MIE-5T4 display a higher frequency of $CD8^+$ cells with a T_{EM} phenotype.

Immunised C57BL/6 mice bearing tumours were sacrificed when the tumours become ulcerated or reached 15-16mm in diameter. Tumours were harvested and processed in single cell suspensions. Cells were stained for CD8α, CD3 and the phenotypic markers CD44, CD62L, PD-1, KLRG1 and CD127. **(A)** Frequency of tumour infiltrating $CD8^+$ cells. Data shown as mean ± SEM. **(B)** PD-1 expression of $CD8^+$ tumour infiltrating lymphocytes. **(C)** Frequencies of effector memory ($CD44^+CD62L^-$), central memory ($CD44^+CD62L^+$) and naïve ($CD44^-CD62L^+$) $CD8^+$ tumour infiltrating cells. **(D)** Frequency of effector memory (T_{EM}) $CD8^+$ TILs expressing KLRG1 and CD127. Data shown as mean + SEM (n=1-3 mice/group).

4.3.2.8 Increased 5T4-specific CD8$^+$ T cell responses in mice protected from tumour development

The association between 5T4-specific T cell responses and protection from LLC1 growth was then examined. Mice that did not develop tumours were monitored until day 61 post-challenge before splenocytes were isolated and stained for CD8, CD4, CD3 and with 5T4-specific tetramers. Responses were compared with splenocytes taken from tumour-bearing mice at the time of sacrifice. An increase in the accumulation of splenic CD4$^+$ and CD8$^+$ cells in mice receiving MCMV in the boost vaccination compared to the control group (PBS + PBS) was observed (Figure 4.25). Furthermore, the data was re-assessed to examine any differences between mice that develop tumours and those that did not, regardless of the immunisation received. Mice that did not develop tumours displayed a higher frequency and total counts of splenic CD4$^+$ and CD8$^+$ T cells (Figure 4.26).

CD8$^+$ T cells specific for 5T4 were examined and no differences were observed in the number of 5T4-tetramer$^+$ CD8$^+$ T cells between the groups studied (Figure 4.27A). Furthermore, functional analysis did not reveal any significant differences in the total number of 5T4-responding CD8$^+$ T cells between the groups studied (Figure 4.27B). However, mice receiving RAd-5T4 + MCMV-MIE-5T4 and RAd-5T4 + RAd-5T4 displayed increased polyfunctional 5T4-specific CD8$^+$ T cells, producing both IFN-γ and TNF-α (Figure 4.27B, left panel). As above, 5T4-specific CD8$^+$ T cells were examined in mice that developed tumours and those that did not. Mice that did not develop tumours in the period studied displayed a significantly higher accumulation of $5T4_{170\text{-}178}$- and $5T4_{253\text{-}260}$- specific CD8$^+$ T cells than mice that developed tumours (Figure 4.28A&B). Furthermore, mice that did not develop tumours exhibited significantly higher numbers of splenic 5T4-specific CD8$^+$ T cells that produced solely TNF-α (IFN-γ^-TNF-α^+) (Figure 4.28C, right panel). Of note,

In addition, similar to data obtained from peripheral blood analysis, MCMV-specific $CD8^+$ T cell responses were decreased in mice receiving RAd-5T4 + MCMV-MIE-5T4 compared to RAd-CTL + MCMV-MIE-5T4 group or the MCMV control group challenged with RAd-5T4 + MCMV-ΔIE2 (Figure 4.29).

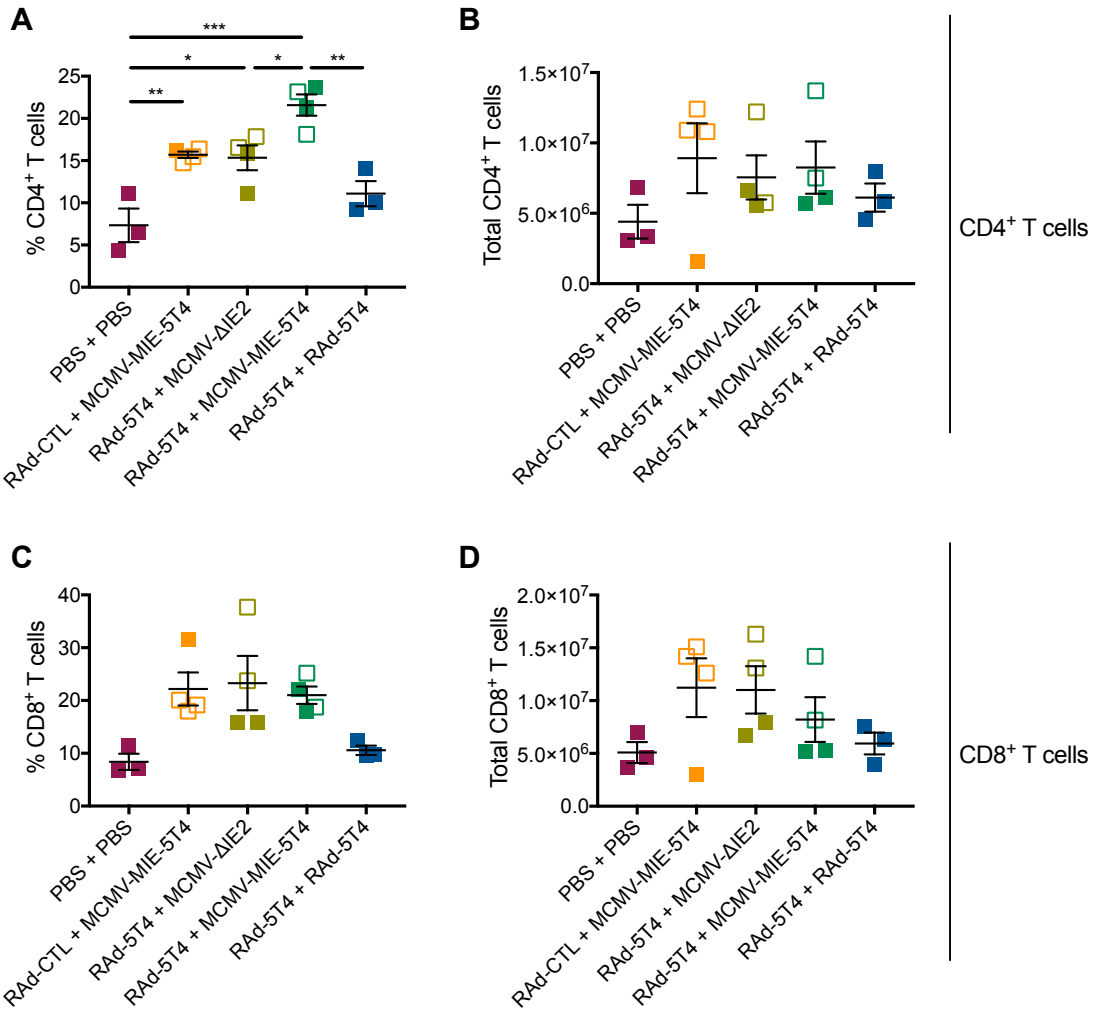

Figure 4.25 Mice receiving MCMV in their vaccination regime have a higher frequency of splenic CD4$^+$ and CD8$^+$ T cells.

Spleens were harvested form the mice in the above study (Figure 4.21A) at the point of sacrifice. These were processed into single cell suspensions and stained for CD8α and CD4. **(A)** Frequency and **(B)** total numbers of splenic CD4$^+$ T cells. **(C)** Frequency and **(D)** total numbers of splenic CD8$^+$ T cells. Data shown as individual mice with mean $\pm$ SEM (n=3-4 mice/group). Filled squares represent mice that developed tumours while empty squares represent mice that did not develop tumours across the duration of the study. Significance was assessed by one-way ANOVA with Bonferroni's for multiple comparisons. *p<0.05, **p<0.01 and ***p<0.005.

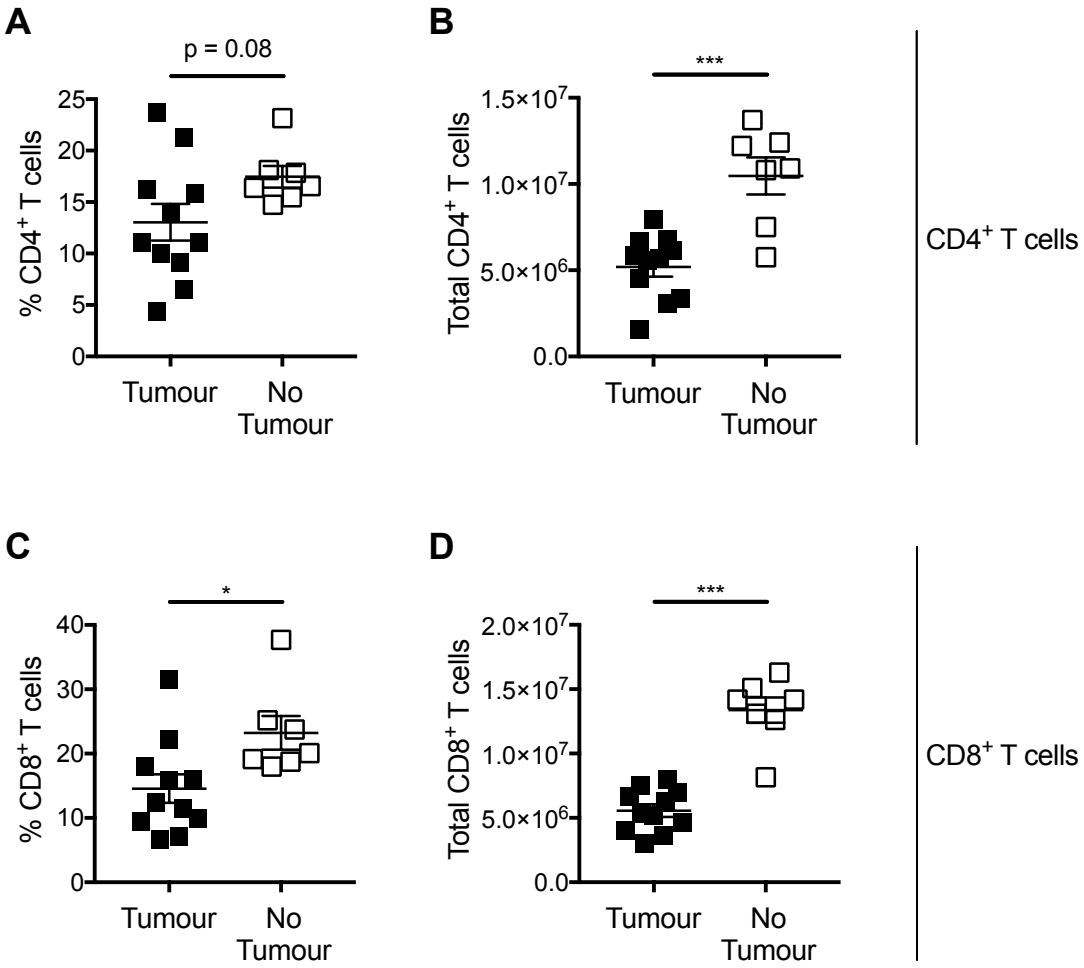

Figure 4.26 Mice that did not develop tumours during the study mount higher splenic CD4$^+$ and CD8$^+$ T cell responses.

Data from Figure 4.25 was re-assessed to compare mice that developed tumours with those that didn't, regardless of the immunisation received. **(A)** Frequency and **(B)** total numbers of splenic CD4$^+$ T cells. **(C)** Frequency and **(D)** total numbers of splenic CD8$^+$ T cells. Data shown as individual mice with mean ± SEM (n=11-7 mice/group). Significance was assessed unpaired *t* test. *p<0.05 and ***p<0.005.

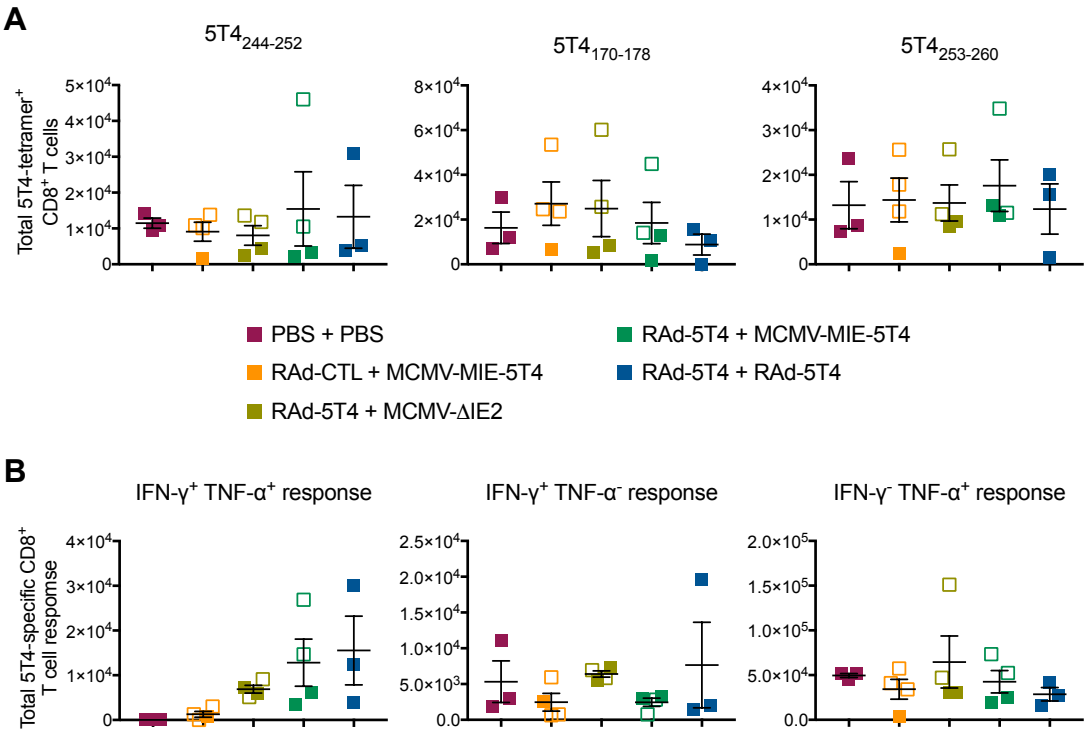

Figure 4.27 Prime-boost does not influence splenic total numbers of 5T4-specific CD8$^+$ T cells.

Spleens were harvested form the mice in the above study (Figure 4.21A) at the point of sacrifice (either after tumour development or day 61 after tumour challenge). **(A)** Splenocytes were stained for CD8α, CD3 and with tetramers specific for the 5T4 immunodominant peptides to obtain total numbers of tumour-specific CD8$^+$ T cells. Left graph: 5T4$_{244\text{-}252}$-tetramer$^+$ CD8$^+$ T cells; middle graph: 5T4$_{170\text{-}178}$-tetramer$^+$ CD8$^+$ cells; and right graph: 5T4$_{253\text{-}260}$-tetramer$^+$ CD8$^+$ T cells. **(B)** Splenocytes were stimulated *ex vivo* with a mix of the three 5T4 peptides followed by staining for CD8α, IFN-γ and TNF-α to obtain total numbers of CD8$^+$ T cells responding to 5T4. Left graph: IFN-γ^+TNF-α^+ 5T4-specific CD8$^+$ T cells; middle graph: IFN-γ^+TNF-α^- 5T4-specific CD8$^+$ T cells; right graph: IFN-γ^-TNF-α^+ 5T4-specific CD8$^+$ T cells. Filled squares represent mice that developed tumours and empty squares represent mice that did not develop tumours during the duration of the study. Data shown as individual mice with mean $\pm$ SEM (n=3-4 mice/group).

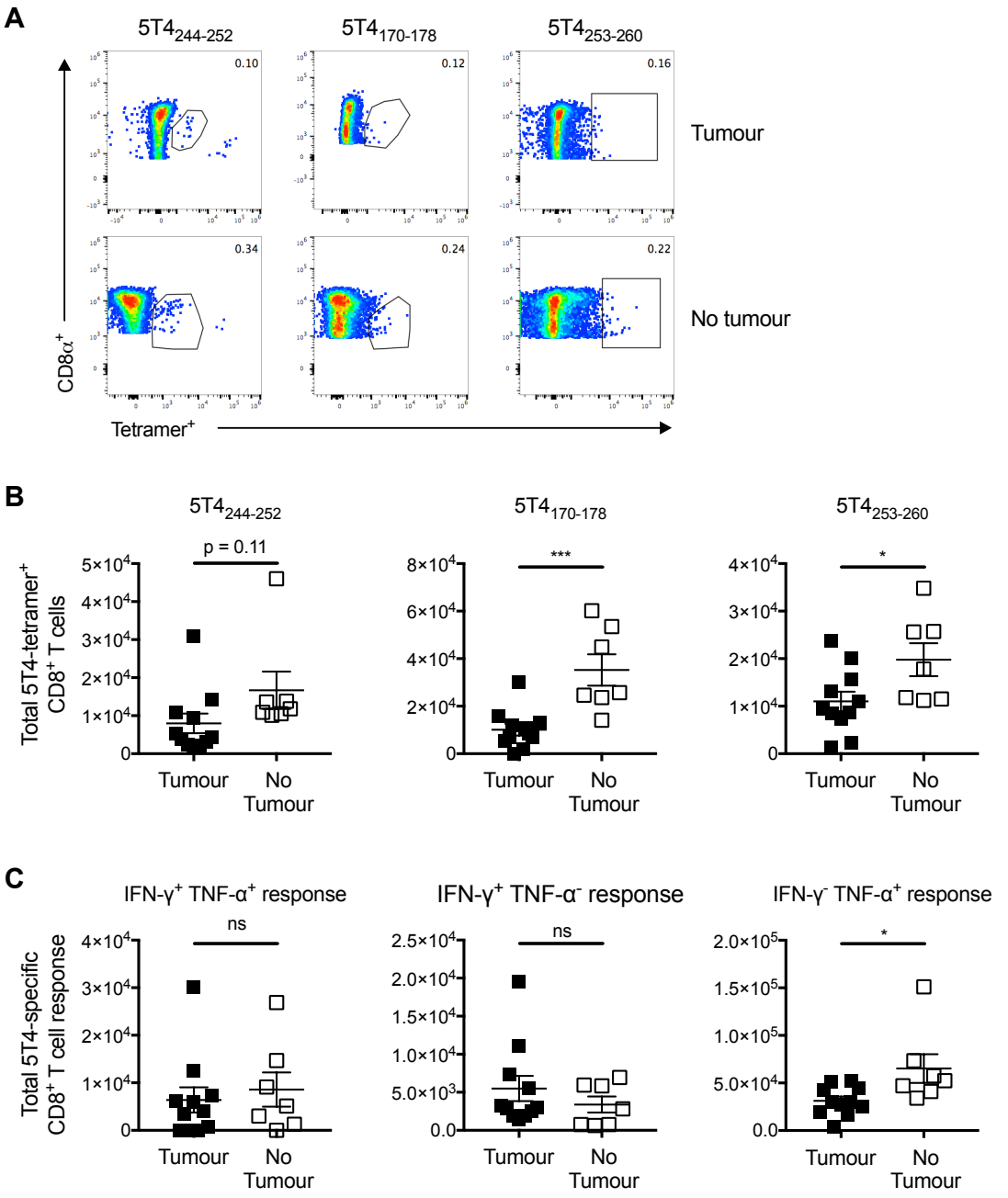

Figure 4.28 5T4-specific immunity correlates with tumour protection in mice.

Data from Figure 4.27 was re-assessed to compare mice that developed tumours with those that did not. **(A)** Representative flow cytometry plots of CD8α versus $5T4_{244-252}$-tetramer (left plots), $5T4_{170-178}$-tetramer (middle plots) and $5T4_{253-260}$-tetramer (right plots). Data representative of 11 (tumour) and 7 (no tumour) mice. **(B)** Total numbers of tumour-specific $CD8^+$ T cells. Left graph: $5T4_{244-252}$-tetramer$^+$ $CD8^+$ T cells; middle graph: $5T4_{170-178}$-tetramer$^+$ $CD8^+$ T cells; and right graph: $5T4_{253-260}$-tetramer$^+$ $CD8^+$ T cells. **(C)** Total numbers of $CD8^+$ T cells responding to 5T4. Left graph: IFN-γ^+TNF-α^+ 5T4-specific $CD8^+$ T cells; middle graph: IFN-γ^+TNF-α^- 5T4-specific $CD8^+$ T cells; right graph: IFN-γ^-TNF-α^+ 5T4-specific $CD8^+$ T cells. Data shown as individual mice with mean ± SEM (n=11-7 mice/group). Significance was assessed unpaired *t* test. *p<0.05, ***p<0.005 and ns = not significant.

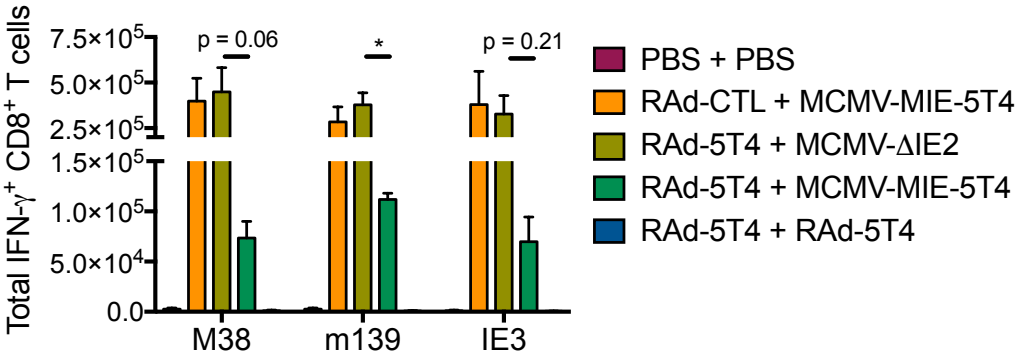

Figure 4.29 Prime-boost with RAd-5T4 + MCMV-MIE-5T4 results in lower MCMV-specific CD8$^+$ T cell responses.

Spleens were harvested from the mice in the above study (Figure 4.21A) at the point of sacrifice and processed into single cell suspensions. Splenocytes were stimulated *ex vivo* for 6 hours with the MCMV endogenous peptides M38, m139 and IE3. Subsequently, cells were stained for CD8α and IFN-γ to obtain the total numbers of virus-specific IFN-γ^+ CD8$^+$ T cells. Data shown as mean + SEM (n=3-4 mouse/group). Significance assessed by one-way ANOVA with Dunnett's correction, comparing those groups receiving MCMV-MIE-5T4 with control group receiving MCMV-ΔIE2. *p<0.05.

4.4 Discussion

4.4.1 Immunogenicity of single dose MCMV vectors

In this chapter, the use of recombinant MCMV vectors expressing the human tumour-associated antigens NY-ESO-1 and 5T4 (Chapter 3) in cancer immunotherapy was evaluated. Single challenge with the vectors MCMV-NY-ESO-1, MCMV-5T4 and MCMV-IE3-P2A-5T4 did not elicit detectable levels of tumour-specific $CD8^+$ T cells. In contrast, MCMV-IE1-P2A-5T4 and MCMV-MIE-5T4 induced 5T4-specific $CD8^+$ T cells, although the response induced by the latter was debateable due to the high background responses at early time-points. The most apparent explanation for the lack of tumour-specific responses in the first three vectors was low NY-ESO-1 and 5T4 protein expression, since MCMV-IE1-P2A-5T4 and MCMV-MIE-5T4 expressed 5T4 at higher levels (Chapter 3, Figure 3.13) and induced 5T4-specific immune responses. This suggests that the site of gene insertion within the MCMV genome as well as the promoter driving its expression influence exogenous protein expression and subsequent vector immunogenicity. Studies using MCMV vaccines encoding single MHC class I restricted immunodominant epitopes tagged to the C-terminus of the *ie2* gene have shown to induce improved $CD8^+$ T cell response as compared to those expressing the entire protein (472), indicating that peptide processing influences T cell responses. Although this strategy is attractive, in a clinical setting for cancer immunotherapy it is not optimal given the diverse repertoire of HLA alleles expressed by humans. Furthermore, this method would restrict the immune response towards a $CD8^+$ T cell response only, while $CD4^+$ T cells and antibodies are also important in mediating protection against tumours in mice (432, 465, 473, 474). Another strategy used to improve $CD8^+$ T cell responses is to mutate the tumour-associated antigen epitope to increase its affinity for MHC class I molecules. Qiu *et al.* (433) showed that an MCMV vector expressing the native gp100 protein did not generate gp100-specific

$CD8^+$ T cells, while that expressing gp100 with the mutated epitope resulted in a robust tumour-specific immune response. Lastly, homologous prime-boost immunisation with a MCMV based vector has been shown to induce detectable levels of antigen-specific immune responses (431) and prime-boost regimens have been successfully explored in cancer immunotherapy to augment tumour-specific $CD8^+$ T cells (230, 269).

MCMV-IE1-P2A-5T4 vector

Sequencing data of the MCMV-IE1-P2A-5T4 vector revealed that the viral genome had the genes from *m07* to *m18* deleted. The proteins encoded by the genes *m07* to *m16* are members of the *m02* gene family (369). Although the function of most of them remain unknown, as a group they have been implicated in evasion of NK cell mediated immunity. This was originally concluded based on experiments in which MCMV lacking genes from *m02* to *m16* grew like WT-MCMV *in vitro* and in C57BL/6 mice depleted of NK cells, but produced less infectious virus in BALB/c and C57BL/6 (475). The protein encoded by the gene *m17* is a member of the *m145* gene family with unknown function to date (369). Lastly, it has been suggested that *m18* gene product inhibits histone deacetylases which in turn increases the expression of several host genes that favours viral fitness *in vivo* (476, 477). These results suggest that the deletion of this region within MCMV-IE1-P2A-5T4 resulted in a less virulent vector perhaps due to elevated NK cell responses. However, as shown in Chapter 3, MCMV-IE1-P2A-5T4 exhibited impaired replication *in vitro* in the absence of immune pressure, suggesting that the site of *5T4* insertion affected IE1 function. Thus, impaired 5T4-specific memory T cell responses induced by this vector may be due to impaired initial virus replication and/or persistence due to defective IE1 function. Nonetheless, inserting *5T4* within the *ie1* locus appears to be a promising site to induce inflationary anti-tumour responses. In order to avoid any interference with IE1 function, in the future it will be interesting to examine whether inserting *5T4* at the beginning of the *ie1* ORF could induce 5T4-specific immunity without influencing IE1 function.

MCMV-MIE-5T4 vector

The lack of 5T4-specific $CD8^+$ T cell inflation observed after the acute response upon intraperitoneal infection with MCMV-MIE-5T4 might be due to the time point chosen to analyse tumour-specific T cell responses. Several studies using MCMV vectors engineered to express tumour-associated antigens gp100 and PSA did not observe an inflationary anti-tumour response until day 320 (433) and week 32 (431) post-infection, respectively. Thus, it is possible that the last time when 5T4-specific $CD8^+$ T cells were analysed after MCMV-MIE-5T4 challenge (i.e. week 26) was too early. Therefore, it would be interesting to examine 5T4 immune responses after ~1 year post-infection. Furthermore, 5T4 expression in this vector is driven by an exogenous promoter (i.e. HCMV MIE promoter). It is not known whether this promoter becomes silenced during MCMV latency, which could result in the loss of inflationary responses.

4.4.2 Immunogenicity of prime-boost immunisation with RAd and MCMV vectors

In this project, RAd vectors expressing NY-ESO-1 or 5T4 were used in combination with MCMV-NY-ESO-1 and MCMV-MIE-5T4, respectively, which resulted in polyfunctional tumour-specific $CD8^+$ T cells. A much higher frequency of tumour-specific $CD8^+$ T cells was observed in the NY-ESO-1 vaccination because this antigen is an exogenous protein while 5T4 protein is a 'self-protein' and tolerance mechanisms might suppress 5T4-reactive immune responses.

In contrast to MCMV-NY-ESO-1, RAd-NY-ESO-1 induced a strong NY-ESO-1_{81-88}-specific $CD8^+$ T cell response after a single administration. As mentioned above, this might be due to strong NY-ESO-1 protein expression driven by the HCMV MIE promoter, while in the MCMV vector the *NY-ESO-1* was placed under the endogenous MCMV *ie2* promoter. A study has suggested that the amount of IE2 protein synthesised during *in vivo* infection is very low as IE2 protein could not be

detected using sera from infected mice (456). Thus, the low level of NY-ESO-1 expression by the MCMV vector might lead to inefficient antigen processing and presentation resulting in the absence of anti-tumour immune response.

During the NY-ESO-1 prime-boost immunisation, mice receiving RAd-NY-ESO-1 + MCMV-NY-ESO-1 and vice versa, displayed a lower magnitude of tumour-specific $CD8^+$ T cells in the circulation compared to that of RAd-NY-ESO-1 + RAd-NY-ESO-1 or RAd-NY-ESO-1 alone at day 7 post-boost. This could be due to the strong immunogenic nature of the MCMV vector that contains antigens that may 'compete' with the inserted tumour-associated antigen, skewing the immune response towards the MCMV antigens rather than to NY-ESO-1. However, by day 29 NY-ESO-1 responses continued to decrease in mice immunised with RAd-NY-ESO-1 + MCMV-NY-ESO-1, while mice administered with MCMV-NY-ESO-1 + RAd-NY-ESO-1 displayed comparable frequencies of NY_{81-88}-specific $CD8^+$ T cells as RAd-NY-ESO-1 + RAd-NY-ESO-1. This suggests the order of the vector given in a prime-boost regime may affect the induction of antigen-specific $CD8^+$ T cell responses. Indeed, this correlates with recently published data where in sequential infections, first with MCMV followed by Ad-lacZ (expressing β-galactosidase), the induced Ad-lacZ-specific cells did not have an impact on the pre-existing MCMV-specific effector cell population. In contrast, mice infected with Ad-lacZ first followed by MCMV resulted in a rapid decline of pre-existing Ad-lacZ-specific population, which was associated with the activation of Fas-dependent apoptotic pathways (478). However, re-exposure to Ad-lacZ resulted in the rapid re-expansion of the remaining pool of the depleted Ad-lacZ-specific population (478). In addition, 100 days after MCMV infection, slow recovery of Ad-lacZ-specific $CD8^+$ T cells was observed in the lungs of mice receiving Ad-lacZ followed by MCMV infection (478). The authors stated that this site displayed a higher expression of β-galactosidase, than other tissues such as the liver, which could drive the expansion of the Ad-lacZ-specific $CD8^+$ T cells owing to increased antigen levels

(478). This compares to the data described in my prime-boost experiment using 5T4-expressing RAd and MCMV vectors. RAd-5T4 + MCMV-ΔIE2 resulted in a decrease in 5T4-specific $CD8^+$ T response, while the anti-tumour response was maintained in mice administered with RAd-5T4 + MCMV-MIE-5T4, most probably due to the expression of 5T4 by the MCMV vector. However, RAd-5T4 + RAd-5T4 still displayed the highest magnitude of 5T4-specific response, probably due to its replicative-defective nature rendering the vector less immunogenic than MCMV. Nonetheless, prime-boosting with RAd-5T4 and MCMV-MIE-5T4 resulted in the induction of polyfunctional 5T4-specific $CD8^+$ T cell responses; although, these did not inflate by day 68 post-boost. Although time restrictions precluded further studies of these responses, it will be interesting to following these immune responses for a longer period to ascertain whether RAd-MCMV prime-boost strategies can induce inflationary 5T4-specific $CD8^+$ T cell responses.

4.4.3 Protective efficacy of prime-boost immunisation with RAd and MCMV vectors

Prime-boost immunisation with NY-ESO-1-expressing vectors resulted in delayed tumour onset that was associated with increased infiltration of NY_{81-88}-specific $CD8^+$ T cells at the tumour site. As mentioned in section 4.3.1.3 there is a possibility that the implanted CT26-NY-ESO-1 cells might have lost the expression of NY-ESO-1 due to the immune responses induced by the vaccines which, apart from targeting NY-ESO-1 expressing cells, may select for antigen-loss cell variants *in vivo* that eventually form a tumour unresponsive to NY-ESO-1 specific T cell immunity. Indeed, studies from melanoma cancer patients have reported a decreased antigen expression in tumours after peptide vaccination (479–481).

Regarding the 5T4 prime-boost study, upon tumour challenge not all the vaccinated mice developed tumours during the period studied. Interestingly, at first glance the magnitude of 5T4-specific $CD8^+$ T cell response in the circulation observed at day 68 post-boost did not correlate with tumour protection since all mice challenged with RAd-5T4 + RAd-5T4, which exhibited the highest 5T4-specific $CD8^+$ T cell response, developed tumours. However, it is not possible to rule out the possibility that 5T4-specific $CD8^+$ T cells countered tumour development since anti-tumour immune responses were not analysed just before tumour challenge. Moreover, it would have been interesting to examine peripheral 5T4 responses following tumour challenge. Nonetheless, immunisation with RAd-5T4 + RAd-5T4 delayed the onset of tumour development, suggesting that 5T4-specific $CD8^+$ T cells may restrict LLC1 growth. Furthermore, I cannot rule out the possibility that LLC1 cells lost 5T4 expression, thus affecting the protective capacity of vector-induced 5T4-specific T cell immunity.

At the end of the study, splenocytes were analysed and compared between mice that developed tumour and those that didn't. Encouragingly, mice that did not develop tumours exhibited significantly higher accumulation of $CD4^+$ and $CD8^+$ T cells. The latter is not surprising since MCMV (all the mice that did not develop tumour had received either MCMV-ΔIE2 or MCMV-MIE-5T4) induce robust, long-lived $CD8^+$ T cell responses. However, these data also suggest that 5T4-specific $CD4^+$ T cells could be involved in tumour protection, although these were not examined. In addition, mice in which tumours did not develop displayed a higher magnitude of 5T4-specific $CD8^+$ T cells that produced only TNFα, suggesting a possible role for tumour-specific production of this cytokine in protection. Intriguingly, not all the mice receiving MCMV boost were protected from LLC1 tumour challenge. The differences within the same group might lie in the ability of 5T4-specific immune cells to rapidly access the tumour. For example, in mice that did not develop tumours, 5T4-specific immune cells might have arrived at the site of tumour challenge before the tumour cells established an

immunosuppressive environment, allowing the cells to exert their anti-tumour activity. In contrast, in tumour-bearing mice, the tumour cells might have been able to establish an immunosuppressive environment, preventing lymphocytes exerting their anti-tumour activity.

Data suggests that MCMV is mediating protection against tumour development as at least half of the mice boosted with the MCMV vector did not develop palpable tumours. Other immune mediators, such as 5T4-specific $CD4^+$ T cells (as an increased accumulation of splenic $CD4^+$ T cells was observed in tumour-free mice) and antibodies may have been induced by the MCMV vector and might have contributed to tumour protection. Indeed, several tumour immunotherapy models have shown that $CD4^+$ T cells and antibodies can be essential for anti-tumour activity *in vivo*. For example, immunisation with VV or Ad vectors expressing HPV E6 or E7 generated $CD4^+$ or $CD8^+$ T cells that were protective upon tumour challenge, depending on the mouse model used (473). In a study using the melanoma B16 model, mice immunised with a VV vector expressing TRP-1 were protected from tumour challenge that was dependent on $CD4^+$ T cells (474). These mice also exhibited high titers of IgG anti-TRP-1 antibodies (474). Another study using the same tumour model, but immunised with an MCMV vector expressing TRP-2 induced rejection of B16 melanoma cells via induction of TRP-2-specific antibodies (432). In both studies, no evidence of $CD8^+$ T cells recognising the tumour-associated antigens was reported. Furthermore, immunisation with MVA expressing human 5T4 induced protective immunity to CT26- and B16- expressing human 5T4 tumour challenge but $CD8^+$ T cells against 5T4 were not detected (465). Authors reported the presence of IgG2 5T4-specifc antibodies, although $CD4^+$ T cell responses cannot be excluded. (465). Taken together, these data suggest that the mechanism for successful anti-tumour therapy, either humoral or cellular immunity, may vary for different types of tumour and tumour-associated antigen target.

Mice boosted with the MCMV vector in the NY-ESO-1 and 5T4 immunisation studies displayed increased influx of $CD8^+$ T cells into tumours, suggesting that MCMV may alter the tumour microenvironment by creating a more immunogenic site or impacting on $CD8^+$ T cell responses, making these cells more likely to infiltrate the tumour irrespective of the tumour environment. A study recently described that independent of antigen, intratumoural MCMV immunisation resulted in significantly delay in subcutaneous B16 tumour growth that was dependent on $CD8^+$ T cells (482). The magnitude of T cell recruitment into the tumour was comparable to that induced when MCMV was administered intraperitoneally, which did not result in delay in tumour growth, suggesting that intratumoural MCMV immunisation affects the tumour microenvironment, which ultimately leads to a delay in tumour growth (482). In addition, tumour-associated macrophages (TAMs) became infected with MCMV. TAMs found in tumours often exhibit an anti-inflammatory phenotype, producing high levels of IL-10 and TGF-β, lose expression of pro-inflammatory T_H1-inducing cytokines and MHC class II, and release CCL2 that can promote Treg infiltration (483). Macrophages are targets for CMV during normal viral infection resulting in the release of cytokines that recruit monocytes to the site of infection that will differentiate into pro-inflammatory macrophages (484). After HCMV infection, macrophages release pro-inflammatory cytokines, have increased TLR expression and improved MyD88 signalling, leading to increased T cell proliferation (485). Thus, if MCMV vectors in my studies gained access to the tumour microenvironment and TAMs, these vaccines may non-specifically induce intra-tumoural T cell responses.

Furthermore, recently it has been suggested that anti-tumour effects can be mediated by 'bystander activated' memory T cells that do not need antigen-specific TCR engagement for activation (486–488). A study in mice by Tietze *et al*. described the antigen-independent expansion of memory $CD8^+$ T cells following cytokine-based immunotherapies (e.g. CD40 agonist and IL-2), resulting in the expansion of memory

$CD8^+$ T cells expressing NKG2D and possessing elevated lytic capabilities without CD25 upregulation (which is associated with TCR activation) and PD-1 expression (486). Additionally, the authors showed that these antigen-independent expanded $CD8^+$ T cells exerted anti-tumour effects, partially, via the detection of NKG2D ligand on tumour cells (486). Moreover, human melanoma biopsies from patients after receiving local immunomodulatory treatment displayed an increased infiltration of $CD8^+$ T cells with a similar phenotype ($CD8^+CD25^-$) (486). Further reports have described the presence of non-tumour-specific $CD8^+$ TILs (including virus-specific $CD8^+$ TILs) in human lung cancer and CRC, that lack the hallmarks of chronic antigen stimulation (489). It is well established that MCMV induces the accumulation of memory $CD8^+$ T cells in different sites throughout the host. Thus, MCMV may improve anti-LLC1 protection by inducing local non-specific memory $CD8^+$ T cell activation. In this regard, bystander activated cells might have an advantage over activated antigen-specific $CD8^+$ T cells. Tumour cells often downregulate MHC molecules and tumour antigen expression to avoid recognition by T cells. In contrast, bystander-activated $CD8^+$ T cells do not rely on the recognition of MHC-bound peptides. Furthermore, non-specific $CD8^+$ T cells do not upregulate PD-1 expression when activated, thus it may render them less susceptible to the immunosuppressive tumour microenvironment. An effective anti-tumour therapy would combine the induction of both antigen-specific and antigen-nonspecific responses to allow maximal anti-tumour effects.

To conclude, prime-boost strategies using RAd and MCMV vectors have the potential to break tolerance and induce high frequencies of tumour-associated antigen-specific T cells. Encouragingly, prime-boost immunisation with NY-ESO-1- and 5T4-expressing vectors delayed tumour onset, and resulted in complete tumour protection for some mice. Hence, the combination of RAd + MCMV may be a promising approach for cancer vaccine development. However, further studies are needed to investigate what

anti-tumour mechanisms elicited by MCMV vectors contribute to anti-tumour protection.

Chapter 5 - Examining the immunogenicity of spread- sufficient and deficient MCMV via different administration routes

5.1 Introduction

5.1.1 Safety profile of CMV

HCMV is generally asymptomatic in immunocompetent individuals but can cause severe disease and sometimes death in immunocompromised patients such as HIV-infected persons, organ transplant recipients and those with hereditary severe combined immunodeficiency, in addition to the immunologically immature (new-born infants) (321, 322). Patients with weakened immune systems, which may include cancer patients, are at high risk of reactivation of latent CMV, causing diseases such as hepatitis, retinitis, colitis and pneumonitis. The severity of medical problems associated with HCMV in these vulnerable populations clearly demonstrate the need to develop a replication-defective CMV vector to achieve an acceptable safety profile in order to exploit the attractive immunological characteristics this virus offers to be used in a vaccine to treat diseases.

5.1.2 Spread-defective MCMV

The ability to genetically manipulate genomes has allowed the identification of many essential genes for viral replication and assembly of viral particles. These can be targeted to generate virus particles that are replication-deficient or unable to spread between cells. Replication-defective viral mutants require propagation in

complementary cell lines that express the missing viral gene(s) to allow viral replication. In normal recipient cells the process for viral replication cannot be completed hence no virus progeny is produced. Nevertheless, viral genes are still expressed within the infected cell, which can result in the induction of an immune response (246). A good example is the generation of a replication-defective HSV-I strain that protects against HSV-I infection (490, 491). A slightly different approach is the generation of single-cycle viral mutants. These viral vectors lack a protein that is essential following viral assembly (492–494). As for the replication-deficient mutants, these need to be propagated in complementing cells expressing the missing gene product. In contrast, in normal cells replication occurs as usual and progeny virions are produced; however, these are non-infectious and cannot infect other cells. The demand for replication-defective vaccines emerge from the fact that these have improved safety profiles as compared to replicating viral vectors.

Regarding CMV, several attempts have been made to generate a safe and immunogenic CMV vector either to be used to protect against CMV itself or as a vaccine for other diseases. In mice, a temperature-sensitive MCMV vector unable to replicate failed to induce robust virus-specific $CD8^+$ T cell memory responses (495). On the other hand, spread-defective MCMV vectors have revealed to be promising vectors due to their ability to induce a strong T cell immunity (410, 496). These MCMVs are replication competent but are unable to generate infectious virus particles. For example, MCMV lacking the essential gene *M94* deleted (MCMV-ΔM94) expressing OVA induced robust OVA-specific $CD4^+$ and $CD8^+$ T cell responses comparable to those induced by WT-MCMV-expressing OVA, upon intraperitoneal challenge (496). In addition, MCMV-ΔM94 was non-pathogenic and protective against challenge with WT-MCMV, even in highly susceptible $IFN\alpha\beta R^{-/-}$ mice (496). A spread-defective MCMV used to investigate the *in vivo* immunogenicity of attenuated CMV-based vectors when administered via various routes lacked the viral glycoprotein L (gL), ΔgL-MCMV, which

is an essential protein for viral entry into the host cell (refer to Chapter 1, section 1.4.2.1). Briefly, gL forms a heterodimer with gH, which along gB, initiates membrane fusion and viral entry (reviewed in (497)). Thus, elimination of gL from the viral genome renders the virus unable to enter cells, but it can still replicate within the infected cell and produce virions. Due to its inability to enter cells, ΔgL-MCMV is grown in a complementary cell line in which NIH-3T3s stably express gL (gL-3T3), which will incorporate the gL onto the virions' envelope, allowing ΔgL-MCMV to infect cells but not spread/re-infect after the initial infection. When administered intraperitoneally, ΔgL-MCMV retained its immunogenic properties, driving MCMV-specific $CD8^+$ T cell memory inflation. However, the magnitude of these responses were much lower as compared to those induced by WT-MCMV (410).

5.1.3 Routes of administration

The route by which a vaccine is administered to an individual is of highly importance for the immunisation to be a success. In order to maximize effectiveness, vaccines can be given either by intramuscular injection, subcutaneous injection, intradermal injection, intranasal spray or oral administration. Experimental studies of immunity against CMV in the well-studied animal model of adult mouse infection have largely relied on infection by the intraperitoneal or intravenous route (400, 401). During the acute phase of intraperitoneal infection, MCMV propagates in multiple tissues including the spleen, liver and lung prior to dissemination to the salivary glands. MCMV eventually establishes latency in multiple tissues including salivary glands, lung, kidney and spleen. Acute MCMV infection results in a robust $CD8^+$ T cell response where virus-specific $CD8^+$ T cells accumulate overtime, consisting predominantly of effector memory cells. However, this site of challenge is not clinically relevant for vaccine administration. Few groups have used mucosal infection routes, such as intranasal challenge for MCMV research (498–500). Intranasal infection results in robust virus

replication in the lung and efficient spread to the salivary glands but limited replication in the spleen (498). $CD8^+$ T cell responses upon intranasal infection are reduced as compared to intraperitoneal infection, yet MCMV-specific $CD8^+$ T cells have similar inflation kinetics and phenotype (498). Intragastric infection on the other hand, results in poor virus replication and induces impaired MCMV-specific T cells responses (498). Another site of infection commonly used in MCMV research is injection by the footpad. Although it results in the accumulation of MCMV-specific $CD8^+$ T cells, the frequency of these cells are substantially lower compared to intraperitoneal infection (410, 501). However, in terms of vaccine development, this route of administration is not a viable option. In this study, I propose to study the immunogenicity of local MCMV challenge via the clinically relevant subcutaneous immunisation route.

5.1.4 Aims

The aims of the studies outlined in this chapter were the following:

1. Examine the induction of T cell memory within tissues following intraperitoneal challenge with ΔgL-MCMV;

2. Examine the immunogenicity of ΔgL-MCMV following subcutaneous challenge.

5.2 Results

5.2.1 Confirmation that ΔgL-MCMV is spread-deficient

Since the spread-defective MCMV vector ΔgL-MCMV requires growth using a complementary cell line, there was a possibility that the virus could acquire the gL gene through recombination, and thus become capable of spreading *in vivo*. Hence, for each new stock of ΔgL-MCMV generated it was necessary to confirm that ΔgL-MCMV was indeed spread defective. As described in section 5.1.2, ΔgL-MCMV grown on the supporting cell line will contain the gL in the viral envelope but not in the viral genome and will only be capable of a single round of infection in non-complementing cells. NIH-3T3 cells were infected at a low multiplicity of infection (MOI 0.1) with either ΔgL-MCMV or WT-MCMV (K181 MCMV). At day 3 p.i, cells infected with ΔgL-MCMV exhibited the typical MCMV-induced cytopathic/rounding effect (Figure 5.1A). At day 6 p.i, ΔgL-MCMV-infected cells had grown more confluent than cells infected with WT-MCMV (Figure 5.1A), indicating infection by ΔgL-MCMV was defective. To confirm that the virus could not spread beyond this initial round of infection, supernatant from cultures already infected with either ΔgL-MCMV or WT-MCMV were transferred to fibroblasts not exposed to virus. Six days after adding the supernatant, no cytopathic cells were observed in ΔgL-MCMV-infected cells, while those receiving supernatant from WT-MCMV-infected cultures predominantly exhibited a morphology indicative of active MCMV infection (Figure 5.1B). These experiments demonstrated that the stocks of ΔgL-MCMV used in *in vivo* experiments were unable to spread *in vitro* and did not contain contaminating virions that might have acquired the *gL* gene.

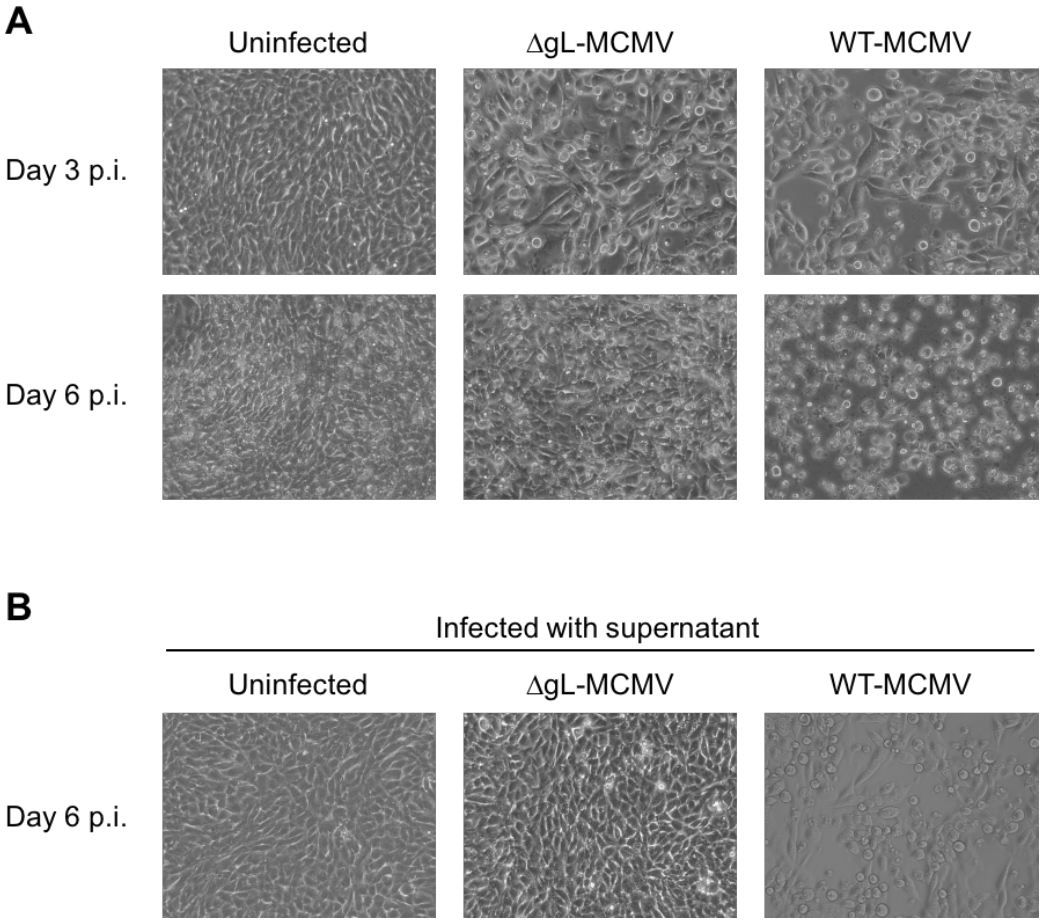

Figure 5.1 ΔgL-MCMV cannot spread *in vitro* after first round of infection.

(A) $1x10^5$ NIH-3T3 cells were infected or not at an MOI = 0.1 with either ΔgL-MCMV or WT-MCMV and incubated for several days. Images were captured at day 3 (top three images) and day 6 (bottom three images) p.i at a magnification of 20x. **(B)** $1x10^5$ 3T3 cells were infected with 200μL of day 6 p.i supernatant from ΔgL-MCMV or WT-MCMV-infected cultures and incubated for several days. Images were captured at day 6 p.i at a magnification of 20x.

5.2.2 Immune responses induced by ΔgL-MCMV after intraperitoneal challenge

5.2.2.1 ΔgL-MCMV infection induces sub-optimal CMV-specific CD8$^+$ T cell accumulation in spleen and salivary glands

Both CD4$^+$ and CD8$^+$ T cells are necessary in the defence against CMV. MCMV-specific CD8$^+$ T cells are important in controlling MCMV infection during the acute phase (502) while CD4$^+$ T cells are required for viral clearance from the salivary glands (392, 396, 397). ΔgL-MCMV has been previously shown to be immunogenic, inducing the generation of MCMV-specific CD8$^+$ T cells, though substantially smaller in numbers than after WT-MCMV infection (410, 494). These studies were done predominantly in C57BL/6 mice, which are more "resistant" to MCMV infection than BALB/c (503–507) . Snyder *et al.* (410) also examined MCMV responses to ΔgL-MCMV in BALB/c, demonstrating that they induced similar inflation levels to WT-MCMV infection. These responses were only examined in the peripheral blood, based on measurements of frequency of MCMV-specific cells within circulating CD8$^+$ T cells and were not characterised further. Hence, I first determined in detail the impact that a spread-defective MCMV has on the immunogenicity of the vector in BALB/c mice following intraperitoneal infection, with either ΔgL-MCMV or WT-MCMV.

Following infection, blood was withdrawn from the lateral tail vein at different time points for a period of 4 months, when mice were sacrificed and multiple organs harvested to examine CD8$^+$ T cell responses. Infection with ΔgL-MCMV induced an expansion of CD8$^+$ T cells in the peripheral blood over time as observed following infection with WT-MCMV (Figure 5.2A). However, CD8$^+$ T cell accumulation in the blood during ΔgL-MCMV infection was delayed and did not reach the levels seen during WT-MCMV infection until week 16 p.i. This was associated with reduced CD8$^+$ T cell

accumulation in the spleen, lung and salivary glands, although this was only statistically significant in the spleen (Figure 5.2B). In addition, MCMV-specific $CD8^+$ T cell responses were followed over time in the peripheral blood. As previously described in experiments using BALB/c mice, ΔgL-MCMV infection induced an inflationary pp89-specific $CD8^+$ T cell response comparable to that induced by WT-MCMV infection (Figure 5.3A). However, in contrast with what has been previously reported, in our hands pp89-specific $CD8^+$ T cells were detectable from week 1 after ΔgL-MCMV infection, although these were almost four times lower than those induced by WT-MCMV infection (1.6% vs 6.3%) (Figure 5.3A). To analyse T cell location during chronic ΔgL-MCMV infection, lymphocytes were isolated from different tissues at week 17 p.i and stained for pp89-specific cells. Overall, pp89-specific $CD8^+$ T cell infiltration was found in all the peripheral organs studied (spleen, lung and salivary glands) of ΔgL-MCMV infected mice (Figure 5.3B&C). However, there was a significantly reduced accumulation of these cells in the spleen and salivary glands compared to WT-MCMV infected mice (Figure 5.3B&C). Taken together, these results suggest that ΔgL-MCMV induced reduced inflationary T cell responses as compared to WT-MCMV.

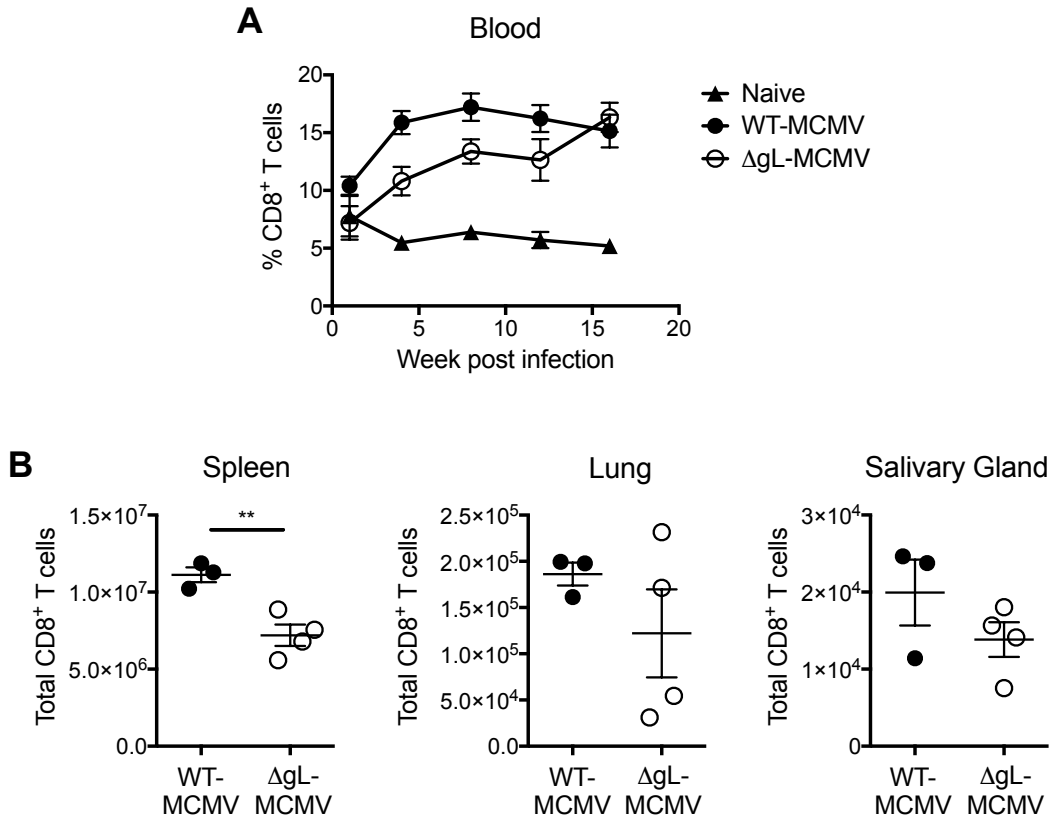

Figure 5.2 Systemic ΔgL-MCMV infection leads to reduced CD8$^+$ T cell accumulation.

(A) BALB/c mice were infected i.p or not with 2x10^5 pfu of either WT-MCMV or ΔgL-MCMV and blood withdrawn at week 1, 4, 8, 12 and 16 p.i. **(B)** At week 17 mice were culled and spleen, lung and salivary glands were harvested, processed into single cell suspension and stained for CD8α. **(A)** Frequency of CD8$^+$ Tcells in the peripheral blood. Data shown as mean ± SEM (n=3-4 mice/group), representing two different experiments. **(B)** Total number of CD8$^+$ T cells in the spleen, lung and salivary gland. Data shown as individual mice with mean ± SEM (n=3-4 mice/group), representing two different experiments. Significance was assessed by unpaired *t* test, **p<0.01.

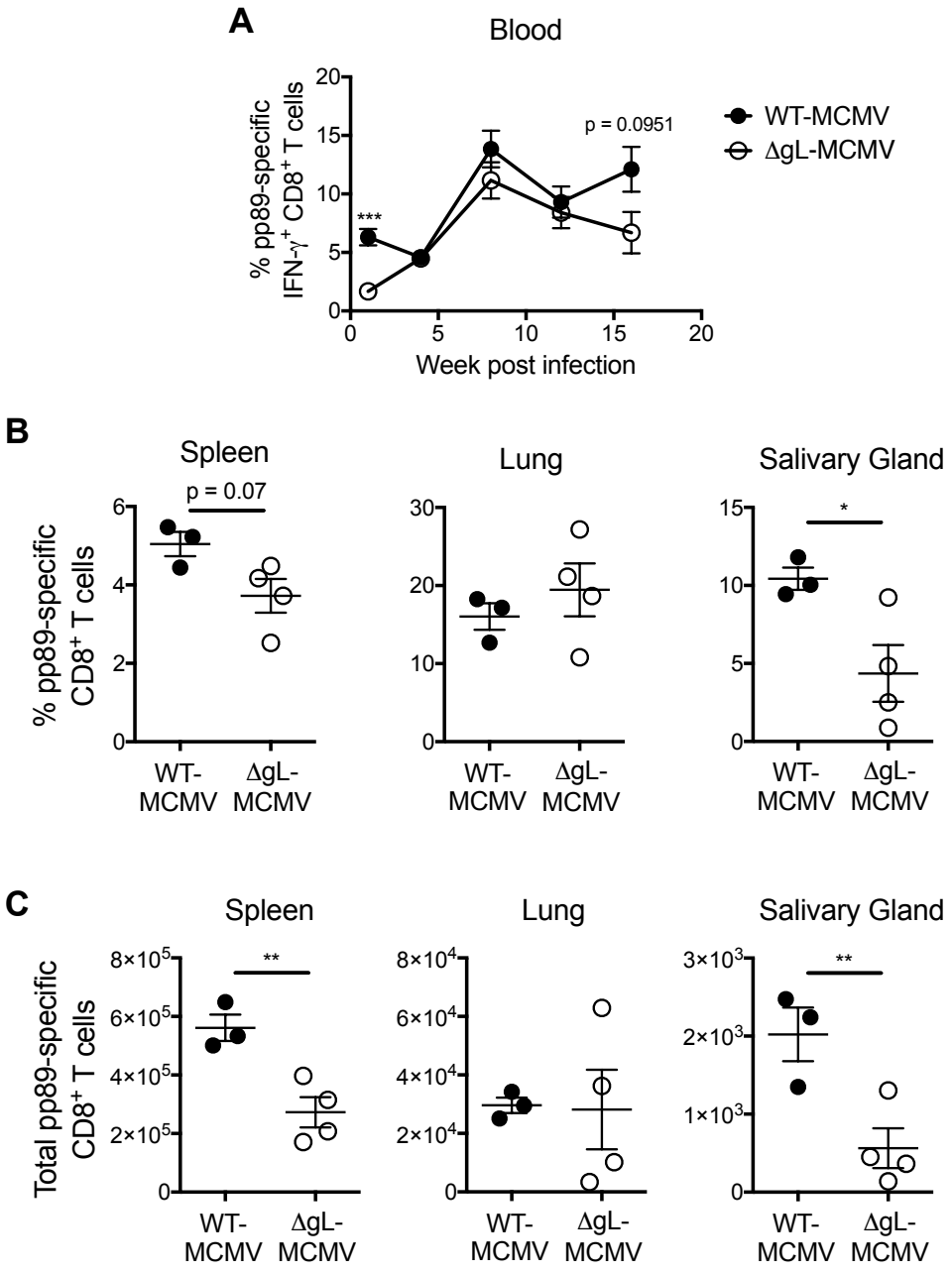

Figure 5.3 Systemic ΔgL-MCMV infection results in reduced MCMV-specific T cells in tissues during chronic infection.

(A) BALB/c mice were infected i.p or not with $2x10^5$ pfu of either WT-MCMV or ΔgL-MCMV and blood withdrawn at week 1, 4, 8, 12 and 16 p.i. Cells were stimulated *ex vivo* with pp89 for 6 hours and then stained for CD8α and IFN-γ to measure virus-specific responses. Data shown as mean ± SEM (n = 3-4 mice/group), representing two separate experiments. **(B&C)** At week 17 p.i mice were culled and spleen, lung and salivary glands were harvested. Cells were stained with CD8α, CD3 and pp89-tetramer to obtain **(B)** frequency and **(C)** total numbers of pp89-specific $CD8^+$ T cells in the different tissues. Data shown as individual mice with mean ± SEM (n = 3-4 mice/group), representing two separate experiments. Significance was assessed by unpaired *t* test, **p<0.01, ***p<0.05.

5.2.2.2 ΔgL-MCMV display reduced accumulation of MCMV-specific T_{EM} and T_{RM} cells as compared to WT-MCMV

As mentioned previously, most investigations of ΔgL-MCMV immunogenicity have used C57BL/6 mice in which inflationary $CD8^+$ T cells induced by this spread-deficient virus were phenotypically similar to those induced by WT-MCMV, with the majority of $MCMV^-$specific cells expressing high levels of KLRG-1 and low levels of CD127 and CD27 (410), markers of an effector memory phenotype (400, 401, 405, 408). To first identify whether the same was true following infection of BALB/c mice, I characterised MCMV-specific $CD8^+$ T cells during an infection time-course. Inflationary $CD8^+$ T cells measured by pp89-tetramer staining showed similar frequencies T_{CM}, T_{EM} and T_N, cells in the spleen, lung and salivary glands of all mice regardless of the virus used for infection, with the majority of pp89-specific $CD8^+$ T cells displaying an antigen experienced ($CD44^{high}CD62L^{low}$) T_{EM} phenotype (Figure 5.4A). In the spleen and salivary glands, ΔgL-MCMV-infected mice had slightly decreased frequencies of pp89-specific $CD8^+$ T_{EM} cells which was associated with higher frequencies of T_N and T_{CM} cells in the spleen and salivary glands, respectively (Figure 5.4A). Furthermore, in accordance with reduced pp89-specific $CD8^+$ T cells in the spleen and salivary glands during ΔgL-MCMV infection (Figure 5.3C), these sites exhibited a significantly reduced accumulation in total numbers pp89-specific T_{EM} cells compared to WT-MCMV infection (Figure 5.4B). In addition, ΔgL-MCMV-infected mice also displayed a substantially lower number of pp89-specific T_{CM} cells in the spleen (Figure 5.4B). In contrast, total number of pp89-specific T_{EM} and T_{CM} cells in the lungs induced by ΔgL-MCMV were comparable to those induced by WT-MCMV (Figure 5.4B).

The expression of KLRG1 and CD127 by pp89-specific $CD8^+$ T_{EM} cells induced by WT-MCMV and ΔgL-MCMV was next examined. KLRG1 is an inhibitory NK cell receptor expressed by T cells and has been reported to be induced by repetitive and

persistent antigen stimulation, and is used as a marker of terminally differentiated T cells (508). The cytokine IL-7 is important in the maintenance of memory T cells and expression of the IL-7 receptor α chain, CD127, has been associated with long-lived memory T cells (44, 509). As described in other studies, heterogeneity in KLRG1 and CD127 expression distinguishes between short-lived effector memory cells ($KLRG1^+CD127^-$), lacking proliferative capacity but exhibiting immediate effector functions, such as IFN-γ and TNF-α; and long-lived memory cells ($KLRG1^-CD127^+$). Both viruses induced comparable frequencies of $KLRG1^+$ pp89-specific T_{EM} cells in all the tissues examined (Figure 5.4D&E). In addition, during chronic infection, WT-MCMV and ΔgL-MCMV displayed similar frequencies of $CD127^+$ pp89-specific $CD8^+$ T_{EM} cells in the spleen and lung (Figure 5.4F&G). Interestingly, in ΔgL-MCMV infected mice, frequency of CD127-expressing pp89-specific $CD8^+$ T_{EM} cells in the salivary gland was significantly higher than those receiving WT-MCMV (Figure 5.4G). Taken together, these data indicate that, although MCMV-specific $CD8^+$ T cells were phenotypically similar in BALB/c mice regardless of the virus used for infection, ΔgL-MCMV failed to induce the accumulation of MCMV-specific T_{EM} cells in tissues to the same extent as WT-MCMV.

Chronic MCMV infection drives the accumulation of MCMV-specific $CD8^+$ T_{RM} cells in mucosal tissues (500, 510, 511). $CD8^+$ T_{RM} cells can be characterised by the expression of CD103, the α-chain of the integrin $\alpha_E\beta_7$ involved in the localization of T cells and mediating their interaction with epithelial cells; and CD69, a marker of activation and tissue resident memory cells that acts as a costimulatory molecule for lymphocyte proliferation. T_{RM} cells provide local immediate protection against re-infection by rapidly proliferating and killing infected cells (50, 512, 513). Establishing T_{RM} cells in large numbers may be important in maintaining immune-surveillance in these sites as part of an effective vaccine. Therefore, the impact of the spread-deficient MCMV vector, ΔgL-MCMV, on the development of MCMV-specific T_{RM} cells was

assessed *in vivo* (Figure 5.5). Spleens and lungs from ΔgL-MCMV and WT-MCMV infected mice had comparable frequencies and total number of pp89-specific $CD8^+$ T_{RM} cells on week 17 p.i (Figure 5.5A-C). In contrast, ΔgL-MCMV infection resulted in impaired accumulation of pp89-specific $CD8^+$ T_{RM} cells in salivary glands as compared to WT-MCMV (Figure 5.5A-C). Collectively, these data show that a spread-deficient vector can induce inflationary effector memory T cells with similar phenotype to WT-MCMV, yet, vector spread is required for optimal induction of T_{RM} cell formation.

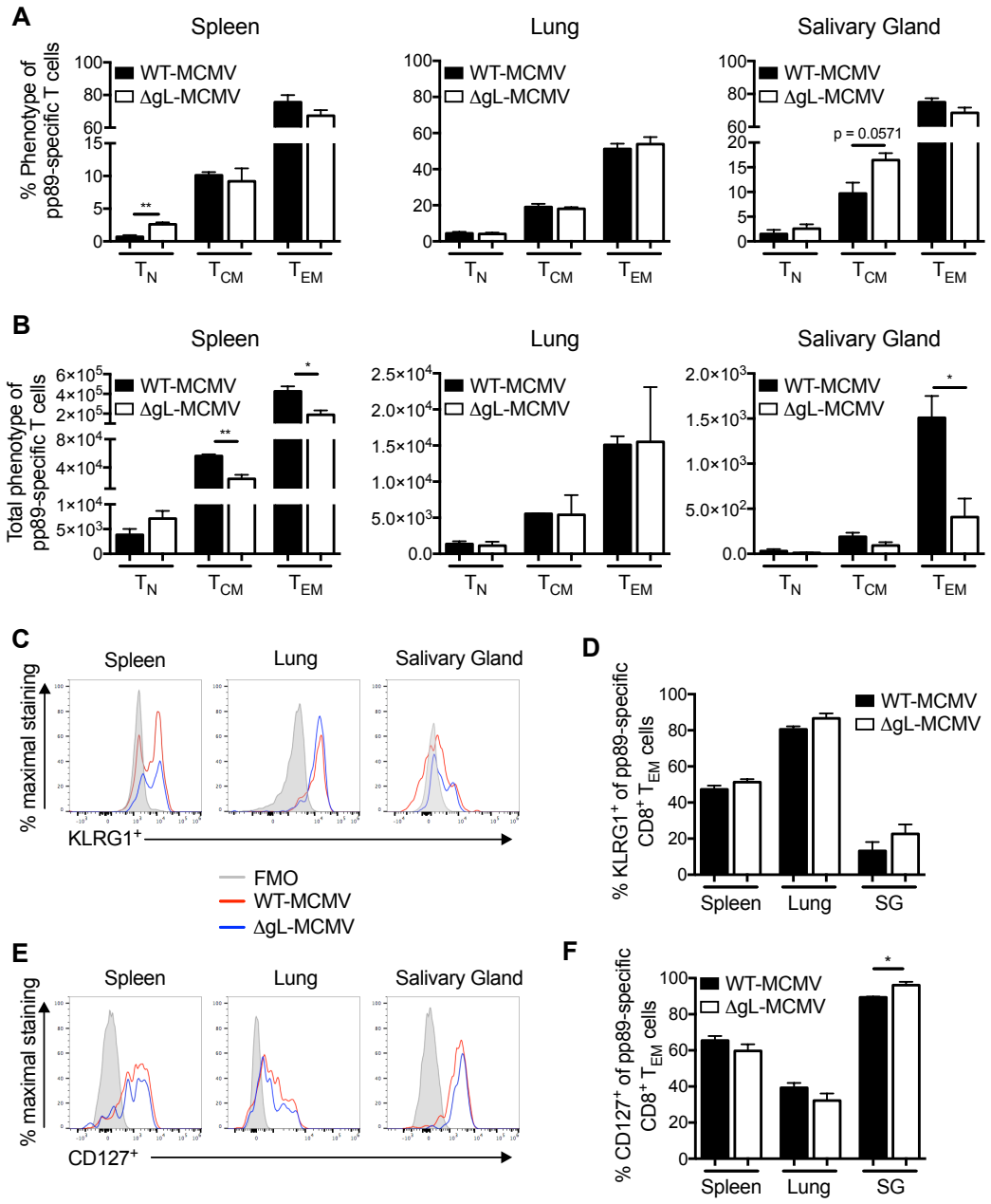

Figure 5.4 ΔgL-MCMV infection results in reduced accumulation of MCMV-specific T_{EM} cells in the spleen and salivary glands.

The phenotype of inflationary pp89-specific $CD8^+$ T cells in tissues from the experiment shown in Figure 5.3 was determined by co-staining cells with antibodies for CD44, CD62L, KLRG1 and CD127 at week 17 p.i. **(A)** Frequencies and **(B)** total numbers of naïve (T_N) and central and effector memory T (T_{CM} and T_{EM}, respectively) cells of pp89-tetramer$^+$ $CD8^+$ T cells in the spleen, lung and salivary glands were determined by CD44 and CD62L staining. **(C & E)** Representative histogram overlays of **(C)** KLRG1 and **(E)** CD127 expression by pp89-specific T_{EM} cells ($CD44^+CD62L^-$) in spleen, lung and salivary glands. Grey – FMO, red - WT-MCMV-infected, blue - ΔgL-MCMV-infected. **(D&F)** Frequency of pp89-specific $CD8^+$ T_{EM} cells expressing **(D)** KLRG1 and **(F)** CD127 in the spleen, lung and salivary gland (SG). Data shown as mean + SEM, (n=3-4 mice/group), representing two separate experiments. Significance was assessed by unpaired *t* test, * p<0.05 and **p<0.01.

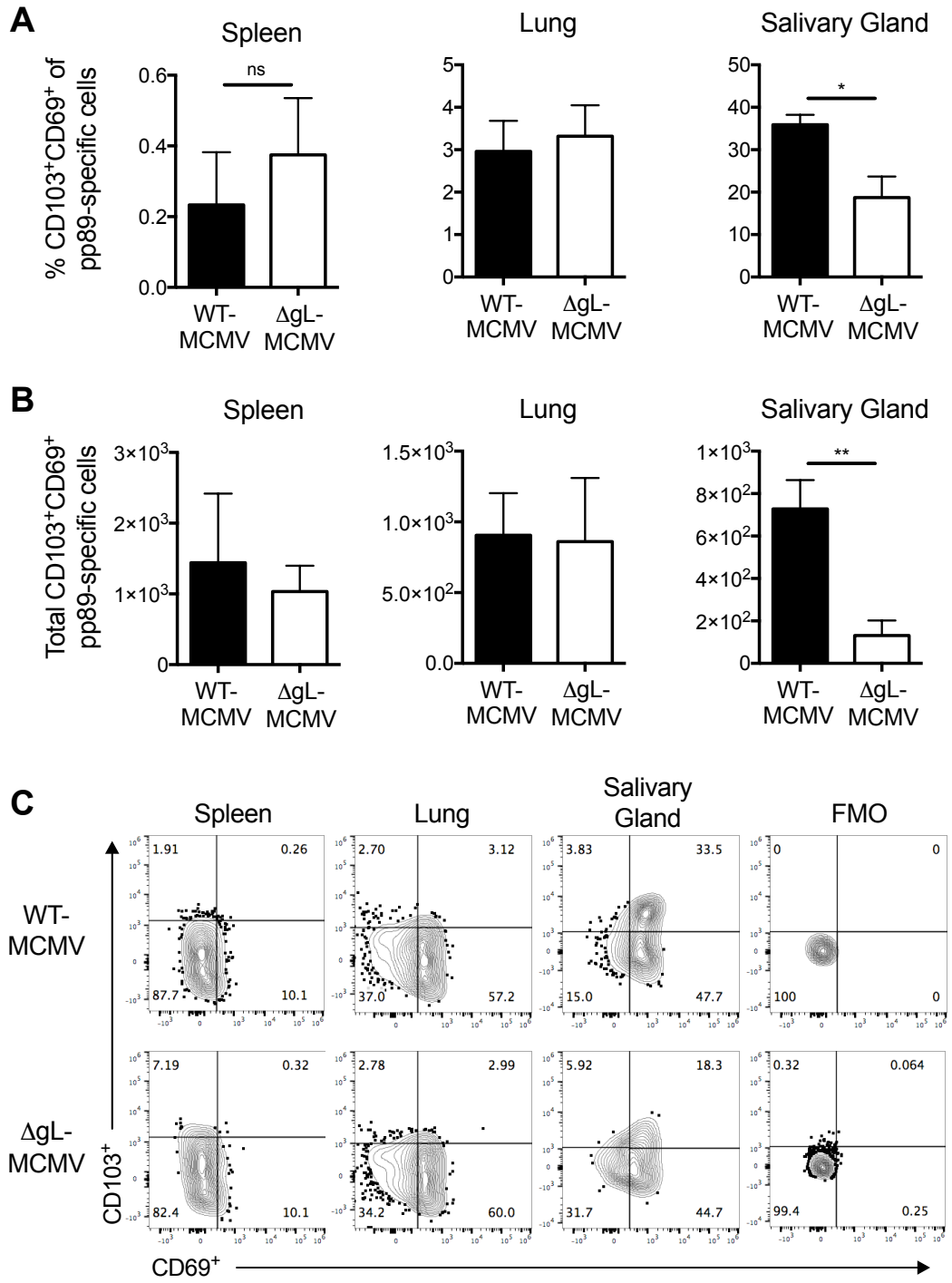

Figure 5.5 Systemic ΔgL-MCMV infection results in altered frequency of MCMV-specific T_{RM} cells in salivary gland.

(A-C) Expression levels of CD103 and CD69 were quantified on pp89-tetramer$^+$ CD8$^+$ T cells from different tissues at week 17 p.i. **(A)** Frequency and **(B)** total numbers of CD103$^+$CD69$^+$ pp89-specific CD8$^+$ T cells in the spleen (left graph), lung (middle graph) and salivary gland (right graph). Data shown as mean + SEM (n=3-4 mice/group), representing two separate experiments. Significance was assessed by unpaired *t* test, ns = not significant, * $p<0.05$ and ** $p<0.01$. **(C)** Representative flow cytometry plots of CD103 versus CD69. Plots show concatenated samples from 3 (WT-MCMV infected) and 4 (ΔgL-MCMV infected) mice.

5.2.3 Subcutaneous challenge with WT-MCMV results in a reduced immune response compared to intraperitoneal challenge

Most of the research using MCMV has been done via intraperitoneal challenge, yet this route of immunization is not inappropriate for clinical vaccination strategies. Although there are studies using different administration routes such as intranasal and foot-pad infection, these have not been studied in the context of vaccine administration. Hence, to determine the impact that the site of viral administration has on the immunogenicity of MCMV, we compared infection via the peritoneum to subcutaneous infection. Firstly, to determine the immunogenicity of virus administered subcutaneously, BALB/c mice were subcutaneously infected with increasing amounts of MCMV-IE2KO. MCMV-IE2KO was used in this experiment because as mentioned in Chapter 4 various MCMV vectors had the *ie2* ORF deleted and this would serve to determine what dose to administer subcutaneously in future vaccination experiments. At day 7 post-infection, viral load in salivary gland was significantly higher in mice infected with $1x10^6$ pfu as compared to infection with $2x10^5$ and $5x10^5$ pfu (Figure 5.6A). However, this did not result in increased MCMV-specific $CD8^+$ T cell responses as measured by the ability of $CD8^+$ T cells to generate IFN-γ in response to the MCMV-derived peptide pp89 (Figure 5.6B). Consequently, mice were challenged either i.p or s.c with $2x10^5$ pfu WT-MCMV. Splenic lymphocytes from day 7 and 123 p.i were stimulated *ex-vivo* with pp89-derived peptide and responses were measured by flow cytometry. In the acute phase of infection, mice from both groups had comparable numbers of $CD8^+$ T cells in the spleen but the accumulation of the inflationary pp89-specific $CD8^+$ T cells was more than two-fold reduced in mice receiving MCMV via the subcutaneous route (Figure 5.6C&D). Furthermore, during the chronic phase of infection the difference in splenic pp89-specific $CD8^+$ T cells remained two-fold lower in s.c challenged mice and was accompanied with reduced $CD8^+$ T cell accumulation (Figure 5.6E&F). These

findings show that subcutaneous challenge induces a diminished $CD8^+$ T cell response as compared to intraperitoneal infection.

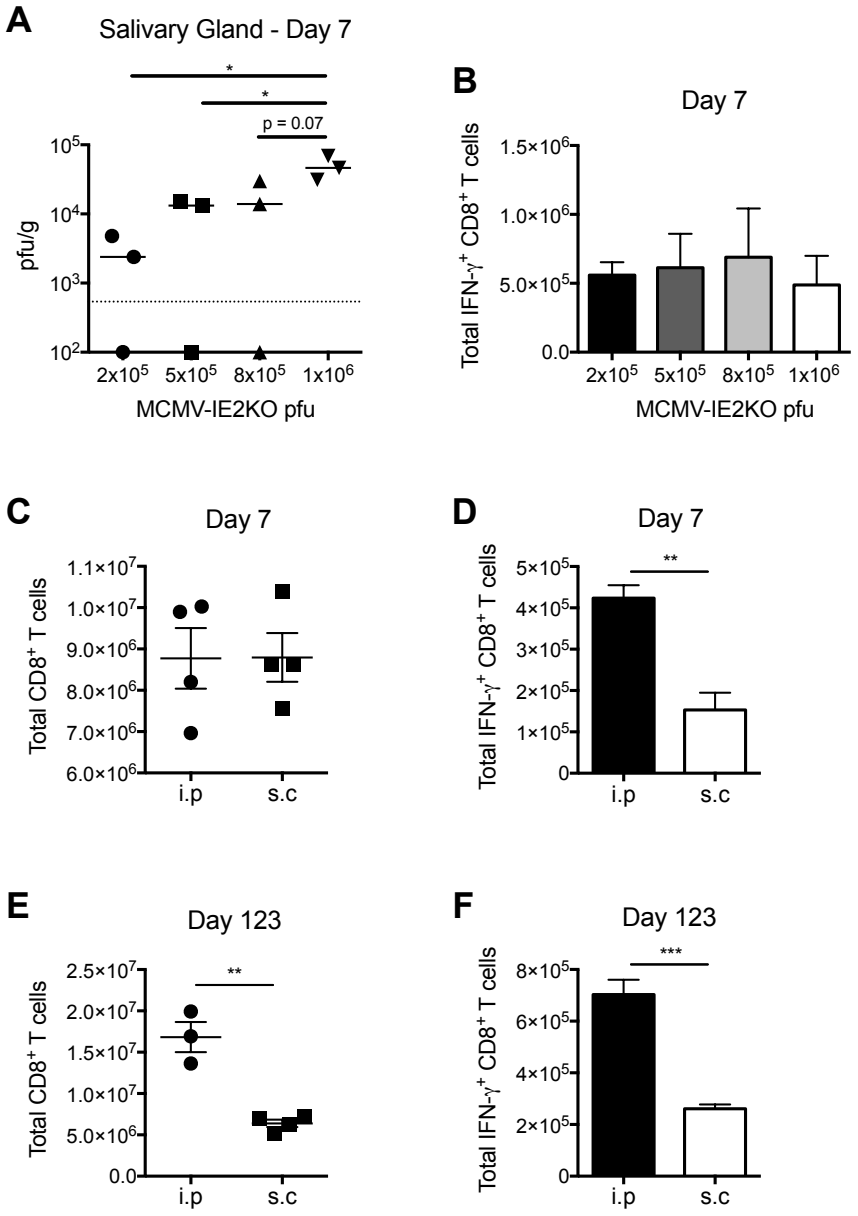

Figure 5.6 Subcutaneous challenge with WT-MCMV results in reduced immune response compared to systemic challenge.

(A&B) BALB/c mice were infected s.c with the indicated doses of MCMV-IE2KO. Spleens and salivary glands were harvested on day 7 p.i. **(A)** Salivary glands were used to measure replicating MCMV load by plaque assay. Individual mice and median are shown. Horizontal dashed line delineates limit of detection. Significance was assessed by one-way ANOVA with Bonferroni's correction for multiple comparisons. **(B)** Splenocytes were stimulated *ex vivo* with pp89 and stained for CD8α and IFN-γ to measure virus-specific T cell responses. Data shown as mean + SEM (n=3 mice/group) **(C-F)** BALB/c mice were infected either i.p or s.c with 2 x10^5 pfu WT-MCMV and spleens harvested on **(C&D)** day 7 and **(E&F)** 123 p.i. Splenocytes were stimulated *ex vivo* with pp89 and stained for CD8α and IFN-γ. **(C&E)** Total splenic $CD8^+$ T cells. Data shown as individual mice with mean $\pm$ SEM (n=3-4 mice/group). **(D&F)** Total virus-specific $CD8^+$ T cell responses. Data shown as mean + SEM (n=3-4 mice/group). Significance was assessed by unpaired *t* test. *p<0.05, ** p<0.01, *** p<0.005.

5.2.4 Immune response induced by ΔgL-MCMV after subcutaneous administration

5.2.4.1 ΔgL-MCMV induces functional MCMV-specific CD8$^+$ T cells that do not inflate over time

As described above, MCMV spread influences the magnitude of T cell responses induced upon intraperitoneal infection (Section 5.2.2). Furthermore, as shown in section 5.2.3, the site of administration also influenced the response to MCMV. Hence, the ability of ΔgL-MCMV to elicit an immune response and drive CD8$^+$ T cell memory inflation after local administration of the vector was investigated. BALB/c mice were challenged subcutaneously with either WT-MCMV or ΔgL-MCMV. MCMV responses were followed in the peripheral blood for four months, at which point mice were culled and organs harvested to study and characterize immune responses in different tissues. Subcutaneous challenge with ΔgL-MCMV led to an expansion of CD8$^+$ T cells in the circulation comparable to that with s.c WT-MCMV infection, albeit with different kinetics (Figure 5.7A). Subcutaneous infection with WT-MCMV induced an increase in circulating CD8$^+$ T cells that peaked at week 4 p.i (17.2% CD8$^+$ T cells) which then contracted to remain stable with ~11% of circulating lymphocytes being CD8$^+$ cells (Figure 5.7A). In contrast, ΔgL-MCMV s.c. infection resulted in a slow progressive accumulation of CD8$^+$ T cells in the blood reaching similar levels to WT-MCMV infection by week 12 p.i (~10% CD8$^+$ T cells) (Figure 5.7A). In accordance with circulating CD8$^+$ cells, no significant differences were seen in the accumulation of CD8$^+$ T cells in the spleen, lung and salivary glands of mice receiving s.c ΔgL-MCMV compared to WT-MCMV (Figure 5.7B). In addition, MCMV-specific responses were examined in these tissues by pp89-tetramer stain. A trend was observed in which s.c ΔgL-MCMV infection resulted in decreased infiltration of pp89-specific CD8$^+$ T cells in the spleen,

lung and salivary glands, compared to WT-MCMV infection (Figure 5.7C). Furthermore, by following pp89-specific $CD8^+$ T cell responses in the peripheral blood, differences in the inflationary $CD8^+$ T cell responses were observed between the two groups of virus-exposed mice. Although both MCMV vectors induced similar frequencies of pp89-specific $CD8^+$ T cells in the acute phase of infection, these responses diverged at week 4 p.i, with ΔgL-MCMV mice harbouring significantly lower frequencies of pp89-specific $CD8^+$ T cells thereafter (Figure 5.8A). Whilst $CD8^+$ T cell responses induced by WT-MCMV resulted in increased frequencies of pp89-specific $CD8^+$ T cells over time, these responses in ΔgL-MCMV infected mice remained stable (~4.5% of $CD8^+$ T cells) from week 12 (Figure 5.8A).

Chronic antigen stimulation has been associated with gradual loss of function and/or proliferation of $CD8^+$ T cells in certain chronic viral infections, including LCMV and hepatitis C virus (HCV) (514, 515). However, T cells reactive to CMV retain the ability to produce IFN-γ and TNF-α over time (427, 516, 517). Thus, the ability of MCMV-specific memory $CD8^+$ T cells to produce IFN-γ and TNF-α following s.c ΔgL-MCMV immunization was investigated. On week 16 p.i, ΔgL-MCMV infected mice exhibited lower overall responses to pp89 in the peripheral blood than WT-MCMV, yet the majority of the responding cells were polyfunctional (IFN-γ^+TNF-α^+), as observed after WT-MCMV infection (Figure 5.8B&D). A similar trend was observed in the spleen, lung and liver on week 17 p.i. ΔgL-MCMV infection, resulting in a diminished pp89-specific $CD8^+$ T cell response in all three tissues. However, most cells induced were capable of producing both cytokines (Figure 5.8C&D). Collectively, these data show that ΔgL-MCMV can elicit functional MCMV-specific $CD8^+$ T cells when administered subcutaneously, but these responses do not exhibit the 'inflationary' pattern observed in response to WT-MCMV infection.

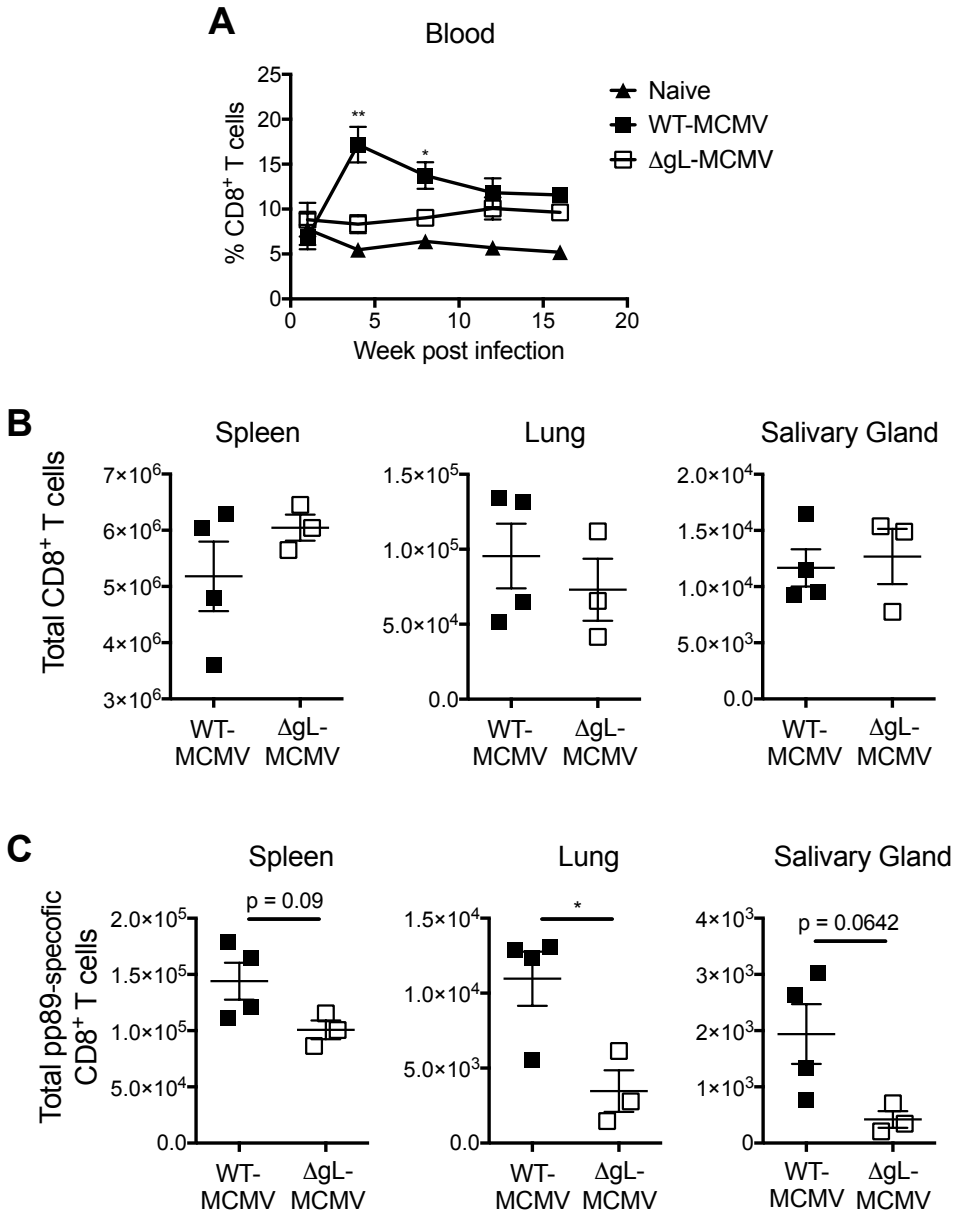

Figure 5.7 Subcutaneous infection with ΔgL-MCMV results in reduced MCMV-specific CD8$^+$ T cell responses in tissues.

(A-C) BALB/c mice were infected s.c or not with 2x10^5 pfu of either WT-MCMV or ΔgL-MCMV. **(A)** Blood was withdrawn week 1, 4, 8, 12 and 16 p.i and stained for CD8α to obtain frequencies of C8$^+$ T cells in peripheral blood. Data shown as mean ± SEM (n=3-4 mice/group), representing two separate experiments. Significance was assessed by unpaired *t* test comparing ΔgL-MCMV with WT-MCMV on the different time points. **(B&C)** Mice were culled at week 17 p.i and spleen, lung and salivary glands harvested. Tissues were processed to obtain single cell suspensions and cells were then stained for CD8α, CD3 and with pp89-tetramer. Total numbers of **(B)** CD8$^+$ T cells and **(C)** pp89-tetramer$^+$, gated on CD8$^+$CD3$^+$ cells, were quantified. Data shown as individual mice with mean ± SEM (n=3-4 mice/group), representing two separate experiments. Significance was assessed by unpaired *t* test. *p<0.05 and **p<0.01.

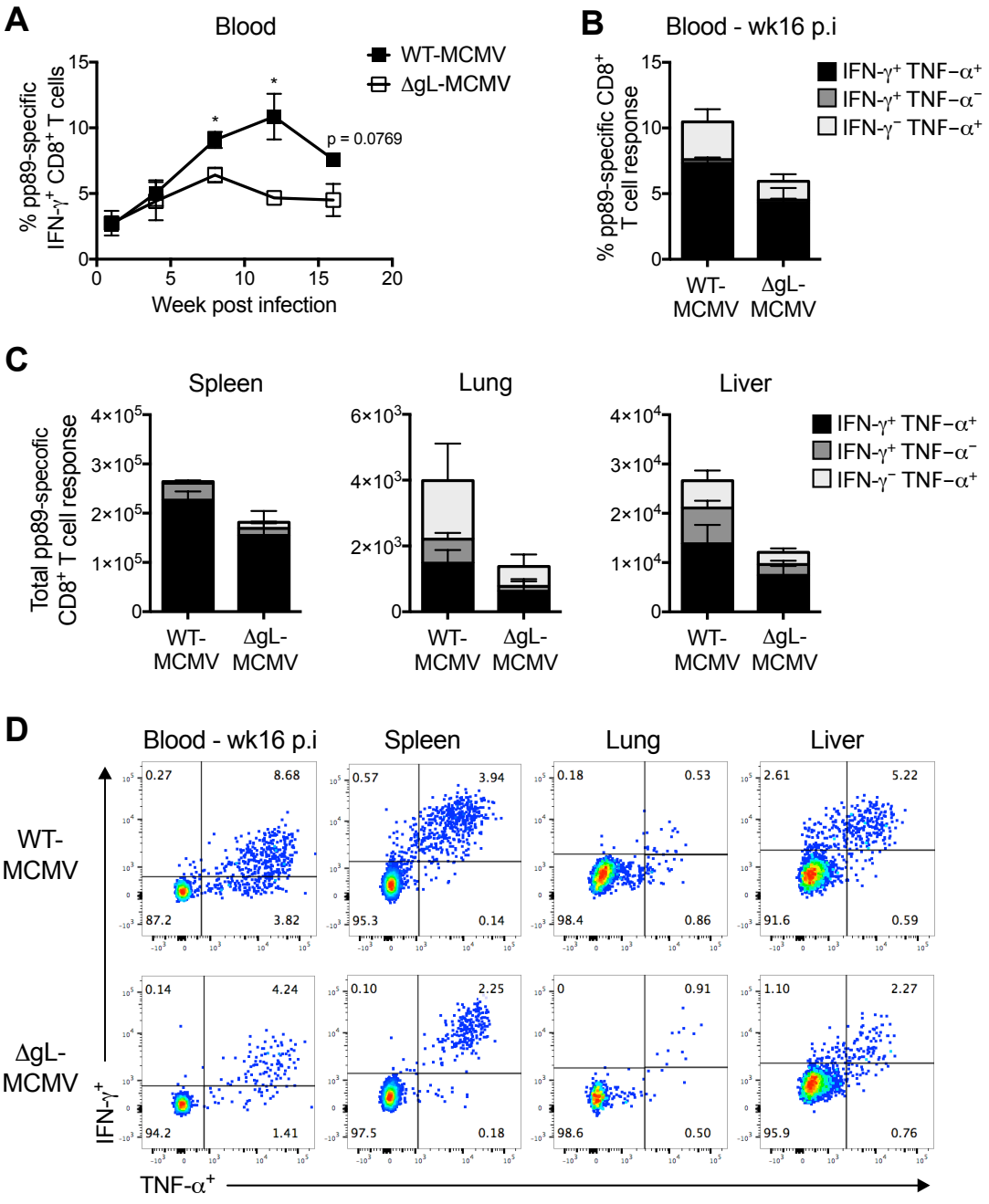

Figure 5.8 ΔgL-MCMV subcutaneous infection induces polyfunctional CMV-specific CD8$^+$ T cells.

BALB/c mice were infected s.c. with 2x10^5 pfu of either WT-MCMV or ΔgL-MCMV. **(A&B)** Blood was withdrawn on week 1, 4, 8, 12 and 16 p.i and **(C)** spleen, lung and liver were harvested on week 17 p.i. **(A-C)** Cells were stimulated ex *vivo* with pp89 for 6 hours and then stained for CD8α, IFN-γ and TNF-α to quantify virus-specific CD8$^+$ T cell responses. Data shown as mean ± SEM (n = 3-4 mice/group), representing two separate experiments. **(A)** Significance was assessed by unpaired *t* test on individual time points, *p<0.05. **(D)** Representative flow cytometry showing of IFN-γ vs TNF-α, gated on live CD8$^+$ T cells. Representative of 3-4 mice per group.

5.2.4.2 Subcutaneous administration of ΔgL-MCMV induces similar phenotype of CMV-specific CD8$^+$ T cells as WT-MCMV

Having established that the inability of MCMV to spread influences the generation of MCMV-specific CD8$^+$ T cells, the phenotype of these cells was next investigated. As with intraperitoneal viral challenge, ΔgL-MCMV and WT-MCMV induced comparable frequencies of pp89-specific T_N, T_{CM}, and T_{EM} in the spleen, lung and salivary glands (Figure 5.9A). Yet, mice challenged with ΔgL-MCMV displayed reduced total numbers of pp89-specific T_{CM}, and T_{EM} in the spleen, lung and salivary glands (Figure 5.9B), which could be a result of the reduced number of pp89-specific CD8$^+$ T cells observed in these tissues (Figure 5.7C). In addition, expression of KLRG1 and CD127 on pp89-specific CD8$^+$ T_{EM} cells was assessed. No significant differences were observed in the frequency of pp89-specific CD8$^+$ T_{EM} cells displaying CD127$^+$KLRG1$^-$ and CD127$^-$KLRG1$^+$ expression in mice receiving ΔgL-MCMV compared to those administered WT-MCMV (Figure 5.9C). The development of CD8$^+$ T_{RM} cells during chronic WT-MCMV and ΔgL-MCMV infection after subcutaneous challenge was assessed in the lung and salivary glands. Although there was no statistical difference between frequencies of pp89-specific CD8$^+$ T_{RM} cells between WT-MCMV and ΔgL-MCMV in these tissues (Figure 5.10A&C), a strong trend was observed in the total numbers of T_{RM} cells in the major site of T_{RM} development after intraperitoneal MCMV infection, the salivary glands. Here, ΔgL-MCMV-infected mice displayed a lower accumulation of CD103$^+$CD69$^+$ pp89-specific CD8$^+$ T_{RM} cells (Figure 5.10B).

In addition to pp89-specific CD8$^+$ T cells, another inflationary MCMV-specific CD8$^+$ T cell response (m164) was assessed during ΔgL-MCMV and WT-MCMV chronic infection. BALB/c mice infected with ΔgL-MCMV or WT-MCMV were culled on week 21 p.i and spleen, lung and salivary glands harvested. Infiltration of m164-specific CD8$^+$ T cells in the spleen and lung was reduced in ΔgL-MCMV compared to WT-MCMV

infected mice, although it did not reach statistical difference (Figure 5.11A&B). This might be due to the number of mice in the experiment (n=3) leading to the statistical analysis being under-powered. The characterisation of these cells revealed that ΔgL-MCMV induced lower accumulation of m164-specific $CD8^+$ T_{EM} cells in the spleen and lung (Figure 5.11D&E). Furthermore, in the lungs, ΔgL-MCMV infection also resulted in reduced numbers of m164-specific $CD8^+$ T_{CM} cells (Figure 5.11E). In contrast, in the salivary glands WT-MCMV and ΔgL-MCMV induced comparable quantities of m164-specific $CD8^+$ T cells with equivalent magnitude of T_N, T_{CM} and T_{EM} cells (Figure 5.11C&F).

Taken together, these results suggest that s.c ΔgL-MCMV can drive the development of pp89-specific and m164-specific $CD8^+$ T cell responses without the ability to spread from the first cells infected. However, these responses were reduced in multiple tissues of ΔgL-MCMV infected mice relative to WT-MCMV, and was associated with a reduction in MCMV-specific T_{EM} and T_{RM} cells.

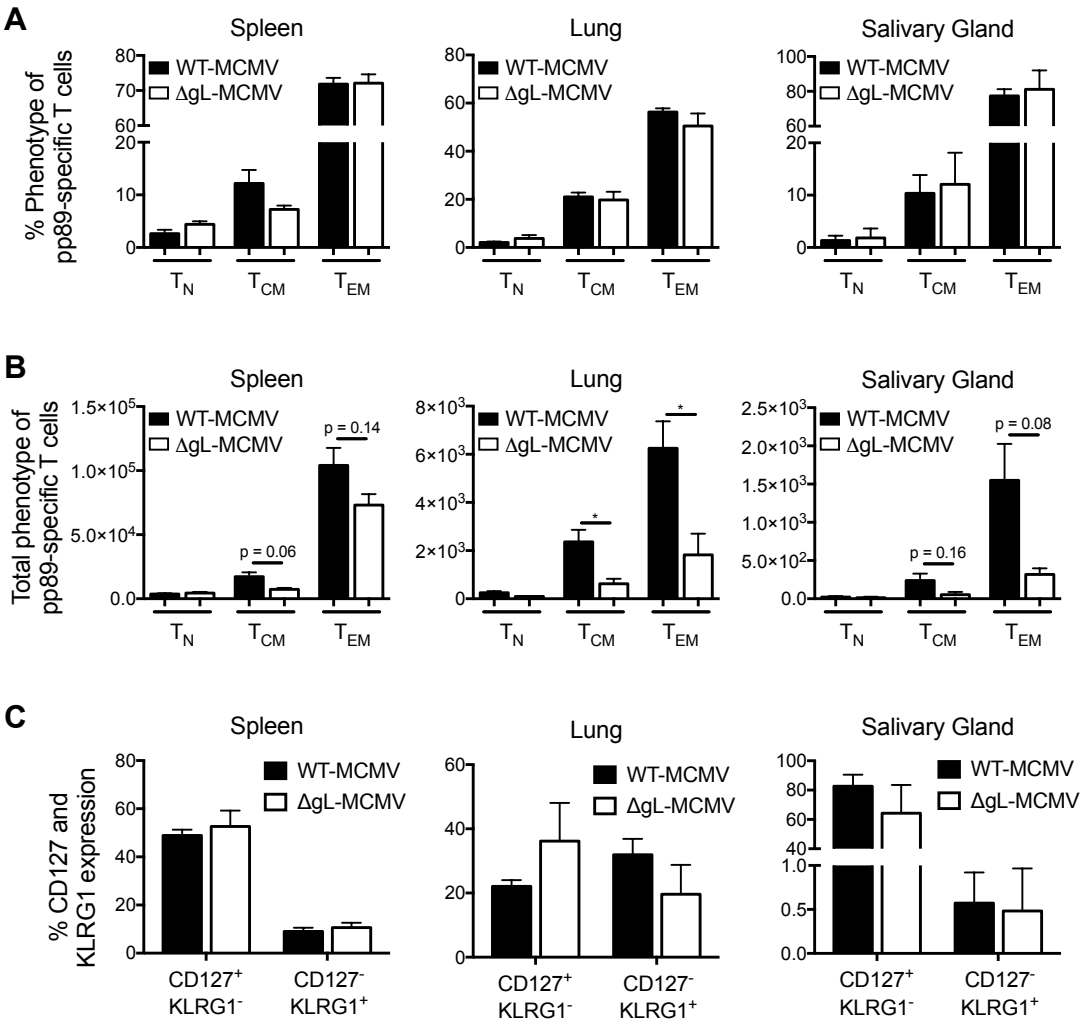

Figure 5.9 Subcutaneous ΔgL-MCMV infection induces similar phenotype of pp89-specific cells in tissues.

The phenotype of inflationary pp89-specific $CD8^+$ T cells in tissues from the experiment shown in Figure 5.7C was determined by co-staining cells with antibodies for CD44, CD62L, KLRG1 and CD127 on week 17 p.i. **(A)** Frequencies and **(B)** total numbers of naïve (T_N) and central and effector memory T (T_{CM} and T_{EM}, respectively) cells of pp89-$tetramer^+$ $CD8^+$ T cells in the spleen (left graph), lung (middle graph) and salivary glands (right graph) determined by CD44 and CD62L staining. **(C)** Frequency of pp89-specific $CD8^+$ T_{EM} cells expressing CD127 and KLRG1 in the spleen, lung and salivary glands. Data shown as mean + SEM, (n=3-4 mice/group), representing two separate experiments. Significance was assessed by unpaired *t* test, *p<0.05.

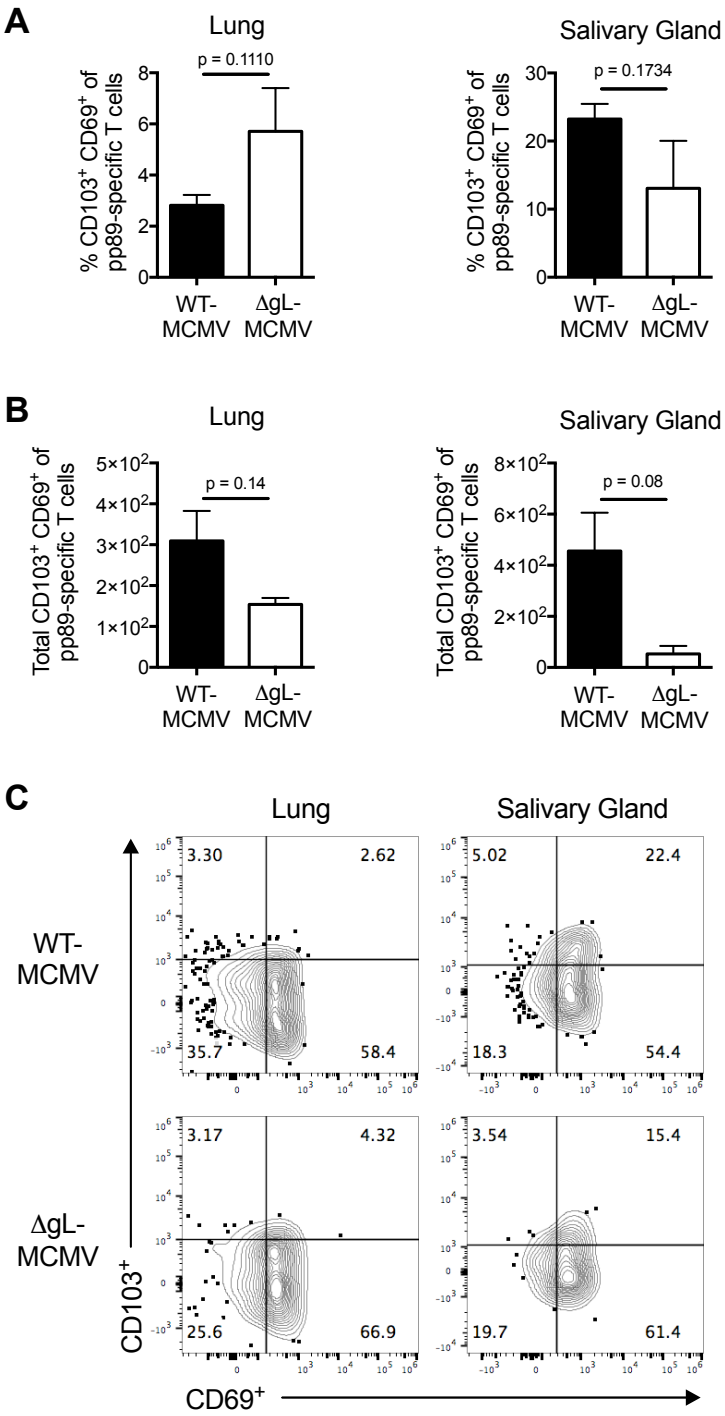

Figure 5.10 Subcutaneous challenge with ΔgL-MCMV results in a reduced accumulation of pp89-specific T_{RM} cells.

(A-C) Expression levels of CD103 and CD69 were quantified on pp89-tetramer$^+$ cells from lung and salivary glands week 17 p.i. **(A)** Frequency and **(B)** total numbers of CD103$^+$CD69$^+$ pp89-specific CD8$^+$ T cells in the lungs (left graphs) and salivary glands (right graphs). Data shown as mean + SEM (n=3-4 mice/group), representing two separate experiments. Significance was assessed by unpaired *t* test. **(C)** Representative flow cytometry plots of CD103 versus CD69. Plots show concatenated samples from 4 (WT-MCMV infected) and 3 (ΔgL-MCMV infected) mice.

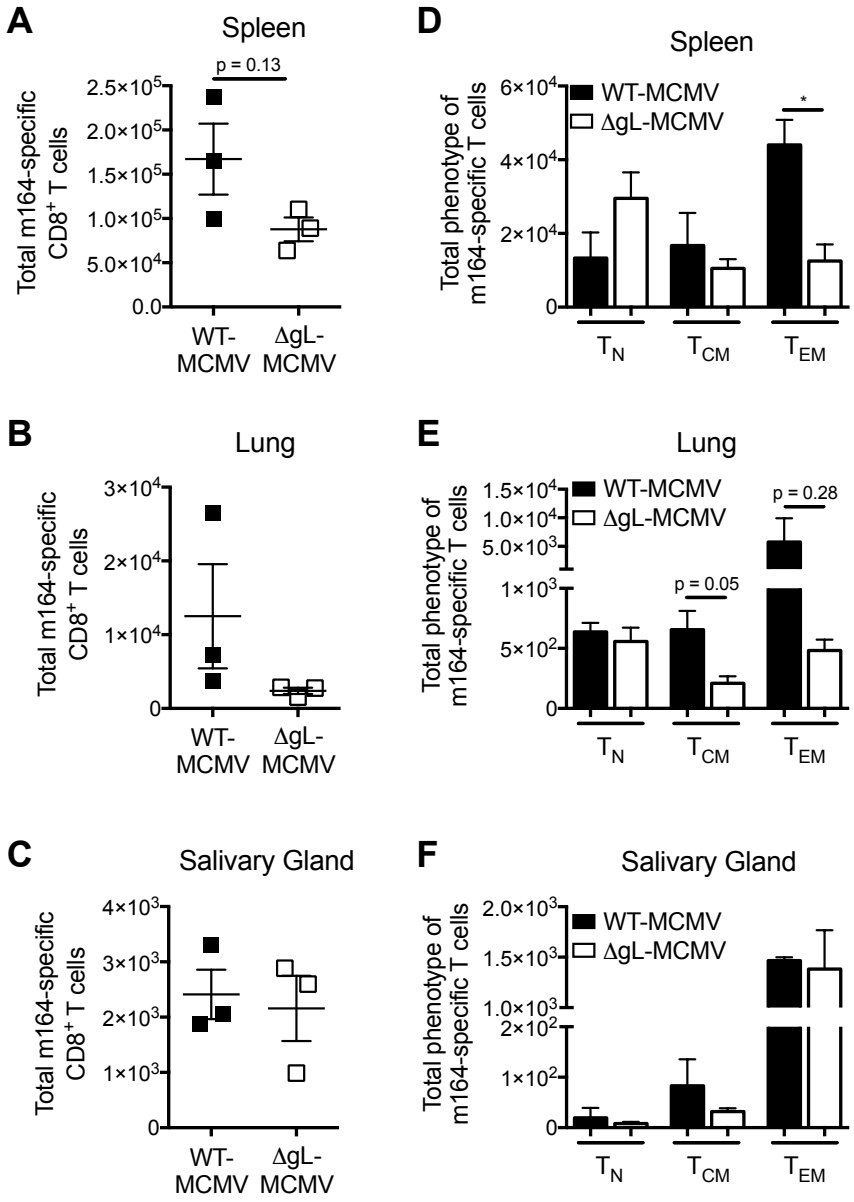

Figure 5.11 Subcutaneous ΔgL-MCMV infection reduced accumulation of m164-specific CD8$^+$ T_{EM} cells in the spleen.

(A-F) BALB/c mice were infected s.c with 2x10^5 pfu of either WT-MCMV or ΔgL-MCMV. On week 21 p.i spleen, lung and salivary glands were harvested and processed to obtain single cell suspension. Cells were then stained for CD8α, CD3 and with m164-tetramer. **(A-C)** Total number of m164-tetramer$^+$ cells, gated on CD8α$^+$CD3$^+$ cells. Data are shown as individual mice with mean ± SEM (n=3 mice/group). **(D-E)** m164-specifc CD8$^+$ T cells in the different tissues were further stained for CD44 and CD62L to determine the total numbers of naïve (T_N), central memory (T_{CM}) and effector memory T (T_{EM}) cells. Data shown as mean + SEM (n=3 mice/group). Significance was assessed by unpaired *t* test, * p<0.05.

5.2.4.3 Subcutaneous administration of WT-MCMV and ΔgL-MCMV in C57BL/6 impacts on MCMV inflationary responses

The immunogenicity of ΔgL-MCMV was also examined in C57BL/6 following subcutaneous administration of the virus. C57BL/6 mice were challenged subcutaneously with $2x10^5$ pfu WT-MCMV or ΔgL-MCMV and blood was withdrawn on week 1, 4, 8, 12 and 16 p.i to measure MCMV-specific responses. Subcutaneous challenge with ΔgL-MCMV resulted in impaired induction of IE3- and M38- specific $CD8^+$ T cells during the acute phase of infection (week 1 p.i), as compared to WT-MCMV (Figure 5.12A&B). Interestingly, IE3 responses in the peripheral circulation of ΔgL-MCMV infected mice 'inflated' to comparable levels as WT-MCMV infection (Figure 5.12A). This contrasts with previously published data, where foot-pad infection of C57BL/6 mice with ΔgL-MCMV yielded no detectable maintenance of IE3-specific T cells in the circulation (410). In contrast, circulating M38-specific responses did not inflate, regardless of the virus used to infect mice; although M38 responses remained lower in ΔgL-MCMV infected mice than in those receiving WT-MCMV (Figure 5.12B). This correlated with previously published data, where foot-pad infection of C57BL/6 mice resulted in the lack of inflationary M38 responses in both viral infections (ΔgL-MCMV and WT-MCMV) (410). Furthermore, MCMV responses in the circulation correlated to those seen in different tissues at the time of sacrifice (week 21 p.i) – WT-MCMV and ΔgL-MCMV induced comparable numbers of IE3-specific $CD8^+$ T cells in the spleen and lung, but exhibited reduced accumulation of M38-specific $CD8^+$ T cells (Figure 5.12C&D). Overall, these data demonstrate that both, site of virus administration and virus spread, impacts on MCMV inflationary responses in C57BL/6 mice.

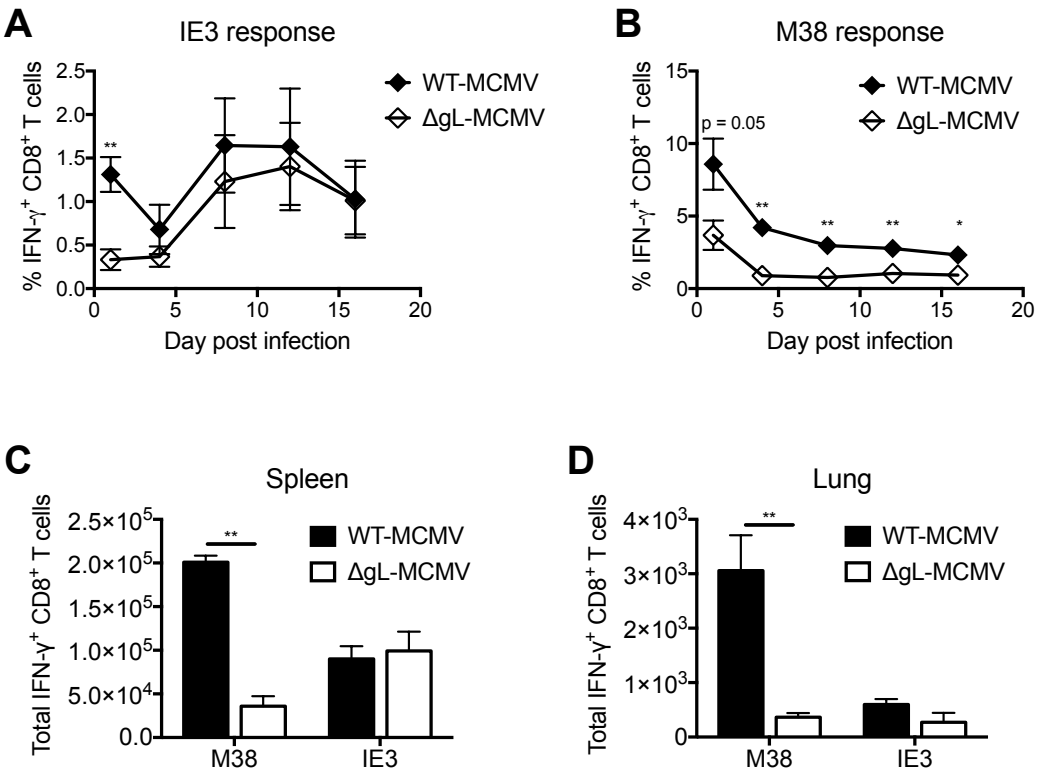

Figure 5.12 Subcutaneous infection results in impaired epitope-specific inflationary responses after infection in C57BL/6 mice.

C57B/6 mice were challenged s.c with $2x10^5$ pfu WT-MCMV or ΔgL-MCMV. **(A&B)** Blood withdrawn from the lateral tail vein on week 1, 4, 8, 12 and 16 p.i and lymphocytes stimulated *ex vivo* with IE3- and M38-derived peptides for 6 hours, followed by staining for CD8 and IFN-γ. **(A)** IE3-specific and **(B)** M38-specific IFN-γ^+ $CD8^+$ T cells. **(A&B)** Data shown as mean ± SEM (n = 4 mice/group). Significance was assessed by unpaired *t* test at individual time points, *p<0.05 and **p<0.01. **(C&D)** Mice were sacrificed on week 21 p.i and spleen and lung harvested. Cells were stimulated and stained as for **(A)** and **(B)** to obtain total numbers of M38-specific and IE3-specific IFN-γ^+ $CD8^+$ T cells in the **(C)** spleen and **(D)** lung. Data shown as mean + SEM (n = 4 mice/group). Significance was assessed by unpaired *t* test, **p<0.01.

5.2.4.3.1 MCMV-induced CD4$^+$ T cell responses are not affected by a spread defective MCMV virus

In order to elucidate the lack of MCMV-specific CD8$^+$ T cell 'inflation' observed during s.c ΔgL-MCMV infection in BALB/c mice, different cell populations during the acute response to MCMV were investigated. CD4$^+$ T cells have been described to promote MCMV-specific CD8$^+$ T cell responses and to prolong their persistence (398, 399, 418). Thus, to explore whether the reduced inflationary CD8$^+$ T cell responses observed were due to impaired CD4$^+$ T cell responses induced by ΔgL-MCMV infection, BALB/c mice were s.c challenged with WT-MCMV or ΔgL-MCMV and at day 7 p.i total CD4$^+$ T cells were measured in the spleen. Comparable numbers of total splenic CD4$^+$ T cells were observed in the two infection models (Figure 5.13A). In addition, responses to two MCMV class II peptides recently described for BALB/c, M53 and M78 (518), was examined. Both vectors induced polyfunctional M53- and M78- specific responses with no significantly differences detected in the magnitude of the response (Figure 5.13B&C). Consequently, CD4$^+$ T cell responses appeared not to be the determinant of the differences seen in the chronic phase of ΔgL-MCMV infection.

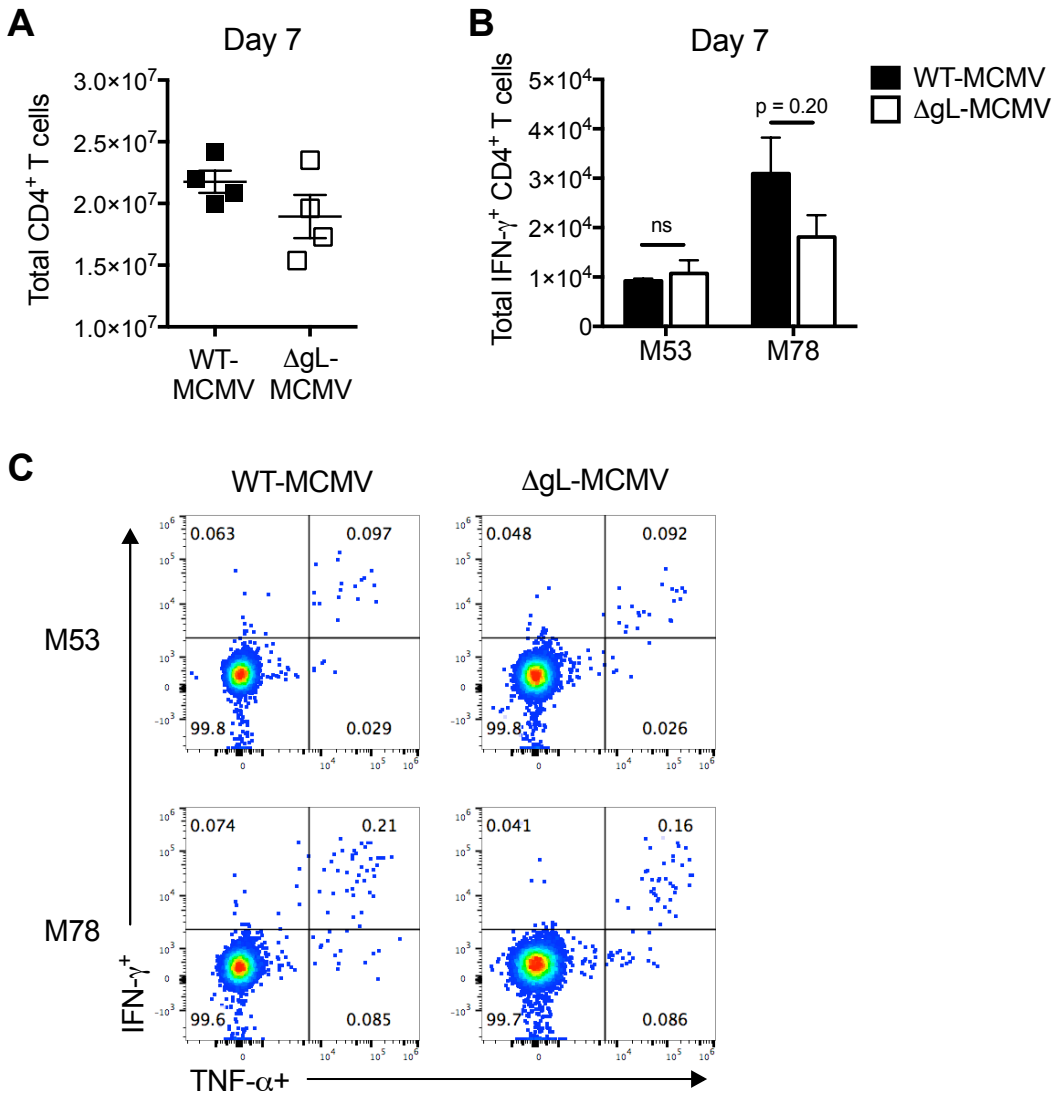

Figure 5.13 ΔgL-MCMV induces comparable CMV-specific CD4$^+$ T cell responses to WT-MCMV.

BALB/c mice were infected s.c with 2x10^5 pfu WT-MCMV or ΔgL-MCMV and spleens harvested on day 7 p.i. Splenocytes were stimulated *ex vivo* with M53 and M78 peptides for 6 hours and stained for CD4, IFN-γ and TNF-α to measure virus-specific T cell responses. **(A)** Total numbers of splenic CD4$^+$ T cells. Data shown as individual mice with mean ± SEM (n = 3 mice/group). **(B)** Total numbers of IFN-γ$^+$ CD4$^+$ T cells responding to M53 or M78. Data shown as mean + SEM (n = 3 mice/group). (A&B) Significance was assessed by unpaired *t* test, ns = not significant. **(C)** Representative flow cytometry plots showing IFN-γ and TNF-α expression of live, CD4$^+$ cells.

5.2.4.4 Altered activation of CD8$^+$ cDCs after ΔgL-MCMV challenge

Dendritic cells (DCs) are known to initiate adaptive immune responses through antigen-specific activation of naïve T cells (519, 520). Hence, I sought to elucidate whether ΔgL-MCMV infection had an impact on DCs and their ability to prime CD8$^+$ T cells. DCs can be divided into three major subsets: CD8α^+ CD11b$^-$ (later referred to as CD8$^+$ cDCs), CD8α^- CD11b$^+$ (CD11b$^+$ cDCs) and CD11c^{int} CD11b$^-$ SiglecH$^+$ (plasmacytoid DCs; pDCs). DC subsets have different specialised functions. For example, both CD8$^+$ and CD11b$^+$ cDCs can be potent activators of naïve T lymphocytes, but while CD11b$^+$ cDCs are most efficient at priming CD4$^+$ T cells, CD8$^+$ cDCs are more efficient for CD8$^+$ T cell priming due to their unique ability to cross-present exogenous antigens in association with MHC class I molecules (521). In contrast, pDCs are specialised in rapid and high level production of antiviral proteins (e.g. type I IFN) and facilitate NK cell activation (386). Thus, activation of these subsets may lead to specific pathways for differential regulation of downstream immune responses.

BALB/c mice were challenged s.c with 2x10^5 pfu WT-MCMV or ΔgL-MCMV and on day 2 p.i spleen and draining lymph nodes (axillary lymph node) were harvested to examine the different DC subsets. The gating strategy to delineate the different subtypes of DCs in the spleen and lymph nodes is shown in Figure 5.14. Total numbers of splenic pDCs, CD8$^+$ cDCs and CD11b$^+$ cDCs were obtained and revealed a greater accumulation of these cells during ΔgL-MCMV infection (Figure 5.15A-C). During intraperitoneal infection, MCMV infects splenic DCs by 48hrs p.i (522). Consequently, it is possible that the lower numbers of the three subsets of DCs in WT-MCMV may be a consequence of direct virus infection. Alternatively, activated DCs die and higher numbers of DCs during ΔgL-MCMV infection may reflect impaired DC activation. In

contrast to the spleen, different subsets of DCs from the draining axillary lymph nodes displayed comparable numbers between both infection models (Figure 5.15D-F).

The maturation status and antigen presentation potential of the different DC subsets was next compared between WT-MCMV and ΔgL-MCMV infection. A dysregulation in the expression of costimulatory molecules on $CD8^+$ cDC from ΔgL-MCMV infected mice was observed (Figure 5.16). During acute ΔgL-MCMV infection, expression of CD80 was not efficiently upregulated on $CD8^+$ cDC and showed levels comparable to that of naïve mice (Figure 5.16C&D). Taken together, these data suggest that ΔgL-MCMV may be less efficient at activating $CD8^+$ cDC for T cell priming than WT-MCMV.

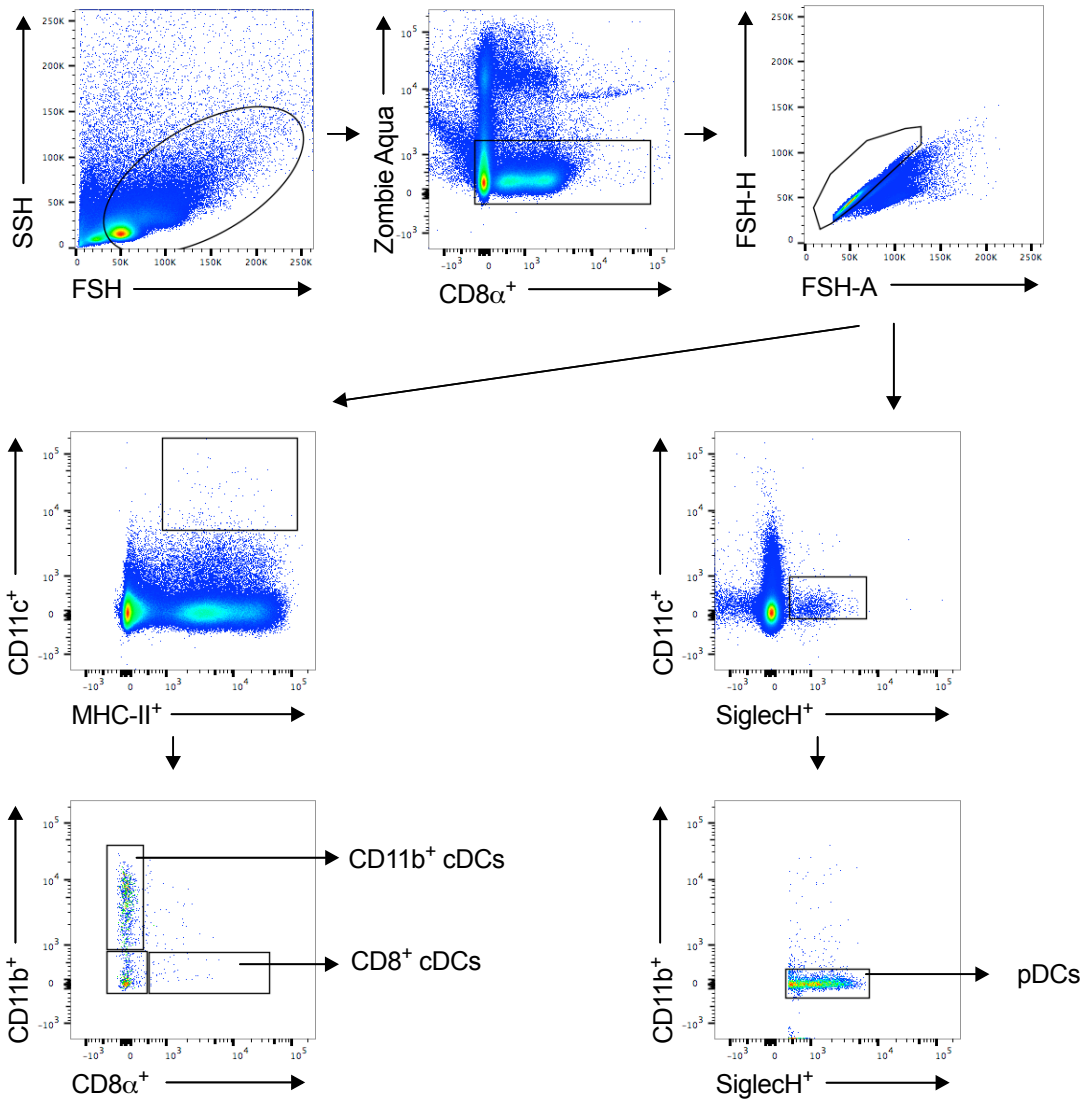

Figure 5.14 Different subsets of dendritic cells delineated by flow cytometry.

Gating strategy for defining different subsets of dendritic cells (DCs): plasmacytoid DCs (pDCs), $CD8^+$ conventional DCs (cDCs) and $CD11b^+$ cDCs. Representative flow cytometry plots are shown of cells isolated from the axillary lymph node d2 p.i with s.c WT-MCMV.

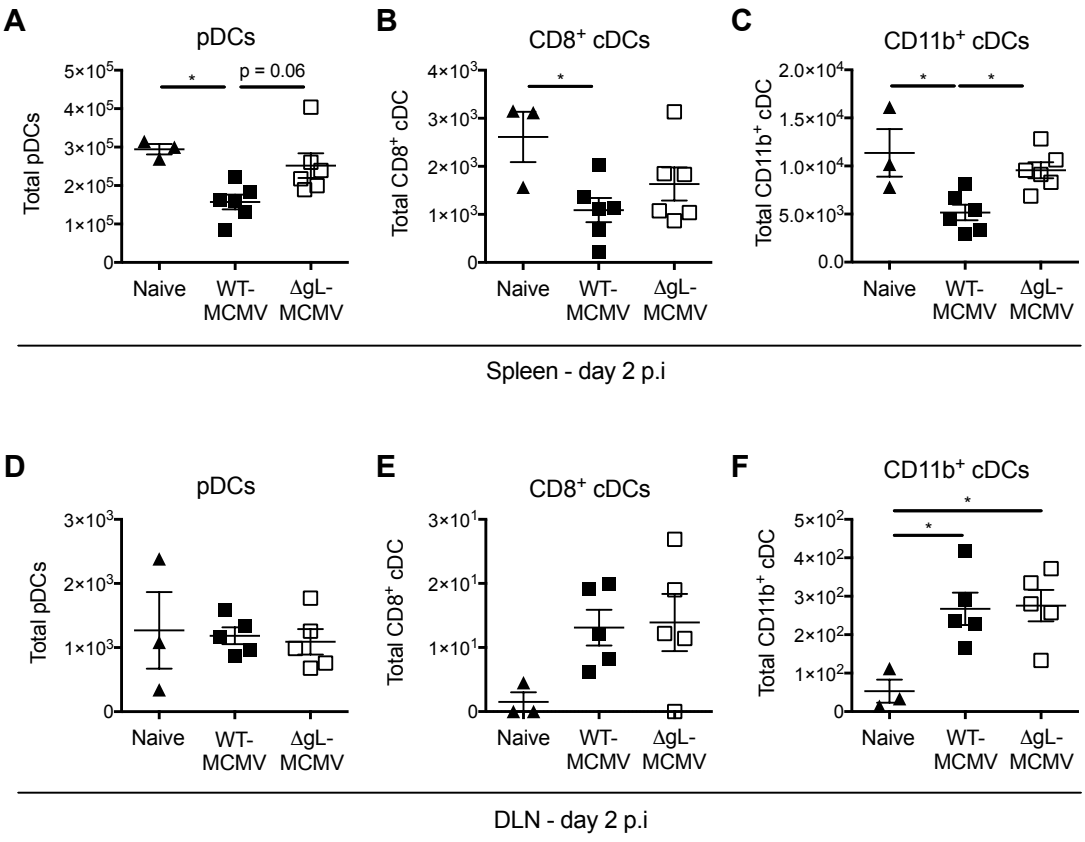

Figure 5.15 Accumulation of DCs in the spleen and lymph nodes of WT-MCMV and ΔgL-MCMV infection.

(A-F) BALB/c mice were infected s.c with WT-MCMV or ΔgL-MCMV and at day 2 p.i, spleen and draining axillary lymph nodes (DLN) were harvested. Naïve mice were used as a control. Cells were stained for MHC class II, CD11c, Siglec H, CD11b and CD8α to obtain total numbers of **(A&D)** pDCs ($CD11c^{int}$ $CD11b^{-}$ Siglec H^{+}), **(B&E)** $CD8^{+}$ DCs (II^{+} $CD11c^{+}$ $CD8\alpha^{+}$) and **(C&F)** $CD11b^{+}$ DCs (II^{+} $CD11c^{+}$ $CD11b^{+}$). Data shown as individual mice withmean ± SEM (n = 3-5 mice/group), representing two separate experiments. Significance was assessed by one-way ANOVA with Bonferroni's correction for multiple comparisons, * $p<0.05$.

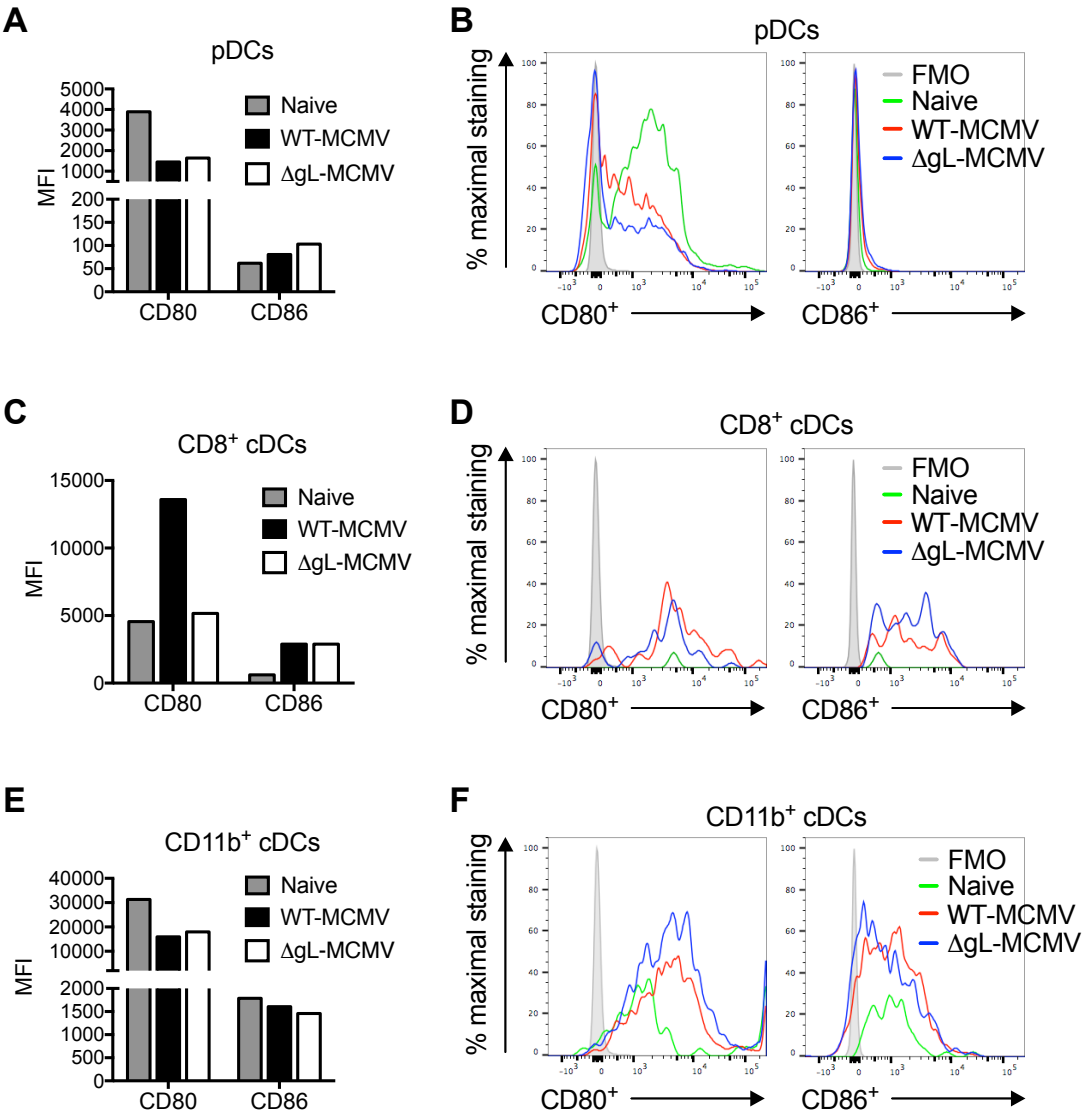

Figure 5.16 CD8$^+$ cDCs during acute ΔgL-MCMV infection display dysregulated expression of costimulatory molecules.

(A-F) The DC subsets from the draining lymph nodes in Figure 5.15 were further stained for CD80 and CD86. **(A, C & E)** The mean fluorescence intensity (MFI) for **(A)** pDCs, **(C)** CD8$^+$ cDCs and **(E)** CD11b$^+$ cDCs was obtained. **(B, D & F)** Histogram overlays of CD80and CD86 expression by **(B)** pDCs, **(D)** CD8$^+$ cDCs and **(F)** CD11b$^+$ cDCs. Graphs and histograms show MFIs from concatenated samples from 3-5 mice in each group.

5.3 Discussion

Development of long-term $CD8^+$ T cell memory is an important goal for vaccination because it can provide protection against re-infection and disease. This protection stems from their longevity and their unique ability to rapidly expand in numbers and produce cytokines and cytotoxic molecules more rapidly than naïve $CD8^+$ T cells upon exposure to the antigen. Thus, the spread-defective MCMV vector, ΔgL-MCMV, was assessed for its ability to induce a long-lasting inflationary immune response.

The data collected here, in accordance with previous studies (410, 494, 496), suggests that a spread-competent MCMV vector is not necessary for the induction of inflationary memory $CD8^+$ T cells upon intraperitoneal infection. Regarding local virus administration, Snyder *et al.* examined ΔgL-MCMV challenge via the hind foot-pad, and reported impaired M38-, IE3- and m139- specific $CD8^+$ T cell memory inflation in C57BL/6 mice (410). In this study, C57BL/6 mice locally administered via s.c injection of ΔgL-MCMV above the sternum failed to induce inflationary responses specific for M38, in accordance with the aforementioned study. WT-MCMV also failed to induce inflationary M38 responses in the peripheral circulation upon subcutaneous challenge, but these responses were significantly higher than those induced by ΔgL-MCMV infection. Nonetheless, in this study, upon s.c administration, ΔgL-MCMV induced IE3-specific $CD8^+$ T cell accumulation to levels comparable to WT-MCMV. In addition, BALB/c mice challenged s.c with ΔgL-MCMV successfully induced memory inflation in the peripheral circulation, albeit with lower magnitude than WT-MCMV. Moreover, infection with ΔgL-MCMV substantially impaired the seeding of MCMV-specific $CD8^+$ T cell responses within tissues, regardless of the administration route and this was associated with reduced accumulation of MCMV-specific T_{EM} and T_{CM} cells in several tissues following i.p and s.c ΔgL-MCMV administration. Most importantly, MCMV-specific $CD8^+$ T cells remained functional during chronic ΔgL-MCMV infection

after subcutaneous challenge. Overall, these data demonstrate that a spread-defective MCMV vector can drive memory inflation upon subcutaneous administration of the virus, suggesting that ΔgL-MCMV can persist and remain antigenically active. How spread-defective MCMV vector drives inflationary responses is unclear. Due to the inability of ΔgL-MCMV to re-infect cells after the first round of infection, for ΔgL-MCMV to be able to drive memory inflation first-target cells might not be eliminated by the immune system, thus enabling carriage of latent virus. Similarly, cells in mice infected with a replication-deficient gamma-herpesvirus (MHV68) were reported to not be targeted by the adaptive immune system (523). Thus, it would be interesting to identify in which cells ΔgL-MCMV establishes latency, understand how long these cells and latent virus is maintained *in vivo* and whether loss of these cells correlates with waning of MCMV-induced T cell immunity.

In the initial days of infection, I observed the lower accumulation of pDCs, $CD8^+$ cDCs and $CD11b^+$ cDCs in the spleen of mice infected with WT-MCMV as compared to ΔgL-MCMV. It was not surprising that WT-MCMV infection in BALB/c mice induced loss of DCs, as it is known that in the absence of effective NK cell control (BALB/c lack the NK cell activator receptor Ly49H), MCMV depletes $CD11c^+$ cDCs from the spleen during acute infection (524–526). It is unclear whether these cells die in the spleen. It is possible that DCs undergo viral induced apoptosis upon direct infection. However this seems unlikely as, although MCMV can infect $CD11c^+$ DCs, it is thought that a very small fraction gets infected *in vivo* (522, 524). Another explanation might be that MCMV blocks the generation of these cells. CMV is capable of infecting haematopoietic progenitors (527), thus these may prevent the generation of DC populations. This correlates with the findings that the spread-defective MCMV vector did not deplete DCs in the spleen probably due to inability to spread from the first infected cells, and subsequently would not spread to haematopoietic progenitors. Alternatively, and the more likely explanation, is that ΔgL-MCMV induces sub-optimal DC activation since

DCs undergo apoptosis after activation (528). This correlates with the findings that $CD8^+$ cDCs in the draining lymph node of ΔgL-MCMV infected mice had lower expression levels of the costimulatory molecule CD80 compared to WT-MCMV. Thus, these results suggest that the reduced accumulation of MCMV-specific $CD8^+$ T cells in tissues might be due to the impaired ability of $CD8^+$ cDCs to prime these cells, as this subset of DCs have been described to be the major contributors of $CD8^+$ T cell priming in MCMV (386). The results observed here are in accordance with previous studies where it has been shown that cross-presentation is necessary and sufficient for the induction of anti-viral $CD8^+$ T cells during acute MCMV infection, and that $CD8^+$ cDCs are responsible for this function (494). Further experiments with $CD8^+$ cDC depletion during WT-MCMV and ΔgL-MCMV infection would highlight the importance of this DC subtype in priming T lymphocytes in s.c immunisation.

Another important aspect for successful vaccine development is the generation of T_{RM} cells, which provide local immediate immunity. It is well known that MCMV-specific $CD8^+$ T_{RM} develop in mucosal tissues after MCMV infection (500, 510, 511). Challenge with ΔgL-MCMV via i.p or s.c resulted in lower accumulation of pp89-specific $CD8^+$ T_{RM} cells in the salivary glands indicating a dysregulation in T_{RM} formation. Indeed, unpublished data from McLaren *et al.* shows ΔgL-MCMV infection displayed defective IL-33 induction. IL-33 is an IL-1 family cytokine member released by necrotic cells as a danger signal in response to infection or cellular stress (529). IL-33 is induced by replicating MCMV and promotes MCMV-specific $CD8^+$ memory T cell infiltration and the accumulation of T_{RM} cells (McLaren *et al.* unpublished), indicating that the reduced accumulation of inflationary MCMV-specific $CD8^+$ T cells and T_{RM} seen in this study is a downstream consequence of impaired IL-33 production. Collectively, these data show that ΔgL-MCMV is less efficient at inducing MCMV-specific T cell responses than WT-MCMV. Consequently, adjuvants might be needed to augment the immunogenicity and efficacy of spread-defective MCMV vectors. Indeed, McLaren *et al.* (unpublished)

showed that administering exogenous recombinant IL-33 augmented long-term MCMV-specific T cell responses induced by ΔgL-MCMV, providing proof-of-principle that sub-optimal responses induced by ΔgL-MCMV can be enhanced by immune modulation.

In conclusion, exciting progress has been made regarding the use of CMV as a vaccine vector due to the generation of a safe and immunogenic spread-defective vector. $CD8^+$ T cells elicited by ΔgL-MCMV do not assume an exhausted phenotype, but instead remain functional. Yet, improvements are necessary to augment the magnitude of $CD8^+$ T cell responses in the circulation and tissues.

Chapter 6 - General Discussion

Despite the relative effectiveness of current cancer therapies, most patients with cancer experience tumour progression or regression, and ultimately die of the disease. There is a need for better treatments for both advanced disease and to prevent relapse. An encouraging cancer immunotherapy approach appears to be the induction and stimulation of immune responses to generate large numbers of tumour-specific T cells. Over the past recent years, CMV has emerged as a potential candidate to be used as a vaccine viral vector due to its ability to induce robust, long-lasting effector memory T cells that remain functional throughout the life of the host.

The aims of this thesis were to construct several MCMV vectors expressing the tumour-associated antigens NY-ESO-1 or 5T4, and to examine the immunogenicity and efficacy of these to induce a strong anti-tumour immune response *in vivo*; in addition to investigate the immunogenicity of MCMV immunisation using a clinically relevant route of delivery. The results of these experiments provide further evidence of the potential of CMV as a cancer vaccine vector. Initially, I demonstrated the ability of MCMV-based vectors to break tolerance and induce an immune response against 5T4. Additionally, I demonstrated that MCMV-based vectors can be used in combination with recombinant adenoviruses in prime-boost approaches to generate polyfunctional tumour-specific $CD8^+$ T cells, which may be protective upon tumour challenge. Finally, I demonstrated that subcutaneous administration of spread-sufficient and spread-deficient MCMV-based vectors can induce memory T cell inflation.

6.1 MCMV-based vectors

MCMV is the best characterised and most widely used animal model for CMV and is a powerful tool for examining the host's immune response to CMV infection. In addition, recombinant MCMV-based vectors can be easily engineered due to the advances in BAC technology and homologous recombination. The use of MCMV infection model and BAC technology have been used in this thesis to investigate the use of CMV as a vaccine platform with the ultimate goal to translate findings from these experiments to help develop HCMV as a vaccine vector.

Experiments described in Chapter 4 demonstrated that CMV-based vectors have the potential to induce a robust anti-tumour $CD8^+$ T cell response. It is important to note that not all the vectors constructed induced detectable tumour-specific $CD8^+$ T cell responses, indicating the importance of the site of gene insertion within the CMV genome for vector immunogenicity. As mentioned before, several factors can affect the immunogenicity of tumour-associated antigens expressed by MCMV vectors such as effective antigen expression, processing and presentation; and gene expression kinetics (401, 420, 472). Thus, further studies are needed to elucidate the appropriate insertion site within the CMV genome to fully exploit the inflationary properties of the CMV vector. In addition, other external factors can influence the immunogenicity of the vector, including route of administration. In Chapter 5, I showed that subcutaneous administration of WT-MCMV resulted in reduced accumulation of MCMV-specific $CD8^+$ T cells. Hence, an MCMV-based vaccine engineered to elicit a strong anti-tumour immune response with inflationary properties upon intraperitoneal challenge, should be examined to see whether it can still induce anti-tumour immune responses via a clinical relevant route of administration such as subcutaneous or intramuscular.

HCMV is a ubiquitous virus and many individuals are infected with multiple virus strains. Therefore, introducing a CMV-based vaccine would not be expected to pose additional risks that are not already present in the population. Nevertheless, although

most primary infections are asymptomatic in healthy adults, HCMV infection can cause a variety of clinical conditions in immune-compromised individuals, making therapeutic vaccination for cancer patients possibly dangerous, especially if they are seronegative. Thus, there is a need to develop a CMV vaccine that exhibits an excellent safety profile to protect the vulnerable population but maintain immunogenicity. Data presented in Chapter 5, and in accordance with several published studies (410, 530), demonstrated the ability of spread-defective MCMV vectors to induce virus-specific inflationary response upon intraperitoneal administration. Importantly, the spread-defective MCMV vectors, ΔgL-MCMV and MCMV-ΔM94, were reported to be safe in immune-deficient SCID mice (410) and highly susceptible IFN$\alpha\beta R^{-/-}$ mice (530), respectively, hence indicating that similarly spread-defective HCMV strains may be safe vaccines. Subcutaneous administration of the spread-defective MCMV vector ΔgL-MCMV induced memory inflation of T cells reactive to endogenous epitopes, although with a reduced magnitude as compared to those induced by WT-MCMV. Whilst promising, the reduced inflationary responses might reflect a reduced induction of tumour-specific responses when a tumour-associated antigen is inserted in the spread-defective vector. Thus, generating a spread-defective MCMV vector expressing a tumour-associated antigen and examining the induction of anti-tumour immune responses will be critical for the validation CMV-based cancer vectors prior to clinical exploitation.

Infiltration of tumours with $CD8^+$ T cells correlates with improved patient survival (Chapter 1, section 1.2.5) and the presence of T_{RM} cells has been reported to improve anti-tumour efficacy in several pre-clinical studies (531, 532). MCMV infection has been shown to induce large numbers of MCMV-specific $CD8^+$ T_{RM} cells in the salivary glands, and to a lesser extend in other mucosal sites such as the female reproductive tract and small intestine (511). In Chapter 5 I have shown that intraperitoneal and subcutaneous administration of the spread-defective MCMV led to a reduced

accumulation of MCMV-specific $CD8^+$ T_{EM} cells in multiple tissues and T_{RM} cells in the salivary gland compared to WT-MCMV. Thus, the use of immune modulators might be an important aspect to consider in order to augment these responses. A number of reagents have been developed to block and enhance signalling pathways to augment and promote more efficient immune responses. An example includes recombinant IL-33, and as mentioned before, administration of IL-33 augmented MCMV-specific T cell responses induced by ΔgL-MCMV (McLaren *et al*. unpublished), demonstrating that immune responses can be enhanced by immune modulators. Other agents that can be used with CMV-based vectors are check-point inhibitors, such as PD-L1 blocking agents, which have proven to synergize with the actions of MCMV-based vectors to delay tumour growth (482). In addition, the use of a spread-defective CMV-based vectors could be used in combination with other non-replicating viral vectors, such as adenovirus, in a prime-boost immunisation approach, as shown in Chapter 4.

6.2 Future development of HCMV-based vectors

In the laboratory, HCMV is most frequently propagated in fibroblasts, but serial passage through these cells results in the accumulation of mutations in the HCMV genome in the process of adaptation. Consequently, the genetic integrity of highly passaged HCMV strains such as AD169 and Towne is severely compromised (277, 298–300). AD169 has been reported to be over attenuated as when administered subcutaneously to healthy individuals only half exhibited detectable amounts of CMV-specific antibody responses when evaluated 8 years post vaccination (reviewed in (533)). Similar studies have been reported with Towne (533). These studies suggest that these strains would not be suitable for generating CMV-based vectors for cancer therapy due to their inability to induce an immune response. Of the current strains used in the lab, the low passage strain Merlin is considered to be the closest to wild-type

HCMV (277). It is now evident that wild-type HCMV strains are not readily propagated *in vitro* as correcting the mutations in UL128 and RL13 (which are normally found in *in vitro* passaged viruses (295)) impairs the ability of the virus to grow in different cell types, including fibroblasts (534). Nonetheless, stable propagation of phenotypically wild-type Merlin virus has been achieved by placing both regions under conditional expression, where UL128 and RL13 expression is repressed during *in vitro* growth (535). In addition, similarly to MCMV, cloning and manipulation of the HCMV genome has been aided by BAC technology which offers means of working with stable and genetically defined strains. To this end, the low-passage HCMV strain Merlin genome has been cloned into a self-excising BAC by Stanton *et al*. (535), making it suitable for rapid manipulation of the viral genome by recombineering technology. Thus, the generation of HCMV-based vectors expressing tumour-associated antigens for cancer immunotherapy is feasible. Furthermore, HCMV can replicate at high titers *in vitro* to then be used in the clinic.

An important aspect to consider when translating CMV-based vectors into the clinic, is the dose to be administered to individuals. Several studies using the mouse model of CMV reported that the viral inoculum dose has an impact on memory T cell inflation (422, 536). Following a low dose MCMV inoculum, the accumulation of inflationary memory $CD8^+$ T cells was severely hampered (422, 536) and turned the characteristic effector memory-like phenotype of inflationary T cells into a more central memory-like phenotype (536). Thus, for a HCMV-based vaccine the dose of inoculum should be high enough to drive $CD8^+$ T_{EM} inflation, but not too high to cause disease. Furthermore, many individuals are seropositive for HCMV, yet unlike many viruses, CMV can re-infect previously infected individuals. However, pre-existing immunity targeting the vector might limit the induction of potent anti-tumour responses. A study using MCMV reported that re-infection with high MCMV titer significantly contributed to memory inflation, while low titer MCMV re-infection induced a transient MCMV-specific

T cell increase, that rapidly returned to baseline levels (422). This suggests that in subsequent CMV encounters, such as immunisation with CMV-based vectors, the vaccination dose needs to be carefully chosen to induce desirable immunity to heterologous proteins. Nonetheless, this allows for vaccination and boosting with CMV-based vectors even in individuals with pre-existing CMV-specific immunity.

Due to the ability to induce durable effector memory $CD8^+$ T cells that infiltrate tissues at a steady state, CMV-based vectors appear to be an attractive strategy to target metastasis. Hence, CMV-based vectors could be given to cancer patients after resection of primary tumours and/or to patients who are at high risk of recurrence. A concern that is closely associated with viral-based vectors is that attenuated viruses may gain virulence *in vivo*. In the case of HCMV, due to the persistent nature of the virus, the use of attenuated HCMV as vaccine vectors bears the risk that it might recombine with endogenous HCMV resulting in the restoration of virulence. Another potential risk is that the administration of an attenuated HCMV vector could stimulate reactivation of latent wild-type virus already present in the individual. Yet, no such reports have been described to date were CMV used in pre-clinical studies have undergone recombineering *in vivo* or reactivated latent virus. For a recombination event to occur, the attenuated virus and the wild-type must co-infect single cells. The likelihood of this to happen in the host under natural conditions is low, suggesting that recombination and its potential consequences are rare (537). Nevertheless, the potential for recombination events between the attenuated CMV vector and wild-type viruses *in vivo* exists and should be assessed.

6.3 Conclusion

I have shown that MCMV expressing tumour-associated antigens can induce an anti-tumour immune response, but this depends on the insertion site within the vector's genome. Furthermore, MCMV vectors can be used in combination with adenoviruses to promote tumour-specific $CD8^+$ T cells that can delay tumour onset. I have also demonstrated that, upon tumour challenge, MCMV immunisation results in increased influx of $CD8^+$ T cells into the tumour site, potentially skewing the tumour environment to be more immunogenic. Finally, the spread-defective MCMV vector ΔgL-MCMV has been proven to be effective in driving memory inflation upon local administration of the virus. Although further studies are needed to determine the best strategy for vector construction, elucidate how MCMV might be driving anti-tumour activity and how to optimise responses induced by replication-deficient vectors following immunisation via clinically relevant routes, overall data presented here suggests that CMV has significant potential to be developed as an effective cancer vaccine vector.

Chapter 7 - References

1. Kondo, M., I. L. Weissman, and K. Akashi. 1997. Identification of Clonogenic Common Lymphoid Progenitors in Mouse Bone Marrow. *Cell* 91: 661–672.

2. Nielsen, M. M., D. A. Witherden, and W. L. Havran. 2017. γδ T cells in homeostasis and host defence of epithelial barrier tissues. *Nat. Rev. Immunol.* 17: 733–745.

3. Starr, T. K., S. C. Jameson, and K. A. Hogquist. 2003. Positive and Negative Selection of T Cells. *Annu. Rev. Immunol.* 21: 139–176.

4. Tao, X., S. Constant, P. Jorritsma, and K. Bottomly. 1997. Strength of TCR signal determines the costimulatory requirements for Th1 and Th2 CD4+ T cell differentiation. *J. Immunol.* 159: 5956–63.

5. Abbas, A. K., K. M. Murphy, and A. Sher. 1996. Functional diversity of helper T lymphocytes. *Nature* 383: 787–93.

6. Kuchroo, V. K., M. Prabhu Das, J. A. Brown, A. M. Ranger, S. S. Zamvil, R. A. Sobel, H. L. Weiner, N. Nabavi, and L. H. Glimcher. 1995. B7-1 and B7-2 costimulatory molecules activate differentially the Th1/Th2 developmental pathways: Application to autoimmune disease therapy. *Cell* 80: 707–718.

7. Hosken, N. A., K. Shibuya, A. W. Heath, K. M. Murphy, and A. O'Garra. 1995. The effect of antigen dose on CD4+ T helper cell phenotype development in a T cell receptor-alpha beta-transgenic model. *J. Exp. Med.* 182: 1579–84.

8. Pfeiffer, C., J. Stein, S. Southwood, H. Ketelaar, A. Sette, and K. Bottomly. 1995. Altered peptide ligands can control CD4 T lymphocyte differentiation in vivo. *J. Exp. Med.* 181: 1569–74.

9. Nakamura, T., Y. Kamogawa, K. Bottomly, and R. A. Flavell. 1997. Polarization of IL-4- and IFN-gamma-producing CD4+ T cells following activation of naive CD4+ T cells. *J Immunol* 158: 1085–1094.

10. Trinchieri, G., S. Pflanz, and R. A. Kastelein. 2003. The IL-12 family of heterodimeric cytokines: New players in the regulation of T cell responses. *Immunity* 19: 641–644.

11. Szabo, S. J., S. T. Kim, G. L. Costa, X. Zhang, C. G. Fathman, and L. H. Glimcher. 2000. A novel transcription factor, T-bet, directs Th1 lineage commitment. *Cell* 100: 655–69.

12. Zheng, W., and R. A. Flavell. 1997. The transcription factor GATA-3 is necessary and sufficient for Th2 cytokine gene expression in CD4 T cells. *Cell* 89: 587–96.

13. Stevens, T. L., A. Bossie, V. M. Sanders, R. Fernandez-Botran, R. L. Coffman, T. R. Mosmann, and E. S. Vitetta. 1988. Regulation of antibody isotype secretion by subsets of antigen-specific helper T cells. *Nature* 334: 255–258.

14. Mowen, K. A., and L. H. Glimcher. 2004. Signaling pathways in Th2 development. *Immunol. Rev.* 202: 203–222.

15. Bao, K., and R. L. Reinhardt. 2015. The differential expression of IL-4 and IL-13 and its impact on type-2 immunity. *Cytokine* 75: 25–37.

16. Nakamura, T., R. K. Lee, S. Y. Nam, E. R. Podack, K. Bottomly, and R. A. Flavell. 1997. Roles of IL-4 and IFN-gamma in stabilizing the T helper cell type 1 and 2 phenotype. *J. Immunol.* 158: 2648–2653.

17. Veldhoen, M., R. J. Hocking, C. J. Atkins, R. M. Locksley, and B. Stockinger. 2006. TGFβ in the context of an inflammatory cytokine milieu supports de novo differentiation of IL-17-producing T cells. *Immunity* 24: 179–189.

18. Weaver, C. T., R. D. Hatton, P. R. Mangan, and L. E. Harrington. 2007. IL-17 Family Cytokines and the Expanding Diversity of Effector T Cell Lineages. *Annu. Rev. Immunol.* 25: 821–852.

19. Ivanov, I. I., B. S. McKenzie, L. Zhou, C. E. Tadokoro, A. Lepelley, J. J. Lafaille, D. J. Cua, and D. R. Littman. 2006. The Orphan Nuclear Receptor RORγt Directs the Differentiation Program of Proinflammatory IL-17+ T Helper Cells. *Cell* 126: 1121–1133.

20. Cosmi, L., L. Maggi, V. Santarlasci, F. Liotta, and F. Annunziato. 2014. T helper cells plasticity in inflammation. *Cytom. Part A* 85: 36–42.

21. Hori, S., T. Nomura, and S. Sakaguchi. 2003. Control of regulatory T cell development by the transcription factor Foxp3. *Science* 299: 1057–61.

22. Fontenot, J. D., J. P. Rasmussen, L. M. Williams, J. L. Dooley, A. G. Farr, and A. Y. Rudensky. 2005. Regulatory T cell lineage specification by the forkhead transcription factor Foxp3. *Immunity* 22: 329–341.

23. Chen, W., W. Jin, N. Hardegen, K. Lei, L. Li, N. Marinos, G. McGrady, and S. M. Wahl. 2003. Conversion of Peripheral CD4 $^{+}$ CD25 $^{-}$ Naive T Cells to CD4 $^{+}$ CD25 $^{+}$ Regulatory T Cells by TGF-β Induction of Transcription Factor *Foxp3*. *J. Exp. Med.* 198: 1875–1886.

24. Crotty, S. 2011. Follicular Helper CD4 T Cells (T FH). *Annu. Rev. Immunol.* 29: 621–663.

25. Nurieva, R. I., Y. Chung, D. Hwang, X. O. Yang, H. S. Kang, L. Ma, Y. hong Wang, S. S. Watowich, A. M. Jetten, Q. Tian, and C. Dong. 2008. Generation of T Follicular Helper Cells Is Mediated by Interleukin-21 but Independent of T Helper 1, 2, or 17 Cell Lineages. *Immunity* 29: 138–149.

26. Nurieva, R. I., Y. Chung, G. J. Martinez, X. O. Yang, S. Tanaka, T. D. Matskevitch, Y.-H. Wang, and C. Dong. 2009. Bcl6 mediates the development of T follicular helper cells. *Science* 325: 1001–5.

27. Linterman, M. A., L. Beaton, D. Yu, R. R. Ramiscal, M. Srivastava, J. J. Hogan, N. K. Verma, M. J. Smyth, R. J. Rigby, and C. G. Vinuesa. 2010. IL-21 acts directly on B cells to regulate Bcl-6 expression and germinal center responses. *J. Exp. Med.* 207: 353–363.

28. Reinhardt, R. L., H. E. Liang, and R. M. Locksley. 2009. Cytokine-secreting follicular T cells shape the antibody repertoire. *Nat. Immunol.* 10: 385–393.

29. Geginat, J., M. Paroni, S. Maglie, J. S. Alfen, I. Kastirr, P. Gruarin, M. de Simone, M. Pagani, and S. Abrignani. 2014. Plasticity of human CD4 T cell subsets. *Front. Immunol.* 5: 1–10.

30. Kolumam, G. A., S. Thomas, L. J. Thompson, J. Sprent, and K. Murali-Krishna. 2005. Type I interferons act directly on CD8 T cells to allow clonal expansion and memory formation in response to viral infection. *J. Exp. Med.* 202: 637–650.

31. Curtsinger, J. M., and M. F. Mescher. 2011. Inflammatory Cytokines as a Third Signal for T Cell Activation Julie. *Curr Opin Immunol* 22: 333–340.

32. Curtsinger, J. M., J. O. Valenzuela, P. Agarwal, D. Lins, and M. F. Mescher. 2005. Cutting Edge: Type I IFNs Provide a Third Signal to CD8 T Cells to Stimulate Clonal Expansion and Differentiation. *J. Immunol.* 174: 4465–4469.

33. Schmidt, C. S., and M. F. Mescher. 2002. Peptide Antigen Priming of Naive, But Not Memory, CD8 T Cells Requires a Third Signal That Can Be Provided by IL-12. *J. Immunol.* 168: 5521–5529.

34. Moser, M. 2003. Dendritic cells in immunity and tolerance - Do they display opposite functions? *Immunity* 19: 5–8.

35. Boehm, U., T. Klamp, M. Groot, and J. C. Howard. 1997. Cellular responses to interferon-γ. *Annu. Rev. Immunol.* 15: 749–795.

36. Harty, J. T., A. R. Tvinnereim, and D. W. White. 2000. Cd8+ T C Ell Effector Mechanisms in R Esistance To Infection. *Annu. Rev. Immunol.* 25: 275–308.

37. Oehen, S., and K. Brduscha-Riem. 1998. Differentiation of naive CTL to effector and memory CTL: correlation of effector function with phenotype and cell division. *J. Immunol.* 161: 5338–46.

38. Baaten, B. J. G., R. Tinoco, A. T. Chen, and L. M. Bradley. 2012. Regulation of antigen-experienced T cells: Lessons from the quintessential memory marker CD44. *Front. Immunol.* 3: 1–12.

39. Arens, R., and S. P. Schoenberger. 2010. Plasticity in programming of effector and memory CD8 T-cell formation. *Immunol. Rev.* 235: 190–205.

40. Obar, J. J., and L. Lefrançois. 2010. Early events governing memory CD8 + T-cell differentiation. *Int. Immunol.* 22: 619–625.

41. Obar, J. J., M. J. Molloy, E. R. Jellison, T. A. Stoklasek, W. Zhang, E. J. Usherwood, and L. Lefrancois. 2010. CD4+ T cell regulation of CD25 expression controls development of short-lived effector CD8+ T cells in primary and secondary responses. *Proc. Natl. Acad. Sci.* 107: 193–198.

42. Joshi, N. S., W. Cui, A. Chandele, H. K. Lee, D. R. Urso, J. Hagman, L. Gapin, and S. M. Kaech. 2007. Inflammation Directs Memory Precursor and Short-Lived Effector CD8+ T Cell Fates via the Graded Expression of T-bet Transcription Factor. *Immunity* 27: 281–295.

43. Sarkar, S., V. Kalia, W. N. Haining, B. T. Konieczny, S. Subramaniam, and R. Ahmed. 2008. Functional and genomic profiling of effector CD8 T cell subsets with distinct memory fates. *J. Exp. Med.* 205: 625–640.

44. Kaech, S. M., J. T. Tan, E. J. Wherry, B. T. Konieczny, C. D. Surh, and R. Ahmed. 2003. Selective expression of the interleukin 7 receptor identifies effector CD8 T cells that give rise to long-lived memory cells. *Nat. Immunol.* 4: 1191–1198.

45. Rutishauser, R. L., G. A. Martins, S. Kalachikov, A. Chandele, I. A. Parish, E. Meffre, J. Jacob, K. Calame, and S. M. Kaech. 2009. Transcriptional Repressor Blimp-1 Promotes CD8+T Cell Terminal Differentiation and Represses the Acquisition of Central Memory T Cell Properties. *Immunity* 31: 296–308.

46. Kallies, A., A. Xin, G. T. Belz, and S. L. Nutt. 2009. Blimp-1 Transcription Factor Is Required for the Differentiation of Effector CD8+ T Cells and Memory Responses. *Immunity* 31: 283–295.

47. Tan, J. T., B. Ernst, W. C. Kieper, E. LeRoy, J. Sprent, and C. D. Surh. 2002. Interleukin (IL)-15 and IL-7 Jointly Regulate Homeostatic Proliferation of Memory Phenotype CD8 $^{+}$ Cells but Are Not Required for Memory Phenotype CD4 $^{+}$ Cells. *J. Exp. Med.* 195: 1523–1532.

48. Schluns, K. S., K. Williams, A. Ma, X. X. Zheng, and L. Lefrancois. 2002. Cutting Edge: Requirement for IL-15 in the Generation of Primary and Memory Antigen-Specific CD8 T Cells. *J. Immunol.* 168: 4827–4831.

49. Kaech, S. M., and W. Cui. 2012. Transcriptional control of effector and memory CD8+ T cell differentiation. *Nat. Rev. Immunol.* 12: 749–761.

50. Schenkel, J. M., and D. Masopust. 2014. Tissue-resident memory T cells. *Immunity* 41: 886–897.

51. Mackay, L. K., A. Rahimpour, J. Z. Ma, N. Collins, A. T. Stock, M.-L. Hafon, J. Vega-Ramos, P. Lauzurica, S. N. Mueller, T. Stefanovic, D. C. Tscharke, W. R. Heath, M. Inouye, F. R. Carbone, and T. Gebhardt. 2013. The developmental pathway for CD103+CD8+ tissue-resident memory T cells of skin. *Nat. Immunol.* 14: 1294–1301.

52. Sheridan, B. S., Q. M. Pham, Y. T. Lee, L. S. Cauley, L. Puddington, and L. Lefrançois. 2014. Oral infection drives a distinct population of intestinal resident memory cd8+ t cells with enhanced protective function. *Immunity* 40: 747–757.

53. Hanahan, D., and R. A. Weinberg. 2000. The hallmarks of cancer. *Cell* 100: 57–70.

54. Hanahan, D., and R. A. Weinberg. 2011. Hallmarks of Cancer: The Next Generation. *Cell* 144: 646–674.

55. Burnet, M. 1957. Cancer; a biological approach. I. The processes of control. *Br. Med. J.* 1: 779–86.

56. Burnet, M. 1964. Immunological factors in the process of carcinogenesis. *Br. Med. Bull.* 20: 154–158.

57. Burnet, F. M. 1970. The concept of immunological surveillance. *Prog. Exp. Tumor Res.* 13: 1–27.

58. Burnet, F. M. 1971. Immunological surveillance in neoplasia. *Transplant. Rev.* 7.

59. Stutman, O. 1974. Tumor development after 3-methylcholanthrene in immunologically deficient athymic-nude mice. *Science* 183: 534–6.

60. Stutman, O. 1979. Chemical carcinogenesis in nude mice: Comparison between nude mice from homozygous matings and heterozygous matings and effect of age and carcinogen dose. *J. Natl. Cancer Inst.* 62: 353–358.

61. Ikehara, S., R. N. Pahwat, G. Fernandest, C. T. Hansen, R. A. Good, and A. A. Con. 1984. Functional T cells in athymic nude mice. 81: 886–888.

62. Maleckar, J. R., and L. A. Sherman. 1987. The composition of the T cell receptor repertoire in nude mice. *J. Immunol.* 138: 3873–6.

63. Stutman, O., C. J. Paige, and E. F. Figarella. 1978. Natural cytotoxic cells against solid tumors in mice I. Strain and age distribution and target cell susceptibility. *J. Immunol.* 121: 1819–1826.

64. Kaplan, D. H., V. Shankaran, A. S. Dighe, E. Stockert, M. Aguet, L. J. Old, and R. D. Schreiber. 1998. Demonstration of an interferon gamma-dependent tumor surveillance system in immunocompetent mice. *Proc. Natl. Acad. Sci. U. S. A.* 95: 7556–61.

65. Street, S. E., E. Cretney, and M. J. Smyth. 2001. Perforin and interferon-gamma activities independently control tumor initiation, growth, and metastasis. *Blood* 97: 192–7.

66. Shankaran, V., H. Ikeda, A. T. Bruce, J. M. White, P. E. Swanson, L. J. Old, and R. D. Schreiber. 2001. IFNγ, and lymphocytes prevent primary tumour development and shape tumour immunogenicity. *Nature* 410: 1107–1111.

67. Smyth, M. J., N. Y. Crowe, and D. I. Godfrey. 2008. NK cells and NKT cells collaborate in host protection from methylcholanthrene-induced fibrosarcoma. *Int. Immunol.* 20: 631.

68. Svane, I. M., A. M. Engel, M. B. Nielsen, H. G. Ljunggren, J. Rygaard, and O. Werdelin. 1996. Chemically induced sarcomas from nude mice are more immunogenic than similar sarcomas from congenic normal mice. *Eur. J. Immunol.* 26: 1844–1850.

69. Engel, A. M., I. M. Svane, S. Mouritsen, J. Rygaard, J. Clausen, and O. Werdelin. 1996. Methylcholanthrene-induced sarcomas in nude mice have short induction times and relatively low levels of surface MHC class I expression. *APMIS* 104: 629–39.

70. Dunn, G. P., A. T. Bruce, H. Ikeda, L. J. Old, and R. D. Schreiber. 2002. Cancer immunoediting: From immunosurveillance to tumor escape. *Nat. Immunol.* 3: 991–998.

71. Dunn, G. P., L. J. Old, and R. D. Schreiber. 2004. The immunobiology of cancer immunosurveillance and immunoediting. *Immunity* 21: 137–48.

72. Schreiber, R. D., L. J. Old, and M. J. Smyth. 2011. Cancer Immunoediting: Integrating Immunity's Roles in Cancer Suppression and Promotion. *Science (80-.).* 331: 1565–1570.

73. Myron Kauffman, H., M. a McBride, W. S. Cherikh, P. C. Spain, W. H. Marks, and A. M. Roza. 2002. Transplant tumor registry: donor related malignancies. *Transplantation* 74: 358–62.

74. MacKie, R. M., R. Reid, and B. Junor. 2003. Fatal Melanoma Transferred in a Donated Kidney 16 Years after Melanoma Surgery. *N. Engl. J. Med.* 348: 567–568.

75. Hicklin, D. J., Z. Wang, F. Arienti, L. Rivoltini, G. Parmiani, and S. Ferrone. 1998. beta2-Microglobulin mutations, HLA class I antigen loss, and tumor progression in melanoma. *J. Clin. Invest.* 101: 2720–9.

76. Algarra, I., T. Cabrera, and F. Garrido. 2000. The HLA crossroad in tumor immunology. *Hum. Immunol.* 61: 65–73.

77. Marincola, F. M., E. M. Jaffee, D. J. Hicklin, and S. Ferrone. 2000. Escape of human solid tumors from T-cell recognition: molecular mechanisms and functional significance. *Adv. Immunol.* 74: 181–273.

78. Seliger, B., C. Harders, S. Lohmann, F. Momburg, S. Urlinger, R. Tampé, and C. Huber. 1998. Down-regulation of the MHC class I antigen-processing machinery after oncogenic transformation of murine fibroblasts. *Eur. J. Immunol.* 28: 122–133.

79. Vitale, M., R. Rezzani, L. Rodella, T. A. P. Down-regulation, H. P. Breast, and G. Zauli. 1998. HLA Class I Antigen and Transporter Associated with Antigen Processing (TAP1 and TAP2) Down-Regulation in High-Grade Primary Breast Carcinoma Lesions HLA Class I Antigen and Transporter Associated with Antigen Processing. *Cancer Res.* 58: 737–742.

80. Seliger, B., M. J. Maeurer, and S. Ferrone. 2000. Antigen-processing machinery breakdown and tumor growth. *Immunol. Today* 21: 455–464.

81. Placzek, W. J., J. Wei, S. Kitada, D. Zhai, J. C. Reed, and M. Pellecchia. 2010. A survey of the anti-apoptotic Bcl-2 subfamily expression in cancer types provides a platform to predict the efficacy of Bcl-2 antagonists in cancer therapy. *Cell Death Dis.* 1: e40-9.

82. Wang, T., G. Niu, M. Kortylewski, L. Burdelya, K. Shain, S. Zhang, R. Bhattacharya, D. Gabrilovich, R. Heller, D. Coppola, W. Dalton, R. Jove, D. Pardoll, and H. Yu. 2004. Regulation of the innate and adaptive immune responses by Stat-3 signaling in tumor cells. *Nat. Med.* 10: 48–54.

83. Medema, J. P., J. de Jong, L. T. Peltenburg, E. M. Verdegaal, a Gorter, S. a Bres, K. L. Franken, M. Hahne, J. P. Albar, C. J. Melief, and R. Offringa. 2001. Blockade of the granzyme B/perforin pathway through overexpression of the serine protease inhibitor PI-9/SPI-6 constitutes a mechanism for immune escape by tumors. *Proc. Natl. Acad. Sci. U. S. A.* 98: 11515–20.

84. Khong, H. T., and N. P. Restifo. 2002. Natural selection of tumor variants in the generation of “tumor escape” phenotypes. *Nat. Immunol.* 3: 999–1005.

85. Zelenay, S., A. G. Van Der Veen, J. P. Böttcher, K. J. Snelgrove, N. Rogers, S. E. Acton, P. Chakravarty, M. R. Girotti, R. Marais, S. A. Quezada, E. Sahai, and C. Reis E Sousa. 2015. Cyclooxygenase-Dependent Tumor Growth through Evasion of Immunity. *Cell* 162: 1257–1270.

86. Huang, M., M. Stolina, S. Sharma, J. T. Mao, L. Zhu, P. W. Miller, J. Wollman, H. Herschman, and S. M. Dubinett. 1998. Non-Small Cell Lung Cancer Cyclooxygenase-2-dependent Balance in Lymphocytes and Macrophages : Up-Regulation and Down-Regulation of Interleukin 12 Production1 Regulation of Cytokine of Interleukin 10. 1208–1216.

87. Rubinstein, N., M. Alvarez, N. W. Zwirner, M. A. Toscano, J. M. Ilarregui, A. Bravo, J. Mordoh, L. Fainboim, O. L. Podhajcer, and G. A. Rabinovich. 2004. Targeted inhibition of galectin-1 gene expression in tumor cells results in heightened T cell-mediated rejection: A potential mechanism of tumor-immune privilege. *Cancer Cell* 5: 241–251.

88. Uyttenhove, C., L. Pilotte, I. Théate, V. Stroobant, D. Colau, N. Parmentier, T. Boon, and B. J. Van den Eynde. 2003. Evidence for a tumoral immune resistance mechanism based on tryptophan degradation by indoleamine 2,3-dioxygenase. *Nat. Med.* 9: 1269–1274.

89. Mougiakakos, D., A. Choudhury, A. Lladser, R. Kiessling, and C. C. Johansson. 2010. Regulatory T cells in cancer. *Adv. Cancer Res.* 107: 57–117.

90. Ostrand-Rosenberg, S., and P. Sinha. 2009. Myeloid-Derived Suppressor Cells: Linking Inflammation and Cancer. *J. Immunol.* 182: 4499–4506.

91. Barnd, D. L., M. S. Lan, R. S. Metzgar, and O. J. Finn. 1989. Specific, major histocompatibility complex-unrestricted recognition of tumor-associated mucins by human cytotoxic T cells. *Proc. Natl. Acad. Sci. U. S. A.* 86: 7159–63.

92. Türeci, Ö.¨, U. Sahin, and M. Pfreundschuh. 1997. Serological analysis of human tumor antigens: Molecular definition and implications. *Mol. Med. Today* 3: 342–349.

93. Coulie, P. G., B. J. Van den Eynde, P. van der Bruggen, and T. Boon. 2014. Tumour antigens recognized by T lymphocytes: at the core of cancer immunotherapy. *Nat. Rev. Cancer* 14: 135–46.

94. Robbins, P. F., M. El-Gamil, Y. F. Li, Y. Kawakami, D. Loftus, E. Appella, and S. A. Rosenberg. 1996. A mutated beta-catenin gene encodes a melanoma-specific antigen recognized by tumor infiltrating lymphocytes. *J. Exp. Med.* 183: 1185–92.

95. Southall, P. J., G. M. Boxer, K. D. Bagshawe, N. Hole, M. Bromley, and P. L. Stern. 1990. Immunohistological distribution of 5T4 antigen in normal and malignant tissues. *Br. J. Cancer* 61: 89–95.

96. Hole, N., and P. L. Stern. 1988. A 72 kD trophoblast glycoprotein defined by a monoclonal antibody. *Br. J. Cancer* 57: 239–246.

97. Carsberg, C. J., K. A. Myers, G. S. Evans, T. D. Allen, and P. L. Stern. 1995. Metastasis-associated 5T4 oncofoetal antigen is concentrated at microvillus projections of the plasma membrane. *J. Cell Sci.* 108: 2905–16.

98. Carsberg, C. J., K. A. Myers, and P. L. Stern. 1996. Metastasis-associated 5T4 antigen disrupts cell-cell contacts and induces cellular motility in epithelial cells. *Int. J. Cancer* 68: 84–92.

99. Awan, A., M. R. Lucic, D. M. Shaw, F. Sheppard, C. Westwater, P. L. Stern, and S. A. Lyons. 2002. 5T4 interacts with TIP-2/GIPC, a PDZ protein, with implications for metastasis. *Biochem. Biophys. Res. Commun.* 290: 1030–1036.

100. Starzynska, T., V. Rahi, and P. L. Stern. 1992. The expression of 5T4 antigen in colorectal and gastric carcinoma. *Br. J. Cancer* 66: 867–9.

101. Starzynska, T., P. J. Marsh, P. F. Schofield, S. a Roberts, K. a Myers, and P. L. Stern. 1994. Prognostic significance of 5T4 oncofetal antigen expression in colorectal carcinoma. *Br. J. Cancer* 69: 899–902.

102. Wrigley, E., a. T. McGown, J. Rennison, R. Swindell, D. Crowther, T. Starzynska, and P. L. Stern. 1995. 5T4 oncofetal antigen expression in ovarian carcinoma. *Int. J. Gynecol. Cancer* 5: 269–274.

103. Ward, C. M., K. Barrow, A. M. Woods, and P. L. Stern. 2003. The 5T4 oncofoetal antigen is an early differentiation marker of mouse ES cells and its absence is a useful means to assess pluripotency. *J. Cell Sci.* 116: 4533–42.

104. Ward, C. M., A. M. Eastham, and P. L. Stern. 2006. Cell surface 5T4 antigen is transiently upregulated during early human embryonic stem cell differentiation: Effect of 5T4 phenotype on neural lineage formation. *Exp. Cell Res.* 312: 1713–1726.

105. Eastham, A. M., H. Spencer, F. Soncin, S. Ritson, C. L. R. R. Merry, P. L. Stern, and C. M. Ward. 2007. Epithelial-Mesenchymal Transition Events during Human Embryonic Stem Cell Differentiation. *Cancer Res.* 67: 11254–11262.

106. Spencer, H. L., A. M. Eastham, C. L. R. Merry, T. D. Southgate, F. Perez-Campo, F. Soncin, S. Ritson, R. Kemler, P. L. Stern, and C. M. Ward. 2007. E-Cadherin Inhibits Cell Surface Localization of the Pro-Migratory 5T4 Oncofetal Antigen in Mouse Embryonic Stem Cells. *Mol. Biol. Cell* 18: 2838–2851.

107. Moon, R. T., A. D. Kohn, G. V. De Ferrari, A. Kaykas, G. V. De Ferrari, and A. Kaykas. 2004. WNT and β-catenin signalling: Diseases and therapies. *Nat. Rev. Genet.* 5: 691–701.

108. Kagermeier-Schenk, B., D. Wehner, G. Özhan-Kizil, H. Yamamoto, J. Li, K. Kirchner, C. Hoffmann, P. Stern, A. Kikuchi, A. Schambony, and G. Weidinger. 2011. Waif1/5T4 Inhibits Wnt/β-Catenin Signaling and Activates Noncanonical Wnt Pathways by Modifying LRP6 Subcellular Localization. *Dev. Cell* 21: 1129–1143.

109. Southgate, T. D., O. J. McGinn, F. V. Castro, A. J. Rutkowski, M. Al-Muftah, G. Marinov, G. J. Smethurst, D. Shaw, C. M. Ward, C. J. Miller, and P. L. Stern. 2010. CXCR4 mediated chemotaxis is regulated by 5T4 oncofetal glycoprotein in mouse embryonic cells. *PLoS One* 5.

110. McGinn, O. J., G. Marinov, S. Sawan, and P. L. Stern. 2012. CXCL12 receptor preference, signal transduction, biological response and the expression of 5T4 oncofoetal glycoprotein. *J. Cell Sci.* 125: 5467–5478.

111. Smyth, L. J. C., E. Elkord, T. E. I. Taher, H. R. Jiang, D. J. Burt, A. Clayton, P. A. Van Veelen, A. De Ru, F. Ossendorp, C. J. M. Melief, J. W. Drijfhout, S. Dermime, R. E. Hawkins, and P. L. Stern. 2006. CD8 T-cell recognition of human 5T4 oncofetal antigen. *Int. J. Cancer* 119: 1638–1647.

112. Redchenko, I., R. Harrop, M. G. Ryan, R. E. Hawkins, and M. W. Carroll. 2006. Identification of a major histocompatibility complex class I-restricted T-cell epitope in the tumour-associated antigen, 5T4. *Immunology* 118: 50–57.

113. Elkord, E., D. J. Burt, J. W. Drijfhout, R. E. Hawkins, and P. L. Stern. 2008. CD4+T-cell recognition of human 5T4 oncofoetal antigen: Implications for initial depletion of CD25+T cells. *Cancer Immunol. Immunother.* 57: 833–847.

114. Scurr, M., T. Pembroke, A. Bloom, D. Roberts, A. Thomson, K. Smart, H. Bridgeman, R. Adams, A. Brewster, R. Jones, S. Gwynne, D. Blount, R. Harrop, R. Hills, A. Gallimore, and A. Godkin. 2017. Low-dose cyclophosphamide induces antitumor T-cell responses, which associate with survival in metastatic colorectal cancer. *Clin. Cancer Res.* 23: 6771–6780.

115. Scurr, M., T. Pembroke, A. Bloom, D. Roberts, A. Thomson, K. Smart, H. Bridgeman, R. Adams, A. Brewster, R. Jones, S. Gwynne, D. Blount, R. Harrop, M. Wright, R. Hills, A. Gallimore, and A. Godkin. 2017. Effect of modified vaccinia Ankara–5T4 and low-dose cyclophosphamide on antitumor immunity in metastatic colorectal cancer: A randomized clinical trial. *JAMA Oncol.* 3: 1–9.

116. Chen, Y. T., M. J. Scanlan, U. Sahin, O. Türeci, A. O. Gure, S. Tsang, B. Williamson, E. Stockert, M. Pfreundschuh, and L. J. Old. 1997. A testicular antigen aberrantly expressed in human cancers detected by autologous antibody screening. *Proc. Natl. Acad. Sci. U. S. A.* 94: 1914–8.

117. Stockert, E., E. Jäger, Y.-T. Chen, M. J. Scanlan, I. Gout, J. Karbach, M. Arand, A. Knuth, and L. J. Old. 1998. A Survey of the Humoral Immune Response of Cancer Patients to a Panel of Human Tumor Antigens. *J. Exp. Med.* 187: 1349–1354.

118. Wang, R. F., S. L. Johnston, G. Zeng, S. L. Topalian, D. J. Schwartzentruber, S. A. Rosenberg, L. Suzanne, D. J. Schwartzentruber, A. Steven, S. L. Topalian, and S. A. Rosenberg. 1998. A Breast and Melanoma-Shared Tumor Antigen: T Cell Responses to Antigenic Peptides Translated from Different Open Reading Frames. *J. Immunol.* 161: 3598–606.

119. Jungbluth, A. A., Y.-T. Chen, E. Stockert, K. J. Busam, D. Kolb, K. Iversen, K. Coplan, B. Williamson, N. Altorki, and L. J. Old. 2001. Immunohistochemical analysis of NY-ESO-1 antigen expression in normal and malignant human tissues. *Int. J. Cancer* 92: 856–860.

120. Szender, J. B., A. Papanicolau-Sengos, K. H. Eng, A. J. Miliotto, A. A. Lugade, S. Gnjatic, J. Matsuzaki, C. D. Morrison, and K. Odunsi. 2017. NY-ESO-1 expression predicts an aggressive phenotype of ovarian cancer. *Gynecol. Oncol.* 145: 420–425.

121. Jäger, E., Y. T. Chen, J. W. Drijfhout, J. Karbach, M. Ringhoffer, D. Jäger, M. Arand, H. Wada, Y. Noguchi, E. Stockert, L. J. Old, and a Knuth. 1998. Simultaneous humoral and cellular immune response against cancer-testis antigen NY-ESO-1: definition of human histocompatibility leukocyte antigen (HLA)-A2-binding peptide epitopes. *J. Exp. Med.* 187: 265–270.

122. Zeng, G., C. E. Touloukian, X. Wang, N. P. Restifo, S. A. Rosenberg, and R.-F. Wang. 2000. Identification of CD4+ T Cell Epitopes from NY-ESO-1 Presented by HLA-DR Molecules. *J. Immunol.* 165: 1153–1159.

123. Valmori, D., V. Dutoit, D. Liénard, D. Lie, D. Rimoldi, J. Pittet, P. Champagne, K. Ellefsen, U. Sahin, D. Speiser, F. Lejeune, J. Cerottini, and P. Romero. 2000. Naturally Occurring Human Lymphocyte Antigen-A2 Restricted CD8 + T-Cell Response to the Cancer Testis Antigen NY-ESO-1 in Melanoma Patients Naturally Occurring Human Lymphocyte Antigen-A2 Restricted CD8 T-Cell Response to the Cancer Testis Antigen NY-ES. 7: 4499–4506.

124. Robbins, P. F., R. A. Morgan, S. A. Feldman, J. C. Yang, R. M. Sherry, M. E. Dudley, J. R. Wunderlich, A. V. Nahvi, L. J. Helman, C. L. Mackall, U. S. Kammula, M. S. Hughes, N. P. Restifo, M. Raffeld, C. C. R. Lee, C. L. Levy, Y. F. Li, M. El-Gamil, S. L. Schwarz, C. Laurencot, and S. A. Rosenberg. 2011. Tumor regression in patients with metastatic synovial cell sarcoma and melanoma using genetically engineered lymphocytes reactive with NY-ESO-1. *J. Clin. Oncol.* 29: 917–924.

125. Robbins, P. F., S. H. Kassim, T. L. N. Tran, J. S. Crystal, R. A. Morgan, S. A. Feldman, J. C. Yang, M. E. Dudley, J. R. Wunderlich, R. M. Sherry, U. S. Kammula, M. S. Hughes, N. P. Restifo, M. Raffeld, C. C. R. Lee, Y. F. Li, M. El-Gamil, and S. A. Rosenberg. 2015. A pilot trial using lymphocytes genetically engineered with an NY-ESO-1-reactive T-cell receptor: Long-term follow-up and correlates with response. *Clin. Cancer Res.* 21: 1019–1027.

126. MacCarty, W. C. 1931. Principles of prognosis in cancer. *JAMA J. Am. Med. Assoc.* 96: 30.

127. Clark, W. H., D. E. Elder, D. Guerry, L. E. Braitman, B. J. Trock, D. Schultz, M. Synnestvedt, and A. C. Halpern. 1989. Model predicting survival in stage I melanoma based on tumor progression. *J. Natl. Cancer Inst.* 81: 1893–1904.

128. Ropponen, K. M., M. J. Eskelinen, P. K. Lipponen, E. Alhava, and V. M. Kosma. 1997. Prognostic value of tumour-infiltrating lymphocytes (TILs) in colorectal cancer. *J. Pathol.* 182: 318–324.

129. Schumacher, K., W. Haensch, C. Röefzaad, C. Ro, and P. M. Schlag. 2001. Prognostic Significance of Activated CD8 + T Cell Infiltrations within Esophageal Carcinomas Prognostic Significance of Activated CD8 ¾ T Cell Infiltrations within Esophageal Carcinomas. 3932–3936.

130. Zhang, L., J. R. Conejo-Garcia, D. Katsaros, P. A. Gimotty, M. Massobrio, G. Regnani, A. Makrigiannakis, H. Gray, K. Schlienger, M. N. Liebman, S. C. Rubin, and G. Coukos. 2003. Intratumoral T Cells, Recurrence, and Survival in Epithelial Ovarian Cancer. *N. Engl. J. Med.* 348: 203–213.

131. Marrogi, a J., a Munshi, a J. Merogi, Y. Ohadike, a El-Habashi, O. L. Marrogi, and S. M. Freeman. 1997. Study of tumor infiltrating lymphocytes and transforming growth factor-beta as prognostic factors in breast carcinoma. *Int. J. Cancer* 74: 492–501.

132. Kawai, O., G. Ishii, K. Kubota, Y. Murata, Y. Naito, T. Mizuno, K. Aokage, N. Saijo, Y. Nishiwaki, A. Gemma, S. Kudoh, and A. Ochia. 2008. Predominant infiltration of macrophages and CD8+ T cells in cancer nests is a significant predictor of survival in stage IV nonsmall cell lung cancer. *Cancer* 113: 1387–1395.

133. Shibuya, T. Y., S. Kim, T. Y. Shibuya, C. E. McLaren, K. T. Li, S. Kim, N. Nugyen, G. H. Yoo, W. Z. Wei, J. Ensley, W. Sakr, C. E. McLaren, W. Z. Wei, A. Rogowski, J. Ensley, and W. Sakr. 2002. Clinical significance of poor CD3 response in head and neck cancer. *Clin. Cancer Res.* 8: 745–751.

134. Vesalainen, S., P. Lipponen, M. Talja, and K. Syrjänen. 1994. Histological grade, perineural infiltration, tumour-infiltrating lymphocytes and apoptosis as determinants of long-term prognosis in prostatic adenocarcinoma. *Eur. J. Cancer* 30: 1797–1803.

135. Pagès, F., A. Berger, M. Camus, F. Sanchez-cabo, A. Costes, R. Molidor, B. Mlecnik, A. Kirilovsky, M. Nilsson, D. Damotte, T. Meatchi, P. Bruneval, P. Cugnenc, Z. Trajanoski, W.-H. Fridman, J. Galon, D. Ph, A. Costes, R. Molidor, D. Ph, B. Mlecnik, M. Sc, A. Kirilovsky, M. Sc, M. Nilsson, D. Damotte, D. Ph, T. Meatchi, P. Bruneval, D. Ph, P. Cugnenc, D. Ph, Z. Trajanoski, and D. Ph. 2008. Effector memory T cells, early metastasis, and survival in colorectal cancer. *N. Engl. J. Med.* 353: 2654–66.

136. Galon, J., A. Costes, F. Sanchez-Cabo, A. Kirilovsky, B. Mlecnik, C. Lagorce-Pagès, M. Tosolini, M. Camus, A. Berger, P. Wind, F. Zinzindohoué, P. Bruneval, P. H. Cugnenc, Z. Trajanoski, W. H. Fridman, and F. Pagès. 2006. Type, density, and location of immune cells within human colorectal tumors predict clinical outcome. *Science (80-.).* 313: 1960–1964.

137. Geng, Y., Y. Shao, W. He, W. Hu, Y. Xu, J. Chen, C. Wu, and J. Jiang. 2015. Prognostic role of tumor-infiltrating lymphocytes in lung cancer: A meta-analysis. *Cell. Physiol. Biochem.* 37: 1560–1571.

138. Curiel, T. J., G. Coukos, L. Zou, X. Alvarez, P. Cheng, P. Mottram, M. Evdemon-Hogan, J. R. Conejo-Garcia, L. Zhang, M. Burow, Y. Zhu, S. Wei, I. Kryczek, B. Daniel, A. Gordon, L. Myers, A. Lackner, M. L. Disis, K. L. Knutson, L. Chen, and W. Zou. 2004. Specific recruitment of regulatory T cells in ovarian carcinoma fosters immune privilege and predicts reduced survival. *Nat. Med.* 10: 942–949.

139. Steidl, C., T. Lee, S. P. Shah, P. Farinha, G. Han, T. Nayar, A. Delaney, S. J. Jones, J. Iqbal, D. D. Weisenburger, M. A. Bast, A. Rosenwald, H.-K. Muller-Hermelink, L. M. Rimsza, E. Campo, J. Delabie, R. M. Braziel, J. R. Cook, R. R. Tubbs, E. S. Jaffe, G. Lenz, J. M. Connors, L. M. Staudt, W. C. Chan, and R. D. Gascoyne. 2010. Tumor-associated macrophages and survival in classic Hodgkin's lymphoma. *N. Engl. J. Med.* 362: 875–85.

140. Wu, M. H., W. J. Lee, K. T. Hua, M. L. Kuo, and M. T. Lin. 2015. Macrophage infiltration induces gastric cancer invasiveness by activating the β-catenin pathway. *PLoS One* 10: 1–13.

141. Hiraoka, N., K. Onozato, T. Kosuge, and S. Hirohashi. 2006. Prevalence of FOXP3+ regulatory T cells increases during the progression of pancreatic ductal adenocarcinoma and its premalignant lesions. *Clin. Cancer Res.* 12: 5423–5434.

142. Fu, J., D. Xu, Z. Liu, M. Shi, P. Zhao, B. Fu, Z. Zhang, H. Yang, H. Zhang, C. Zhou, J. Yao, L. Jin, H. Wang, Y. Yang, Y.-X. Fu, and F.-S. Wang. 2007. Increased regulatory T cells correlate with CD8 T-cell impairment and poor survival in hepatocellular carcinoma patients. *Gastroenterology* 132: 2328–39.

143. Betts, G., E. Jones, S. Junaid, T. El-Shanawany, M. Scurr, P. Mizen, M. Kumar, S. Jones, B. Rees, G. Williams, A. Gallimore, and A. Godkin. 2012. Suppression of tumour-specific CD4 $^{+}$ T cells by regulatory T cells is associated with progression of human colorectal cancer. *Gut* 61: 1163–1171.

144. Carreras, J., A. López-Guillermo, B. C. Fox, L. Colomo, A. Martínez, G. Roncador, E. Montserrat, E. Campo, and A. H. Banham. 2006. High numbers of tumor-infiltrating FOXP3-positive regulatory T cells are associated with improved overall survival in follicular lymphoma. *Blood* 108: 2957–2964.

145. Salama, P., M. Phillips, F. Grieu, M. Morris, N. Zeps, D. Joseph, C. Platell, and B. Iacopetta. 2009. Tumor-infiltrating FOXP3+ T regulatory cells show strong prognostic significance in colorectal cancer. *J. Clin. Oncol.* 27: 186–92.

146. Tzankov, A., C. Meier, P. Hirschmann, P. Went, S. A. Pileri, and S. Dirnhofer. 2008. Correlation of high numbers of intratumoral FOXP3+ regulatory T cells with improved survival in germinal center-like diffuse large B-cell lymphoma, follicular lymphoma and classical Hodgkin's lymphoma. *Haematologica* 93: 193–200.

147. Frey, D. M., R. A. Droeser, C. T. Viehl, I. Zlobec, A. Lugli, U. Zingg, D. Oertli, C. Kettelhack, L. Terracciano, and L. Tornillo. 2010. High frequency of tumor-infiltrating FOXP3 $^{+}$ regulatory T cells predicts improved survival in mismatch repair-proficient colorectal cancer patients. *Int. J. Cancer* NA-NA.

148. Scurr, M., A. Gallimore, and A. Godkin. 2012. T cell subsets and colorectal cancer: Discerning the good from the bad. *Cell. Immunol.* 279: 21–24.

149. Redmond, W. L., and L. A. Sherman. 2005. Peripheral tolerance of CD8 T lymphocytes. *Immunity* 22: 275–284.

150. Liu, G. Y., P. J. Fairchild, R. M. Smith, J. R. Prowle, D. Kioussis, and D. C. Wraith. 1995. Low avidity recognition of self-antigen by T cells permits escape from central tolerance. *Immunity* 3: 407–415.

151. Cole, D. K., N. J. Pumphrey, J. M. Boulter, M. Sami, J. I. Bell, E. Gostick, D. A. Price, G. F. Gao, A. K. Sewell, and B. K. Jakobsen. 2007. Human TCR-Binding Affinity is Governed by MHC Class Restriction. *J. Immunol.* 178: 5727–5734.

152. Schmid, D. A., M. B. Irving, V. Posevitz, M. Hebeisen, A. Posevitz-Fejfar, J. C. F. Sarria, R. Gomez-Eerland, M. Thome, T. N. M. Schumacher, P. Romero, D. E. Speiser, V. Zoete, O. Michielin, and N. Rufer. 2010. Evidence for a TCR Affinity Threshold Delimiting Maximal CD8 T Cell Function. *J. Immunol.* 184: 4936–4946.

153. Baitsch, L., S. A. Fuertes-Marraco, A. Legat, C. Meyer, and D. E. Speiser. 2012. The three main stumbling blocks for anticancer T cells. *Trends Immunol.* 33: 364–372.

154. Ahmadzadeh, M., L. a Johnson, B. Heemskerk, J. R. Wunderlich, M. E. Dudley, D. E. White, S. a Rosenberg, and W. Dc. 2009. Tumor antigen − specific CD8 T cells infiltrating the tumor express high levels of PD-1 and are functionally impaired Tumor antigen – specific CD8 T cells infiltrating the tumor express high levels of PD-1 and are functionally impaired. *Blood* 114: 1537–1544.

155. Matsuzaki, J., S. Gnjatic, P. Mhawech-Fauceglia, A. Beck, A. Miller, T. Tsuji, C. Eppolito, F. Qian, S. Lele, P. Shrikant, L. J. Old, and K. Odunsi. 2010. Tumor-infiltrating NY-ESO-1–specific CD8 $^{+}$ T cells are negatively regulated by LAG-3 and PD-1 in human ovarian cancer. *Proc. Natl. Acad. Sci.* 107: 7875–7880.

156. Fourcade, J., Z. Sun, M. Benallaoua, P. Guillaume, I. F. Luescher, C. Sander, J. M. Kirkwood, V. Kuchroo, and H. M. Zarour. 2010. Upregulation of Tim-3 and PD-1 expression is associated with tumor antigen–specific CD8 $^{+}$ T cell dysfunction in melanoma patients. *J. Exp. Med.* 207: 2175–2186.

157. Riches, J. C., J. K. Davies, F. McClanahan, R. Fatah, S. Iqbal, S. Agrawal, A. G. Ramsay, and J. G. Gribben. 2013. T cells from CLLpatients exhibit features of T-cell exhaustion but retain capacity for cytokine production. *Blood* 121: 1612–1621.

158. Zippelius, A., P. Batard, V. Rubio-Godoy, G. Bioley, D. Liénard, F. Lejeune, D. Rimoldi, P. Guillaume, N. Meidenbauer, A. Mackensen, N. Rufer, N. Lubenow, D. Speiser, J. C. Cerottini, P. Romero, M. J. Pittet, D. Lie, F. Lejeune, D. Rimoldi, P. Guillaume, N. Meidenbauer, A. Mackensen, N. Rufer, N. Lubenow, D. Speiser, J. C. Cerottini, and P. Romero. 2004. Effector Function of Human Tumor-Specific CD8 T Cells in Melanoma Lesions : A State of Local Functional Tolerance Effector Function of Human Tumor-Specific CD8 T Cells in Melanoma Lesions : A State of Local Functional Tolerance. *Cancer Res.* 64: 2865–2873.

159. Baitsch, L., P. Baumgaertner, E. Devevre, S. K. Raghav, A. Legat, L. Barba, S. Wieckowski, H. Bouzourene, B. Deplancke, P. Romero, N. Rufer, and D. E. Speiser. 2011. Exhaustion of tumour-specific CD8+ T cells in metastases from melanoma patients. *J Clin Invest* 121: 2350–2360.

160. Coley, W. B. 1893. The treatment of malignant tumors by repeated inoculations of erysipelas. With a report of ten original cases. 1893. *Am. J. Med. Sci.* 487–511.

161. Rosenberg, S. A., B. S. Packard, P. M. Aebersold, D. Solomon, S. L. Topalian, S. T. Toy, P. Simon, M. T. Lotze, J. C. Yang, and C. A. Seipp. 1988. Use of tumor-infiltrating lymphocytes and interleukin-2 in the immunotherapy of patients with metastatic melanoma. A preliminary report. *N. Engl. J. Med.* 319: 1676–80.

162. Dudley, M. E., J. C. Yang, R. Sherry, M. S. Hughes, R. Royal, U. Kammula, P. F. Robbins, J. Huang, D. E. Citrin, S. F. Leitman, J. Wunderlich, N. P. Restifo, A. Thomasian, S. G. Downey, F. O. Smith, J. Klapper, K. Morton, C. Laurencot, D. E. White, and S. A. Rosenberg. 2008. Adoptive cell therapy for patients with metastatic melanoma: Evaluation of intensive myeloablative chemoradiation preparative regimens. *J. Clin. Oncol.* 26: 5233–5239.

163. Rosenberg, S. A., J. C. Yang, R. M. Sherry, U. S. Kammula, M. S. Hughes, G. Q. Phan, D. E. Citrin, N. P. Restifo, P. F. Robbins, J. R. Wunderlich, K. E. Morton, C. M. Laurencot, S. M. Steinberg, D. E. White, and M. E. Dudley. 2011. Durable complete responses in heavily pretreated patients with metastatic melanoma using T-cell transfer immunotherapy. *Clin. Cancer Res.* 17: 4550–4557.

164. Besser, M. J., R. Shapira-Frommer, O. Itzhaki, A. J. Treves, D. B. Zippel, D. Levy, A. Kubi, N. Shoshani, D. Zikich, Y. Ohayon, D. Ohayon, B. Shalmon, G. Markel, R. Yerushalmi, S. Apter, A. Ben-Nun, E. Ben-Ami, A. Shimoni, A. Nagler, and J. Schachter. 2013. Adoptive transfer of tumor-infiltrating lymphocytes in patients with metastatic melanoma: Intent-to-treat analysis and efficacy after failure to prior immunotherapies. *Clin. Cancer Res.* 19: 4792–4800.

165. Dudley, M. E. 2002. Cancer Regression and Autoimmunity in Patients After Clonal Repopulation with Antitumor Lymphocytes. *Science (80-.).* 298: 850–854.

166. Rosenberg, S. A. 2011. Cell transfer immunotherapy for metastatic solid cancer-what clinicians need to know. *Nat. Rev. Clin. Oncol.* 8: 577–585.

167. Robbins, P. F., M. E. Dudley, J. Wunderlich, M. El-Gamil, Y. F. Li, J. Zhou, J. Huang, D. J. Powell, and S. A. Rosenberg. 2004. Cutting edge: persistence of transferred lymphocyte clonotypes correlates with cancer regression in patients receiving cell transfer therapy. *J. Immunol.* 173: 7125–30.

168. Robbins, P. F., Y. F. Li, M. El-Gamil, Y. Zhao, J. A. Wargo, Z. Zheng, H. Xu, R. A. Morgan, S. A. Feldman, L. A. Johnson, A. D. Bennett, S. M. Dunn, T. M. Mahon, B. K. Jakobsen, and S. A. Rosenberg. 2008. Single and Dual Amino Acid Substitutions in TCR CDRs Can Enhance Antigen-Specific T Cell Functions. *J. Immunol.* 180: 6116–6131.

169. Liu, K., and S. a Rosenberg. 2001. Transduction of an IL-2 gene into human melanoma-reactive lymphocytes results in their continued growth in the absence of exogenous IL-2 and maintenance of specific antitumor activity. *J. Immunol.* 167: 6356–6365.

170. Hsu, C., S. A. Jones, C. J. Cohen, Z. Zheng, K. Kerstann, J. Zhou, P. F. Robbins, P. D. Peng, X. Shen, T. J. Gomes, C. E. Dunbar, D. J. Munroe, C. Stewart, K. Cornetta, D. Wangsa, T. Ried, S. A. Rosenberg, and R. A. Morgan. 2007. Cytokine-independent growth and clonal expansion of a primary human CD8+T-cell clone following retroviral transduction with the IL-15 gene. *Blood* 109: 5168–5177.

171. Charo, J., S. E. Finkelstein, N. Grewal, N. P. Restifo, P. F. Robbins, and S. A. Rosenberg. 2005. Bcl-2 overexpression enhances tumor-specific T-cell survival. *Cancer Res.* 65: 2001–2008.

172. Stephan, M. T., V. Ponomarev, R. J. Brentjens, A. H. Chang, K. V. Dobrenkov, G. Heller, and M. Sadelain. 2007. T cell-encoded CD80 and 4-1BBL induce auto- and transcostimulation, resulting in potent tumor rejection. *Nat. Med.* 13: 1440–1449.

173. Peng, W., Y. Ye, B. A. Rabinovich, C. Liu, Y. Lou, M. Zhang, M. Whittington, Y. Yang, W. W. Overwijk, G. Lizée, and P. Hwu. 2010. Transduction of tumor-specific T cells with CXCR2 chemokine receptor improves migration to tumor and antitumor immune responses. *Clin. Cancer Res.* 16: 5458–5468.

174. Zhou, J., X. Shen, J. Huang, R. J. Hodes, S. A. Rosenberg, and P. F. Robbins. 2005. Telomere Length of Transferred Lymphocytes Correlates with In Vivo Persistence and Tumor Regression in Melanoma Patients Receiving Cell Transfer Therapy. *J. Immunol.* 175: 7046–7052.

175. Parkhurst, M. R., J. C. Yang, R. C. Langan, M. E. Dudley, D. A. N. Nathan, S. A. Feldman, J. L. Davis, R. A. Morgan, M. J. Merino, R. M. Sherry, M. S. Hughes, U. S. Kammula, G. Q. Phan, R. M. Lim, S. A. Wank, N. P. Restifo, P. F. Robbins, C. M. Laurencot, and S. A. Rosenberg. 2011. T cells targeting carcinoembryonic antigen can mediate regression of metastatic colorectal cancer but induce severe transient colitis. *Mol. Ther.* 19: 620–626.

176. Johnson, L. a, R. a Morgan, M. E. Dudley, L. Cassard, J. C. Yang, M. S. Hughes, U. S. Kammula, R. E. Royal, R. M. Sherry, J. R. Wunderlich, C.-C. R. C. R. Lee, N. P. Restifo, S. L. Schwarz, A. P. Cogdill, R. J. Bishop, H. Kim, C. C. Brewer, S. F. Rudy, C. VanWaes, J. L. Davis, A. Mathur, R. T. Ripley, D. A. Nathan, C. M. Laurencot, and S. A. Rosenberg. 2009. Gene therapy with human and mouse T-cell receptors mediates cancer regression and targets normal tissues expressing cognate antigen. *Blood* 114: 535–546.

177. Gross, G., T. Waks, and Z. Eshhar. 1989. Expression of immunoglobulin-T-cell receptor chimeric molecules as functional receptors with antibody-type specificity. *Proc. Natl. Acad. Sci.* 86: 10024–10028.

178. Park, T. S., S. A. Rosenberg, and R. A. Morgan. 2011. Treating cancer with genetically engineered T cells. *Trends Biotechnol.* 29: 550–557.

179. Pule, M. A., B. Savoldo, G. D. Myers, C. Rossig, H. V. Russell, G. Dotti, M. H. Huls, E. Liu, A. P. Gee, Z. Mei, E. Yvon, H. L. Weiss, H. Liu, C. M. Rooney, H. E. Heslop, and M. K. Brenner. 2008. Virus-specific T cells engineered to coexpress tumor-specific receptors: Persistence and antitumor activity in individuals with neuroblastoma. *Nat. Med.* 14: 1264–1270.

180. Kochenderfer, J. N., W. H. Wilson, J. E. Janik, M. E. Dudley, S. a Feldman, I. Maric, M. Raffeld, D. N. Nathan, J. Brock, R. a Morgan, S. a Rosenberg, M. Stetler-stevenson, and B. J. Lanier. 2010. Eradication of B-lineage cells and regression of lymphoma in a patient treated with autologous T cells genetically engineered to recognize Brief report Eradication of B-lineage cells and regression of lymphoma in a patient treated with autologous T cells. 116: 4099–4102.

181. J.N., K., D. M.E., S.-S. M., W. W.H., J. J.E., N. D.-A.N., M. I., R. M., F. S.A., M. R.A., and R. S.A. 2010. A phase I clinical trial of treatment of B-cell malignancies with autologous anti-CD19-CAR-transduced T cells. *Blood* 116.

182. Lamers, C. H. J., R. Willemsen, P. Van Elzakker, S. Van Steenbergen-langeveld, M. Broertjes, J. Oosterwijk-wakka, E. Oosterwijk, S. Sleijfer, R. Debets, J. W. Gratama, and W. Dc. 2011. Immune responses to transgene and retroviral vector in patients treated with ex vivo − engineered T cells Immune responses to transgene and retroviral vector in patients treated with ex vivo – engineered T cells. *Blood* 117: 72–82.

183. Adams, G. P., and L. M. Weiner. 2005. Monoclonal antibody therapy of cancer. *Nat. Biotechnol.* 23: 1147–1157.

184. Hudis, C. A. 2007. Trastuzumab — Mechanism of Action and Use in Clinical Practice Clifford. *new Engl. J. o f Med.* 39–51.

185. Cunningham, D., Y. Humblet, S. Siena, D. Khayat, H. Bleiberg, A. Santoro, D. Bets, M. Mueser, A. Harstrick, C. Verslype, I. Chau, and E. Van Cutsem. 2004. Cetuximab Monotherapy and Cetuximab plus Irinotecan in Irinotecan-Refractory Metastatic Colorectal Cancer. *N. Engl. J. Med.* 351: 337–345.

186. Weiner, L. M., A. S. Belldegrun, J. Crawford, A. W. Tolcher, P. Lockbaum, R. H. Arends, L. Navale, R. G. Amado, G. Schwab, and R. A. Figlin. 2008. Dose and schedule study of panitumumab monotherapy in patients with advanced solid malignancies. *Clin. Cancer Res.* 14: 502–508.

187. Kindler, H. L., G. Friberg, D. A. Singh, G. Locker, S. Nattam, M. Kozloff, D. A. Taber, T. Karrison, A. Dachman, W. M. Stadler, and E. E. Vokes. 2005. Phase II trial of bevacizumab plus gemcitabine in patients with advanced pancreatic cancer. *J. Clin. Oncol.* 23: 8033–8040.

188. Bukowski, R. M., F. F. Kabbinavar, R. A. Figlin, K. Flaherty, S. Srinivas, U. Vaishampayan, H. A. Drabkin, J. Dutcher, S. Ryba, Q. Xia, F. A. Scappaticci, and D. McDermott. 2007. Randomized phase II study of erlotinib combined with bevacizumab compared with bevacizumab alone in metastatic renal cell cancer. *J. Clin. Oncol.* 25: 4536–4541.

189. Keating, M. J., I. Flinn, V. Jain, J.-L. Binet, P. Hillmen, J. Byrd, M. Albitar, L. Brettman, P. Santabarbara, B. Wacker, and K. R. Rai. 2002. Therapeutic role of alemtuzumab (Campath-1H) in patients who have failed udarabine: results of a large international study. *Blood* 99: 3554–3561.

190. Bross, P. F., J. Beitz, G. Chen, Xiao Hong Chen, E. Duffy, L. Kieffer, S. Roy, R. Sridhara, A. Rahman, G. Williams, and R. Pazdur. 2001. Approval summary: Gemtuzumab ozogamicin in relapsed acute myeloid leukemia. *Clin. Cancer Res.* 7: 1490–1496.

191. Coiffier, B., E. Lepage, J. Brière, R. Herbrecht, H. Tilly, R. Bouabdallah, P. Morel, E. Van Den Neste, G. Salles, P. Gaulard, F. Reyes, P. Lederlin, and C. Gisselbrecht. 2002. CHOP Chemotherapy plus Rituximab Compared with CHOP Alone in Elderly Patients with Diffuse Large-B-Cell Lymphoma. *N. Engl. J. Med.* 346: 235–242.

192. Witzig, T. E., L. I. Gordon, F. Cabanillas, M. S. Czuczman, C. Emmanouilides, R. Joyce, B. L. Pohlman, N. L. Bartlett, G. A. Wiseman, N. Padre, A. J. Grillo-López, P. Multani, and C. A. White. 2002. Randomized controlled trial of yttrium-90-labeled ibritumomab tiuxetan radioimmunotherapy versus rituximab immunotherapy for patients with relapsed or refractory low-grade, follicular, or transformed B-cell non-Hodgkin's lymphoma. *J. Clin. Oncol.* 20: 2453–2463.

193. Fisher, R. I., M. S. Kaminski, R. L. Wahl, S. J. Knox, A. D. Zelenetz, J. M. Vose, J. P. Leonard, S. Kroll, S. J. Goldsmith, and M. Coleman. 2005. Tositumomab and iodine-131 tositumomab produces durable complete remissions in a subset of heavily pretreated patients with low-grade and transformed non-Hodgkin's lymphomas. *J. Clin. Oncol.* 23: 7565–7573.

194. Cohen, M. H., J. Gootenberg, P. Keegan, and R. Pazdur. 2007. FDA Drug Approval Summary: Bevacizumab (Avastin(R)) Plus Carboplatin and Paclitaxel as First-Line Treatment of Advanced/Metastatic Recurrent Nonsquamous Non-Small Cell Lung Cancer. *Oncologist* 12: 713–718.

195. Cohen, M. H., J. Gootenberg, P. Keegan, and R. Pazdur. 2007. FDA Drug Approval Summary: Bevacizumab Plus FOLFOX4 as Second-Line Treatment of Colorectal Cancer. *Oncologist* 12: 356–361.

196. Miller, K. D., L. I. Chap, F. A. Holmes, M. A. Cobleigh, P. K. Marcom, L. Fehrenbacher, M. Dickler, B. A. Overmoyer, J. D. Reimann, A. P. Sing, V. Langmuir, and H. S. Rugo. 2005. Randomized phase III trial of capecitabine compared with bevacizumab plus capecitabine in patients with previously treated metastatic breast cancer. *J. Clin. Oncol.* 23: 792–799.

197. Chambers, C. A., M. S. Kuhns, J. G. Egen, and J. P. Allison. 2001. CTLA-4-mediated inhibition in regulation of T cell responses: mechanisms and manipulation in tumor immunotherapy. *Annu. Rev. Immunol.* 19: 565–94.

198. Hodi, F. S., S. J. O'Day, D. F. McDermott, R. W. Weber, J. A. Sosman, J. B. Haanen, R. Gonzalez, C. Robert, D. Schadendorf, J. C. Hassel, W. Akerley, A. J. M. van den Eertwegh, J. Lutzky, P. Lorigan, J. M. Vaubel, G. P. Linette, D. Hogg, C. H. Ottensmeier, C. Lebbé, C. Peschel, I. Quirt, J. I. Clark, J. D. Wolchok, J. S. Weber, J. Tian, M. J. Yellin, G. M. Nichol, A. Hoos, and W. J. Urba. 2010. Improved survival with ipilimumab in patients with metastatic melanoma. *N. Engl. J. Med.* 363: 711–23.

199. Robert, C., L. Thomas, I. Bondarenko, S. O'Day, J. Weber, C. Garbe, C. Lebbe, J.-F. Baurain, A. Testori, J.-J. Grob, N. Davidson, J. Richards, M. Maio, A. Hauschild, W. H. Miller, P. Gascon, M. Lotem, K. Harmankaya, R. Ibrahim, S. Francis, T.-T. Chen, R. Humphrey, A. Hoos, and J. D. Wolchok. 2011. Ipilimumab plus dacarbazine for previously untreated metastatic melanoma. *N. Engl. J. Med.* 364: 2517–26.

200. Ribas, A., and J. D. Wolchok. 2018. Cancer immunotherapy using checkpoint blockade. 1: 1350–1355.

201. Brahmer, J. R., C. G. Drake, I. Wollner, J. D. Powderly, J. Picus, W. H. Sharfman, E. Stankevich, A. Pons, T. M. Salay, T. L. McMiller, M. M. Gilson, C. Wang, M. Selby, J. M. Taube, R. Anders, L. Chen, A. J. Korman, D. M. Pardoll, I. Lowy, and S. L. Topalian. 2010. Phase I study of single-agent anti-programmed death-1 (MDX-1106) in refractory solid tumors: Safety, clinical activity, pharmacodynamics, and immunologic correlates. *J. Clin. Oncol.* 28: 3167–3175.

202. Robert, C., J. Schachter, G. V. Long, A. Arance, J. J. Grob, L. Mortier, A. Daud, M. S. Carlino, C. McNeil, M. Lotem, J. Larkin, P. Lorigan, B. Neyns, C. U. Blank, O. Hamid, C. Mateus, R. Shapira-Frommer, M. Kosh, H. Zhou, N. Ibrahim, S. Ebbinghaus, and A. Ribas. 2015. Pembrolizumab versus Ipilimumab in Advanced Melanoma. *N. Engl. J. Med.* 372: 2521–2532.

203. McLaughlin-Drubin, M. E., and K. Munger. 2008. Viruses associated with human cancer. *Biochim. Biophys. Acta - Mol. Basis Dis.* 1782: 127–150.

204. Chang, M. H., S. L. You, C. J. Chen, C. J. Liu, C. M. Lee, S. M. Lin, H. C. Chu, T. C. Wu, S. S. Yang, H. S. Kuo, and D. S. Chen. 2009. Decreased incidence of hepatocellular carcinoma in hepatitis B vaccinees: A 20-year follow-up study. *J. Natl. Cancer Inst.* 101: 1348–1355.

205. Dimberu, P. M., and R. M. Leonhardt. 2011. Cancer immunotherapy takes a multi-faceted approach to kick the immune system into gear. *Yale J. Biol. Med.* 84: 371–380.

206. Garland, S. M., M. Hernandez-Avila, C. M. Wheeler, G. Perez, D. M. Harper, S. Leodolter, G. W. K. Tang, D. G. Ferris, M. Steben, J. Bryan, F. J. Taddeo, R. Railkar, M. T. Esser, H. L. Sings, M. Nelson, J. Boslego, C. Sattler, E. Barr, L. a Koutsky, and Females United to Unilaterally Reduce Endo/Ectocervical Disease (FUTURE) I Investigators. 2007. Quadrivalent vaccine against human papillomavirus to prevent anogenital diseases. *N. Engl. J. Med.* 356: 1928–43.

207. FUTURE II Study Group. 2007. Quadrivalent Vaccine against Human Papillomavirus to Prevent High-Grade Cervical Lesions. *N. Engl. J. Med.* 356: 1915–1927.

208. Slingluff, C. L., G. R. Petroni, K. A. Chianese-Bullock, M. E. Smolkin, M. I. Ross, N. B. Haas, M. Von Mehren, and W. W. Grosh. 2011. Randomized multicenter trial of the effects of melanoma-associated helper peptides and cyclophosphamide on the immunogenicity of a multipeptide melanoma vaccine. *J. Clin. Oncol.* 29: 2924–2932.

209. Walter, S., T. Weinschenk, A. Stenzl, R. Zdrojowy, A. Pluzanska, C. Szczylik, M. Staehler, W. Brugger, P. Y. Dietrich, R. Mendrzyk, N. Hilf, O. Schoor, J. Fritsche, A. Mahr, D. Maurer, V. Vass, C. Trautwein, P. Lewandrowski, C. Flohr, H. Pohla, J. J. Stanczak, V. Bronte, S. Mandruzzato, T. Biedermann, G. Pawelec, E. Derhovanessian, H. Yamagishi, T. Miki, F. Hongo, N. Takaha, K. Hirakawa, H. Tanaka, S. Stevanovic, J. Frisch, A. Mayer-Mokler, A. Kirner, H. G. Rammensee, C. Reinhardt, and H. Singh-Jasuja. 2012. Multipeptide immune response to cancer vaccine IMA901 after single-dose cyclophosphamide associates with longer patient survival. *Nat. Med.* 18: 1254–1261.

210. Disis, M. L., J. R. Gralow, H. Bernhard, S. L. Hand, W. D. Rubin, and M. A. Cheever. 1996. Peptide-based, but not whole protein, vaccines elicit immunity to HER-2/neu, oncogenic self-protein. *J. Immunol.* 156: 3151–8.

211. Zwaveling, S., S. C. F. Mota, J. Nouta, M. Johnson, G. B. Lipford, R. Offringa, S. H. van der Burg, and C. J. M. Melief. 2002. Established Human Papillomavirus Type 16-Expressing Tumors Are Effectively Eradicated Following Vaccination with Long Peptides. *J. Immunol.* 169: 350–358.

212. Li, M., H. Shi, Y. Mu, Z. Luo, H. Zhang, Y. Wan, D. Zhang, L. Lu, K. Men, Y. Tian, X. Wu, X. Liu, Y. Pan, Y. Fan, C. Yu, B. Zhou, R. Xiang, X. Chen, and L. Yang. 2014. Effective inhibition of melanoma tumorigenesis and growth via a new complex vaccine based on NY-ESO-1-alum-polysaccharide-HH2. *Mol. Cancer* 13: 179.

213. Butts, C., M. A. Socinski, P. L. Mitchell, N. Thatcher, L. Havel, M. Krzakowski, S. Nawrocki, T. E. Ciuleanu, L. Bosquée, J. M. Trigo, A. Spira, L. Tremblay, J. Nyman, R. Ramlau, G. Wickart-Johansson, P. Ellis, O. Gladkov, J. R. Pereira, W. E. E. Eberhardt, C. Helwig, A. Schröder, and F. A. Shepherd. 2014. Tecemotide (L-BLP25) versus placebo after chemoradiotherapy for stage III non-small-cell lung cancer (START): A randomised, double-blind, phase 3 trial. *Lancet Oncol.* 15: 59–68.

214. Rini, B. I., A. Stenzl, R. Zdrojowy, M. Kogan, M. Shkolnik, S. Oudard, S. Weikert, S. Bracarda, S. J. Crabb, J. Bedke, J. Ludwig, D. Maurer, R. Mendrzyk, C. Wagner, A. Mahr, J. Fritsche, T. Weinschenk, S. Walter, A. Kirner, H. Singh-Jasuja, C. Reinhardt, and T. Eisen. 2016. IMA901, a multipeptide cancer vaccine, plus sunitinib versus sunitinib alone, as first-line therapy for advanced or metastatic renal cell carcinoma (IMPRINT): a multicentre, open-label, randomised, controlled, phase 3 trial. *Lancet Oncol.* 17: 1599–1611.

215. Suzuki, N., S. Hazama, H. Iguchi, K. Uesugi, H. Tanaka, K. Hirakawa, A. Aruga, T. Hatori, H. Ishizaki, Y. Umeda, T. Fujiwara, T. Ikemoto, M. Shimada, K. Yoshimatsu, R. Shimizu, H. Hayashi, K. Sakata, H. Takenouchi, H. Matsui, Y. Shindo, M. Iida, Y. Koki, H. Arima, H. Furukawa, T. Ueno, S. Yoshino, Y. Nakamura, M. Oka, and H. Nagano. 2017. Phase II clinical trial of peptide cocktail therapy for patients with advanced pancreatic cancer: VENUS-PC study. *Cancer Sci.* 108: 73–80.

216. Melief, C. J. M., and S. H. Van Der Burg. 2008. Immunotherapy of established (pre)malignant disease by synthetic long peptide vaccines. *Nat. Rev. Cancer* 8: 351–360.

217. Berzofsky, J. A., J. D. Ahlers, and I. M. Belyakov. 2001. Strategies for Designing and Optimizing New Generation Vaccines. *Nat. Rev. Immunol.* 1: 209–219.

218. Rosenberg, S. A., J. C. Yang, D. J. Schwartzentruber, P. Hwu, F. M. Marincola, S. L. Topalian, N. P. Restifo, M. E. Dudley, S. L. Schwarz, P. J. Spiess, J. R. Wunderlich, M. R. Parkhurst, Y. Kawakami, C. A. Seipp, J. H. Einhorn, and D. E. White. 1998. Immunologic and therapeutic evaluation of a synthetic peptide vaccine for the treatment of patients with metastatic melanoma. *Nat. Med.* 4: 321–7.

219. Rivoltini, L., P. Squarcina, D. J. Loftus, C. Castelli, P. Tarsini, A. Mazzocchi, F. Rini, V. Viggiano, F. Belli, and G. Parmiani. 1999. A superagonist variant of peptide MART1/Melan A27-35 elicits anti-melanoma CD8+ T cells with enhanced functional characteristics: implication for more effective immunotherapy. *Cancer Res.* 59: 301–6.

220. Brinckerhoff, L. H., V. V Kalashnikov, L. W. Thompson, G. V Yamshchikov, R. A. Pierce, H. S. Galavotti, V. H. Engelhard, and C. L. Slingluff. 1999. Terminal modifications inhibit proteolytic degradation of an immunogenic MART-1(27-35) peptide: implications for peptide vaccines. *Int. J. cancer* 83: 326–34.

221. Arens, R., T. van Hall, S. H. van der Burg, F. Ossendorp, and C. J. M. Melief. 2013. Prospects of combinatorial synthetic peptide vaccine-based immunotherapy against cancer. *Semin. Immunol.* 25: 182–190.

222. Krieg, A. M., A. K. Yi, J. Schorr, and H. L. Davis. 1998. The role of CpG dinucleotides in DNA vaccines. *Trends Microbiol.* 6: 23–27.

223. Hemmi, H., O. Takeuchi, T. Kawai, T. Kaisho, S. Sato, H. Sanjo, M. Matsumoto, K. Hoshino, H. Wagner, K. Takeda, and S. Akira. 2000. A Toll-like receptor recognizes bacterial DNA.[In Process Citation]. *Nature* 408: 740–745.

224. Conry, R. M., A. F. LoBuglio, J. Kantor, J. Schlom, F. Loechel, S. E. Moore, L. A. Sumerel, D. L. Barlow, S. Abrams, and D. T. Curiel. 1994. Immune response to a carcinoembryonic antigen polynucleotide vaccine. *Cancer Res.* 54: 1164–8.

225. Syrengelas, A. D., T. T. Chen, and R. Levy. 1996. DNA immunization induces protective immunity against B-cell lymphoma. *Nat. Med.* 2: 1038–41.

226. Biragyn, A., K. Tani, M. C. Grimm, S. Weeks, and L. W. Kwak. 1999. Genetic fusion of chemokines to a self tumor antigen induces protective, T-cell dependent antitumor immunity. *Nat. Biotechnol.* 17: 253–258.

227. Timmerman, J. M., G. Singh, G. Hermanson, P. Hobart, D. K. Czerwinski, B. Taidi, R. Rajapaksa, C. B. Caspar, A. Van Beckhoven, and R. Levy. 2002. Immunogenicity of a Plasmid DNA Vaccine Encoding Chimeric Idiotype in Patients with B-Cell Lymphoma 1. 5845–5852.

228. Conry, R. M., D. T. Curiel, T. V Strong, S. E. Moore, K. O. Allen, D. L. Barlow, D. R. Shaw, and A. F. LoBuglio. 2002. Safety and immunogenicity of a DNA vaccine encoding carcinoembryonic antigen and hepatitis B surface antigen in colorectal carcinoma patients. *Clin.Cancer Res.* 8: 2782–2787.

229. Rosenberg, S. A., J. C. Yang, R. M. Sherry, P. Hwu, S. L. Topalian, D. J. Schwartzentruber, N. P. Restifo, L. R. Haworth, C. A. Seipp, L. J. Freezer, K. E. Morton,

S. A. Mavroukakis, and D. E. White. 2003. Inability to Immunize Patients with Metastatic Melanoma Using Plasmid DNA Encoding the gp100 Melanoma-Melanocyte Antigen. *Hum. Gene Ther.* 14: 709–714.

230. Mincheff, M., S. Tchakarov, S. Zoubak, D. Loukinov, C. Botev, I. Altankova, G. Georgiev, S. Petrov, and H. T. Meryman. 2000. Naked DNA and adenoviral immunizations for immunotherapy of prostate cancer: a phase I/II clinical trial. *Eur. Urol.* 38: 208–17.

231. Nestle, F. O., S. Alijagic, M. Gilliet, Y. Sun, S. Grabbe, R. Dummer, G. Burg, and D. Schadendorf. 1998. Vaccination of melanoma patients with peptide- or tumor lysate-pulsed dendritic cells. *Nat. Med.* 4: 328–332.

232. Hsu, F. J., F. Fagnoni, C. BENIKE, T. M. Liles, D. Czerwinski, B. Taidi, E. G. Engleman, and R. Levy. 1996. Vaccination of patients with B-cell lymphoma using autologous antigen-pulsed dendritic cells. *Nat. Med.* 2: 52–58.

233. Van Tendeloo, V. F., A. Van de Velde, A. Van Driessche, N. Cools, S. Anguille, K. Ladell, E. Gostick, K. Vermeulen, K. Pieters, G. Nijs, B. Stein, E. L. Smits, W. A. Schroyens, A. P. Gadisseur, I. Vrelust, P. G. Jorens, H. Goossens, I. J. de Vries, D. A. Price, Y. Oji, Y. Oka, H. Sugiyama, and Z. N. Berneman. 2010. Induction of complete and molecular remissions in acute myeloid leukemia by Wilms' tumor 1 antigen-targeted dendritic cell vaccination. *Proc. Natl. Acad. Sci.* 107: 13824–13829.

234. Wierecky, J., M. R. Müller, S. Wirths, E. Halder-Oehler, D. Dörfel, S. M. Schmidt, M. Häntschel, W. Brugger, S. Schröder, M. S. Horger, L. Kanz, and P. Brossart. 2006. Immunologic and clinical responses after vaccinations with peptide-pulsed dendritic cells in metastatic renal cancer patients. *Cancer Res.* 66: 5910–5918.

235. Small, E. J., P. F. Schellhammer, C. S. Higano, C. H. Redfern, J. J. Nemunaitis, F. H. Valone, S. S. Verjee, L. A. Jones, and R. M. Hershberg. 2006. Placebo-controlled phase III trial of immunologic therapy with Sipuleucel-T (APC8015) in patients with metastatic, asymptomatic hormone refractory prostate cancer. *J. Clin. Oncol.* 24: 3089–3094.

236. Kantoff, P. W., C. S. Higano, N. D. Shore, E. R. Berger, E. J. Small, D. F. Penson, C. H. Redfern, A. C. Ferrari, R. Dreicer, R. B. Sims, Y. Xu, M. W. Frohlich, P. F. Schellhammer, and IMPACT Study Investigators. 2010. Sipuleucel-T immunotherapy for castration-resistant prostate cancer. *N. Engl. J. Med.* 363: 411–22.

237. Banchereau, J., and A. K. Palucka. 2005. Dendritic cells as therapeutic vaccines against cancer. *Nat. Rev. Immunol.* 5: 296–306.

238. Palucka, K., and J. Banchereau. 2013. Dendritic-Cell-Based Therapeutic Cancer Vaccines. *Immunity* 39: 38–48.

239. Sancho, D., D. Mourão-Sá, O. P. Joffre, O. Schulz, N. C. Rogers, D. J. Pennington, J. R. Carlyle, and C. Reis e Sousa. 2008. Tumor therapy in mice via antigen targeting to a novel, DC-restricted C-type lectin. *J. Clin. Invest.* 118: 2098–110.

240. Wei, H., S. Wang, D. Zhang, S. Hou, W. Qian, B. Li, H. Guo, G. Kou, J. He, H. Wang, and Y. Guo. 2009. Targeted delivery of tumor antigens to activated dendritic cells via CD11c molecules induces potent antitumor immunity in mice. *Clin. Cancer Res.* 15: 4612–4621.

241. Wang, B., N. Zaidi, L. He, L. Zhang, J. M. Y. Kuroiwa, T. Keler, and R. M. Steinman. 2012. Targeting of the non-mutated tumor antigen HER2 / neu to mature dendritic cells induces an integrated immune response that protects against breast cancer in mice. *Breast Cancer Res.* 14: R39.

242. Neubert, K., C. H. K. Lehmann, L. Heger, A. Baranska, A. M. Staedtler, V. R. Buchholz, S. Yamazaki, G. F. Heidkamp, N. Eissing, H. Zebroski, M. C. Nussenzweig, F. Nimmerjahn, and D. Dudziak. 2014. Antigen Delivery to CD11c+CD8- Dendritic Cells Induces Protective Immune Responses against Experimental Melanoma in Mice In Vivo. *J. Immunol.* 192: 5830–5838.

243. Moss, B., G. L. Smith, J. L. Gerin, and R. H. Purcell. 1984. Live recombinant vaccinia virus protects chimpanzees against hepatitis B. *Nature* 311: 67–69.

244. Humphreys, I. R., and S. Sebastian. 2017. Novel viral vectors in infectious diseases. *Immunology* 1–9.

245. Liu, M. A. 2010. Immunologic basis of vaccine vectors. *Immunity* 33: 504–515.

246. Dudek, T., and D. M. Knipe. 2006. Replication-defective viruses as vaccines and vaccine vectors. *Virology* 344: 230–239.

247. Uusi-Kerttula, H., S. Hulin-Curtis, J. Davies, and A. L. Parker. 2015. Oncolytic adenovirus: Strategies and insights for vector design and immuno-oncolytic applications. *Viruses* 7: 5987–6020.

248. Tatsis, N., and H. C. J. Ertl. 2004. Adenoviruses as vaccine vectors. *Mol. Ther.* 10: 616–629.

249. Rosenberg, S. A., Y. Zhai, J. C. Yang, D. J. Schwartzentruber, P. Hwu, F. M. Marincola, S. L. Topalian, N. P. Restifo, C. A. Seipp, J. H. Einhorn, B. Roberts, and D. E. White. 1998. Immunizing patients with metastatic melanoma using recombinant adenoviruses encoding MART-1 or gp100 melanoma antigens. *J. Natl. Cancer Inst.* 90: 1894–900.

250. Lubaroff, D. M., B. R. Konety, B. Link, J. Gerstbrein, T. Madsen, M. Shannon, J. Howard, J. Paisley, D. Boeglin, T. L. Ratliff, and R. D. Williams. 2009. Phase I clinical trial of an adenovirus/prostate-specific antigen vaccine for prostate cancer: Safety and immunologic results. *Clin. Cancer Res.* 15: 7375–7380.

251. Überla, K. 2008. HIV vaccine development in the aftermath of the STEP study: Re-focus on occult hiv infection? *PLoS Pathog.* 4: 4–6.

252. Harrop, R., and M. W. Carroll. 2006. Viral vectors for cancer immunotherapy. *Front Biosci* 11: 804.

253. Conry, R. M., M. B. Khazaeli, M. N. Saleh, K. O. Allen, D. L. Barlow, S. E. Moore, D. Craig, R. B. Arani, J. Schlom, and A. F. LoBuglio. 1999. Phase I trial of a recombinant vaccinia virus encoding carcinoembryonic antigen in metastatic adenocarcinoma: Comparison of intradermal versus subcutaneous administration. *Clin. Cancer Res.* 5: 2330–2337.

254. Sanda, M. G., D. C. Smith, L. G. Charles, C. Hwang, K. J. Pienta, J. Schlom, D. Milenic, D. Panicali, and J. E. Montie. 1999. Recombinant vaccinia-PSA (PROSTVAC) can induce a prostate-specific immune response in androgen-modulated human prostate cancer. *Urology* 53: 260–266.

255. Eder, J. P., P. W. Kantoff, K. Roper, G. X. Xu, G. J. Bubley, J. Boyden, L. Gritz, G. Mazzara, W. K. Oh, P. Arlen, K. Y. Tsang, D. Panicali, J. Schlom, and D. W. Kufe. 2000. A phase I trial of a recombinant vaccinia virus expressing prostate-specific antigen in advanced prostate cancer. *Clin. Cancer Res.* 6: 1632–8.

256. Gulley, J., A. P. Chen, W. Dahut, P. M. Arlen, A. Bastian, S. M. Steinberg, K. Tsang, D. Panicali, D. Poole, J. Schlom, and J. M. Hamilton. 2002. Phase I study of a vaccine using recombinant vaccinia virus expressing PSA (rV-PSA) in patients with metastatic androgen-independent prostate cancer. *Prostate* 53: 109–117.

257. Jager, E., J. Karbach, S. Gnjatic, A. Neumann, A. Bender, D. Valmori, M. Ayyoub, E. Ritter, G. Ritter, D. Jager, D. Panicali, E. Hoffman, L. Pan, H. Oettgen, L. J. Old, and A. Knuth. 2006. Recombinant vaccinia/fowlpox NY-ESO-1 vaccines induce both humoral and cellular NY-ESO-1-specific immune responses in cancer patients. *Proc. Natl. Acad. Sci.* 103: 14453–14458.

258. Rosenberg, S. A., J. C. Yang, D. J. Schwartzentruber, P. Hwu, S. L. Topalian, R. M. Sherry, N. P. Restifo, J. R. Wunderlich, C. A. Seipp, L. Rogers-Freezer, K. E. Morton, S. A. Mavroukakis, L. Gritz, D. L. Panicali, and D. E. White. 2003. Recombinant fowlpox viruses encoding the anchor-modified gp100 melanoma antigen can generate antitumor immune responses in patients with metastatic melanoma. *Clin. Cancer Res.* 9: 2973–2980.

259. von Mehren, M., P. Arlen, K. Y. Tsang, A. Rogatko, N. Meropol, H. S. Cooper, M. Davey, S. McLaughlin, J. Schlom, and L. M. Weiner. 2000. Pilot study of a dual gene recombinant avipox vaccine containing both carcinoembryonic antigen (CEA) and B7.1 transgenes in patients with recurrent CEA-expressing adenocarcinomas. *Clin. Cancer Res.* 6: 2219–28.

260. von Mehren, M., P. Arlen, J. Gulley, A. Rogatko, H. S. Cooper, N. J. Meropol, R. K. Alpaugh, M. Davey, S. McLaughlin, M. T. Beard, K. Y. Tsang, J. Schlom, and L. M. Weiner. 2001. The influence of granulocyte macrophage colony-stimulating factor and prior chemotherapy on the immunological response to a vaccine (ALVAC-CEA B7.1) in patients with metastatic carcinoma. *Clin. Cancer Res.* 7: 1181–91.

261. Sutter, G., and C. Staib. 2003. Vaccinia Vectors as Candidate Vaccines: The Development of Modified Vaccinia Virus Ankara for Antigen Delivery. *Curr. Drug Target -Infectious Disord.* 3: 263–271.

262. Pastoret, P. P., and A. Vanderplasschen. 2003. Poxviruses as vaccine vectors. *Comp. Immunol. Microbiol. Infect. Dis.* 26: 343–355.

263. Harrop, R. 2006. Vaccination of Colorectal Cancer Patients with Modified Vaccinia Ankara Delivering the Tumor Antigen 5T4 (TroVax) Induces Immune Responses which Correlate with Disease Control: A Phase I/II Trial. *Clin. Cancer Res.* 12: 3416–3424.

264. Elkord, E., A. Dangoor, N. L. Drury, R. Harrop, D. J. Burt, J. W. Drijfhout, C. Hamer, D. Andrews, S. Naylor, D. Sherlock, R. E. Hawkins, and P. L. Stern. 2008. An MVA-based Vaccine Targeting the Oncofetal Antigen 5T4 in Patients Undergoing Surgical Resection of Colorectal Cancer Liver Metastases. *J. Immunother.* 31: 820–829.

265. Amato, R. J., N. Drury, S. Naylor, J. Jac, S. Saxena, A. Cao, J. Hernandez-McClain, and R. Harrop. 2008. Vaccination of Prostate Cancer Patients With Modified Vaccinia Ankara Delivering the Tumor Antigen 5T4 (TroVax). *J. Immunother.* 31: 577–585.

266. Amato, R. J., W. Shingler, S. Naylor, J. Jac, J. Willis, S. Saxena, J. Hernandez-McClain, and R. Harrop. 2008. Vaccination of Renal Cell Cancer Patients with Modified Vaccinia Ankara Delivering Tumor Antigen 5T4 (TroVax) Administered with Interleukin 2: A Phase II Trial. *Clin. Cancer Res.* 14: 7504–7510.

267. Amato, R. J., W. Shingler, M. Goonewardena, J. de Belin, S. Naylor, J. Jac, J. Willis, S. Saxena, J. Hernandez-McClain, and R. Harrop. 2009. Vaccination of Renal Cell Cancer Patients With Modified Vaccinia Ankara Delivering the Tumor Antigen 5T4 (TroVax) Alone or Administered in Combination With Interferon-α (IFN-α). *J. Immunother.* 32: 765–772.

268. Kaufman, H. L., B. Taback, W. Sherman, D. Kim, W. H. Shingler, D. Moroziewicz, G. DeRaffele, J. Mitcham, M. W. Carroll, R. Harrop, S. Naylor, and S. Kim-Schulze. 2009. Phase II trial of Modified Vaccinia Ankara (MVA) virus expressing 5T4 and high dose Interleukin-2 (IL-2) in patients with metastatic renal cell carcinoma. *J. Transl. Med.* 7: 2.

269. Kantoff, P. W., T. J. Schuetz, B. A. Blumenstein, L. Michael Glode, D. L. Bilhartz, M. Wyand, K. Manson, D. L. Panicali, R. Laus, J. Schlom, W. L. Dahut, P. M. Arlen, J. L. Gulley, and W. R. Godfrey. 2010. Overall survival analysis of a phase II randomized controlled trial of a poxviral-based PSA-targeted immunotherapy in metastatic castration-resistant prostate cancer. *J. Clin. Oncol.* 28: 1099–1105.

270. McGeoch, D. J., F. J. Rixon, and A. J. Davison. 2006. Topics in herpesvirus genomics and evolution. *Virus Res.* 117: 90–104.

271. Davison, A. J., R. Eberle, B. Ehlers, G. S. Hayward, D. J. McGeoch, A. C. Minson, P. E. Pellett, B. Roizman, M. J. Studdert, and E. Thiry. 2009. The order Herpesvirales. *Arch. Virol.* 154: 171–177.

272. Weir, J. P. 1998. Genomic organization and evolution of the human herpesviruses. *Virus Genes* 16: 85–93.

273. Mocarski, E. S., T. Shenk, and R. F. Pass. 2013. Cytomegalovirus. In *Fields Virology* 1960–2014.

274. Lilja, A. E., and T. Shenk. 2008. Efficient replication of rhesus cytomegalovirus variants in multiple rhesus and human cell types. *Proc. Natl. Acad. Sci. U. S. A.* 105: 19950–5.

275. Jurak, I., and W. Brune. 2006. Induction of apoptosis limits cytomegalovirus cross-species infection. *EMBO J.* 25: 2634–2642.

276. Tang, Q., and G. G. Maul. 2006. Mouse Cytomegalovirus Crosses the Species Barrier with Help from a Few Human Cytomegalovirus Proteins. *J. Virol.* 80: 7510–7521.

277. Dolan, A., C. Cunningham, R. D. Hector, A. F. Hassan-Walker, L. Lee, C. Addison, D. J. Dargan, D. J. McGeoch, D. Gatherer, V. C. Emery, P. D. Griffiths, C. Sinzger, B. P. McSharry, G. W. G. Wilkinson, and A. J. Davison. 2004. Genetic content of wild-type human cytomegalovirus. *J. Gen. Virol.* 85: 1301–1312.

278. Dölken, L., S. Pfeffer, and U. H. Koszinowski. 2009. Cytomegalovirus microRNAs. *Virus Genes* 38: 355–64.

279. Roizman, B. 1980. Genome variation and evolution among herpes viruses. *Ann. N. Y. Acad. Sci.* 354: 472–83.

280. Spaete, R. R., and E. S. Mocarski. 1985. The alpha sequence of the cytomegalovirus genome functions as a cleavage/packaging signal for herpes simplex virus defective genomes. *J. Virol.* 54: 817–824.

281. Kemble, G. W., and E. S. Mocarski. 1989. A host cell protein binds to a highly conserved sequence element (pac-2) within the cytomegalovirus a sequence. *J. Virol.* 63: 4715–4728.

282. Weststrate, M. W., J. L. Geelen, and J. van der Noordaa. 1980. Human cytomegalovirus DNA: physical maps for restriction endonucleases BglII, hindIII and XbaI. *J. Gen. Virol.* 49: 1–21.

283. Sinzger, C., A. Grefte, B. Plachter, A. S. H. Gouw, T. H. The, and G. Jahn. 1995. Fibroblasts, epithelial cells, endothelial cells and smooth muscle cells are major targets of human cytomegalovirus infection in lung and gastrointestinal tissues. *J. Gen. Virol.* 76: 741–750.

284. Sinzger, C., a L. Bissinger, R. Viebahn, H. Oettle, C. Radke, C. a Schmidt, and G. Jahn. 1999. Hepatocytes are permissive for human cytomegalovirus infection in human liver cell culture and In vivo. *J. Infect. Dis.* 180: 976–986.

285. Bissinger, A. L., C. Sinzger, E. Kaiserling, and G. Jahn. 2002. Human cytomegalovirus as a direct pathogen: Correlation of multiorgan involvement and cell distribution with clinical and pathological findings in a case of congenital inclusion disease. *J. Med. Virol.* 67: 200–206.

286. Ibanez, C. E., R. Schrier, P. Ghazal, C. Wiley, and J. A. Nelson '. 1991. Human Cytomegalovirus Productively Infects Primary Differentiated Macrophages. *J. Virol.* 65: 6581–6588.

287. Riegler, S., H. Hebart, H. Einsele, P. Brossart, G. Jahn, and C. Sinzger. 2000. Monocyte-derived dendritic cells are permissive to the complete replicative cycle of human cytomegalovirus. *J. Gen. Virol.* 81: 393–399.

288. Rice, G. P. A., R. D. Schrier, and M. B. A. Oldstone. 1984. Cytomegalovirus infects human lymphocytes and monocytes: Virus expression is restricted to immediate-early gene products (abortive infection). *Immunology* 81: 6134–6138.

289. Kondo, K., H. Kaneshima, and E. S. Mocarski. 1994. Human cytomegalovirus latent infection of granulocyte-macrophage progenitors. *Proc. Natl. Acad. Sci.* 91: 11879–11883.

290. Minton, E. J., C. Tysoe, J. H. Sinclair, and J. G. Sissons. 1994. Human cytomegalovirus infection of the monocyte/macrophage lineage in bone marrow. *J. Virol.* 68: 4017–21.

291. Mendelson, M., S. Monard, P. Sissons, and J. Sinclair. 1996. Detection of endogenous human cytomegalovirus in CD34+bone marrow progenitors. *J. Gen. Virol.* 77: 3099–3102.

292. Hahn, G., R. Jores, and E. S. Mocarski. 1998. Cytomegalovirus remains latent in a common precursor of dendritic and myeloid cells. *Proc. Natl. Acad. Sci.* 95: 3937–3942.

293. Taylor-Wiedeman, J., P. Sissons, and J. Sinclair. 1994. Induction of Endogenous Human Cytomegalovirus Gene Expression after Differentiation of Monocytes from Healthy Carriers. *J. Virol.* 68: 1597–1604.

294. Reeves, M. B., and J. H. Sinclair. 2013. Circulating Dendritic Cells Isolated from Healthy Seropositive Donors Are Sites of Human Cytomegalovirus Reactivation In Vivo. *J. Virol.* 87: 10660–10667.

295. Dargan, D. J., E. Douglas, C. Cunningham, F. Jamieson, R. J. Stanton, K. Baluchova, B. P. McSharry, P. Tomasec, V. C. Emery, E. Percivalle, A. Sarasini, G. Gerna, G. W. G. Wilkinson, and A. J. Davison. 2010. Sequential mutations associated with adaptation of human cytomegalovirus to growth in cell culture. *J. Gen. Virol.* 91: 1535–1546.

296. Sinzger, C., K. Schmidt, J. Knapp, M. Kahl, R. Beck, J. Waldman, H. Hebart, H. Einsele, and G. Jahn. 1999. Modification of human cytomegalovirus tropism through propagation in vitro is associated with changes in the viral genome. *J. Gen. Virol.* 80: 2867–2877.

297. Grazia Revello, M., F. Baldanti, E. Percivalle, A. Sarasini, L. De-Giuli, E. Genini, D. Lilleri, N. Labò, and G. Gerna. 2001. In vitro selection of human cytomegalovirus variants unable to transfer virus and virus products from infected cells to polymorphonuclear leukocytes and to grow in endothelial cells. *J. Gen. Virol.* 82: 1429–1438.

298. Cha, T. a, E. Tom, G. W. Kemble, G. M. Duke, E. S. Mocarski, and R. R. Spaete. 1996. Human cytomegalovirus clinical isolates carry at least 19 genes not found in laboratory strains. *J. Virol.* 70: 78–83.

299. Murphy, E., D. Yu, J. Grimwood, J. Schmutz, M. Dickson, M. A. Jarvis, G. Hahn, J. A. Nelson, R. M. Myers, and T. E. Shenk. 2003. Coding potential of laboratory and clinical strains of human cytomegalovirus. *Proc. Natl. Acad. Sci.* 100: 14976–14981.

300. Cunningham, C., D. Gatherer, B. Hilfrich, K. Baluchova, D. J. Dargan, M. Thomson, P. D. Griffiths, G. W. G. Wilkinson, T. F. Schulz, and A. J. Davison. 2010. Sequences of complete human cytomegalovirus genomes from infected cell cultures and clinical specimens. *J. Gen. Virol.* 91: 605–615.

301. Feire, A. L., H. Koss, and T. Compton. 2004. Cellular integrins function as entry receptors for human cytomegalovirus via a highly conserved disintegrin-like domain. *Proc. Natl. Acad. Sci. U. S. A.* 101: 15470–5.

302. Wang, X., S. M. Huong, M. L. Chiu, N. Raab-Traub, and E. S. Huang. 2003. Epidermal growth factor receptor is a cellular receptor for human cytomegalovirus. *Nature* 424: 456–461.

303. Isaacson, M. K., A. L. Feire, and T. Compton. 2007. Epidermal Growth Factor Receptor Is Not Required for Human Cytomegalovirus Entry or Signaling. *J. Virol.* 81: 6241–6247.

304. Wang, X., D. Y. Huang, S. M. Huong, and E. S. Huang. 2005. Integrin αvβ3 is a coreceptor for human cytomegalovirus. *Nat. Med.* 11: 515–521.

305. Huber, M. T., and T. Compton. 1998. The human cytomegalovirus UL74 gene encodes the third component of the glycoprotein H-glycoprotein L-containing envelope complex. *J. Virol.* 72: 8191–8197.

306. Kabanova, A., J. Marcandalli, T. Zhou, S. Bianchi, U. Baxa, Y. Tsybovsky, D. Lilleri, C. Silacci-Fregni, M. Foglierini, B. M. Fernandez-Rodriguez, A. Druz, B. Zhang, R. Geiger, M. Pagani, F. Sallusto, P. D. Kwong, D. Corti, A. Lanzavecchia, and L. Perez. 2016. Platelet-derived growth factor-α receptor is the cellular receptor for

human cytomegalovirus gHgLgO trimer. *Nat. Microbiol.* 1: 1–8.

307. Vanarsdall, A. L., M. C. Chase, and D. C. Johnson. 2011. Human Cytomegalovirus Glycoprotein gO Complexes with gH/gL, Promoting Interference with Viral Entry into Human Fibroblasts but Not Entry into Epithelial Cells. *J. Virol.* 85: 11638–11645.

308. Ryckman, B. J., M. A. Jarvis, D. D. Drummond, J. A. Nelson, and D. C. Johnson. 2006. Human Cytomegalovirus Entry into Epithelial and Endothelial Cells Depends on Genes UL128 to UL150 and Occurs by Endocytosis and Low-pH Fusion. *J. Virol.* 80: 710–722.

309. Patrone, M., M. Secchi, L. Fiorina, M. Ierardi, G. Milanesi, and A. Gallina. 2005. Human Cytomegalovirus UL130 Protein Promotes Endothelial Cell Infection through a Producer Cell Modification of the Virion Human Cytomegalovirus UL130 Protein Promotes Endothelial Cell Infection through a Producer Cell Modification of the Virion †. 79: 8361–8373.

310. Wang, D., and T. Shenk. 2005. Human cytomegalovirus virion protein complex required for epithelial and endothelial cell tropism. *Proc. Natl. Acad. Sci. U. S. A.* 102: 18153–18158.

311. Ryckman, B. J., B. L. Rainish, M. C. Chase, J. A. Borton, J. A. Nelson, M. A. Jarvis, and D. C. Johnson. 2008. Characterization of the Human Cytomegalovirus gH/gL/UL128-131 Complex That Mediates Entry into Epithelial and Endothelial Cells. *J. Virol.* 82: 60–70.

312. Vanarsdall, A. L., and D. C. Johnson. 2012. Human cytomegalovirus entry into cells. *Curr. Opin. Virol.* 2: 37–42.

313. Ogawa-Goto, K., K. Tanaka, W. Gibson, E. Moriishi, Y. Miura, T. Kurata, S. Irie, and T. Sata. 2003. Microtubule network facilitates nuclear targeting of human cytomegalovirus capsid. *J. Virol.* 77: 8541–7.

314. Kalejta, R. F. 2008. Tegument Proteins of Human Cytomegalovirus. *Microbiol. Mol. Biol. Rev.* 72: 249–265.

315. McVoy, M. A., and S. P. Adler. 1994. Human cytomegalovirus DNA replicates after early circularization by concatemer formation, and inversion occurs within the concatemer. *J. Virol.* 68: 1040–51.

316. Freed, E., and M. Martin. 2013. *Fields Virology*,.

317. Tandon, R., and E. S. Mocarski. 2012. Viral and host control of cytomegalovirus maturation. *Trends Microbiol.* 20: 392–401.

318. Buser, C., P. Walther, T. Mertens, and D. Michel. 2007. Cytomegalovirus Primary Envelopment Occurs at Large Infoldings of the Inner Nuclear Membrane. *J. Virol.* 81: 3042–3048.

319. Silva, M. C., J. Schröer, and T. Shenk. 2005. Human cytomegalovirus cell-to-cell spread in the absence of an essential assembly protein. *Proc. Natl. Acad. Sci. U. S. A.* 102: 2081–6.

320. Murrell, I., C. Bedford, K. Ladell, K. L. Miners, D. A. Price, P. Tomasec, G. W. G. Wilkinson, and R. J. Stanton. 2017. The pentameric complex drives immunologically covert cell–cell transmission of wild-type human cytomegalovirus. *Proc. Natl. Acad. Sci.* 114: 6104–6109.

321. Fowler, K. B., S. Stagno, R. F. Pass, W. J. Britt, T. J. Boll, and C. A. Alford. 1992. The outcome of congenital cytomegalovirus infection in relation to maternal antibody status. *N. Engl. J. Med.* 326: 663–7.

322. Selik, R. M., S. Y. Chu, and J. W. Ward. 1997. Trends in infectious diseases and cancers among persons dying of HIV infection in the United States from 1987 to 1992 (Reprinted from Annals of Internal Medicine, vol 123, pg 933-936, 1995). *Formulary* 32: S43–S47.

323. Kenneson, A., and M. J. Cannon. 2007. Review and meta-analysis of the epidemiology of congenital cytomegalovirus (CMV) infection. *Rev. Med. Virol.* 17: 253–276.

324. Griffiths, P. D. 2012. Burden of disease associated with human cytomegalovirus and prospects for elimination by universal immunisation. *Lancet Infect. Dis.* 12: 790–798.

325. Dollard, S. C., S. D. Grosse, and D. S. Ross. 2007. New estimates of the prevalence of neurological and sensory sequelae and mortality associated with congenital cytomegalovirus infection. *Rev. Med. Virol.* 17: 355–363.

326. Reynolds, D. W., S. Stagno, R. Reynolds, and C. A. Alford. 1978. Perinatal cytomegalovirus infection: Influence of placentally transferred maternal antibody. *J. Infect. Dis.* 137: 564–567.

327. Fowler, K. B., S. Stagno, R. F. Pass, J. Stanley, and A. Plotkin. 2003. Cytomegalovirus Infection Maternal Immunity and Prevention of Congenital Maternal Immunity and Prevention of Congenital Cytomegalovirus Infection. *JAMA Public Heal. Immunization; Women's Heal. Pregnancy Breast Feed. Relat. Lett.* 2898290: 24–27.

328. Emery, V. C. 2001. Investigation of CMV disease in immunocompromised patients. *J. Clin. Pathol.* 54: 84–88.

329. Fishman, J. A., and R. H. Rubin. 1998. Infection in organ-transplant recipients. *N. Engl. J. Med.* 338: 1741–51.

330. Fishman, J. A., V. Emery, R. Freeman, M. Pascual, L. Rostaing, H. J. Schlitt, D. Sgarabotto, J. Torre-cisneros, and M. E. Uknis. 2007. Cytomegalovirus in transplantation - Challenging the status quo. *Clin. Transplant.* 21: 149–158.

331. Deayton, J. R., C. a Prof Sabin, M. a Johnson, V. C. Emery, P. Wilson, and P. D. Griffiths. 2004. Importance of cytomegalovirus viraemia in risk of disease progression and death in HIV-infected patients receiving highly active antiretroviral therapy. *Lancet* 363: 2116–2121.

332. Komatsu, T. E., A. Pikis, L. K. Naeger, and P. R. Harrington. 2014. Resistance of human cytomegalovirus to ganciclovir/valganciclovir: A comprehensive review of putative resistance pathways. *Antiviral Res.* 101: 12–25.

333. Compton, T., E. a. Kurt-Jones, K. W. Boehme, J. Belko, E. Latz, D. T. Golenbock, and R. W. Finberg. 2003. Human cytomegalovirus activates inflammatory cytokine responses via CD14 and Toll-like receptor 2. *J. Virol.* 77: 4588–4596.

334. Boehme, K. W., M. Guerrero, and T. Compton. 2006. Human Cytomegalovirus Envelope Glycoproteins B and H Are Necessary for TLR2 Activation in Permissive Cells. *J. Immunol.* 177: 7094–7102.

335. Yew, K. H., B. Carsten, and C. Harrison. 2010. Scavenger receptor A1 is required for sensing HCMV by endosomal TLR-3/-9 in monocytic THP-1 cells. *Mol. Immunol.* 47: 883–893.

336. Amsler, L., M. C. Verweij, and V. R. Defilippis. 2013. The tiers and dimensions of evasion of the type i interferon response by human cytomegalovirus. *J. Mol. Biol.* 425: 4857–4871.

337. Sedger, L. M., D. M. Shows, R. A. Blanton, J. J. Peschon, R. G. Goodwin, D. Cosman, and S. R. Wiley. 1999. IFN-gamma mediates a novel antiviral activity through dynamic modulation of TRAIL and TRAIL receptor expression. *J. Immunol.* 163: 920–6.

338. Benedict, C. A., T. A. Banks, L. Senderowicz, M. Ko, W. J. Britt, A. Angulo, P. Ghazal, and C. F. Ware. 2001. Lymphotoxins and cytomegalovirus cooperatively induce interferon-β, establishing host-virus Détente. *Immunity* 15: 617–626.

339. Iversen, A.-C., P. S. Norris, C. F. Ware, and C. A. Benedict. 2005. Human NK Cells Inhibit Cytomegalovirus Replication through a Noncytolytic Mechanism Involving Lymphotoxin-Dependent Induction of IFN- . *J. Immunol.* 175: 7568–7574.

340. Biron, C. A., K. S. Byron, and J. L. Sullivan. 1989. Severe Herpesvirus Infections in an Adolescent without Natural Killer Cells. *N. Engl. J. Med.* 320: 1731–1735.

341. Wilkinson, G. W. G., P. Tomasec, R. J. Stanton, M. Armstrong, V. Prod'homme, R. Aicheler, B. P. McSharry, C. R. Rickards, D. Cochrane, S. Llewellyn-Lacey, E. C. Y. Wang, C. A. Griffin, and A. J. Davison. 2008. Modulation of natural killer cells by human cytomegalovirus. *J. Clin. Virol.* 41: 206–212.

342. Ahn, K., A. Angulo, P. Ghazal, P. A. Peterson, Y. Yang, and K. Früh. 1996. Human cytomegalovirus inhibits antigen presentation by a sequential multistep process. *Proc. Natl. Acad. Sci. U. S. A.* 93: 10990–5.

343. Jones, T. R., E. J. Wiertz, L. Sun, K. N. Fish, J. A. Nelson, and H. L. Ploegh. 1996. Human cytomegalovirus US3 impairs transport and maturation of major histocompatibility complex class I heavy chains. *Proc. Natl. Acad. Sci. U. S. A.* 93: 11327–11333.

344. Wiertz, E. J. H. J., T. R. Jones, L. Sun, M. Bogyo, H. J. Geuze, and H. L. Ploegh. 1996. The human cytomegalovirus US11 gene product dislocates MHC class I heavy chains from the endoplasmic reticulum to the cytosol. *Cell* 84: 769–779.

345. Cebulla, C. M., D. M. Miller, Y. Zhang, B. M. Rahill, P. Zimmerman, J. M. Robinson, and D. D. Sedmak. 2002. Human cytomegalovirus disrupts constitutive MHC class II expression. *J. Immunol.* 169: 167–76.

346. Spencer, J. V, K. M. Lockridge, P. A. Barry, G. Lin, M. Tsang, M. E. T. Penfold, and T. J. Schall. 2002. Potent immunosuppressive activities of cytomegalovirus-encoded interleukin-10. *J. Virol.* 76: 1285–92.

347. Odeberg, J., B. Plachter, L. Brandén, and C. Söderberg-Nauclér. 2003. Human cytomegalovirus protein pp65 mediates accumulation of HLA-DR in lysosomes and destruction of the HLA-DR alpha-chain. *Blood* 101: 4870–7.

348. Sinzger, C., K. Eberhardt, Y. Cavignac, C. Weinstock, T. Kessler, G. Jahn, and J. L. Davignon. 2006. Macrophage cultures are susceptible to lytic productive infection by endothelial-cell-propagated human cytomegalovirus strains and present viral IE1

protein to CD4+T cells despite late downregulation of MHC class II molecules. *J. Gen. Virol.* 87: 1853–1862.

349. Arrode, G., C. Boccaccio, J. Lulé, S. Allart, N. Moinard, J. P. Abastado, A. Alam, and C. Davrinche. 2000. Incoming human cytomegalovirus pp65 (UL83) contained in apoptotic infected fibroblasts is cross-presented to CD8(+) T cells by dendritic cells. *J. Virol.* 74: 10018–24.

350. Tabi, Z., M. Moutaftsi, and L. K. Borysiewicz. 2001. Human cytomegalovirus pp65- and immediate early 1 antigen-specific HLA class I-restricted cytotoxic T cell responses induced by cross-presentation of viral antigens. *J. Immunol.* 166: 5695–703.

351. Arrode, G., C. Boccaccio, J.-P. Abastado, and C. Davrinche. 2002. Cross-presentation of human cytomegalovirus pp65 (UL83) to CD8+ T cells is regulated by virus-induced, soluble-mediator-dependent maturation of dendritic cells. *J. Virol.* 76: 142–50.

352. Nowak, B., C. Sullivan, P. Sarnow, R. Thomas, F. Bricout, J. C. Nicolas, B. Fleckenstein, and A. J. Levine. 1984. Characterization of monoclonal antibodies and polyclonal immune sera directed against human cytomegalovirus virion proteins. *Virology* 132: 325–338.

353. Britt, W. J., L. Vugler, E. J. Butfiloski, and E. B. Stephens. 1990. Cell surface expression of human cytomegalovirus (HCMV) gp55-116 (gB): use of HCMV-recombinant vaccinia virus-infected cells in analysis of the human neutralizing antibody response. *J. Virol.* 64: 1079–1085.

354. Rasmussen, L., C. Matkin, R. Spaete, C. Pachl, and T. Merigan. 1991. Antibody response to human cytomegalovirus glycoproteins gB and gH after natural infection in humans. *J. Infect. Dis.* 164: 835–42.

355. Steffens, H. P., S. Kurz, R. Holtappels, and M. J. Reddehase. 1998. Preemptive CD8 T-cell immunotherapy of acute cytomegalovirus infection prevents lethal disease, limits the burden of latent viral genomes, and reduces the risk of virus recurrence. *J. Virol.* 72: 1797–804.

356. Reusser, P., S. R. Riddell, J. D. Meyers, and P. D. Greenberg. 1991. Cytotoxic T-lymphocyte response to cytomegalovirus after human allogeneic bone marrow transplantation: pattern of recovery and correlation with cytomegalovirus infection and disease. *Blood* 78: 1373–1380.

357. Walter, E. A., P. D. Greenberg, M. J. Gilbert, R. J. Finch, K. S. Watanabe, E. D. Thomas, and S. R. Riddell. 1995. Reconstitution of cellular immunity against cytomegalovirus in recipients of allogeneic bone marrow by transfer of T-cell clones from the donor. *N. Engl. J. Med.* 333: 1038–1044.

358. Jacobson, M. A., H. T. Maecker, P. L. Orr, R. D'Amico, M. Van Natta, X. Li, R. B. Pollard, and B. M. Bredt. 2004. Results of a Cytomegalovirus (CMV)–Specific $CD8^{+}$ /Interferon-γ^{+} Cytokine Flow Cytometry Assay Correlate with Clinical Evidence of Protective Immunity in Patients with AIDS with CMV Retinitis. *J. Infect. Dis.* 189: 1362–1373.

359. Tu, W., S. Chen, M. Sharp, C. Dekker, A. M. Manganello, E. C. Tongson, H. T. Maecker, T. H. Holmes, Z. Wang, G. Kemble, S. Adler, A. Arvin, and D. B. Lewis. 2004. Persistent and selective deficiency of CD4+ T cell immunity to cytomegalovirus in immunocompetent young children. *J Immunol* 172: 3260–3267.

360. Sester, U., B. C. Gärtner, H. Wilkens, B. Schwaab, R. Wössner, I. Kindermann, M. Girndt, A. Meyerhans, N. Mueller-Lantzsch, H. J. Schäfers, G. W. Sybrecht, H. Köhler, and M. Sester. 2005. Differences in CMV-specific T-cell levels and long-term susceptibility to CMV infection after kidney, heart and lung transplantation. *Am. J. Transplant.* 5: 1483–1489.

361. Sylwester, A. A. W., B. B. L. Mitchell, J. B. J. Edgar, C. Taormina, C. Pelte, F. Ruchti, P. P. R. Sleath, K. K. H. Grabstein, N. A. Hosken, F. Kern, J. A. Nelson, and L. L. J. Picker. 2005. Broadly targeted human cytomegalovirus-specific CD4+ and CD8+ T cells dominate the memory compartments of exposed subjects. *J. Exp. Med.* 202: 673–685.

362. Khan, N., N. Shariff, M. Cobbold, R. Bruton, J. A. Ainsworth, A. J. Sinclair, L. Nayak, and P. A. H. Moss. 2002. Cytomegalovirus Seropositivity Drives the CD8 T Cell Repertoire Toward Greater Clonality in Healthy Elderly Individuals. *J. Immunol.* 169: 1984–1992.

363. Khan, N., A. Hislop, N. Gudgeon, M. Cobbold, R. Khanna, L. Nayak, A. B. Rickinson, and P. A. H. Moss. 2004. Herpesvirus-Specific CD8 T Cell Immunity in Old Age: Cytomegalovirus Impairs the Response to a Coresident EBV Infection. *J. Immunol.* 173: 7481–7489.

364. Pourgheysari, B., N. Khan, D. Best, R. Bruton, L. Nayak, and P. a H. Moss. 2007. The cytomegalovirus-specific CD4+ T-cell response expands with age and markedly alters the CD4+ T-cell repertoire. *J. Virol.* 81: 7759–7765.

365. Weekes, M. P., A. J. Carmichael, M. R. Wills, K. Mynard, and J. G. Sissons. 1999. Human CD28-CD8+ T cells contain greatly expanded functional virus-specific memory CTL clones. *J Immunol* 162: 7569–7577.

366. Hertoghs, K. M. L., P. D. Moerland, A. Van Stijn, E. B. M. Remmerswaal, S. L. Yong, P. J. E. J. Van De Berg, S. M. Van Ham, F. Baas, I. J. M. Berge, and R. a W. Van Lier. 2010. Molecular profiling of cytomegalovirus- induced human CD8 + T cell differentiation. *J. Clin. Invest.* 120: 4077–4090.

367. Powers, C., and K. Früh. 2008. Rhesus CMV: An emerging animal model for human CMV. *Med. Microbiol. Immunol.* 197: 109–115.

368. Ebeling, A., G. M. Keil, E. Knust, and U. H. 1983. Molecular Cloning and Physical Mapping of Murine. *Cloning* 47: 421–433.

369. Rawlinson, W. D., H. E. Farrell, B. G. Barrell, H. E. Farrell, and B. G. Barrell. 1996. Analysis of the complete DNA sequence of murine cytomegalovirus. *J. Virol.* 70: 8833–8849.

370. Smith, M. G. 1954. Propagation of salivary gland virus of the mouse in tissue cultures. *Proc Soc Exp Biol Med* 86: 435–440.

371. Misra, V., and J. B. Hudson. 1980. Minor base sequence differences between the genomes of two strains of murine cytomegalovirus differing in virulence. *Arch. Virol.* 64: 1–8.

372. Fitzgerald, N. A., J. M. Papadimitriou, and G. R. Shellam. 1990. Cytomegalovirus-induced pneumonitis and myocarditis in newborn mice. A model for perinatal human cytomegalovirus infection. *Arch. Virol.* 115: 75–88.

373. Hayashi, K., Y. Suwa, Y. Shimomura, and Y. Ohashi. 1995. Pathogenesis of Ocular Cytomegalovirus-Infection in the Immunocompromised Host. *J. Med. Virol.* 47: 364–369.

374. Trgovcich, J., D. Stimac, B. Polić, A. Krmpotić, E. Pernjak-Pugel, J. Tomac, M. Hasan, B. Wraber, and S. Jonjić. 2000. Immune responses and cytokine induction in the development of severe hepatitis during acute infections with murine cytomegalovirus. *Arch. Virol.* 145: 2601–18.

375. Krmpotic, A., I. Bubic, B. Polic, P. Lucin, and S. Jonjic. 2003. Pathogenesis of murine cytomegalovirus infection. *Microbes Infect.* 5: 1263–1277.

376. Reddehase, M. J., J. Podlech, and N. K. a Grzimek. 2002. Mouse models of cytomegalovirus latency: overview. *J. Clin. Virol.* 25 Suppl 2: S23-36.

377. Wu, C. A., S. A. Paveglio, E. G. Lingenheld, L. Zhu, L. Lefrancois, and L. Puddington. 2011. Transmission of Murine Cytomegalovirus in Breast Milk: a Model of Natural Infection in Neonates. *J. Virol.* 85: 5115–5124.

378. Kashiwai, A., N. Kawamura, C. Kadota, and Y. Tsutsui. 1992. Susceptibility of mouse embryo to murine cytomegalovirus infection in early and mid-gestation stages. *Arch. Virol.* 127: 37–48.

379. Tsutsui, Y., A. Kashiwai, N. Kawamura, and C. Kadota. 1993. Microphthalmia and cerebral atrophy induced in mouse embryos by infection with murine cytomegalovirus in midgestation. *Am. J. Pathol.* 143: 804–813.

380. Tsutsui, Y. 1995. Developmental disorders of the mouse brain induced by murine cytomegalovirus: Animal models for congenital cytomegalovirus infection. *Pathol. Int.* 45: 91–102.

381. Tabeta, K., P. Georgel, E. Janssen, X. Du, K. Hoebe, K. Crozat, S. Mudd, L. Shamel, S. Sovath, J. Goode, L. Alexopoulou, R. A. Flavell, and B. Beutler. 2004. Toll-like receptors 9 and 3 as essential components of innate immune defense against mouse cytomegalovirus infection. *Proc Natl Acad Sci U S A* 101: 3516–3521.

382. Zucchini, N., G. Bessou, S. Traub, S. H. Robbins, S. Uematsu, S. Akira, L. Alexopoulou, and M. Dalod. 2008. Cutting Edge: Overlapping Functions of TLR7 and TLR9 for Innate Defense against a Herpesvirus Infection. *J. Immunol.* 180: 5799–5803.

383. Yamaguchi, T., Y. Shinagawa, and R. B. Pollard. 1988. Relationship between the production of murine cytomegalovirus and interferon in macrophages. *J. Gen. Virol.* 69: 2961–2971.

384. Orange, J. J. S. J., and C. A. Biron. 1996. Characterization of early IL-12, IFN-αβ, and TNF effects on antiviral state and NK cell responses during murine cytomegalovirus infection. *J Immunol* 156: 4746–4756.

385. Yerkovich, S. T., S. D. Olver, J. C. Lenzo, and C. D. Peacock. 1997. The roles of tumour necrosis factor-a, interleukin-1 and interleukin-12 in murine cytomegalovirus infection. *Immunology* 91: 45–52.

386. Dalod, M., T. Hamilton, R. Salomon, T. P. Salazar-Mather, S. C. Henry, J. D. Hamilton, and C. A. Biron. 2003. Dendritic cell responses to early murine cytomegalovirus infection: subset functional specialization and differential regulation by interferon alpha/beta. *J. Exp. Med.* 197: 885–98.

387. Shellam, G. R., J. E. Allan, J. M. Papadimitriou, and G. J. Bancroft. 1981. Increased susceptibility to cytomegalovirus infection in beige mutant mice. *Proc. Natl. Acad. Sci. U. S. A.* 78: 5104–8.

388. Bukowski, J. F., B. a Woda, and R. M. Welsh. 1984. Pathogenesis of murine cytomegalovirus infection in natural killer cell-depleted mice. *J. Virol.* 52: 119–128.

389. Bukowski, J. F., J. F. Warner, G. Dennert, and R. M. Welsh. 1985. Adoptive transfer studies demonstrating the antiviral effect of natural killer cells in vivo. *J. Exp. Med.* 161: 40–52.

390. Jonjić, S., I. Pavić, B. Polić, I. Crnković, P. Lucin, and U. H. Koszinowski. 1994. Antibodies are not essential for the resolution of primary cytomegalovirus infection but limit dissemination of recurrent virus. *J. Exp. Med.* 179: 1713–7.

391. Reddehase, M. J., M. Balthesen, M. Rapp, S. Jonjić, I. Pavić, and U. H. Koszinowski. 1994. The conditions of primary infection define the load of latent viral genome in organs and the risk of recurrent cytomegalovirus disease. *J. Exp. Med.* 179: 185–93.

392. Jonjic, S., I. Pavic, P. Lucin, D. Rukavina, and U. H. Koszinowski. 1990. Efficacious control of cytomegalovirus infection after long-term depletion of CD8+ T lymphocytes. *J Virol* 64: 5457–5464.

393. Salem, M. L., and M. S. Hossain. 2000. In vivo acute depletion of CD8(+) T cells before murine cytomegalovirus infection upregulated innate antiviral activity of natural killer cells. *Int. J. Immunopharmacol.* 22: 707–18.

394. Jonjić, S., W. Mutter, F. Weiland, M. J. Reddehase, and U. H. Koszinowski. 1989. Site-restricted persistent cytomegalovirus infection after selective long-term depletion of CD4+ T lymphocytes. *J. Exp. Med.* 169: 1199–212.

395. Lucin, P., I. Pavić, B. Polić, S. Jonjić, and U. H. Koszinowski. 1992. Gamma interferon-dependent clearance of cytomegalovirus infection in salivary glands. *J. Virol.* 66: 1977–84.

396. Walton, S. M., S. Mandaric, N. Torti, A. Zimmermann, H. Hengel, and A. Oxenius. 2011. Absence of cross-presenting cells in the salivary gland and viral immune evasion confine cytomegalovirus immune control to effector CD4 T cells. *PLoS Pathog.* 7.

397. Lu, X., A. K. Pinto, A. M. Kelly, K. S. Cho, and A. B. Hill. 2006. Murine Cytomegalovirus Interference with Antigen Presentation Contributes to the Inability of CD8 T Cells To Control Virus in the Salivary Gland Murine Cytomegalovirus Interference with Antigen Presentation Contributes to the Inability of CD8 T Cells To C. 80: 4200–4202.

398. Snyder, C. M., A. Loewendorf, E. L. Bonnett, M. Croft, C. a Benedict, and A. B. Hill. 2009. CD4+ T cell help has an epitope-dependent impact on CD8+ T cell memory inflation during murine cytomegalovirus infection. *J. Immunol.* 183: 3932–3941.

399. Walton, S. M., N. Torti, S. Mandaric, and A. Oxenius. 2011. T-cell help permits memory CD8+ T-cell inflation during cytomegalovirus latency. *Eur. J. Immunol.* 41: 2248–2259.

400. Karrer, U., S. Sierro, M. Wagner, A. Oxenius, H. Hengel, U. H. Koszinowski, R. E. Phillips, and P. Klenerman. 2003. Memory inflation: continuous accumulation of antiviral CD8+ T cells over time. *J. Immunol.* 170: 2022–2029.

401. Munks, M. W., K. S. Cho, A. K. Pinto, S. Sierro, P. Klenerman, and A. B. Hill. 2006. Four Distinct Patterns of Memory CD8 T Cell Responses to Chronic Murine Cytomegalovirus Infection. *J. Immunol.* 177: 450–458.

402. Holtappels, R., D. Thomas, J. Podlech, G. Geginat, H. P. Steffens, and M. J. Reddehase. 2000. The putative natural killer decoy early gene m04 (gp34) of murine cytomegalovirus encodes an antigenic peptide recognized by protective antiviral CD8 T cells. *J. Virol.* 74: 1871–84.

403. Holtappels, R., N. K. A. Grzimek, D. Thomas, and M. J. Reddehase. 2002. Early gene m18, a novel player in the immune response to murine cytomegalovirus. *J. Gen. Virol.* 83: 311–316.

404. Holtappels, R., D. Thomas, J. Podlech, and M. J. Reddehase. 2002. Two antigenic peptides from genes m123 and m164 of murine cytomegalovirus quantitatively dominate CD8 T-cell memory in the H-2d haplotype. *J. Virol.* 76: 151–64.

405. Sierro, S., R. Rothkopf, and P. Klenerman. 2005. Evolution of diverse antiviral CD8+ T cell populations after murine cytomegalovirus infection. *Eur. J. Immunol.* 35: 1113–1123.

406. Arens, R., P. Wang, J. Sidney, A. Loewendorf, A. Sette, S. P. Schoenberger, B. Peters, and C. A. Benedict. 2008. Cutting edge: murine cytomegalovirus induces a polyfunctional CD4 T cell response. *J. Immunol.* 180: 6472–6.

407. Clement, M., M. Marsden, M. A. Stacey, J. Abdul-Karim, S. Gimeno Brias, D. Costa Bento, M. J. Scurr, P. Ghazal, C. T. Weaver, G. Carlesso, S. Clare, S. A. Jones, A. Godkin, G. W. Jones, and I. R. Humphreys. 2016. Cytomegalovirus-Specific IL-10-Producing CD4+T Cells Are Governed by Type-I IFN-Induced IL-27 and Promote Virus Persistence. *PLoS Pathog.* 12: 1–26.

408. Snyder, C. M., K. S. Cho, E. L. Bonnett, S. van Dommelen, G. R. Shellam, and A. B. Hill. 2008. Memory Inflation during Chronic Viral Infection Is Maintained by Continuous Production of Short-Lived, Functional T Cells. *Immunity* 29: 650–659.

409. Wherry, E. J. 2011. T cell exhaustion. *Nat. Immunol.* 12: 492–499.

410. Snyder, C. M., K. S. Cho, E. L. Bonnett, J. E. Allan, and A. B. Hill. 2011. Sustained CD8+ T cell memory inflation after infection with a single-cycle Cytomegalovirus. *PLoS Pathog.* 7.

411. Smith, C. J., H. Turula, and C. M. Snyder. 2014. Systemic Hematogenous Maintenance of Memory Inflation by MCMV Infection. *PLoS Pathog.* 10.

412. Torti, N., S. M. Walton, T. Brocker, T. Rülicke, and A. Oxenius. 2011. Non-hematopoietic cells in lymph nodes drive memory CD8 t cell inflation during murine cytomegalovirus infection. *PLoS Pathog.* 7.

413. Seckert, C. K., S. I. Schader, S. Ebert, D. Thomas, K. Freitag, A. Renzaho, J. Podlech, M. J. Reddehase, and R. Holtappels. 2011. Antigen-presenting cells of haematopoietic origin prime cytomegalovirus-specific CD8 T-cells but are not sufficient for driving memory inflation during viral latency. *J. Gen. Virol.* 92: 1994–2005.

414. Seckert, C. K., M. Grießl, J. K. Büttner, S. Scheller, C. O. Simon, K. A. Kropp, A. Renzaho, B. Kühnapfel, N. K. A. Grzimek, and M. J. Reddehase. 2012. Viral latency drives 'memory inflation': a unifying hypothesis linking two hallmarks of cytomegalovirus infection. *Med. Microbiol. Immunol.* 201: 551–566.

415. Torti, N., S. M. Walton, K. M. Murphy, and A. Oxenius. 2011. Batf3 transcription factor-dependent DC subsets in murine CMV infection: Differential impact on T-cell priming and memory inflation. *Eur. J. Immunol.* 41: 2612–2618.

416. Hutchinson, S., S. Sims, G. O'Hara, J. Silk, U. Gileadi, V. Cerundolo, and P. Klenerman. 2011. A dominant role for the immunoproteasome in CD8+ T cell responses to murine cytomegalovirus. *PLoS One* 6.

417. Van den Eynde, B. J., and S. Morel. 2001. Differential processing of class-I-restricted epitopes by the standard proteasome and the immunoproteasome. *Curr. Opin. Immunol.* 13: 147–153.

418. Ware, C. F., M. Croft, K. Schneider, C. A. Benedict, M. W. Munks, I. R. Humphreys, A. Loewendorf, and C. De Trez. 2007. CD4-Dependent Mechanism Cytomegalovirus-Specific CD8 T Cells: A OX40 Costimulation Promotes Persistence of OX40 Costimulation Promotes Persistence of Cytomegalovirus-Specific CD8 T Cells: A CD4-Dependent Mechanism. *J Immunol Ref. J. Immunol. Genzyme Novemb. J. Immu-nology* 179: 2195–2202.

419. Humphreys, I. R., S. W. Lee, M. Jones, A. Loewendorf, E. Gostick, D. A. Price, C. A. Benedict, C. F. Ware, and M. Croft. 2010. Biphasic role of 4-1BB in the regulation of mouse cytomegalovirus-specific CD8+ T cells. *Eur. J. Immunol.* 40: 2762–2768.

420. Dekhtiarenko, I., M. A. Jarvis, Z. Ruzsics, and L. Cicin-Sain. 2013. The Context of Gene Expression Defines the Immunodominance Hierarchy of Cytomegalovirus Antigens. *J. Immunol.* 190: 3399–3409.

421. Munks, M. W., M. C. Gold, A. L. Zajac, C. M. Doom, C. S. Morello, D. H. Spector, and A. B. Hill. 2006. Genome-wide analysis reveals a highly diverse CD8 T cell response to murine cytomegalovirus. *J. Immunol. (Baltimore, Md 1950)* 176: 3760–3766.

422. Trgovcich, J., M. Kincaid, A. Thomas, M. Griessl, P. Zimmerman, V. Dwivedi, V. Bergdall, P. Klenerman, and C. H. Cook. 2016. Cytomegalovirus reinfections stimulate CD8 T-Memory inflation. *PLoS One* 11: 1–19.

423. Hansen, S. G., C. Vieville, N. Whizin, L. Coyne-Johnson, D. C. Siess, D. D. Drummond, a W. Legasse, M. K. Axthelm, K. Oswald, C. M. Trubey, M. Piatak Jr., J. D. Lifson, J. a Nelson, M. a Jarvis, and L. J. Picker. 2009. Effector memory T cell responses are associated with protection of rhesus monkeys from mucosal simian immunodeficiency virus challenge. *Nat.Med.* 15: 293–299.

424. Hansen, S. G., J. C. Ford, M. S. Lewis, A. B. Ventura, C. M. Hughes, L. Coyne-Johnson, N. Whizin, K. Oswald, R. Shoemaker, T. Swanson, A. W. Legasse, M. J. Chiuchiolo, C. L. Parks, M. K. Axthelm, J. a Nelson, M. a Jarvis, M. Piatak, J. D. Lifson, and L. J. Picker. 2011. Profound early control of highly pathogenic SIV by an effector memory T-cell vaccine. *Nature* 473: 523–7.

425. Hansen, S. G., D. E. Zak, G. Xu, J. C. Ford, E. E. Marshall, D. Malouli, R. M. Gilbride, C. M. Hughes, A. B. Ventura, E. Ainslie, K. T. Randall, A. N. Selseth, P. Rundstrom, L. Herlache, M. S. Lewis, H. Park, S. L. Planer, J. M. Turner, M. Fischer, C. Armstrong, R. C. Zweig, J. Valvo, J. M. Braun, S. Shankar, L. Lu, A. W. Sylwester, A. W. Legasse, M. Messerle, M. A. Jarvis, L. M. Amon, A. Aderem, G. Alter, D. J. Laddy, M. Stone, A. Bonavia, T. G. Evans, M. K. Axthelm, K. Früh, P. T. Edlefsen, and L. J. Picker. 2018. Prevention of tuberculosis in rhesus macaques by a cytomegalovirus-based vaccine. *Nat. Med.* 24: 130–143.

426. Tierney, R., T. Nakai, C. J. Parkins, P. Caposio, N. F. Fairweather, D. Sesardic, and M. A. Jarvis. 2012. A single-dose cytomegalovirus-based vaccine encoding tetanus toxin fragment C induces sustained levels of protective tetanus toxin antibodies in mice. *Vaccine* 30: 3047–3052.

427. Karrer, U., M. Wagner, S. Sierro, H. Hengel, T. Dumrese, U. H. Koszinowski, R. E. Phillips, P. Klenerman, A. Oxenius, and S. Freigang. 2004. Expansion of Protective CD8 + T-Cell Responses Driven by Recombinant Cytomegaloviruses Expansion of Protective CD8 ∂ T-Cell Responses Driven by Recombinant Cytomegaloviruses. 78: 2255–2264.

428. Tsuda, Y., P. Caposio, C. J. Parkins, S. Botto, I. Messaoudi, L. Cicin-Sain, H. Feldmann, and M. A. Jarvis. 2011. A replicating cytomegalovirus-based vaccine encoding a single Ebola virus nucleoprotein CTL epitope confers protection against Ebola virus. *PLoS Negl. Trop. Dis.* 5.

429. Beverley, P. C. L., Z. Ruzsics, A. Hey, C. Hutchings, S. Boos, B. Bolinger, E. Marchi, G. O 'hara, P. Klenerman, U. H. Koszinowski, and E. Z. Tchilian. 2014. A Novel Murine Cytomegalovirus Vaccine Vector Protects against Mycobacterium tuberculosis. *J. Immunol.* 193: 2306–2316.

430. Lloyd, M. L., G. R. Shellam, J. M. Papadimitriou, and M. A. Lawson. 2003. Immunocontraception is induced in BALB/c mice inoculated with murine cytomegalovirus expressing mouse zona pellucida 3. *Biol Reprod* 68: 2024–2032.

431. Klyushnenkova, E. N., D. V. Kouiavskaia, C. J. Parkins, P. Caposio, S. Botto, R. B. Alexander, and M. A. Jarvis. 2012. A Cytomegalovirus-based Vaccine Expressing a Single Tumor-specific CD8+ T-cell Epitope Delays Tumor Growth in a Murine Model of Prostate Cancer. *J. Immunother.* 35: 390–399.

432. Xu, G., T. Smith, F. Grey, and A. B. Hill. 2013. Cytomegalovirus-based cancer vaccines expressing TRP2 induce rejection of melanoma in mice. *Biochem. Biophys. Res. Commun.* 437: 287–291.

433. Qiu, Z., H. Huang, J. M. Grenier, O. A. Perez, H. M. Smilowitz, B. Adler, and K. M. Khanna. 2015. Cytomegalovirus-Based Vaccine Expressing a Modified Tumor Antigen Induces Potent Tumor-Specific CD8+ T-cell Response and Protects Mice from Melanoma. *Cancer Immunol. Res.* 3: 536–46.

434. Warming, S., N. Costantino, D. L. Court, N. A. Jenkins, and N. G. Copeland. 2005. Simple and highly efficient BAC recombineering using galK selection. *Nucleic Acids Res.* 33: 1–12.

435. Tischer, B. K., G. A. Smith, and N. Osterrieder. 2010. En Passant Mutagenesis: A Two Step Markerless Red Recombination System. In *Methods in Molecular Biology* vol. 634. 421–430.

436. Almazan, F., J. M. Gonzalez, Z. Penzes, A. Izeta, E. Calvo, J. Plana-Duran, and L. Enjuanes. 2000. Engineering the largest RNA virus genome as an infectious bacterial artificial chromosome. *Proc. Natl. Acad. Sci.* 97: 5516–5521.

437. Domi, A., and B. Moss. 2002. Cloning the vaccinia virus genome as a bacterial artificial chromosome in Escherichia coli and recovery of infectious virus in mammalian cells. *Proc. Natl. Acad. Sci. U. S. A.* 99: 12415–12420.

438. Messerle, M., I. Crnkovic, W. Hammerschmidt, H. Ziegler, and U. H. Koszinowski. 1997. Cloning and mutagenesis of a herpesvirus genome as an infectious bacterial artificial chromosome. *Proc. Natl. Acad. Sci. U. S. A.* 94: 14759–63.

439. Borst, E. M., G. Hahn, U. H. Koszinowski, and M. Messerle. 1999. Cloning of the human cytomegalovirus (HCMV) genome as an infectious bacterial artificial chromosome in Escherichia coli: a new approach for construction of HCMV mutants. *J. Virol.* 73: 8320–8329.

440. Shizuya, H., B. Birren, U. J. Kim, V. Mancino, T. Slepak, Y. Tachiiri, and M. Simon. 1992. Cloning and stable maintenance of 300-kilobase-pair fragments of human DNA in Escherichia coli using an F-factor-based vector. *Proc. Natl. Acad. Sci. U. S. A.* 89: 8794–7.

441. Murphy, K. C. 1998. Use of bacteriophage λ recombination functions to promote gene replacement in Escherichia coli. *J. Bacteriol.* 180: 2063–2071.

442. Yu, D., H. M. Ellis, E.-C. Lee, N. A. Jenkins, N. G. Copeland, and D. L. Court. 2000. An efficient recombination system for chromosome engineering in Escherichia coli. *Proc. Natl. Acad. Sci.* 97: 5978–5983.

443. Lee, E.-C., D. Yu, J. Martinez de Velasco, L. Tessarollo, D. A. Swing, D. L. Court, N. A. Jenkins, and N. G. Copeland. 2001. A Highly Efficient Escherichia coli-Based Chromosome Engineering System Adapted for Recombinogenic Targeting and Subcloning of BAC DNA. *Genomics* 73: 56–65.

444. Karsten Tischer, B., G. A. Smith, and N. Osterrieder. 2010. *In Vitro Mutagenesis Protocols*, (J. Braman, ed). Humana Press, Totowa, NJ.

445. Redwood, A. J., M. Messerle, N. L. Harvey, C. M. Hardy, U. H. Koszinowski, a Malcolm, G. R. Shellam, and M. a Lawson. 2005. Use of a Murine Cytomegalovirus K181-Derived Bacterial Artificial Chromosome as a Vaccine Vector for Immunocontraception Use of a Murine Cytomegalovirus K181-Derived Bacterial Artificial Chromosome as a Vaccine Vector for Immunocontraception. 79: 2998–3008.

446. Bloss, T. A., and B. Sugden. 1994. Optimal lengths for DNAs encapsidated by Epstein-Barr virus. *J. Virol.* 68: 8217–22.

447. Bett, A. J., L. Prevec, and F. L. Graham. 1993. Packaging capacity and stability of human adenovirus type 5 vectors. *J. Virol.* 67: 5911–21.

448. Stanton, R., B. McSharry, M. Armstrong, P. Tomasec, and G. Wilkinson. 2008. Re-engineering adenovirus vector systems to enable high-throughput analyses of gene function. *Biotechniques* 45: 659–668.

449. Woods, A. M., W. W. Wang, D. M. Shaw, C. M. Ward, M. W. Carroll, B. R. Rees, and P. L. Stern. 2002. Characterization of the murine 5T4 oncofoetal antigen: a target for immunotherapy in cancer. *Biochem. J.* 366: 353–365.

450. Cardin, R. D., G. B. Abenes, C. A. Stoddart, and E. S. Mocarski. 1995. Murine cytomegalovirus IE2, an activator of gene expression, is dispensable for growth and latency in mice. *Virology* 209: 236–41.

451. Kurz, S. K., and M. J. Reddehase. 1999. Patchwork pattern of transcriptional reactivation in the lungs indicates sequential checkpoints in the transition from murine cytomegalovirus latency to recurrence. *J Virol* 73: 8612–8622.

452. Kurz, S. K., M. Rapp, H. P. Steffens, N. K. Grzimek, S. Schmalz, and M. J. Reddehase. 1999. Focal transcriptional activity of murine cytomegalovirus during latency in the lungs. *J Virol* 73: 482–494.

453. Rodríguez-Martín, S., K. A. Kropp, V. Wilhelmi, V. J. Lisnic, W. Y. Hsieh, M. Blanc, A. Livingston, A. Busche, H. Tekotte, M. Messerle, M. Auer, I. Fraser, S. Jonjic, A. Angulo, M. J. Reddehase, and P. Ghazal. 2012. Ablation of the Regulatory IE1 Protein of Murine Cytomegalovirus Alters In Vivo Pro-inflammatory TNF-alpha Production during Acute Infection. *PLoS Pathog.* 8.

454. Tomko, R. P., R. Xu, and L. Philipson. 1997. HCAR and MCAR: the human and mouse cellular receptors for subgroup C adenoviruses and group B coxsackieviruses. *Proc. Natl. Acad. Sci. U. S. A.* 94: 3352–6.

455. Bergelson, J. M. 1997. Isolation of a Common Receptor for Coxsackie B Viruses and Adenoviruses 2 and 5. *Science.* 275: 1320–1323.

456. Keil, G. M., A. Ebeling-Keil, and U. H. Koszinowski. 1987. Immediate-early genes of murine cytomegalovirus: location, transcripts, and translation products. *J. Virol.* 61: 526–33.

457. Koszinowski, U. H., G. M. Keil, H. Volkmer, M. R. Fibi, A. Ebeling-Keil, and K. Munch. 1986. The 89,000-Mr murine cytomegalovirus immediate-early protein activates gene transcription. *J Virol* 58: 59–66.

458. Ghazal, P., A. E. Visser, M. Gustems, R. García, E. M. Borst, K. Sullivan, M. Messerle, and A. Angulo. 2005. Elimination of ie1 significantly attenuates murine cytomegalovirus virulence but does not alter replicative capacity in cell culture. *J. Virol.* 79: 7182–94.

459. Rosenberg, S. a, J. C. Yang, and N. P. Restifo. 2004. Cancer immunotherapy: moving beyond current vaccines. *Nat. Med.* 10: 909–915.

460. Larocca, C., and J. Schlom. 2011. Viral Vector-Based Therapeutic Cancer Vaccines. *Cancer J.* 17: 359–371.

461. van Rhee, F., S. M. Szmania, F. Zhan, S. K. Gupta, M. Pomtree, P. Lin, R. B. Batchu, A. Moreno, G. Spagnoli, J. Shaughnessy, and G. J. Tricot. 2005. NY-ESO-1 is highly expressed in poor prognosis multiple myeloma and induces spontaneous humoral and cellular immune responses. *Blood* 105: 3939–3944.

462. Gure, A. O., R. Chua, B. Williamson, M. Gonen, C. A. Ferrera, S. Gnjatic, G. Ritter, A. J. G. Simpson, Y. T. Chen, L. J. Old, and N. K. Altorki. 2005. Cancer-testis genes are coordinately expressed and are markers of poor outcome in non-small cell lung cancer. *Clin. Cancer Res.* 11: 8055–8062.

463. Perez, D., F. Hauswirth, D. Jäger, U. Metzger, E. P. Samartzis, P. Went, and A. Jungbluth. 2011. Protein expression of cancer testis antigens predicts tumor recurrence and treatment response to imatinib in gastrointestinal stromal tumors. *Int. J. Cancer* 128: 2947–2952.

464. Al-Taei, S., J. Salimu, J. F. Lester, S. Linnane, M. Goonewardena, R. Harrop, M. D. Mason, and Z. Tabi. 2012. Overexpression and potential targeting of the oncofoetal antigen 5T4 in malignant pleural mesothelioma. *Lung Cancer* 77: 312–318.

465. Mulryan, K., M. G. Ryan, K. a Myers, D. Shaw, W. Wang, S. M. Kingsman, P. L. Stern, and M. W. Carroll. 2002. Attenuated recombinant vaccinia virus expressing oncofetal antigen (tumor-associated antigen) 5T4 induces active therapy of established tumors. *Mol. Cancer Ther.* 1: 1129–1137.

466. Kim, D. W., V. Krishnamurthy, S. D. Bines, and H. L. Kaufman. 2010. Trovax, a recombinant modified vaccinia ankara virus encoding 5T4: Lessons learned and future development. *Hum. Vaccin.* 6: 784–791.

467. Amato, R. J., R. E. Hawkins, H. L. Kaufman, J. A. Thompson, P. Tomczak, C. Szczylik, M. McDonald, S. Eastty, W. H. Shingler, J. De Belin, M. Goonewardena, S. Naylor, and R. Harrop. 2010. Vaccination of metastatic renal cancer patients with MVA-5T4: A randomized, double-blind, placebo-controlled phase III study. *Clin. Cancer Res.* 16: 5539–5547.

468. Odunsi, K., J. Matsuzaki, J. Karbach, A. Neumann, P. Mhawech-Fauceglia, A. Miller, A. Beck, C. D. Morrison, G. Ritter, H. Godoy, S. Lele, N. duPont, R. Edwards, P. Shrikant, L. J. Old, S. Gnjatic, and E. Jager. 2012. Efficacy of vaccination with recombinant vaccinia and fowlpox vectors expressing NY-ESO-1 antigen in ovarian cancer and melanoma patients. *Proc. Natl. Acad. Sci.* 109: 5797–5802.

469. Albershardt, T. C., D. J. Campbell, A. J. Parsons, M. M. Slough, J. ter Meulen, and P. Berglund. 2016. LV305, a dendritic cell-targeting integration-deficient ZVex TM -based lentiviral vector encoding NY-ESO-1, induces potent anti-tumor immune response. *Mol. Ther. - Oncolytics* 3: 16010.

470. Tatsis, N., and H. C. J. Ertl. 2004. Adenoviruses as vaccine vectors. *Mol. Ther.* 10: 616–629.

471. Farrington, L. A., T. A. Smith, F. Grey, A. B. Hill, and C. M. Snyder. 2013. Competition for antigen at the level of the APC is a major determinant of immunodominance during memory inflation in murine cytomegalovirus infection. *J. Immunol.* 190: 3410–6.

472. Dekhtiarenko, I., R. B. Ratts, R. Blatnik, L. N. Lee, S. Fischer, L. Borkner, J. D. Oduro, T. F. Marandu, S. Hoppe, Z. Ruzsics, J. K. Sonnemann, M. Mansouri, C. Meyer, N. A. W. Lemmermann, R. Holtappels, R. Arens, P. Klenerman, K. Früh, M. J. Reddehase, A. B. Riemer, and L. Cicin-Sain. 2016. Peptide Processing Is Critical for T-Cell Memory Inflation and May Be Optimized to Improve Immune Protection by CMV-Based Vaccine Vectors. *PLoS Pathog.* 12: 1–25.

473. He, Z., A. P. Wlazlo, D. W. Kowalczyk, J. Cheng, Z. Q. Xiang, W. Giles-Davis, and H. C. J. Ertl. 2000. Viral recombinant vaccines to the E6 and E7 antigens of HPV-16. *Virology* 270: 146–161.

474. Overwijk, W. W., D. S. Lee, D. R. Surman, K. R. Irvine, C. E. Touloukian, C.-C. Chan, M. W. Carroll, B. Moss, S. A. Rosenberg, and N. P. Restifo. 1999. Vaccination with a recombinant vaccinia virus encoding a ' 'self ' ' antigen induces autoimmune vitiligo and tumor cell destruction in mice: Requirement for CD4 ⅞ T lymphocytes. *Immunology* 96: 2982–2987.

475. Oliveira, S. A., S.-H. Park, P. Lee, A. Bendelac, and T. E. Shenk. 2002. Murine cytomegalovirus m02 gene family protects against natural killer cell-mediated immune surveillance. *J. Virol.* 76: 885–94.

476. Greene, T. T., M. Tokuyama, G. M. Knudsen, M. Kunz, J. Lin, A. L. Greninger, V. R. Defilippis, J. L. Derisi, D. H. Raulet, and L. Coscoy. 2016. A herpesviral induction of RAE-1 NKG2D ligand expression occurs through release of HDAC mediated repression. *Elife* 5.

477. Raulet, D. H., A. Marcus, and L. Coscoy. 2017. Dysregulated cellular functions and cell stress pathways provide critical cues for activating and targeting natural killer cells to transformed and infected cells. *Immunol. Rev.* 280: 93–101.

478. Lee, L. N., B. Bolinger, Z. Banki, C. de Lara, A. J. Highton, J. M. Colston, C. Hutchings, and P. Klenerman. 2017. Adenoviral vaccine induction of CD8+T cell memory inflation: Impact of co-infection and infection order. *PLoS Pathog.* 13: 1–26.

479. Jäger, E., M. Ringhoffer, J. Karbach, M. Arand, F. Oesch, and A. Knuth. 1996. Inverse relationship of melanocyte differentiation antigen expression in melanoma tissues and CD8+ cytotoxic-T-cell responses: Evidence for immunoselection of antigen-loss variantsin vivo. *Int. J. Cancer* 66: 470–476.

480. Lee, K. H., M. C. Panelli, C. J. Kim, A. I. Riker, M. P. Bettinotti, M. M. Roden, P. Fetsch, A. Abati, S. A. Rosenberg, and F. M. Marincola. 1998. Functional dissociation between local and systemic immune response during anti-melanoma peptide vaccination. *J. Immunol.* 161: 4183–94.

481. Riker, A., J. Cormier, M. Panelli, U. Kammula, E. Wang, A. Abati, P. Fetsch, K. H. Lee, S. Steinberg, S. Rosenberg, and F. Marincola. 1999. Immune selection after antigen-specific immunotherapy of melanoma. *Surgery* 126: 112–20.

482. Erkes, D. A., G. Xu, C. Daskalakis, K. A. Zurbach, N. A. Wilski, T. Moghbeli, A. B. Hill, and C. M. Snyder. 2016. Intratumoral Infection with Murine Cytomegalovirus Synergizes with PD-L1 Blockade to Clear Melanoma Lesions and Induce Long-term Immunity. *Mol. Ther.* 24: 1444–1455.

483. Gabrilovich, D. I., S. Ostrand-Rosenberg, and V. Bronte. 2012. Coordinated regulation of myeloid cells by tumours. *Nat. Rev. Immunol.* 12: 253–268.

484. Daley-Bauer, L. P., L. J. Roback, G. M. Wynn, and E. S. Mocarski. 2014. Cytomegalovirus hijacks CX3CR1hi patrolling monocytes as immune-privileged vehicles for dissemination in mice. *Cell Host Microbe* 15: 351–362.

485. Smith, P. D., M. Shimamura, L. C. Musgrove, E. A. Dennis, D. Bimczok, L. Novak, M. Ballestas, A. Fenton, S. Dandekar, W. J. Britt, and L. E. Smythies. 2014. Cytomegalovirus Enhances Macrophage TLR Expression and MyD88-Mediated Signal Transduction To Potentiate Inducible Inflammatory Responses. *J. Immunol.* 193: 5604–5612.

486. Tietze, J. K., D. E. C. Wilkins, G. D. Sckisel, M. N. Bouchlaka, K. L. Alderson, J. M. Weiss, E. Ames, K. W. Bruhn, N. Craft, R. H. Wiltrout, D. L. Longo, L. L. Lanier, B. R. Blazar, D. Redelman, and W. J. Murphy. 2012. Delineation of antigen-specific and antigen-nonspecific CD8(+) memory T-cell responses after cytokine-based cancer immunotherapy. *Blood* 119: 3073–83.

487. Sckisel, G. D., and W. J. Murphy. 2012. Getting to know the nonspecific side of memory T cells Specificity may be overrated in cancer immunotherapy. 1: 1208–1210.

488. Xu, W., M. Jones, B. Liu, X. Zhu, C. B. Johnson, A. C. Edwards, L. Kong, E. K. Jeng, K. Han, W. D. Marcus, M. P. Rubinstein, P. R. Rhode, and H. C. Wong. 2013. Efficacy and mechanism-of-action of a novel superagonist interleukin-15: Interleukin-

15 receptor αSu/Fc fusion complex in syngeneic murine models of multiple myeloma. *Cancer Res.* 73: 3075–3086.

489. Simoni, Y., E. Becht, M. Fehlings, C. Y. Loh, S.-L. Koo, K. W. W. Teng, J. P. S. Yeong, R. Nahar, T. Zhang, H. Kared, K. Duan, N. Ang, M. Poidinger, Y. Y. Lee, A. Larbi, A. J. Khng, E. Tan, C. Fu, R. Mathew, M. Teo, W. T. Lim, C. K. Toh, B.-H. Ong, T. Koh, A. M. Hillmer, A. Takano, T. K. H. Lim, E. H. Tan, W. Zhai, D. S. W. Tan, I. B. Tan, and E. W. Newell. 2018. Bystander CD8+ T cells are abundant and phenotypically distinct in human tumour infiltrates. *Nature* 1.

490. Morrison, L. A., and D. M. Knipe. 1996. Mechanisms of immunization with a replication-defective mutant of herpes simplex virus. *Virology* 220: 402–413.

491. Nguyen, L. H., D. M. Knipe, and R. W. Finberg. 1992. Replication-defective mutants of herpes simplex virus (HSV) induce cellular immunity and protect against lethal HSV infection. *J. Virol.* 66: 7067–7072.

492. Farrell, H. E., C. S. McLean, C. Harley, S. Efstathiou, S. Inglis, and a C. Minson. 1994. Vaccine potential of a herpes simplex virus type 1 mutant with an essential glycoprotein deleted. *J. Virol.* 68: 927–32.

493. Evans, D. T., J. E. Bricker, H. B. Sanford, S. Lang, A. Carville, B. a Richardson, M. Piatak, J. D. Lifson, K. G. Mansfield, and R. C. Desrosiers. 2005. Immunization of macaques with single-cycle simian immunodeficiency virus (SIV) stimulates diverse virus-specific immune responses and reduces viral loads after challenge with SIVmac239. *J. Virol.* 79: 7707–7720.

494. Snyder, C. M., J. E. Allan, E. L. Bonnett, C. M. Doom, and A. B. Hill. 2010. Cross-presentation of a spread-defective MCMV is sufficient to prime the majority of virus-specific CD8+ T cells. *PLoS One* 5: e9681.

495. Beswick, M., A. Pachnio, A. Al-Ali, C. Sweet, and P. A. Moss. 2013. An attenuated temperature-sensitive strain of cytomegalovirus (tsm5) establishes immunity without development of CD8+ T cell memory inflation. *J. Med. Virol.* 85: 1968–1974.

496. Mohr, C. A., J. Arapovic, H. Muhlbach, M. Panzer, A. Weyn, L. Dolken, A. Krmpotic, D. Voehringer, Z. Ruzsics, U. Koszinowski, and T. Sacher. 2010. A Spread-Deficient Cytomegalovirus for Assessment of First-Target Cells in Vaccination. *J. Virol.* 84: 7730–7742.

497. Heldwein, E. E., and C. Krummenacher. 2008. Entry of herpesviruses into mammalian cells. *Cell. Mol. Life Sci.* 65: 1653–1668.

498. Oduro, J. D., A. Redeker, N. A. W. Lemmermann, L. Ebermann, T. F. Marandu, I. Dekhtiarenko, J. K. Holzki, D. H. Busch, R. Arens, and L. Čičin-Šain. 2016. Murine cytomegalovirus (CMV) infection via the intranasal route offers a robust model of immunity upon mucosal CMV infection. *J. Gen. Virol.* 97: 185–195.

499. Jordan, M. C. 1978. Interstitial pneumonia and subclinical infection after intranasal inoculation of murine cytomegalovirus. *Infect. Immun.* 21: 275–280.

500. Morabito, K. M., T. R. Ruckwardt, A. J. Redwood, S. M. Moin, D. A. Price, and B. S. Graham. 2017. Intranasal administration of RSV antigen-expressing MCMV elicits robust tissue-resident effector and effector memory CD8+ T cells in the lung. *Mucosal Immunol.* 10: 545–554.

501. Mitrovic, M., J. Arapovic, S. Jordan, N. Fodil-Cornu, S. Ebert, S. M. Vidal, A. Krmpotic, M. J. Reddehase, and S. Jonjic. 2012. The NK Cell Response to Mouse Cytomegalovirus Infection Affects the Level and Kinetics of the Early CD8+ T-Cell Response. *J. Virol.* 86: 2165–2175.

502. Reddehase, M. J., W. Mutter, K. Münch, H. J. Bühring, and U. H. Koszinowski. 1987. CD8-positive T lymphocytes specific for murine cytomegalovirus immediate-early antigens mediate protective immunity. *J. Virol.* 61: 3102–8.

503. Shellam, G. R., and J. P. Flexman. 1986. Genetically determined resistance to murine cytomegalovirus and herpes simplex virus in newborn mice. *J. Virol.* 58: 152–6.

504. Quinnan, G. V, and J. F. Manischewitz. 1987. Genetically determined resistance to lethal murine cytomegalovirus infection is mediated by interferon-dependent and -independent restriction of virus replication. *J. Virol.* 61: 1875–81.

505. Lathbury, L. J., J. E. Allan, and G. R. Shellam. 1996. Effect of host genotype in determining the relative roles of natural killer cells and T cells in mediating protection against murine cytomegalovirus infection. 2605–2613.

506. Smith, H. R. C., J. W. Heusel, I. K. Mehta, S. Kim, B. G. Dorner, O. V Naidenko, K. Iizuka, H. Furukawa, D. L. Beckman, J. T. Pingel, A. A. Scalzo, D. H. Fremont, and W. M. Yokoyama. 2002. Recognition of a virus-encoded ligand by a natural killer cell activation receptor. *Proc. Natl. Acad. Sci. U. S. A.* 99: 8826–31.

507. Arase, H., E. S. Mocarski, A. E. Campbell, A. B. Hill, and L. L. Lanier. 2002. Direct recognition of cytomegalovirus by activating and inhibitory NK cell receptors. *Science (80-.).* 296: 1323–1326.

508. Thimme, R., V. Appay, M. Koschella, E. Roth, A. D. Hislop, A. B. Rickinson, S. L. Rowland-Jones, H. E. Blum, and H. Pircher. 2005. Increased Expression of the NK Cell Receptor KLRG1 by Virus-Specific CD8 T Cells during Persistent Antigen Stimulation Increased Expression of the NK Cell Receptor KLRG1 by Virus-Specific CD8 T Cells during Persistent Antigen Stimulation. *J. Virol.* 79: 12112–12116.

509. Goldrath, A. W., P. V. Sivakumar, M. Glaccum, M. K. Kennedy, M. J. Bevan, C. Benoist, D. Mathis, and E. A. Butz. 2002. Cytokine Requirements for Acute and Basal Homeostatic Proliferation of Naive and Memory CD8 $^{+}$ T Cells. *J. Exp. Med.* 195: 1515–1522.

510. Thom, J. T., T. C. Weber, S. M. Walton, N. Torti, and A. Oxenius. 2015. The Salivary Gland Acts as a Sink for Tissue-Resident Memory CD8+ T Cells, Facilitating Protection from Local Cytomegalovirus Infection. *Cell Rep.* 13: 1125–1136.

511. Smith, C. J., S. Caldeira-Dantas, H. Turula, and C. M. Snyder. 2015. Murine CMV Infection Induces the Continuous Production of Mucosal Resident T Cells. *Cell Rep.* 13: 1137–1148.

512. McMaster, S. R., J. J. Wilson, H. Wang, and J. E. Kohlmeier. 2015. Airway-Resident Memory CD8 T Cells Provide Antigen-Specific Protection against Respiratory Virus Challenge through Rapid IFN-γ Production. *J. Immunol.* 195: 203–209.

513. Gebhardt, T., L. M. Wakim, L. Eidsmo, P. C. Reading, W. R. Heath, and F. R. Carbone. 2009. Memory T cells in nonlymphoid tissue that provide enhanced local immunity during infection with herpes simplex virus. *Nat. Immunol.* 10: 524–30.

514. Gruener, N. H., F. Lechner, M.-C. Jung, H. Diepolder, T. Gerlach, G. Lauer, B. Walker, J. Sullivan, R. Phillips, G. R. Pape, and P. Klenerman. 2001. Sustained Dysfunction of Antiviral CD8+ T Lymphocytes after Infection with Hepatitis C Virus. *J. Virol.* 75: 5550–5558.

515. Fuller, M. J., A. Khanolkar, A. E. Tebo, and A. J. Zajac. 2004. Maintenance, Loss, and Resurgence of T Cell Responses During Acute, Protracted, and Chronic Viral Infections. *J. Immunol.* 172: 4204–4214.

516. Mackay, L. K., L. Wakim, C. J. van Vliet, C. M. Jones, S. N. Mueller, O. Bannard, D. T. Fearon, W. R. Heath, and F. R. Carbone. 2012. Maintenance of T Cell Function in the Face of Chronic Antigen Stimulation and Repeated Reactivation for a Latent Virus Infection. *J. Immunol.* 188: 2173–2178.

517. Frank, G. M., A. J. Lepisto, M. L. Freeman, B. S. Sheridan, T. L. Cherpes, and R. L. Hendricks. 2010. Early CD4(+) T cell help prevents partial CD8(+) T cell exhaustion and promotes maintenance of Herpes Simplex Virus 1 latency. *J. Immunol.* 184: 277–86.

518. Verma, S., D. Weiskopf, A. Gupta, B. McDonald, B. Peters, A. Sette, and C. A. Benedict. 2016. Cytomegalovirus-Specific CD4 T Cells Are Cytolytic and Mediate Vaccine Protection. *J. Virol.* 90: 650–658.

519. Shortman, K., and Y. J. Liu. 2002. Mouse and human dendritic cell subtypes. *Nat. Rev. Immunol.* 2: 151–161.

520. Alexandre, Y. O., C. D. Cocita, S. Ghilas, and M. Dalod. 2014. Deciphering the role of DC subsets in MCMV infection to better understand immune protection against viral infections. *Front. Microbiol.* 5: 1–20.

521. Pooley, J. L., W. R. Heath, and K. Shortman. 2001. Cutting edge: intravenous soluble antigen is presented to CD4 T cells by CD8- dendritic cells, but cross-presented to CD8 T cells by CD8+ dendritic cells. *J. Immunol. (Baltimore, Md 1950)* 166: 5327–5330.

522. Hsu, K. M., J. R. Pratt, W. J. Akers, S. I. Achilefu, and W. M. Yokoyama. 2009. Murine cytomegalovirus displays selective infection of cells within hours after systemic administration. *J. Gen. Virol.* 90: 33–43.

523. Tibbetts, S. A., F. Suarez, A. L. Steed, J. A. Simmons, and H. W. Virgin IV. 2006. A γ-herpesvirus deficient in replication establishes chronic infection in vivo and is impervious to restriction by adaptive immune cells. *Virology* 353: 210–219.

524. Andrews, D. M., A. A. Scalzo, W. M. Yokoyama, M. J. Smyth, and M. A. Degli-Esposti. 2003. Functional interactions between dendritic cells and NK cells during viral infection. *Nat. Immunol.* 4: 175–181.

525. Andrews, D. M., C. E. Andoniou, A. A. Scalzo, S. L. H. Van Dommelen, M. E. Wallace, M. J. Smyth, and M. A. Degli-Esposti. 2005. Cross-talk between dendritic cells and natural killer cells in viral infection. *Mol. Immunol.* 42: 547–555.

526. Robbins, S. H., G. Bessou, A. Cornillon, N. Zucchini, B. Rupp, Z. Ruzsics, T. Sacher, E. Tomasello, E. Vivier, U. H. Koszinowski, and M. Dalod. 2007. Natural killer cells promote early CD8 T cell responses against cytomegalovirus. *PLoS Pathog.* 3: 1152–1164.

527. Gibbons, a E., P. Price, and G. R. Shellam. 1995. Analysis of hematopoietic stem and progenitor cell populations in cytomegalovirus-infected mice. *Blood* 86: 473–481.

528. Chen, M., and J. Wang. 2010. Programmed cell death of dendritic cells in immune regulation. *Immunol Rev* 236: 11–27.

529. Bonilla, W. V, A. Fröhlich, K. Senn, S. Kallert, M. Fernandez, P. G. Fallon, R. Klemenz, S. Nakae, H. Adler, and D. Merkler. 2012. The Alarmin Interleukin-33 Drives. .

530. Mohr, C. A., J. Arapovic, H. Muhlbach, M. Panzer, A. Weyn, L. Dolken, A. Krmpotic, D. Voehringer, Z. Ruzsics, U. Koszinowski, and T. Sacher. 2010. A Spread-Deficient Cytomegalovirus for Assessment of First-Target Cells in Vaccination. *J. Virol.* 84: 7730–7742.

531. Enamorado, M., S. Iborra, E. Priego, F. J. Cueto, J. A. Quintana, S. Martýnez-Cano, E. Mejyás-Perez, M. Esteban, I. Melero, A. Hidalgo, and D. Sancho. 2017. Enhanced anti-tumour immunity requires the interplay between resident and circulating memory CD8+T cells. *Nat. Commun.* 8: 1–11.

532. Nizard, M., H. Roussel, M. O. Diniz, S. Karaki, T. Tran, T. Voron, E. Dransart, F. Sandoval, M. Riquet, B. Rance, E. Marcheteau, E. Fabre, M. Mandavit, M. Terme, C. Blanc, J. B. Escudie, L. Gibault, F. L. P. Barthes, C. Granier, L. C. S. Ferreira, C. Badoual, L. Johannes, and E. Tartour. 2017. Induction of resident memory T cells enhances the efficacy of cancer vaccine. *Nat. Commun.* 8.

533. Schleiss, M. R. 2016. Cytomegalovirus vaccines under clinical development. *J. virus Erad.* 2: 198–207.

534. Wilkinson, G. W. G., A. J. Davison, P. Tomasec, C. A. Fielding, R. Aicheler, I. Murrell, S. Seirafian, E. C. Y. Wang, M. Weekes, P. J. Lehner, G. S. Wilkie, and R. J. Stanton. 2015. Human cytomegalovirus: taking the strain. *Med. Microbiol. Immunol.* 204: 273–284.

535. Stanton, R. J., K. Baluchova, D. J. Dargan, C. Cunningham, O. Sheehy, S. Seirafian, B. P. McSharry, M. L. Neale, J. A. Davies, P. Tomasec, A. J. Davison, and G. W. G. Wilkinson. 2010. Reconstruction of the complete human cytomegalovirus genome in a BAC reveals RL13 to be a potent inhibitor of replication. *J. Clin. Invest.* 120: 3191–3208.

536. Redeker, A., S. P. M. Welten, and R. Arens. 2014. Viral inoculum dose impacts memory T-cell inflation. *Eur. J. Immunol.* 44: 1046–1057.

537. Gogev, S., F. Schynts, F. Meurens, I. Bourgot, and E. Thiry. 2003. Biosafety of herpesvirus vectors. *Curr Gene Ther* 3: 597–611.

Chapter 8 - Appendix

8.1 Appendix I

Table 8.1 Primers used for recombineering.

Primer		Sequence	Description
RpsL_IE2	Forward	GGGCGTGAACACGATGTTCTTGAGCACGGGGTCCTCGGGAGTAGCGTACGGAGCGCCGCCGTCCTCGGTGTAGACGTTCCTGTGACGGAAGATCACTTCG	Amplification of *rpsL* cassette with ie2 arms of homology
	Reverse	GGAGCGGGACGCCGATCGACTCTTCCTGGCCGCCGAGTCCCTGCAGTCCTTCGGTAGGGAAGGACTCTGCAGGTGCGACCTGAGGTTCTTATGGCTCTTG	
IE2KO	Oligo	CCTCGTGTCCTCTCACTGAATCTTCTTCCTGACGGTCACCAGGTCTCTGGATCTACAGACAAACAGAACCGTGAGCAGTCGCGTCCCTCACGCCCCCGGA	Oligonucleotide to delete *ie2* ORF
NY-ESO-1_IE2	Forward	CTCTTTATTTATTGATTAAAAACCATGACATACCTCGTGTCCTCTCACTGAATCTTCTTCCTGACGGTCACCAGGTCTCTGGTTATCTCCGCTGGCCGCT	Amplification of NY-ESO-1 gene with *ie2* arms of homology
	Reverse	CGGGGTAGCAGCTGTAGTGAGAGTCTCTCGGGTCCGGGGGCGTGAGGGACGCGACTGCTCACGGTTCTGTTTGTCTGTAGATATGCAGGCCGAGGGCAGA	
5T4_IE2	Forward	CTTTATTTATTGATTAAAAACCATGACATACCTCGTGTCCTCTCACTGAATCTTCTTCCTGACGGTCACCAGGTCTCTGGTCAGACATCGGAGTTGCTGC	Amplification of 5T4 gene with *ie2* arms of homology
	Reverse	GGGGTAGCAGCTGTAGTGAGAGTCTCTCGGGTCCGGGGGCGTGAGGGACGCGACTGCTCACGGTTCTGTTTGTCTGTAGATATGCCTGGCGGCTGTTCTA	
RpsL_IE1	Forward	AAAAGTATCCATCATTGTCCAAGTGTTAGTAAAAAAAACATTGTCCATGGTGATGGGTGGGGAGCTGGGCTTGTGGATC	Amplification of *rpsL* cassette with *ie1* arms of homology
	Reverse	CAAGAGGCAGTACGCCATGGTGCATACCAGATCCAAGTCTTCTGAGAATCAACAGCAGCCCAAGAAGAAGAGCAAGAAGCTGAGGTTCTTATGGCTCTTG	

RpsL_IE3	Forward	GACAGTTAGTTAGTTAGTTATGTATCTACATATTTTACAAAACAGGGTTCATCTTTAATACCAAGTCCACAGTACAGACCTGTGACGGAAGATCACTTCG	Amplification of *rpsL* cassette with *ie3* arms of homology
	Reverse	TTATGTGAACGCCCAGTTTGAGGCAGATGATATAAGCCATCATGAGGATGAGTCTGGGGAGTATGAGTCTGACTGCGAGCTGAGGTTCTTATGGCTCTTG	
P2A-5T4_IE3	Forward	CAGACAGTTAGTTAGTTAGTTATGTATCTACATATTTTACAAAACAGGGTTCATCTTTAATACCAAGTCCACAGTACAGATCAGACATCGGAGTTGCTGC	Amplification of P2A-5T4 with *ie3* arms of homology
	Reverse	AGCAGTTATGTGAACGCCCAGTTTGAGGCAGATGATATAAGCCATCATGAGGATGAGTCTGGGGAGTATGAGTCTGACTGCGAGAGCGGCTCCGGTGCCA	
RAd-NY-ESO-1	Forward	CGTCAGATCGCCTGGAGACGCCATCCACGCTGTTTTGACCTCCATAGAAGACACCGGGACCGATCCAGCCTGGATCCCCACCATGCAGGCCGAGGGCAGA	Amplification of NY-ESO-1 gene with RAd arms of homology
	Reverse	CAGGCGTGACACGTTTATTGAGTAGGATTACAGAGTATAACATAGAGTATAATATAGAGTATACAATAGTGACGTGGGATCCTTATCTCCGCTGGCCGCT	
m157_seq	Forward	GTCAGTAACGATCGCAGAGC	Primers to amplify *m157* locus
	Reverse	CACTCTTGTTAGTGCCGGT	

8.2 Appendix II

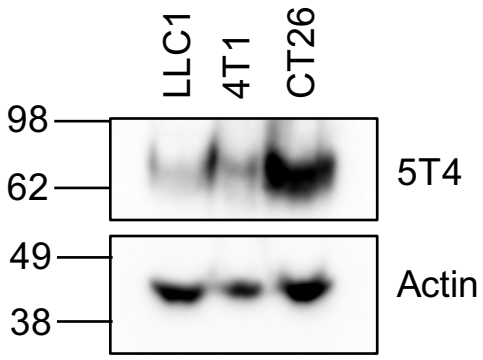

Figure 8.1 Expression of 5T4 by LLC1, 4T1 and CT26 cell lines.

Cell lysates were prepared from $2x10^5$ LLC1, 4T1 or CT26 cells and samples separated by SDSPAGE and transferred to a nitrocellulose membrane. 5T4 was detected prior to stripping and re-probing for actin.